

COORDINATION COMPOUNDS POSSESSING STANNYLAMINES: SYNTHESIS,
CHARACTERIZATION, AND APPLICATION

A Thesis Presented to the Academic Faculty

by

Jack F. Eichler

In Partial Fulfillment of the Requirements for the Degree
Doctor of Philosophy in Chemistry

Georgia Institute of Technology
August 2004

COORDINATION COMPOUNDS POSSESSING STANNYLAMINES: SYNTHESIS,
CHARACTERIZATION, AND APPLICATION

Approved:

William S. Rees, Jr., Committee Chairman

E. Kent Barefield

Angus P. Wilkinson

Z. John Zhang

Dennis W. Hess

20 August 2004

Date Approved

DEDICATION

This work is dedicated to my wife, Angie Gray, my parents, Mr. and Mrs. David Eichler, my grandmother, Rita Eichler, and to the memory of my grandfather, Jack Eichler.

ACKNOWLEDGEMENT

I would like to first acknowledge Professor William S. Rees, Jr. for supporting my graduate career. In addition, I would like to acknowledge Dr. Oliver Just for performing all of the single crystal X-ray diffraction analyses reported in this dissertation and for providing both academic and personal counsel during my time at Georgia Tech. I would also like to thank Dr. Scott Bunge and Dr. Javier Concepcion for providing assistance in general laboratory matters and for providing useful insight regarding my research project, Professor Christoph Fahrni for lending his expertise in the interpretation of the photochemical measurements, Dr. Xi Zeng for performing SEM experiments, Qian Luo for completing all XPS measurements, David Bostwick for assisting in the mass spectrometry analyses, and Dr. Johannes Leissen and Dr. Leslie Gelbaum for their assistance in performing NMR experiments. Finally, I would like to send my gratitude to all of the members of my research group for their support and friendship. The work presented in this dissertation was financially supported by the Office of Naval Research and Molecular Design Institute, and for this I am truly grateful.

TABLE OF CONTENTS

	<u>Page</u>
Acknowledgement	iv
List of Tables	ix
List of Figures	xvii
List of Schemes	xxi
List of Symbols and Abbreviations	xxii
Summary	xxiv
Chapter 1	
Introduction	1
References	11
Chapter 2	
Synthesis and Characterization of Group I and II Stannylamides	
Section A: Synthesis and Characterization of Homoleptic and Heteroleptic Lithium Amides Possessing the Trimethylstannyl Moiety: $[(\text{Me}_3\text{Sn})(\text{Me}_3\text{E})\text{NLi}\bullet(\text{Et}_2\text{O})]_2$ (E = Si, Ge, Sn)	14
Introduction	14
Experimental	15
Results and Discussion	19
Conclusion	26
Section B: Synthesis and Characterization of Beryllium Amides Prepared via Lithiated Stannylamines: $[(\text{Me}_3\text{Sn})_2\text{NBe}(\text{Cl})\bullet(\text{THF})]_2$, $[(\text{Me}_3\text{Sn})_2\text{NBe}(\text{OSO}_2\text{CF}_3)]_2$, and $[(\text{Me}_3\text{Si})(\text{H})\text{NBe}(\text{Cl})\bullet(\text{THF})]_2$	27
Introduction	27
Experimental	28
Results and Discussion	31

Chapter 2	Conclusion	39
	References	39
Chapter 3	Synthesis and Characterization of Luminescent Tetrameric Silver(I) Amides Possessing Group 14 Substituents: [(Me ₃ Si) ₂ NAg] ₄ and [(Me ₃ Sn)(Me ₃ E)NAg] ₄ (E = Si, Ge, Sn)	41
	Introduction	41
	Experimental	42
	Results and Discussion	46
	Conclusion	58
	References	58
Chapter 4	Synthesis and Structure Determination of Zinc(II) and Zirconium(IV) Dimeric Amides: [Zn{N(SnMe ₃) ₂ }(Cl) ₂ •Li(Et ₂ O) ₂] ₂ and [(C ₅ H ₅) ₂ ZrNSnMe ₃] ₂	60
	Introduction	60
	Experimental	60
	Results and Discussion	62
	Conclusion	68
	References	68
Chapter 5	Design and Synthesis of Group 14-Nitrogen Heterocubanes	70
	Section A: Synthesis and Characterization of a Series of Group 14-Nitrogen Heterocubanes: [M(u ₃ -NSiMe ₃) ₄] (M = Ge, Sn, Pb)	70
	Introduction	70
	Experimental	71
	Results and Discussion	74
	Conclusion	81

Chapter 5	Section B: Molecular Design of Group 14-Nitrogen Heterocubanes - Modification of the Exo-cube Substituent: $[\text{Sn}(\text{u}_3\text{-NEMe}_3)]_4$ (E = Ge, Sn)	82
	Introduction	82
	Experimental	82
	Results and Discussion	85
	Conclusion	91
	Section C: Molecular Design of Group 14-Nitrogen Heterocubanes - Modification of Both the Exo- and Endo-cube Substituent: $[\text{M}(\text{u}_3\text{-NGeMe}_3)]_4$ (M = Ge, Pb)	93
	Introduction	93
	Experimental	93
	Results and Discussion	96
	Conclusion	101
	Section D: Reaction of Tin-nitrogen Oxo Cubanes with Tetrakis Titanium Alkoxides: $\text{Sn}_6(\text{u}_3\text{-O})_4(\text{u}_3\text{-O}^i\text{Pr})_4$ and $\text{Sn}_6(\text{u}_3\text{-O})_4(\text{u}_3\text{-O}^t\text{Bu})_4$	102
	Introduction	102
	Experimental	103
	Results and Discussion	105
	Conclusion	109
	References	109
Chapter 6	The MOCVD of ZTT Via the Use of Tin-titanium Amidoalkoxides	112
	Section A: Synthesis and Characterization of Heterometallic Amidoalkoxides for Use as Precursors in the CVD of ZTT: $(\text{Me}_3\text{Sn})(\text{Me}_3\text{E})\text{Ti}(\text{OR})_3$ [E = Sn, Si; R = ^iPr , ^tBu , C_5H_{11}]	112

Chapter 6	Introduction	112
	Experimental	114
	Results and Discussion	117
	Conclusion	122
	Section B: CVD of ZTT Using Bis(trimethylstannyl)amine titanium(IV) tris(alkoxides)	123
	Introduction	123
	Experimental	123
	Results and Discussion	124
	Conclusions	129
	References	130
Chapter 7	Conclusions and Future Work	131
Appendix A	Crystallographic Tables for Compounds 1-19, 21-22	134

LIST OF TABLES

<u>Table</u>		<u>Page</u>
1.1	Metal complexes with N(SnMe ₃) ₃ , ⁻ N(SnMe ₃)(R), or ²⁻ N(SnMe ₃) as a ligand.	4
2.1	Selected average interatomic distances (Å) and angles (degrees) for compounds 1-3 .	24
2.2	Selected average interatomic distances (Å) and angles (degrees) for compounds 4-6 .	36
3.1	Selected average interatomic distances (Å) and angles (degrees) for compounds 7-10 .	52
3.2	UV/VIS absorption, emission, excitation, and lifetime decay for compounds 7,8 , and 10 .	57
4.1	Selected average interatomic distances (Å) and angles (degrees) for compounds 11 and 12 .	67
5.1	Selected average interatomic distances (Å) and angles (degrees) for compounds 13-15 .	79
5.2	Selected average interatomic distances (Å) and angles (degrees) for compounds 16 and 17 .	88
5.3	¹¹⁹ Sn NMR resonances observed for compounds 13 , 16 , and 17 .	90
5.4	Selected average interatomic distances (Å) and angles (degrees) for compounds 16 , 18 , and 19 .	99
5.5	Selected average interatomic distances (Å) and angles (degrees) for compounds 21 and 22 .	108
5.6	Selected average interatomic distances (Å) and angles (degrees) for compounds 21 and 22 .	109
6.1	Experimental conditions for the MOCVD of ZTT using precursors 23-25 and Zr(OBu ^t) ₄ .	126

6.2	Atomic concentration and molar composition of ZTT films calculated from high resolution XPS measurements.	127
A.1	Atomic Coordinates ($\times 10^4$) and Equivalent Isotropic Displacement Parameters ($\text{\AA} \times 10^3$) for $\text{C}_{20}\text{H}_{52}\text{N}_2\text{O}_2\text{Li}_2\text{Sn}_4$ (1).	135
A.2	Interatomic Distances (\AA) and Angles ($^\circ$) for $\text{C}_{20}\text{H}_{52}\text{N}_2\text{O}_2\text{Li}_2\text{Sn}_4$ (1).	136
A.3	Anisotropic displacement parameters ($\text{\AA}^2 \times 10^3$) for $\text{C}_{20}\text{H}_{52}\text{N}_2\text{O}_2\text{Li}_2\text{Sn}_4$ (1).	138
A.4	Hydrogen coordinates ($\times 10^4$) and isotropic displacement parameters ($\text{\AA}^2 \times 10^3$) for $\text{C}_{20}\text{H}_{52}\text{N}_2\text{O}_2\text{Li}_2\text{Sn}_4$ (1).	139
A.5	Atomic Coordinates ($\times 10^4$) and Equivalent Isotropic Displacement Parameters ($\text{\AA} \times 10^3$) for $\text{C}_{20}\text{H}_{52}\text{N}_2\text{O}_2\text{Li}_2\text{Si}_2\text{Sn}_2$ (2).	140
A.6	Interatomic Distances (\AA) and Angles ($^\circ$) for $\text{C}_{20}\text{H}_{52}\text{N}_2\text{O}_2\text{Li}_2\text{Si}_2\text{Sn}_2$ (2).	141
A.7	Anisotropic displacement parameters ($\text{\AA}^2 \times 10^3$) for $\text{C}_{20}\text{H}_{52}\text{N}_2\text{O}_2\text{Li}_2\text{Si}_2\text{Sn}_2$ (2).	143
A.8	Hydrogen coordinates ($\times 10^4$) and isotropic displacement parameters ($\text{\AA}^2 \times 10^3$) for $\text{C}_{20}\text{H}_{52}\text{N}_2\text{O}_2\text{Li}_2\text{Si}_2\text{Sn}_2$ (2).	144
A.9	Atomic Coordinates ($\times 10^4$) and Equivalent Isotropic Displacement Parameters ($\text{\AA} \times 10^3$) for $\text{C}_{20}\text{H}_{56}\text{N}_2\text{O}_2\text{Li}_2\text{Ge}_2\text{Sn}_2$ (3).	145
A.10	Interatomic Distances (\AA) and Angles ($^\circ$) for $\text{C}_{20}\text{H}_{52}\text{N}_2\text{O}_2\text{Li}_2\text{Ge}_2\text{Sn}_2$ (3).	146
A.11	Anisotropic displacement parameters ($\text{\AA}^2 \times 10^3$) for $\text{C}_{20}\text{H}_{52}\text{N}_2\text{O}_2\text{Li}_2\text{Ge}_2\text{Sn}_2$ (3).	148
A.12	Hydrogen coordinates ($\times 10^4$) and isotropic displacement parameters ($\text{\AA}^2 \times 10^3$) for $\text{C}_{20}\text{H}_{52}\text{N}_2\text{O}_2\text{Li}_2\text{Ge}_2\text{Sn}_2$ (3).	149

A.13	Atomic Coordinates ($\times 10^4$) and Equivalent Isotropic Displacement Parameters ($\text{\AA} \times 10^3$) for $\text{C}_{20}\text{H}_{52}\text{N}_2\text{O}_2\text{Cl}_2\text{Be}_2\text{Sn}_4$ (4).	150
A.14	Interatomic Distances (\AA) and Angles ($^\circ$) for $\text{C}_{20}\text{H}_{52}\text{N}_2\text{O}_2\text{Cl}_2\text{Be}_2\text{Sn}_4$ (4).	151
A.15	Anisotropic displacement parameters ($\text{\AA}^2 \times 10^3$) for $\text{C}_{20}\text{H}_{52}\text{N}_2\text{O}_2\text{Cl}_2\text{Be}_2\text{Sn}_4$ (4).	153
A.16	Hydrogen coordinates ($\times 10^4$) and isotropic displacement parameters ($\text{\AA}^2 \times 10^3$) for $\text{C}_{20}\text{H}_{52}\text{N}_2\text{O}_2\text{Cl}_2\text{Be}_2\text{Sn}_4$ (4).	154
A.17	Atomic Coordinates ($\times 10^4$) and Equivalent Isotropic Displacement Parameters ($\text{\AA} \times 10^3$) for $\text{C}_{14}\text{H}_{36}\text{Be}_2\text{F}_6\text{N}_2\text{O}_6\text{S}_2\text{Sn}_4$ (5).	156
A.18	Interatomic Distances (\AA) and Angles ($^\circ$) for $\text{C}_{14}\text{H}_{36}\text{Be}_2\text{F}_6\text{N}_2\text{O}_6\text{S}_2\text{Sn}_4$ (5).	158
A.19	Anisotropic displacement parameters ($\text{\AA}^2 \times 10^3$) for $\text{C}_{14}\text{H}_{36}\text{Be}_2\text{F}_6\text{N}_2\text{O}_6\text{S}_2\text{Sn}_4$ (5).	161
A.20	Hydrogen coordinates ($\times 10^4$) and isotropic displacement parameters ($\text{\AA}^2 \times 10^3$) for $\text{C}_{14}\text{H}_{36}\text{Be}_2\text{F}_6\text{N}_2\text{O}_6\text{S}_2\text{Sn}_4$ (5).	163
A.21	Atomic Coordinates ($\times 10^4$) and Equivalent Isotropic Displacement Parameters ($\text{\AA} \times 10^3$) for $\text{C}_{14}\text{H}_{36}\text{N}_2\text{O}_2\text{Cl}_2\text{Be}_2\text{Si}_2$ (6).	165
A.22	Interatomic Distances (\AA) and Angles ($^\circ$) for $\text{C}_{14}\text{H}_{36}\text{N}_2\text{O}_2\text{Cl}_2\text{Be}_2\text{Si}_2$ (6).	166
A.23	Anisotropic displacement parameters ($\text{\AA}^2 \times 10^3$) for $\text{C}_{14}\text{H}_{36}\text{N}_2\text{O}_2\text{Cl}_2\text{Be}_2\text{Si}_2$ (6).	167
A.24	Hydrogen coordinates ($\times 10^4$) and isotropic displacement parameters ($\text{\AA}^2 \times 10^3$) for $\text{C}_{14}\text{H}_{36}\text{N}_2\text{O}_2\text{Cl}_2\text{Be}_2\text{Si}_2$ (6).	168
A.25	Atomic Coordinates ($\times 10^4$) and Equivalent Isotropic Displacement Parameters ($\text{\AA} \times 10^3$) for $\text{C}_{24}\text{H}_{72}\text{N}_4\text{Sn}_8\text{Ag}_4$ (7).	169

A.26	Interatomic Distances (\AA) and Angles ($^\circ$) for $\text{C}_{24}\text{H}_{72}\text{N}_4\text{Sn}_8\text{Ag}_4$ (7).	171
A.27	Anisotropic displacement parameters ($\text{\AA}^2 \times 10^3$) for $\text{C}_{24}\text{H}_{72}\text{N}_4\text{Sn}_8\text{Ag}_4$ (7).	175
A.28	Hydrogen coordinates ($\times 10^4$) and isotropic displacement parameters ($\text{\AA}^2 \times 10^3$) for $\text{C}_{24}\text{H}_{72}\text{N}_4\text{Sn}_8\text{Ag}_4$ (7).	177
A.29	Atomic Coordinates ($\times 10^4$) and Equivalent Isotropic Displacement Parameters ($\text{\AA}^2 \times 10^3$) for $\text{C}_{24}\text{H}_{72}\text{N}_4\text{Si}_4\text{Sn}_4\text{Ag}_4$ (8).	181
A.30	Interatomic Distances (\AA) and Angles ($^\circ$) for $\text{C}_{24}\text{H}_{72}\text{N}_4\text{Si}_4\text{Sn}_4\text{Ag}_4$ (8).	183
A.31	Anisotropic displacement parameters ($\text{\AA}^2 \times 10^3$) for $\text{C}_{24}\text{H}_{72}\text{N}_4\text{Si}_4\text{Sn}_4\text{Ag}_4$ (8).	189
A.32	Atomic Coordinates ($\times 10^4$) and Equivalent Isotropic Displacement Parameters ($\text{\AA}^2 \times 10^3$) for $\text{C}_{24}\text{H}_{72}\text{N}_4\text{Ge}_4\text{Sn}_4\text{Ag}_4$ (9).	190
A.33	Interatomic Distances (\AA) and Angles ($^\circ$) for $\text{C}_{24}\text{H}_{72}\text{N}_4\text{Ge}_4\text{Sn}_4\text{Ag}_4$ (9).	192
A.34	Anisotropic displacement parameters ($\text{\AA}^2 \times 10^3$) for $\text{C}_{24}\text{H}_{72}\text{N}_4\text{Ge}_4\text{Sn}_4\text{Ag}_4$ (9).	197
A.35	Atomic Coordinates ($\times 10^4$) and Equivalent Isotropic Displacement Parameters ($\text{\AA}^2 \times 10^3$) for $\text{C}_{24}\text{H}_{72}\text{N}_4\text{Si}_4\text{Ag}_4$ (10).	198
A.36	Interatomic Distances (\AA) and Angles ($^\circ$) for $\text{C}_{24}\text{H}_{72}\text{N}_4\text{Si}_4\text{Ag}_4$ (10).	200
A.37	Anisotropic displacement parameters ($\text{\AA}^2 \times 10^3$) for $\text{C}_{24}\text{H}_{72}\text{N}_4\text{Si}_4\text{Ag}_4$ (10).	202
A.38	Hydrogen coordinates ($\times 10^4$) and isotropic displacement parameters ($\text{\AA}^2 \times 10^3$) for $\text{C}_{24}\text{H}_{72}\text{N}_4\text{Si}_8\text{Ag}_4$ (10).	204

A.39	Atomic Coordinates ($\times 10^4$) and Equivalent Isotropic Displacement Parameters ($\text{\AA} \times 10^3$) for $\text{C}_{28}\text{H}_{76}\text{N}_2\text{O}_4\text{Cl}_4\text{Sn}_4\text{Zn}_2$ (11).	206
A.40	Interatomic Distances (\AA) and Angles ($^\circ$) for $\text{C}_{28}\text{H}_{76}\text{N}_2\text{O}_4\text{Cl}_4\text{Sn}_4\text{Zn}_2$ (11).	209
A.41	Anisotropic displacement parameters ($\text{\AA}^2 \times 10^3$) for $\text{C}_{28}\text{H}_{76}\text{N}_2\text{O}_4\text{Cl}_4\text{Sn}_4\text{Zn}_2$ (11).	215
A.42	Hydrogen coordinates ($\times 10^4$) and isotropic displacement parameters ($\text{\AA}^2 \times 10^3$) for $\text{C}_{28}\text{H}_{76}\text{N}_2\text{O}_4\text{Cl}_4\text{Sn}_4\text{Zn}_2$ (11).	217
A.43	Atomic Coordinates ($\times 10^4$) and Equivalent Isotropic Displacement Parameters ($\text{\AA} \times 10^3$) for $\text{C}_{26}\text{H}_{38}\text{N}_2\text{Sn}_2\text{Zr}_2$ (12).	219
A.44	Interatomic Distances (\AA) and Angles ($^\circ$) for $\text{C}_{26}\text{H}_{38}\text{N}_2\text{Sn}_2\text{Zr}_2$ (12).	220
A.45	Anisotropic displacement parameters ($\text{\AA}^2 \times 10^3$) for $\text{C}_{26}\text{H}_{38}\text{N}_2\text{Sn}_2\text{Zr}_2$ (12).	223
A.46	Hydrogen coordinates ($\times 10^4$) and isotropic displacement parameters ($\text{\AA}^2 \times 10^3$) for $\text{C}_{26}\text{H}_{38}\text{N}_2\text{Sn}_2\text{Zr}_2$ (12).	224
A.47	Atomic Coordinates ($\times 10^4$) and Equivalent Isotropic Displacement Parameters ($\text{\AA} \times 10^3$) for $\text{C}_{12}\text{H}_{36}\text{N}_4\text{Si}_4\text{Sn}_4$ (13).	225
A.48	Interatomic Distances (\AA) and Angles ($^\circ$) for $\text{C}_{12}\text{H}_{36}\text{N}_4\text{Si}_4\text{Sn}_4$ (13).	227
A.49	Anisotropic displacement parameters ($\text{\AA}^2 \times 10^3$) for $\text{C}_{12}\text{H}_{36}\text{N}_4\text{Si}_4\text{Sn}_4$ (13).	232
A.50	Hydrogen coordinates ($\times 10^4$) and isotropic displacement parameters ($\text{\AA}^2 \times 10^3$) for $\text{C}_{12}\text{H}_{36}\text{N}_4\text{Si}_4\text{Sn}_4$ (13).	233

A.51	Atomic Coordinates ($\times 10^4$) and Equivalent Isotropic Displacement Parameters ($\text{\AA} \times 10^3$) for $\text{C}_{12}\text{H}_{36}\text{N}_4\text{Ge}_4\text{Si}_4$ (14).	234
A.52	Interatomic Distances (\AA) and Angles ($^\circ$) for $\text{C}_{12}\text{H}_{36}\text{N}_4\text{Ge}_4\text{Si}_4$ (14).	236
A.53	Anisotropic displacement parameters ($\text{\AA}^2 \times 10^3$) for $\text{C}_{12}\text{H}_{36}\text{N}_4\text{Ge}_4\text{Si}_4$ (14).	241
A.54	Hydrogen coordinates ($\times 10^4$) and isotropic displacement parameters ($\text{\AA}^2 \times 10^3$) for $\text{C}_{12}\text{H}_{36}\text{N}_4\text{Ge}_4\text{Si}_4$ (14).	243
A.55	Atomic Coordinates ($\times 10^4$) and Equivalent Isotropic Displacement Parameters ($\text{\AA} \times 10^3$) for $\text{C}_{12}\text{H}_{36}\text{N}_4\text{Pb}_4\text{Si}_4$ (15).	245
A.56	Interatomic Distances (\AA) and Angles ($^\circ$) for $\text{C}_{12}\text{H}_{36}\text{N}_4\text{Pb}_4\text{Si}_4$ (15).	246
A.57	Anisotropic displacement parameters ($\text{\AA}^2 \times 10^3$) for $\text{C}_{12}\text{H}_{36}\text{N}_4\text{Pb}_4\text{Si}_4$ (15).	248
A.58	Hydrogen coordinates ($\times 10^4$) and isotropic displacement parameters ($\text{\AA}^2 \times 10^3$) for $\text{C}_{12}\text{H}_{36}\text{N}_4\text{Pb}_4\text{Si}_4$ (15).	249
A.59	Atomic Coordinates ($\times 10^4$) and Equivalent Isotropic Displacement Parameters ($\text{\AA} \times 10^3$) for $\text{C}_{12}\text{H}_{36}\text{N}_4\text{Sn}_4\text{Ge}_4$ (16).	250
A.60	Interatomic Distances (\AA) and Angles ($^\circ$) for $\text{C}_{12}\text{H}_{36}\text{N}_4\text{Sn}_4\text{Ge}_4$ (16).	251
A.61	Anisotropic displacement parameters ($\text{\AA}^2 \times 10^3$) for $\text{C}_{12}\text{H}_{36}\text{N}_4\text{Sn}_4\text{Ge}_4$ (16).	253
A.62	Hydrogen coordinates ($\times 10^4$) and isotropic displacement parameters ($\text{\AA}^2 \times 10^3$) for $\text{C}_{12}\text{H}_{36}\text{N}_4\text{Sn}_4\text{Ge}_4$ (16).	254
A.63	Atomic Coordinates ($\times 10^4$) and Equivalent Isotropic Displacement Parameters ($\text{\AA} \times 10^3$) for $\text{C}_{12}\text{H}_{36}\text{N}_4\text{Sn}_8$ (17).	255

A.64	Interatomic Distances (\AA) and Angles ($^\circ$) for $\text{C}_{12}\text{H}_{36}\text{N}_4\text{Sn}_8$ (17).	256
A.65	Anisotropic displacement parameters ($\text{\AA}^2 \times 10^3$) for $\text{C}_{12}\text{H}_{36}\text{N}_4\text{Sn}_8$ (17).	257
A.66	Hydrogen coordinates ($\times 10^4$) and isotropic displacement parameters ($\text{\AA}^2 \times 10^3$) for $\text{C}_{12}\text{H}_{36}\text{N}_4\text{Sn}_8$ (17).	258
A.67	Atomic Coordinates ($\times 10^4$) and Equivalent Isotropic Displacement Parameters ($\text{\AA}^2 \times 10^3$) for $\text{C}_{12}\text{H}_{36}\text{N}_4\text{Ge}_8$ (18).	259
A.68	Interatomic Distances (\AA) and Angles ($^\circ$) for $\text{C}_{12}\text{H}_{36}\text{N}_4\text{Ge}_8$ (18).	260
A.69	Anisotropic displacement parameters ($\text{\AA}^2 \times 10^3$) for $\text{C}_{12}\text{H}_{36}\text{N}_4\text{Ge}_8$ (18).	261
A.70	Hydrogen coordinates ($\times 10^4$) and isotropic displacement parameters ($\text{\AA}^2 \times 10^3$) for $\text{C}_{12}\text{H}_{36}\text{N}_4\text{Ge}_8$ (18).	262
A.71	Atomic Coordinates ($\times 10^4$) and Equivalent Isotropic Displacement Parameters ($\text{\AA}^2 \times 10^3$) for $\text{C}_{12}\text{H}_{36}\text{N}_4\text{Pb}_4\text{Ge}_4$ (19).	263
A.72	Interatomic Distances (\AA) and Angles ($^\circ$) for $\text{C}_{12}\text{H}_{36}\text{N}_4\text{Pb}_4\text{Ge}_4$ (19).	264
A.73	Anisotropic displacement parameters ($\text{\AA}^2 \times 10^3$) for $\text{C}_{12}\text{H}_{36}\text{N}_4\text{Pb}_4\text{Ge}_4$ (19).	267
A.74	Hydrogen coordinates ($\times 10^4$) and isotropic displacement parameters ($\text{\AA}^2 \times 10^3$) for $\text{C}_{12}\text{H}_{36}\text{N}_4\text{Pb}_4\text{Ge}_4$ (19).	268
A.75	Atomic Coordinates ($\times 10^4$) and Equivalent Isotropic Displacement Parameters ($\text{\AA}^2 \times 10^3$) for $\text{C}_{12}\text{H}_{28}\text{O}_8\text{Sn}_6$ (21).	269

A.76	Interatomic Distances (\AA) and Angles ($^\circ$) for $\text{C}_{12}\text{H}_{28}\text{O}_8\text{Sn}_6$ (21).	270
A.77	Anisotropic displacement parameters ($\text{\AA}^2 \times 10^3$) for $\text{C}_{12}\text{H}_{28}\text{O}_8\text{Sn}_6$ (21).	273
A.78	Hydrogen coordinates ($\times 10^4$) and isotropic displacement parameters ($\text{\AA}^2 \times 10^3$) for $\text{C}_{12}\text{H}_{28}\text{O}_8\text{Sn}_6$ (21).	274
A.79	Atomic Coordinates ($\times 10^4$) and Equivalent Isotropic Displacement Parameters ($\text{\AA}^2 \times 10^3$) for $\text{C}_{16}\text{H}_{36}\text{O}_8\text{Sn}_6$ (22).	275
A.80	Interatomic Distances (\AA) and Angles ($^\circ$) for $\text{C}_{16}\text{H}_{36}\text{O}_8\text{Sn}_6$ (22).	276
A.81	Anisotropic displacement parameters ($\text{\AA}^2 \times 10^3$) for $\text{C}_{16}\text{H}_{36}\text{O}_8\text{Sn}_6$ (22).	277
A.82	Hydrogen coordinates ($\times 10^4$) and isotropic displacement parameters ($\text{\AA}^2 \times 10^3$) for $\text{C}_{16}\text{H}_{36}\text{O}_8\text{Sn}_6$ (22).	278

LIST OF FIGURES

<u>Figure</u>		<u>Page</u>
1.1	Bridging bonding mode of $\text{}^1\text{N}(\text{SnMe}_3)_2$ (I) and $\text{}^2\text{N}(\text{SnMe}_3)$ (II).	5
1.2	Ball and stick rendering of $[\text{Ti}(\text{Cl})(\eta^5\text{-Cp}^*)\{\mu\text{-N}(\text{SnMe}_3)\}]_2$ (A) and $[\text{In}(\text{Cl})(\text{CH}_3)\{\mu\text{-N}(\text{SnMe}_3)_2\}]_2$ (B).	6
1.3	Ball and stick rendering of $[\text{Li}\{\text{O}(\text{Me})(\text{}^t\text{Bu})\}\{\mu\text{-N}(\text{SnMe}_3)\}]_2$.	7
1.4	Ball and stick rendering of $[\text{Ag}\{\mu\text{-N}(\text{SnMe}_3)\}]_4$.	8
1.5	Ball and stick rendering of $[\text{Sn}\{\mu_3\text{-N}(\text{SiMe}_3)\}]_4$.	9
1.6	Diagram of tris(alkoxy)titanium chloride (A) and heterometallic amino alkoxide (B).	10
2.1	ORTEP plot representation (30% probability) with numbering scheme for (1). Hydrogen atoms have been omitted for clarity.	21
2.2	ORTEP plot representation (30% probability) with numbering scheme for (2). Hydrogen atoms have been omitted for clarity.	22
2.3	ORTEP plot representation (30% probability) with numbering scheme for (3). Hydrogen atoms have been omitted for clarity.	23
2.4	^{119}Sn NMR spectra of compounds 1-3 (chemical shift scale in ppm).	25
2.5	ORTEP plot representation (30% probability) with numbering scheme for (4). Hydrogen atoms have been omitted for clarity.	33
2.6	ORTEP plot representation (30% probability) with numbering scheme for (5). Hydrogen atoms have been omitted for clarity.	34

2.7	ORTEP plot representation (30% probability) with numbering scheme for (6). Hydrogen atoms have been omitted for clarity.	35
2.8	Solid state ^9Be NMR spectrum of compound 4 (chemical shift scale in ppm).	38
3.1	ORTEP plot representation (30% probability) with numbering scheme for (7). Hydrogen atoms have been omitted for clarity.	48
3.2	ORTEP plot representation (30% probability) for (8). Hydrogen atoms have been omitted for clarity.	49
3.3	ORTEP plot representation (30% probability) for (9). Hydrogen atoms have been omitted for clarity.	50
3.4	ORTEP plot representation (30% probability) with numbering scheme for (10). Hydrogen atoms have been omitted for clarity.	51
3.5	^{119}Sn NMR spectra of compounds 7-9 (chemical shift scale in ppm).	53
3.6.A	The UV/VIS absorption, emission (@ 300 nm), and excitation (@ 350 nm) spectra for (7).	55
3.6.B	The decay lifetime for (7).	55
3.7	A: HOMO; B: HOMO(-1); C: LUMO; D: LUMO(-1) for (7). Single point energy calculation (BP/LACVP*).	56
4.1	ORTEP plot representation (30% probability) with numbering scheme for (11). Hydrogen atoms have been omitted for clarity.	65
4.2	ORTEP plot representation (30% probability) with numbering scheme for (12). Hydrogen atoms have been omitted for clarity.	66
5.1	ORTEP plot representation (30% probability) with numbering scheme for (13). Hydrogen atoms have been omitted for clarity.	76

5.2	ORTEP plot representation (30% probability) with numbering scheme for (14) . Hydrogen atoms have been omitted for clarity.	77
5.3	ORTEP plot representation (30% probability) with numbering scheme for (15) . Hydrogen atoms have been omitted for clarity.	78
5.4	TGA plot of percent vs. temperature for (15) .	81
5.5	ORTEP plot representation (30% probability) with numbering scheme for (16) . Hydrogen atoms have been omitted for clarity.	86
5.6	ORTEP plot representation (30% probability) with numbering scheme for (17) . Hydrogen atoms have been omitted for clarity.	87
5.7	¹¹⁹ Sn NMR spectra of compound 17 (chemical shift scale in ppm).	90
5.8	TGA plot of percent weight vs. temperature for compound 17 .	91
5.9	ORTEP plot representation (30% probability) with numbering scheme for (18) . Hydrogen atoms have been omitted for clarity.	97
5.10	ORTEP plot representation (30% probability) with numbering scheme for (19) . Hydrogen atoms have been omitted for clarity.	98
5.11	TGA plot of percent weight vs. temperature for compound 19 .	100
5.12	ORTEP plot representation (30% probability) with numbering scheme for (21) . Hydrogen atoms have been omitted for clarity.	106
5.13	ORTEP plot representation (30% probability) with numbering scheme for (22) . Hydrogen atoms have been omitted for clarity.	107

6.1	Variable temperature ^1H NMR of compound 23 : $-\text{Sn}(\text{CH}_3)_2$ peaks shown (chemical shift scale in ppm).	119
6.2.A	TGA plots of compound 23 , $\text{Zr}(\text{OBu}^t)_4$, and a mixture of the two species.	120
6.2.B	TGA plot of A: compound 24 , $\text{Zr}(\text{OBu}^t)_4$, and a mixture of the two species B: compound 25 and $\text{Zr}(\text{OBu}^t)_4$.	121
6.3	Schematic of MOCVD reactor.	125
6.4.A	SEM picture of film from experiment 1.	128
6.4.B	SEM picture of film from experiment 4.	129

LIST OF SCHEMES

<u>Scheme</u>		<u>Page</u>
2.1	Synthesis of 1-3.	20
2.2	Synthesis of 4-5.	32
2.3	Synthesis of 6.	32
3.1	Synthesis of compounds 7-10.	47
4.1	Synthesis of 11.	63
4.2	Synthesis of 12.	64
5.1	Synthesis of 13-15.	75
5.2	Synthesis of 16-17.	85
5.3	Synthesis of 18-19.	96
5.4	Synthesis of 21-22.	105
6.1	Synthesis of 23-27.	118

LIST OF SYMBOLS AND ABBREVIATIONS

Å	Angstrom
C	Celsius
d	doublet
EI	Electron Ionization
Et ₂ O	diethyl ether
eV	electron volt
HOMO	Highest Occupied Molecular Orbital
IR	Infrared
K	Kelvin
λ	wavelength
LUMO	Lowest Unoccupied Molecular Orbital
m	multiplet
MHz	Megahertz
MOCVD	Metal Organic Chemical Vapor Deposition
MS	Mass Spectrometry
NMR	Nuclear Magnetic Resonance
ORTEP	Oak Ridge Thermal Ellipsoid Plot
ppm	parts per million
s	singlet
sccm	standard cubic centimeters per minute
SEM	Scanning Electron Microscopy
THF	tetrahydrofuran

TGA	Thermogravimetric Analysis
TMS	tetramethyl silane
UV/VIS	Ultraviolet/Visible
XPS	X-ray Photoelectron Spectroscopy
ZTT	Zirconium Tin Titanate

SUMMARY

The marriage of synthetic chemistry to materials science has been well documented in the last decade. The design, synthesis, and utilization of chemical precursors in the MOCVD of electronic materials in particular has received a lot of attention in both academic and industrial circles. The maintenance of this symbiotic relationship is pursued in this work in the hope of discovering chemical forerunners for high-dielectric metal oxide materials. Specifically, it is of interest to isolate chemical precursors for ZTT, a recent entry into the field of high-k dielectrics.

The primary theme of this dissertation is the exploration of the design and synthesis of molecular precursors that possess more than one of the cations found in the final ZTT film. The approach taken to obtain such precursors, referred to in this work as “same-source” precursors, is to investigate the implementation of the anionic stannylamine ligand, $\text{N}(\text{SnMe}_3)_2$ in the preparation of heterometallic coordination complexes. The ultimate goal is to procure volatile, low molecular weight compounds that possess more than one of the metals found in ZTT (tin, titanium, and/or zirconium).

The reason for choosing stannylamine ligands is two-fold. First, as was alluded to above, such ligands might provide convenient access to heterometallic complexes possessing tin as one of the metal constituents. Second, since the coordination chemistry of stannyl amines is relatively unexplored compared to alkyl- and silylamine ligands, it is important from a fundamental standpoint to investigate the synthetic utility of this ligand type.

Thus, this work accomplishes two major objectives: 1) the synthesis and characterization of a variety of metal complexes coordinated by stannylamines and 2) the design, synthesis, and utilization of heterometallic precursors for use in the MOCVD of ZTT. Chapter 1 summarizes the history of stannylamine coordination chemistry and the different binding modes possible in these types of ligands. Chapters 2-4 report the synthesis and complete characterization of lithiated stannylamines and their subsequent use in the preparation of beryllium, silver, zinc, and zirconium amides. Chapter 5 then describes the use of lithiated stannylamines as synthons to Group 14-nitrogen heterocubanes and the subsequent molecular design of tin-nitrogen cubanes for potential use in the MOCVD of ZTT. Finally, Chapter 6 provides details of the synthesis and characterization of a new class of heterometallic aminoalkoxides and their use in the MOCVD of ZTT.

To summarize, in the course of a synthetic investigation towards the goal of “same-source” ZTT precursors for use in MOCVD processes, a number of metal coordination complexes possessing stannylamine ligands have been synthesized and fully characterized. Consequently, the library of known compounds containing these ligands has been significantly expanded and a novel route to volatile, heterobimetallic aminoalkoxide species has been developed.

CHAPTER 1

INTRODUCTION

As the size requirements for integrated circuit devices become smaller, the utility of SiO₂ as the dielectric material in field effect transistors (FET's) will diminish.¹ This is due to the inherently high leakage current that arises when the thickness of the SiO₂ dielectric layer is decreased. Scaling of FET devices is governed by the duality of speed versus power. There is a desire to increase the speed of the device, which is dependent on drive current. Additionally, there is a need to decrease the power consumption, which is dependent on the gate leakage current.

$$(1) I \propto \mu C_{ox}$$

$$(2) C_{ox} \propto k/t$$

$$(3) I_g \propto 1/t$$

I = drive current

k = gate oxide dielectric constant

μ = effective mobility of carriers

t = gate oxide thickness

C_{ox} = gate oxide capacitance

I_g = gate oxide leakage current

Since SiO₂ has a low dielectric constant ($k = 4$), higher capacitance, and hence larger drive currents are obtained by decreasing the thickness of the dielectric layer. However, decreasing the thickness of this layer leads to larger leakage currents, and thus increased power consumption. Current projections indicate that SiO₂ most likely will not meet device performance requirements due to scaling within the next decade.² A potential solution to this problem is to replace the silica dielectric layer with alternative metal

oxide materials possessing higher dielectric constants. Thicker dielectric layers can achieve the necessary capacitance if the material's dielectric constant is higher. Materials with larger dielectric constants thus have the potential to both decrease leakage currents (power consumption) and increase the drive current (transistor speed).

A number of oxide materials have been proposed as candidates to replace SiO₂ as the gate dielectric. Included among these are: Ta₂O₅, TiO₂, Y₂O₃, CeO₂, ZrO₂, HfO₂, Al₂O₃, and barium strontium titanate (BST). However, many of these materials are not easily integrated into the current device technology. A recent entry into this group of potential alternative dielectric materials is zirconium tin titanate (ZTT). High-*k* ZTT films were first deposited by van Dover and coworkers using an on-axis reactive sputtering technique. The electrical properties of these films were observed to be quite promising, possessing dielectric constants between 50-70 and leakage currents on the order of 10⁻⁹-10⁻⁷ A/cm².³ However, MOCVD processes offer distinct advantages relative to sputtering techniques, such as higher uniformity films, and are currently used in the deposition of numerous oxide films in the IC industry.

Hence, recent work by Senzaki, *et al.*, as well as researchers in our group, has investigated the use of metal organic chemical vapor deposition (MOCVD) in the preparation of ZTT films. ZTT films were fabricated by both groups using a CVD precursor mixture comprised of (tBuO)₄M [M = Zr, Sn, Ti], but were found to possess dielectric constants between 20-30.^{4,5} Since the dielectric constant of these films is significantly lower than in the films obtained by van Dover, *et al.*, there is a need to optimize the MOCVD of ZTT. One aspect of the process that can be potentially improved is the nature of the chemical precursor system. Since the previously used

cocktail was a mixture of three individual chemical components, the use of a same-source precursor that contains two or more of the desired metal cations may prove to be a better alternative. Such a precursor system has the potential to limit premature reactions, provide good quality homogenous films, avoid varying decomposition regimes, and control the ratio of cations in the final film.⁶⁻⁸

Thus, the research presented in this dissertation focuses on designing and synthesizing same-source precursors that are to be used in the MOCVD of ZTT. The primary objective is to explore potential metal amide precursors and/or precursors that possess two or more of the metals of interest. The use of stannyl amide metal complexes may provide a route to such precursors.

The use of amido ligands (with amido generally referring to a deprotonated secondary amine; 'NRR') in metal complexes is ubiquitous throughout the periodic table. Extensive research studies involving the synthesis, characterization, and application of metal amide compounds can be readily found in the literature and a number of publications devoted to reviewing the field of amidometal chemistry are available to the reader.⁹⁻¹⁵ Interest in metal amide compounds arises, in part, from the potential for disubstitution on the amide ligand. This allows the electronic and steric properties to be finely tuned, and metal coordination compounds of amides have found application in areas such as homogeneous catalysis,^{16,17} organic synthesis,¹⁸ small molecule activation,¹⁹ and MOCVD of thin films.⁶

Due to the enhanced stability of the metal-nitrogen interaction that results from the steric protection of the bulky trimethyl silyl group and the electronic stabilization that potentially arises from the empty d-orbitals present on the silicon atoms, silyl amide

complexes $[M^{x+}(N(SiR_3)_2)_x]$; R = alkyl, aryl] have been utilized in the preparation of a plethora of complexes.^{13,20-22} Although metal amide compounds containing silyl substituents have been systematically studied, complexes possessing the heavier stannyl amide congener are much less frequent. Table 1.1 contains a list of structurally characterized metal complexes containing amide ligands with at least one trimethyl stannyl moiety.

Table 1.1. Metal complexes with $N(SnMe_3)_3$, $N(SnMe_3)(R)$, or $N(SnMe_3)_2$ as a ligand

Complex	Ref.	Complex	Ref.
$[Ti(Cl)\{O(2,6-(Ph)_2Ph)\}_2\{N(SnMe_3)_2\}]$	23	$[Li\{O(CH_3)(^tBu)\}\{\mu-N(SnMe_3)_2\}]_2$	27
$[In(CH_3)_2\{\mu-N(CH_3)(SnMe_3)\}]_2$	24	$[Li\{\eta^3-N(CH_3)(CH_2CH_2NMe_2)_2\}-\{N(SnMe_3)_2\}]_2$	27
$[In(CH_3)_2\{\mu-N(^iPr)(SnMe_3)\}]_2$	24	$[Ti(\eta^5-Cp)\{\mu_3-N(SnMe_3)\}]_4$	28
$[Al(CH_3)_2\{\mu-N(^iPr)(SnMe_3)\}]_2$	24	$[Li\{\eta^2-N(CH_3)_2CH_2CH_2N(CH_3)_2\}-\{\eta^2-N(Quinoline)(SnMe_3)\}]$	29
$[Ga(CH_3)_2\{\mu-N(n-Propyl)(SnMe_3)\}]_2$	24	$[Li\{\eta^3-N(CH_3)(CH_2CH_2N(CH_3)_2)_2\}-\{N(BC_8H_{14})(SnMe_3)\}]$	29
$[Cu(Cl)\{N(SnMe_3)_3\}]$	25	$[Ti(Cl)(\eta^5-Cp^*)\{\mu-N(SnMe_3)\}]_2$	30
$[Cu\{\mu-N(SnMe_3)_2\}]_4$	25	$[In(CH_3)_3\{N(SnMe_3)_3\}]$	31
$[Al(Cl)_3\{N(SnMe_3)_3\}]$	26	$[In(Cl)(CH_3)\{\mu-N(SnMe_3)_2\}]_2$	31
$[Al(Cl)_2(CH_3)\{N(SnMe_3)_3\}]$	26	$[In(Cl)(Et)\{\mu-N(SnMe_3)_2\}]_2$	31
$[Ga(Cl)_3\{N(SnMe_3)_3\}]$	26	$[Ti(F)\{\eta^5-Cp(Me_4)(Et)\}\{\mu-N(SnMe_3)\}]_2$	32
$[Ga(Br)_3\{N(SnMe_3)_3\}]$	26	$[Ga(CH_3)_2\{\mu-N(^iPr)(SnMe_3)\}]_2$	33
$[Ga(Cl)_2(CH_3)\{N(SnMe_3)_3\}]$	26		
$[In(Cl)_3\{N(SnMe_3)_3\}]$	26		
$[In(Br)_3\{N(SnMe_3)_3\}]$	26		

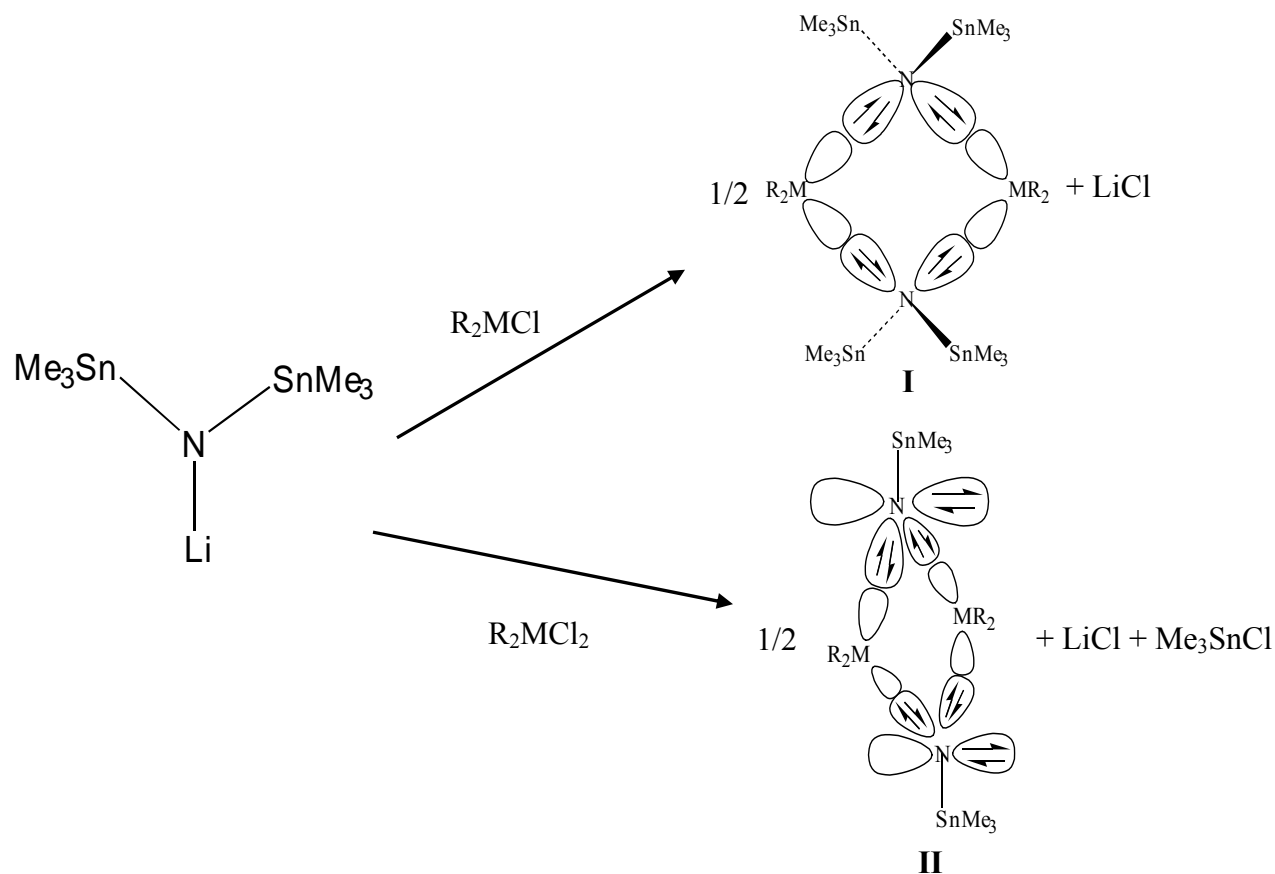


Figure 1.1. Bridging bonding mode of $^1\text{N}(\text{SnMe}_3)_2$ (**I**) and $^2\text{N}(\text{SnMe}_3)$ (**II**)

The following chapters describe the use of either the monoanionic, $^1\text{N}(\text{SnMe}_3)_2$, or dianionic, $^2\text{N}(\text{SnMe}_3)$, stannyl amides (as well as the silicon and germanium congeners) as ligands in metal complexes, with the ultimate aim of preparing heterometallic precursors for the MOCVD of ZTT. Examination of reported stannyl amide metal complexes possessing either mono or dianionic ligands reveals a tendency for these compounds to adopt dimeric or tetrameric structures (see Table 1.1). Figure 1.1 depicts valence bond representations of mono (**I**) and dianionic (**II**) forms of stannyl amide ligands. The ligand type **I** contains an sp^3 hybridized nitrogen, with two electron pairs coordinating to two metal centers in a bridging fashion. The ligand type **II** possesses an

sp^2 hybridized nitrogen, with two electron pairs residing in the sp^2 hybrid orbitals bridging two metal centers and another lone pair of electrons occupying an empty p orbital on the nitrogen atom. Figure 1.2 depicts crystal structures of metal complexes containing both monoanionic and dianionic stannyl amide ligands.

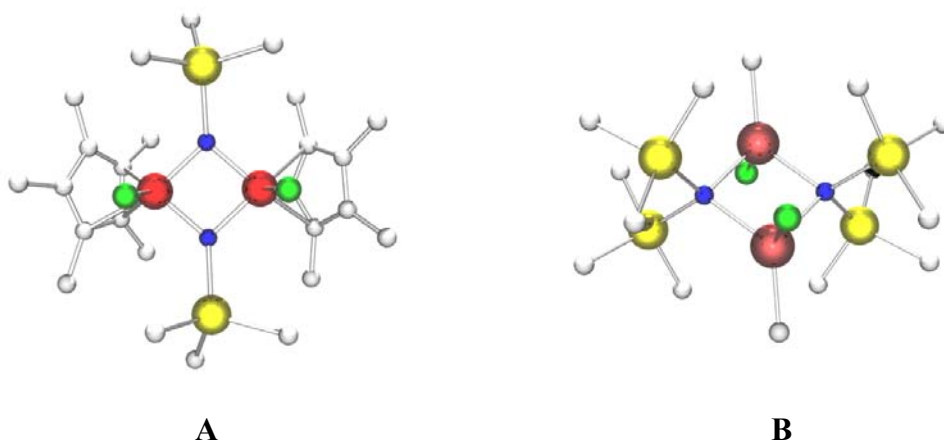


Figure 1.2. Ball and stick rendering of $[\text{Ti}(\text{Cl})(\eta^5\text{-Cp}^*)\{\mu\text{-N}(\text{SnMe}_3)\}]_2^{30}$ (**A**) and $[\text{In}(\text{Cl})(\text{CH}_3)\{\mu\text{-N}(\text{SnMe}_3)_2\}]_2^{31}$ (**B**)



Any design strategy involving the use of stannyl amido metal complexes must consider the potential to form either of these ligand types and their potential to undergo a bridging coordination mode.

The majority of the compounds listed in Table 1.1 were obtained by the reaction of the appropriate metal precursor with the tris(trimethylstannyl)amine $[(\text{Me}_3\text{Sn})_3\text{N}]$ species. Conversely, Fenske and coworkers used the lithiated bis(trimethylstannyl)amine $[(\text{Me}_3\text{Sn})_2\text{NLi}\cdot(\text{THF})]$ in the preparation of the copper tetramer $[\text{Cu}\{\mu\text{-N}(\text{SnMe}_3)_2\}]_4^{25}$. Based on computer database searches of the literature, this is the only stannyl amido metal complex synthesized via a lithium amide precursor. This complex should be

functional in a variety of metathesis reactions and could prove to be useful in the synthesis of ZTT MOCVD precursors. Thus, in an effort to expand the chemistry of this starting material, Chapter 2 explores the synthesis and full characterization of the lithiated bis(stannylamine) ligand. In addition, heteroleptic stannylamide ligands and beryllium complexes possessing stannylamide moieties, synthesized using the lithium amide precursor reported by Fenske, are examined. These Group I and II complexes typically exist as dimers in the solid state, with the stannyl amide acting as a bridging ligand (Figure 1.3).

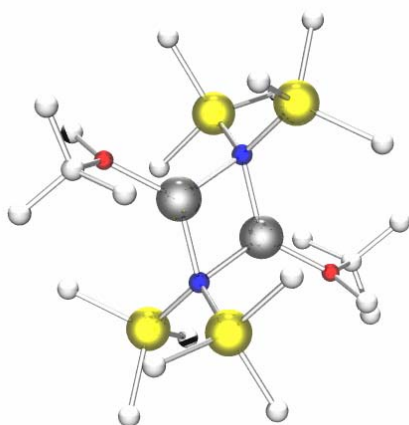


Figure 1.3. Ball and stick rendering of $[\text{Li}\{\text{O}(\text{Me})(\text{tBu})\}\{\mu\text{-N}(\text{SnMe}_3)\}]_2$ ²⁷



Before attempting to procure ZTT precursors, it was first of interest to determine the utility of $[(\text{Me}_3\text{Sn})_2\text{NLi}\bullet(\text{THF})]$ in metathesis reactions with various transition metal halide starting reagents. Thus, the reactivity of homoleptic and heteroleptic lithiated stannyl amides was first investigated with AgBr. The work in Chapter 3 aims to determine if silver tetrameric amido complexes structurally analogous to Fenske's copper tetramer, $[\text{Cu}\{\mu\text{-N}(\text{SnMe}_3)_2\}]_4$, can be synthesized. Lappert and coworkers first reported the synthesis of a silver amide possessing this planar Ag_4N_4 tetrameric core

approximately 8 years ago (Figure 1.4).³⁴ However, until recent work in our laboratory,³⁵ little has been done to investigate the possibility of extending this geometrical design to other ligand systems.

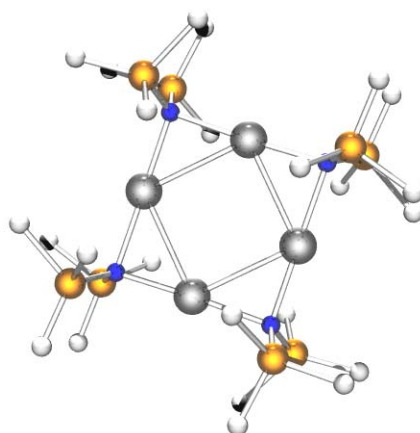


Figure 1.4. Ball and stick rendering of $[\text{Ag}\{\mu\text{-N}(\text{SnMe}_3)\}]_4$ ³⁴



The exploration of the chemistry of $[(\text{Me}_3\text{Sn})_2\text{NLi}\cdot(\text{THF})]$ with metal halide reagents is continued in Chapter 4, which describes reactions of N-lithio bis(trimethylstannyl)amine with zirconium and zinc chloride starting materials. The potential of stannyl amides to form either the monoanionic or dianionic ligand types previously described, and their subsequent complexes with zinc and zirconium are presented. The reaction pathways that are shown here are further explored in Chapter 5, resulting in the use of lithiated stannyl amides to prepare Group 14-nitrogen heterocubanes. Group 14 metal-nitrogen cubane structures have been previously obtained by a variety of alternative synthetic pathways, including the reaction of cyclic stannylenes with primary amines,³⁶ the reaction of magnesium imides with metal

dichlorides,³⁷ the reaction of lithiated primary amines with bis(cyclopentadienyl) metal complexes,³⁸ and the reaction of bis(amido) metal compounds with primary amines.³⁹ These structures exist as tetramers possessing an M_4N_4 core with an additional substituent bound to nitrogen in an exocube fashion (Figure 1.5). The work described here provides a novel, systematic route to a variety of cubane structures that possess unusually heavy exocube substituents, and the molecular design of these structures is probed in an attempt to fabricate ZTT MOCVD precursors.

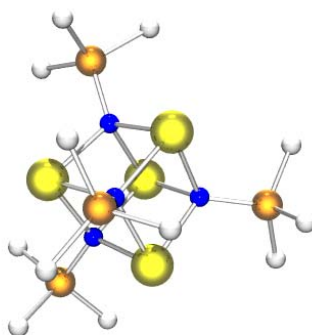


Figure 1.5. Ball and stick rendering of $[Sn\{\mu_3-N(SiMe_3)\}]_4$ ³⁶



Finally, in Chapters 6 and 7, both homoleptic and heteroleptic stannylamines are successfully implemented in the synthesis of same-source ZTT precursors. The resulting heterometallic stannyl amido metal complexes are then applied in the MOCVD of ZTT thin films. Chapter 6 describes the synthesis and characterization of tris(alkoxy)titanium chlorides, and their subsequent reaction with lithiated stannyl amines to produce heterometallic alkoxide-amides (Figure 1.6). A search of the literature indicates that bimetallic species containing nitrogen-bridged alkyl tin and titanium alkoxides have not

been previously reported. The investigation of the thermal properties of the tin-titanium alkoxide-amides and their use in the MOCVD of ZTT are then summarized in Chapter 7.

To conclude, during the course of a synthetic investigation related to the development of MOCVD precursors, a variety of stannyl amidometal complexes have been synthesized and characterized. Whether serendipitous or designed in nature, these complexes have further contributed to the development of the coordination chemistry of stannyl amide ligands, as well as provide potential alternative precursors in the MOCVD of ZTT.

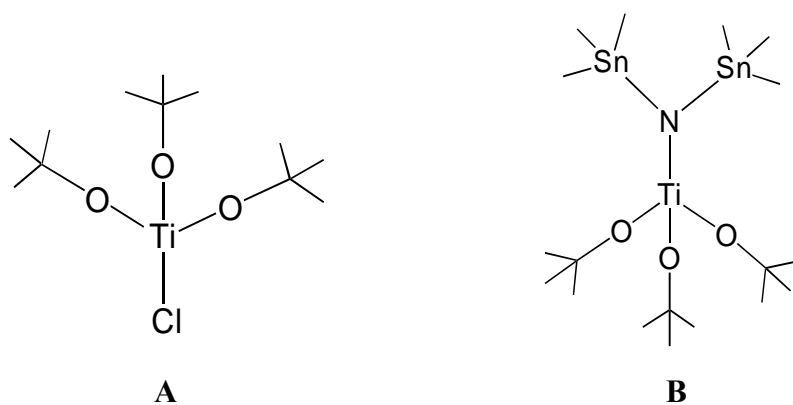


Figure 1.6. Diagram of tris(alkoxy)titanium chloride (**A**)⁴⁰ and heterometallic amido-alkoxide (**B**)

References

- (1) Bersuker, G.; Zeitzoff, P.; Brown, G.; Huff, H. R. *Materials Today* **2004**, 7, 26-33.
- (2) Buchanan, D. A. *IBM J. Res. Develop.* **1999**, 43, 245-264.
- (3) Dover, R. B. v.; Schneemeyer, L. F. *IEEE Electron Device Letters* **1998**, 19, 329-331.
- (4) Mays, E. L.; Hess, D. W.; Rees, W. S., Jr. *Journal of Crystal Growth* **2004**, 261, 309-315.
- (5) Senzaki, Y.; Alers, G. B.; Hochberg, A. K.; Roberts, D. A.; Norman, J. A. T.; Fleming, R. M.; Krautter, H. *Eletrochem. Solid-State Lett.* **2000**, 9, 435-436.
- (6) Just, O.; Rees, W. S., Jr. *Adv. Mater. Opt. Electron.* **2000**, 10, 213.
- (7) Colombo, D. G.; Gilmer, D. C.; Young, V. G.; Campbell, S. A.; Gladfelter, W. L. *Chemical Vapor Deposition* **1998**, 4, 220-222.
- (8) Afzaal, M.; Croch, D.; Malik, M. A.; Motevalli, M.; O'Brien, P.; Park, J. H.; Woolins, J. D. *Eur. J. Inorg. Chem.* **2004**, 171-177.
- (9) Floriani, C. *Chem. Commun.* **1996**, 1257.
- (10) Cummins, C. C. *Chem. Commun.* **1998**, 1777.
- (11) Barker, J.; Killner, M. *Coord. Chem. Rev.* **1994**, 133, 219.
- (12) Kempe, R. *Angew. Chem., Int. Ed. Engl.* **2000**, 39, 468.
- (13) Lappert, M. F.; Power, P. P.; Sanger, A. R.; Srivastava, R. C. *Metal and Metalloid Amides: Syntheses, Structures, and Physical and Chemical Properties*; Ellis Horwood: Chichester, 1980.
- (14) Eller, P. G.; Bradley, D. C.; Hursthouse, M. B.; Meek, D. W. *Coord. Chem. Rev.* **1977**, 24.
- (15) Schrock, R. R. *Acc. Chem. Res.* **1997**, 30, 9.
- (16) Abrams, S. R.; Nucciarone, D. D.; Steck, W. F. *Can. J. Chem.* **1983**, 61, 1073.
- (17) Steinborn, D.; Thies, B.; Wagner, I.; Taube, R. *Zeitschrift fuer Chemie* **1989**, 29, 333.

- (18) Shimano, M.; Matsuo, A. *Tetrahedron* **1998**, *54*, 4787.
- (19) Gambarotta, S. *J. Organomet. Chem.* **1995**, *500*, 117.
- (20) Anderson, R. A.; Faegri, K., Jr.; Green, J. C.; Haaland, A.; Lappert, M. F.; Leung, W. P.; Rypdal, K. *Inorg. Chem.* **1988**, *27*, 1782.
- (21) Veith, M.; Mueller-Becker, S.; Lengert, A.; Engel, N. *Organosilicon Chem.* **1994**, 217.
- (22) Westerhausen, M. *Coord. Chem. Rev.* **1998**, *176*, 157.
- (23) Dilworth, J. R.; Hanich, J.; Krestel, M.; Beck, J.; Strahle, J. *J. Organomet. Chem.* **1986**, *315*, C9.
- (24) Schmid, K.; Hausen, H. D.; Klinkhammer, K. W.; Weidlein, J. Z. *Anorg. Allg. Chem.* **1999**, *625*, 945.
- (25) Reiss, P.; Fenske, D. *Z. Anorg. Allg. Chem.* **2000**, *626*, 1317.
- (26) Cheng, Q. M.; Stark, O.; Merz, K.; Winter, M.; Fischer, R. A. *J. Chem. Soc., Dalton Trans.* **2002**, 2933.
- (27) Neumann, C.; Seifert, T.; Storch, W.; Vosteen, M.; Wrackmeyer, B. *Angew. Chem., Int. Ed. Engl.* **2001**, *40*, 3405.
- (28) Decker, A.; Fenske, D.; Maczek, K. *Angew. Chem., Int. Ed. Engl.* **1996**, *35*, 2863.
- (29) Seifert, T.; Storch, W.; Vosteen, M. *Eur. J. Inorg. Chem.* **1998**, 1343.
- (30) Bal, Y.; Roesky, H. W.; Schmidt, H. G.; Noltmeyer, M. *Z. Naturforsch., B: Chem. Sci.* **1992**, *47*, 603.
- (31) Hillwig, R.; Harms, K.; Dehnicke, K. *J. Organomet. Chem.* **1995**, *501*, 327.
- (32) Liu, F. Q.; Herzog, A.; Roesky, H. W.; Uson, I. *Inorg. Chem.* **1996**, *35*, 741.
- (33) Nutt, W. R.; Murray, K. J.; Gullick, J. M.; Odom, J. D.; Ding, Y.; Lebioda, L. *Organometallics* **1996**, *15*, 1728.
- (34) Hitchcock, P. B.; Lappert, M. F.; Pierssens, L. J. M. *Chem. Comm.* **1996**, 1189-1190.
- (35) Bunge, S. D.; Just, O.; Rees, W. S., Jr. In *The Molecular Design of Metal Amides*; Georgia Institute of Technology: Atlanta, 2001.

- (36) Veith, M.; Opsolder, M.; Zimmer, M.; Huch, V. *Eur. J. Inorg. Chem.* **2000**, 6, 1143-1146.
- (37) Grigsby, W. J.; Hascall, T.; Ellison, J.; Olmstead, M. M.; Power, P. P. *Inorg. Chem.* **1996**, 35, 3254-3261.
- (38) Allan, R. E.; Beswick, M. A.; Davies, M. K.; Raithby, P. R.; Steiner, A.; Wright, D. S. *J. Organomet. Chem.* **1998**, 550, 71-76.
- (39) Chen, H.; Bartlett, R. A.; Dias, H. V. R.; Olmstead, M. M.; Power, P. P. *Inorg. Chem.* **1991**, 30, 3390-3394.
- (40) Selent, D.; Pickardt, J.; Claus, P. *J. Organomet. Chem.* **1994**, 468, 131.

CHAPTER 2

SYNTHESIS AND CHARACTERIZATION OF GROUP I AND II STANNYLAMIDES

SECTION A: SYNTHESIS AND CHARACTERIZATION OF HOMOLEPTIC AND HETEROLEPTIC LITHIUM AMIDES POSSESSING THE TRIMETHYLSTANNYL

MOIETY: $[(\text{Me}_3\text{Sn})(\text{Me}_3\text{E})\text{NLi}\bullet(\text{Et}_2\text{O})]_2$ (E = Si, Ge, Sn)

Introduction

Lithium dialkylamides and related N-lithiated species are an important class of organolithium reagents due to their extensive use in synthetic organic chemistry.¹ In addition, lithium amide species of this type provide convenient access to a wide range of metal amide compounds. Lithium amide species adopt numerous geometries in the solid state, including monomeric,² dimeric,³ trimeric,⁴ tetrameric,⁵ and hexameric arrangements.⁶ The structural characteristics of lithium amides and their use in the synthesis of amidometal compounds have been previously reviewed.^{7,8}

Lithium bis(trimethylsilyl)amide and its derivatives have been used as amido transfer reagents in the preparation of a variety of metal amide complexes.⁹ It was structurally characterized by Mootz and coworkers as a trimer,⁴ and then later by Lappert, *et al.* as an ether-solvated dimer.³ Although extensive research has been performed to understand the structural properties of lithiated silyl amines and their use as synthetic reagents in the preparation of metal amide compounds, little work has been put forth in the extension of this chemistry to the heavier *N*-lithiostannylamine congeners.

Fenske and coworkers first reported the synthesis of lithium bis(trimethylstannyl)amide and its subsequent utilization as a precursor of copper amide species.¹⁰ However, little has been done since to structurally characterize this class of lithium amide complexes or explore their use in the synthesis of amidometal compounds. The lithiated stannylamines, $[(\text{Me}_3\text{Sn})_2\text{NLi}(t\text{BuOMe})]_2$ and $[(\text{Me}_3\text{Sn})_2\text{NLi}(\text{pmdta})]$, ($\text{pmdta} = N,N',N''$ -pentamethyldiethylenetriamine), reported by Wrackmeyer, *et al.* constitute the only examples of structurally characterized lithium stannylamides,¹¹ and these types of lithium amide precursors have not been utilized in the preparation of other amidometal species. Hence, it was desired to synthesize and characterize both homoleptic and heteroleptic lithiated stannylamines and further explore their use in the preparation of other metal amides.

The primary objective of this sub-chapter is to synthesize and isolate lithiated stannylamines as crystalline products. The need to accomplish this goal is two-fold: 1) precursors of this nature will ensure reagent purity and therefore minimize stoichiometric errors in subsequent reactions and 2) ease of manipulation and characterization. Thus, the synthesis and full characterization of the series of lithiated stannylamines, $[(\text{Me}_3\text{Sn})_2\text{NLi}\bullet(\text{THF})]_2$ (**1**), $[(\text{Me}_3\text{Sn})(\text{Me}_3\text{Si})\text{NLi}\bullet(\text{Et}_2\text{O})]_2$ (**2**), and $[(\text{Me}_3\text{Sn})(\text{Me}_3\text{Ge})\text{NLi}\bullet(\text{Et}_2\text{O})]_2$ (**3**) are reported herein.

Experimental

All manipulations were carried out in a dry atmosphere glovebox or by standard Schlenk techniques. All solvents were dried over Na° metal and were freshly distilled under an inert atmosphere prior to use. Me_3GeCl was purchased from Gelest, and MeLi and

Me₃SiCl were purchased from Aldrich and used without further purification. (Me₃Sn)₃N was prepared according to literature procedures.¹² All NMR experiments were performed on a Bruker 400 MHz Spectrometer at 300K using C₆D₆ solvent that was distilled over CaH₂ and stored under argon. ¹H, ¹³C, and ²⁹Si spectra were referenced to TMS. ¹¹⁹Sn and ⁷Li spectra were externally referenced to Me₄Sn and LiBr respectively. Elemental analyses were performed in triplicate on a Perkin Elmer Series II CHNS/O Analyzer 2400.

Synthesis of [(Me₃Sn)₂NLi•(THF)]₂ (1): A 12.4 mL sample of MeLi (1.6 M solution in hexane) was added dropwise at –30°C to a stirred solution of (Me₃Sn)₃N (10.0g, 19.8 mmol) in diethyl ether (40 mL). The reaction mixture was allowed to attain ambient temperature on its own and it was stirred overnight under an argon atmosphere. The resulting pale yellow solution was then reduced in volume, *in vacuo*, to about 30 mL, and from this colorless crystals were grown at –40°C over a two-day period. Yield: 4.62 g (56%); ¹H NMR (400 MHz, C₆D₆, 25°C, TMS): δ 0.31 (s, 36H, CH₃), 1.31 (m, 8H, CH₂), 3.62 (m, 8H, CH₂); ¹³C NMR (100.6 MHz, C₆D₆, 25°C, TMS): δ 1.71 (s, CH₃), 25.22 (s, CH₂), 68.61 (s, CH₂); ¹¹⁹Sn NMR (149.3 MHz, C₆D₆, 25°C, Me₄Sn): δ 63.3 (s, Sn(CH₃)₃); ⁷Li NMR (155.5 MHz, C₆D₆, 25°C, LiBr): δ 1.69 (s); elemental analysis calculated (%) for C₂₀H₅₂N₂O₂Li₂Sn₄: C 28.55, H 6.23; found: C 27.86, H 6.24.

Crystal data for **1**. C₂₀H₅₂N₂O₂Li₂Sn₄: *M*_r = 841.28 g cm^{–3}, crystal dimensions 0.46 x 0.27 x 0.24 mm, tetragonal, space group *P*-4*n*2, *a* = 9.936(3), *c* = 17.727(5) Å, β = 90°; *V* = 1750.0(8) Å³, *Z* = 2, ρ_{calcd} = 1.597 g cm^{–3}, Siemens SMART CCD diffractometer, 2.35 ≤ θ ≤ 28.74°, MoK_α radiation (λ = 0.71073 Å), ω scans, *T* = 193(2) K; of 4898 measured

reflections, 2,113 were independent and 1376 observed with $I > 2\sigma(I)$, $-3 \leq h \leq 13$, $-9 \leq k \leq 10$, $-23 \leq l \leq 23$; $R_1 = 0.0487$, $wR_2 = 0.1290$, GOF = 0.981 for 77 parameters, $\Delta\rho_{\max} = 1.636 \text{ e}\text{\AA}^{-3}$. The structure was solved by direct methods (SHELXS-97) and refined by full-matrix least-squares procedures (SHELXL-97), Lorentz polarization corrections and absorption correction (SADABS) were applied, $\mu = 2.836 \text{ mm}^{-1}$, min./max. transmission 0.5518/0.3560.

Synthesis of $[(\text{Me}_3\text{Sn})(\text{Me}_3\text{Si})\text{NLi}\bullet(\text{Et}_2\text{O})]_2$ (2): Me_3SiCl (1.12 g, 10.30 mmol) was added dropwise at 0°C to a stirred solution of $[(\text{Me}_3\text{Sn})_2\text{NLi}\bullet(\text{THF})]_2$ (4.32 g, 5.15 mmol) in diethyl ether (40 mL). After the reaction mixture reached ambient temperature, a colorless precipitate formed within 10 minutes. The solution was stirred overnight under an argon atmosphere and then it was filtered through a Schlenk frit. The resulting clear, colorless solution was cooled to -30°C and, under vigorous stirring, MeLi (6.4 mL of 1.6 M solution in hexane) was added. The reaction mixture was allowed to reach room temperature on its own and it was subsequently stirred overnight under an argon atmosphere. The volume of solution was reduced, *in vacuo*, to about 30 mL and from this colorless crystals were grown at -40°C over a two-day period. Yield: 2.45 g (72%); ^1H NMR (400 MHz, C_6D_6 , 25°C , TMS): δ 0.22 (s, 18H, SiMe_3), 0.40 (s, 18H, SnMe_3), 1.29 (m, 8H, CH_2), 3.61 (m, 8H, CH_2); ^{13}C NMR (100.6 MHz, C_6D_6 , 25°C , TMS): δ -2.72 (s, SiMe_3), 7.16 (s, SnMe_3), 25.28 (s, CH_2), 68.47 (s, CH_2); ^{29}Si NMR (79 MHz, C_6D_6 , 25°C , Me_4Si): δ -8.41 (s, SiMe_3); ^{119}Sn NMR (149.3 MHz, C_6D_6 , 25°C , Me_4Sn): δ 34.4 (s, SnMe_3); ^7Li NMR (155.5 MHz, C_6D_6 , 25°C , LiBr): δ 1.47 (s); elemental analysis calculated (%) for $\text{C}_{20}\text{H}_{52}\text{N}_2\text{O}_2\text{Li}_2\text{Si}_2\text{Sn}_2$: C 36.39, H 7.94; found: C 38.44, H 8.30.

Crystal data for **2**. $C_{20}H_{56}N_2O_2Li_2Si_2Sn_2$: $M_r = 664.11 \text{ g cm}^{-3}$, crystal dimensions 0.37 x 0.27 x 0.17 mm, tetragonal, space group $P-4n2$, $a = 9.788(3)$, $c = 17.406(9) \text{ \AA}$, $\beta = 90^\circ$; $V = 1667.7(11) \text{ \AA}^3$, $Z = 2$, $\rho_{\text{calcd}} = 1.323 \text{ g cm}^{-3}$, Siemens SMART CCD diffractometer, $2.34 \leq \theta \leq 28.71^\circ$, $Mo_{K\alpha}$ radiation ($\lambda = 0.71073 \text{ \AA}$), ω scans, $T = 193(2) \text{ K}$; of 9,799 measured reflections, 2,074 were independent and 1,739 observed with $I > 2\sigma(I)$, $-13 \leq h \leq 13$, $-12 \leq k \leq 10$, $-23 \leq l \leq 15$; $R_1 = 0.0434$, $wR_2 = 0.0953$, GOF = 1.061 for 79 parameters, $\Delta\rho_{\text{max}} = 0.552 \text{ e\AA}^{-3}$. The structure was solved by direct methods (SHELXS-97) and refined by full-matrix least-squares procedures (SHELXL-97), Lorentz polarization corrections and absorption correction (SADABS) were applied, $\mu = 1.585 \text{ mm}^{-1}$, min./max. transmission 0.7744/0.5887.

*Synthesis of $[(Me_3Sn)(Me_3Ge)NLi\bullet(Et_2O)]_2$ (**3**):* Compound **3** was prepared using $[(Me_3Sn)_2NLi\bullet(THF)]_2$ (4.55 g, 5.40 mmol), Me_3GeCl (1.65 g, 10.80 mmol), and $MeLi$ (6.75 mL of a 1.6 M solution in hexane) in an analogous manner to compound **2**.

Colorless crystals were grown from diethyl ether at -40°C over a two-day period. Yield: 2.22 g (55%); ^1H NMR (400 MHz, C_6D_6 , 25°C , TMS): δ 0.23 (s, 18H; CH_3Sn), 0.42 (s, 18H; CH_3Ge), 1.03 (t, 12H; CH_3), 3.39 (q, 8H; CH_2); ^{13}C NMR (100.6 MHz, C_6D_6 , 25°C , TMS): δ -1.52 (s, CH_3Sn), 6.96 (s, CH_3Ge), 14.85 (s, CH_3), 64.64 (s, CH_2); ^{119}Sn NMR (149.3 MHz, C_6D_6 , 25°C , Me_4Sn): δ 46.73 (s, Me_3Sn); ^7Li NMR (155.5 MHz, C_6D_6 , 25°C , $LiBr$): δ 1.66 (s); elemental analysis calculated (%) for $C_{20}H_{56}N_2O_2Li_2Ge_2Sn_2$: C 31.89, H 7.49, N 3.72; found: C 32.16, H 7.11, N 4.73.

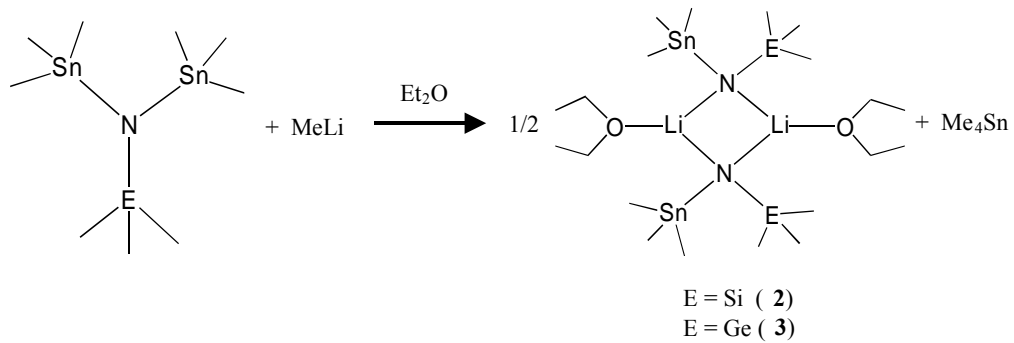
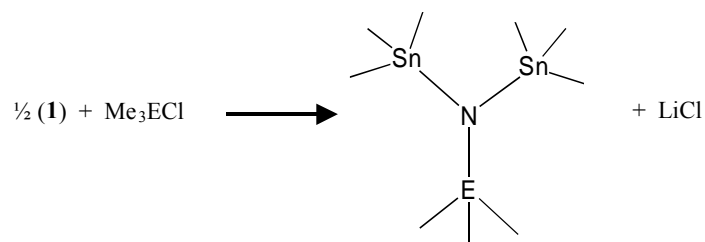
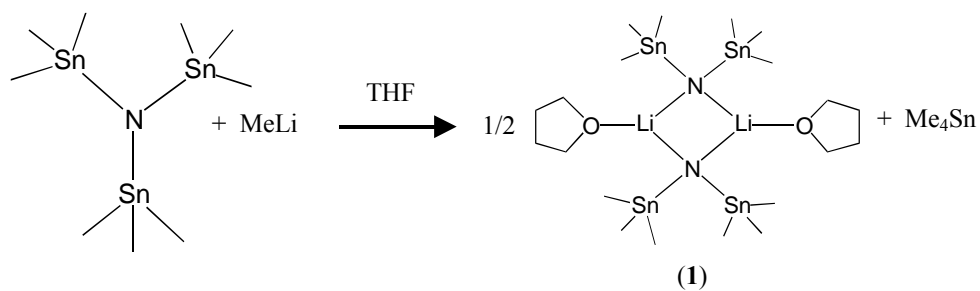
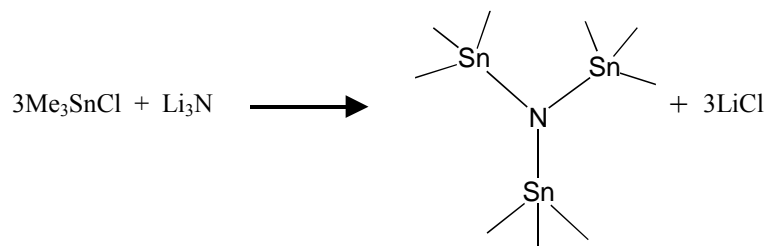
Crystal data for **3**: $C_{20}H_{56}N_2O_2Li_2Ge_2Sn_2$, $M_r = 753.11 \text{ g cm}^{-3}$, crystal dimensions 0.32 x 0.27 x 0.19 mm, tetragonal, space group $P-4n2$, $a = 9.7798(6)$, $c = 17.664(2) \text{ \AA}$, $\beta = 90^\circ$;

$V = 1689.4(3) \text{ \AA}^3$, $Z = 2$, $\rho_{\text{calcd}} = 1.480 \text{ g cm}^{-3}$, Siemens SMART CCD diffractometer, $2.31 \leq \theta \leq 28.73^\circ$, $\text{MoK}\alpha$ radiation ($\lambda = 0.71073 \text{ \AA}$), ω scans, $T = 193(2) \text{ K}$; of 9,503 measured reflections, 2,087 were independent and 1,828 observed with $I > 2\sigma(I)$, $-12 \leq h \leq 12$, $-13 \leq k \leq 11$, $-23 \leq l \leq 11$; $R_1 = 0.0385$, $wR_2 = 0.0977$, $\text{GOF} = 1.075$ for 80 parameters, $\Delta\rho_{\text{max}} = 0.616 \text{ e\AA}^{-3}$. The structure was solved by direct methods (SHELXS-97) and refined by full-matrix least-squares procedures (SHELXL-97), Lorentz polarization corrections and absorption correction (SADABS) were applied, $\mu = 3.238 \text{ mm}^{-1}$, min./max. transmission 0.5827/0.4211.

Results and Discussion

Synthesis

The synthesis of compounds **1-3** is depicted in Scheme 2.1. Compound **1** was synthesized by a modification of the method originally reported by Fenske.¹⁰ In the first step, three equivalents of trimethyltin chloride were reacted with lithium nitride to generate tris(trimethylstannyl)amine, which was then isolated by a vacuum distillation and reacted subsequently with an equivalent amount of methyl lithium. Upon completion of the reaction, compound **1** was recrystallized from THF at -40°C , yielding colorless crystals. Crystals of **1**, found to be dimeric in the solid state, were dissolved in diethyl ether and reacted with two equivalents of Me_3ECI ($\text{E} = \text{Si}, \text{Ge}$). After stirring overnight and filtering off the LiCl precipitate, two equivalents of MeLi were added *in situ*. The reaction was stirred overnight to produce compounds **2** and **3**, which were recrystallized from diethyl ether at -40°C and isolated as colorless crystals in moderate yields.



Scheme 2.1. Synthesis of compounds 1-3.

Characterization

Crystals of compounds **1-3** were each analyzed by a single crystal X-ray diffraction experiment. The results are shown in Figures 2.1-2.3.

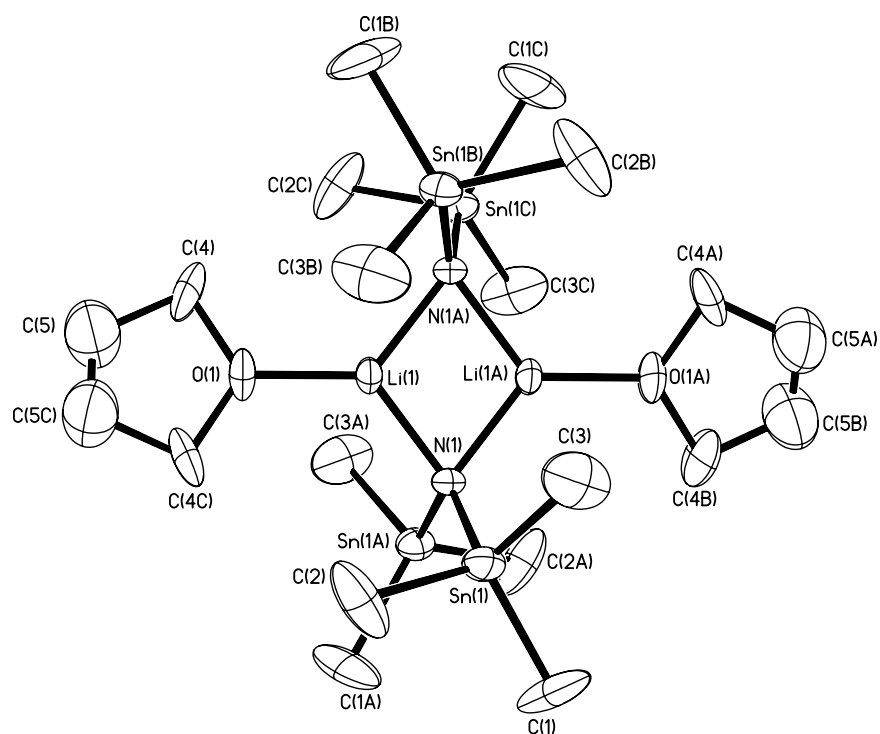


Figure 2.1. ORTEP plot representation (30% probability) with numbering scheme for compound **1**. Hydrogen atoms have been omitted for clarity.

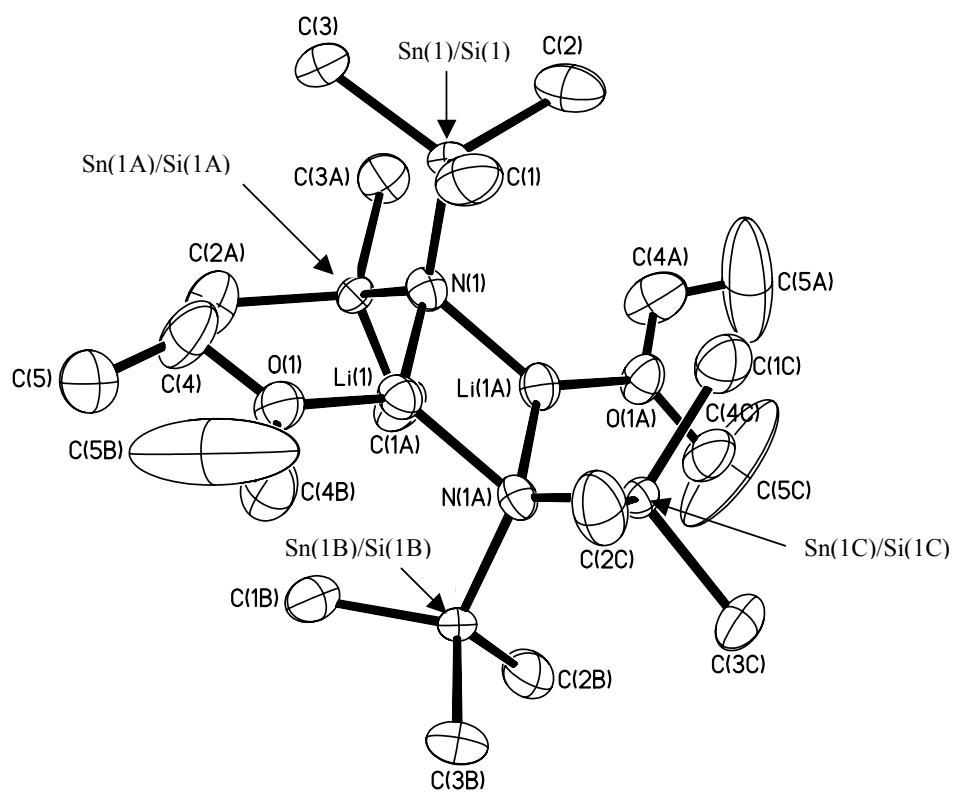


Figure 2.2. ORTEP plot representation (30% probability) with numbering scheme for compound **2**. Hydrogen atoms have been omitted for clarity.

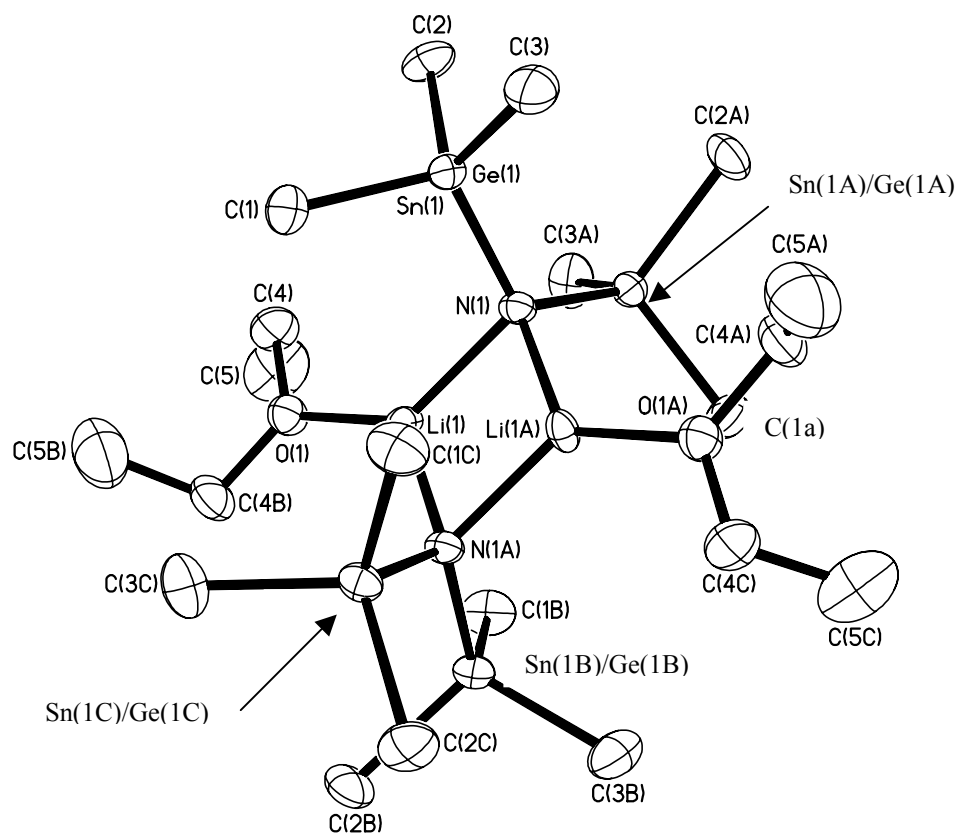


Figure 2.3. ORTEP plot representation (30% probability) with numbering scheme for compound **3**. Hydrogen atoms have been omitted for clarity.

All three complexes exist as lithium dimers in the solid state, with the bis(trimethylstannyl)amide acting as a bridging ligand, and THF or diethyl ether molecules terminally binding to the lithium metal centers. A summary of the principal interatomic distances and angles for compounds **1-3** is provided in Table 2.1, and a complete list of all distances and angles can be found in Tables A.2, A.6, and A.10, respectively.

Table 2.1. Selected average interatomic distances (Å) and angles (degrees) for compounds **1-3**.

(1)	distance/angle	(2)	distance/angle	(3)	distance/angle
Sn-N	2.022(4)	Sn/Si-N	1.919(3)	Sn/Ge-N	1.915(3)
Li-N	1.935(14)	Li-N	1.987(9)	Li-N	1.980(8)
Li-O	1.90(2)	Li-O	1.921(14)	Li-O	1.937(12)
Li-N-Li	74.1(10)	Li-N-Li	75.0(6)	Li-N-Li	75.3(5)
N-Li-N	105.9(10)	N-Li-N	105.0(6)	N-Li-N	104.7(5)

Compounds **1-3** possess a Li_2N_2 rhombic core with the Li-N-Li and N-Li-N angles approximating 75° and 105° , respectively. The Li-N and Li-O interatomic distances are in agreement with previously reported lithium amide dimers with terminally coordinated etherate molecules $\{[(\text{Me}_3\text{Sn})_2\text{NLi}\cdot\text{O}(\text{Me})(^t\text{Bu})]_2$, Li-N = 2.0115 Å and Li-O = 1.987 Å; $[(\text{Me}_3\text{Si})_2\text{NLi}\cdot\text{OEt}_2]_2$, Li-N = 2.06 Å and Li-O = 1.96 Å $\}^{3,11}$. As seen in Table 2.1, a trend of decreasing Li-N interatomic distance can be observed with the second amide substituent being a heavier Group 14 analogue. It suggests increased electron density

localized on the nitrogen atom with two heavier Group 14 elements attached. The tin-nitrogen interatomic distances also fall in the range observed for similar compounds $\{[(\text{Me}_3\text{Sn})_2\text{NLi}(\text{}^t\text{BuMeO})]_2, \text{Sn-N}_{\text{avg}} = 2.093 \text{ \AA}\}^{11}$. For compounds **2** and **3**, the Sn, Si, and Ge atoms were crystallographically indistinguishable. The observed interatomic distances were 1.919 Å for all Sn-N and Si-N interactions, and 1.915 Å for all Sn-N and Ge-N interactions. These values lie between the corresponding interatomic distances registered in the structurally analogous compounds: $[(\text{Me}_3\text{Sn})_2\text{NLi}(\text{}^t\text{BuMeO})]_2$, $\text{Sn-N}_{\text{avg}} = 2.093 \text{ \AA}$ and $[(\text{Me}_3\text{Si})_2\text{NLi}(\text{Et}_2\text{O})]_2$, $\text{Si-N}_{\text{avg}} = 1.705 \text{ \AA}$; $[(\text{Me}_3\text{Sn})_2\text{NLi}(\text{}^t\text{BuMeO})]_2$, $\text{Sn-N}_{\text{avg}} = 2.093 \text{ \AA}$ ¹¹ and $[\text{LiN}(\text{GeMe}_3)_2]_3$, $\text{Ge-N}_{\text{avg}} = 1.837 \text{ \AA}$.¹³ The presence of germanium and silicon in the heteroleptic compounds **2** and **3** was confirmed by the ^{119}Sn NMR chemical shifts for the two compounds (Figure 2.4) and the elemental analyses.

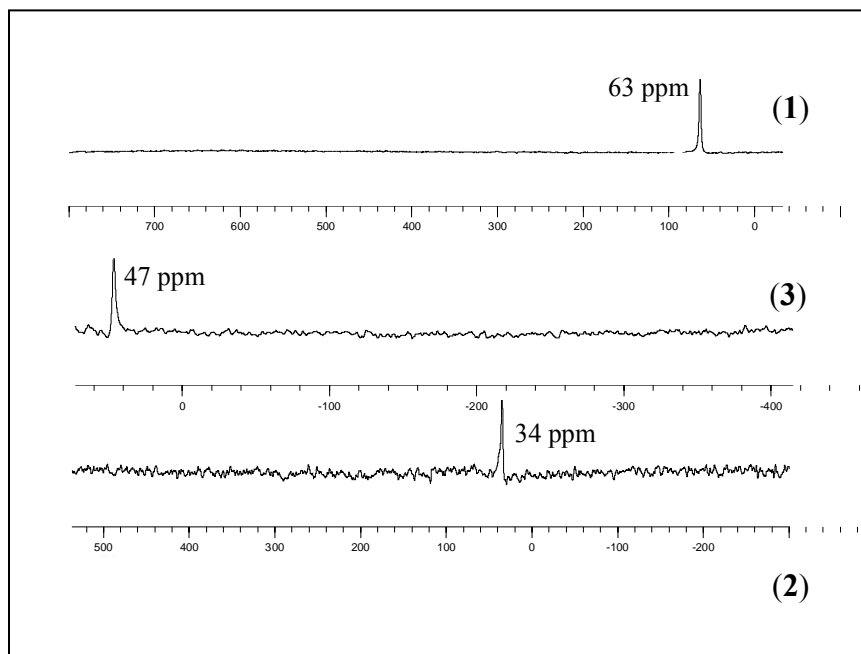


Figure 2.4. ^{119}Sn NMR spectra of compounds **1-3** (chemical shift scale in ppm).

Conclusion

In summary, compound **1** was prepared using a modified version of Fenske's synthesis and used as a precursor to obtain the heteroleptic lithiated stannylamines, **2** and **3**. All three complexes were isolated as analytically pure, colorless crystals. Compounds **1-3** were structurally characterized by a single crystal X-ray diffraction study, and the molecular structures were verified by multinuclear NMR and elemental analyses. These species add to the limited library of lithiated stannylamines and will be subsequently used as synthons to other metal amide compounds.

SECTION B: SYNTHESIS AND CHARACTERIZATION OF BERYLLIUM AMIDES
PREPARED VIA LITHIATED STANNYLAMINES: $[(\text{Me}_3\text{Sn})_2\text{NBe}(\text{Cl})\bullet(\text{THF})]_2$ AND



Introduction

Due to the high toxicity of its compounds, the chemistry of beryllium remains relatively unexplored compared to that of its neighboring elements. A majority of the structurally characterized beryllium amido complexes carry either dialkyl or silyl amide ligands. A comprehensive review of beryllium amide chemistry has been compiled by Lappert and coworkers.⁹

A literature search revealed that beryllium amide compounds possessing stannyl amide ligands have not, to date, been reported. Previous studies show that amido beryllium species can be prepared via the reaction of lithiated amines and BeCl_2 .¹⁴ Thus, the lithiated stannyl amines previously described in Chapter 2 – Part A have the potential to provide an avenue to a new class of beryllium amides. This sub-chapter explores the reaction of compounds **1-3** with BeCl_2 , leading to the synthesis and characterization of the dimeric beryllium amides, $[(\text{Me}_3\text{Sn})_2\text{NBe}(\text{Cl})\bullet(\text{THF})]_2$ (**4**) and $[(\text{Me}_3\text{Si})(\text{H})\text{NBe}(\text{Cl})\bullet(\text{THF})]_2$ (**5**). Additionally, compound **4** was employed as a synthon in the preparation of $[(\text{Me}_3\text{Sn})_2\text{NBe}(\text{OSO}_2\text{CF}_3)]_2$ (**6**).

Experimental

All manipulations were carried out in a dry atmosphere glovebox or by standard Schlenk techniques. All solvents were dried over Na° metal and were freshly distilled under an

inert atmosphere prior to use. BeCl_2 was purchased from Alfa Aesar and compounds (1) and (2) were prepared as described in Chapter 2 – Part A. All solution state NMR experiments were performed on a Bruker 400 MHz Spectrometer at 300 K using C_6D_6 solvent that was distilled over CaH_2 and stored under argon. ^1H and ^{13}C spectra were referenced to TMS. ^{119}Sn and ^9Be spectra were externally referenced to Me_4Sn and BeSO_4 , respectively. All solid state NMR experiments were performed on a Bruker DSX 400 MHz spectrometer and all samples were analysed using a 4 mm MAS rotor. ^9Be spectra were externally referenced to an aqueous solution of BeSO_4 . Elemental analyses were performed in triplicate on a Perkin Elmer Series II CHNS/O Analyzer 2400, FT-IR measurements were performed on a Bruker Equinox 55 Spectrometer, and mass spectrometry analyses were done on a VG Instruments 70SE (Electron Impact ionization; 70eV).

Synthesis of $[(\text{Me}_3\text{Sn})_2\text{NBe}(\text{Cl})\bullet(\text{THF})]_2$ (4): A solution of $[(\text{Me}_3\text{Sn})_2\text{NLi}\bullet(\text{THF})]_2$ (1.00 g, 1.19 mmol) in diethyl ether (40 mL) was added dropwise to a diethyl ether slurry of BeCl_2 (0.19 g, 2.38 mmol) at 0°C . The reaction mixture was allowed to attain ambient temperature on its own, whereby a colorless precipitate formed within 10 minutes. After stirring overnight under an argon atmosphere the reaction mixture was filtered and its volume was reduced, *in vacuo*, to about 30 mL. Colorless crystals were grown from this solution at -40°C over a two-day period. Yield: 0.42 g (38%); ^1H NMR (400 MHz, C_6D_6 , 25°C , TMS): δ 0.40 (s, 36H, SnMe_3), 1.39 (m, 8H, CH_2), 3.58 (m, 8H, CH_2); ^{13}C NMR (100.6 MHz, C_6D_6 , 25°C , TMS): δ -1.89 (s, SnMe_3), 25.66 (s, CH_2), 68.55 (s, CH_2); ^{119}Sn NMR (149.3 MHz, C_6D_6 , 25°C , Me_4Sn): δ 75.1 (s, SnMe_3); ^9Be NMR (56

MHz, CDCl₃, 25°C, BeSO₄): δ 13.71 (s); ⁹Be Solid State NMR (56 MHz, 25°C, BeSO₄): δ 0.3 (s); MS (EI, 245°C): m/z 757 [(M-15)⁺]; elemental analysis calculated (%) for C₂₀H₅₂N₂O₂Cl₂Be₂Sn₄: C 26.21, H 5.72; found: C 26.75, H 5.12.

Crystal data for **4**. C₂₀H₅₂N₂O₂Cl₂Be₂Sn₄: M_r = 458.16 g cm⁻³, crystal dimensions 0.27 x 0.20 x 0.12 mm, monoclinic, space group *P2(1)/n*, a = 11.299(2), b = 13.064(3), c = 11.512(2) Å, α = 90, β = 107.620(3)°; V = 1619.7(5) Å³, Z = 4, ρ_{calcd} = 1.879 g cm⁻³, Siemens SMART CCD diffractometer, $2.21 \leq \theta \leq 28.88^\circ$, MoK α radiation (λ = 0.71073 Å), ω scans, T = 193(2) K; of 10,272 measured reflections, 3909 were independent and 3,283 observed with $I > 2\sigma(I)$, $-14 \leq h \leq 13$, $-17 \leq k \leq 9$, $-14 \leq l \leq 15$; R_1 = 0.0585, wR_2 = 0.1516, GOF = 1.126 for 161 parameters, $\Delta\rho_{\text{max}}$ = 2.085 eÅ⁻³. The structure was solved by direct methods (SHELXS-97) and refined by full-matrix least-squares procedures (SHELXL-97), Lorentz polarization corrections and absorption correction (SADABS) were applied, μ = 3.232 mm⁻¹, min./max. transmission 0.6997/0.4735.

Synthesis of [(Me₃Si)(H)NBe(Cl)•(THF)]₂ (5): Compound **5** was prepared in an analogous fashion to compound **4** using [(Me₃Sn)(Me₃Si)NLi•(Et₂O)]₂ (1.00 g, 1.50 mmol) and BeCl₂ (0.24 g, 3.00 mmol). Colorless crystals were grown at -40°C over a two-day period. Yield: 0.22 g (36%); IR (nujol): 3270 (w), 1261 (m), 1905 (s), 807 (s), 667 (w), 599 (w) cm⁻¹.

Crystal data for **5**. C₁₄H₃₆N₂O₂Cl₂Be₂Si₂: M_r = 409.55 g cm⁻³, crystal dimensions 0.136 x 0.119 x 0.102 mm, tetragonal, space group *P4(3)2(1)2*, a = 11.3551(12), c = 18.865(4) Å, β = 90°; V = 2432.4(6) Å³, Z = 4, ρ_{calcd} = 1.118 g cm⁻³, Siemens SMART CCD diffractometer, $2.09 \leq \theta \leq 25.05^\circ$, MoK α radiation (λ = 0.71073 Å), ω scans, T = 193(2) K;

of 12,348 measured reflections, 2,165 were independent and 1,827 observed with $I > 2\sigma(I)$, $-13 \leq h \leq 13$, $-13 \leq k \leq 13$, $-22 \leq l \leq 16$; $R_1 = 0.0549$, $wR_2 = 0.1332$, $GOF = 1.065$ for 120 parameters, $\Delta\rho_{\max} = 0.621 \text{ e}\text{\AA}^{-3}$. The structure was solved by direct methods (SHELXS-97) and refined by full-matrix least-squares procedures (SHELXL-97), Lorentz polarization corrections and absorption correction (SADABS) were applied, $\mu = 0.374 \text{ mm}^{-1}$, min./max. transmission 0.9629/0.9510.

Synthesis of $[(\text{Me}_3\text{Sn})_2\text{NBe}(\text{OSO}_2\text{CF}_3)]_2$ (6): Compound **6** was prepared by stirring a mixture of 1.0 equivalents of **4** (0.65 g, 0.71 mmol) with 2.0 equivalents of $\text{Ag}(\text{OSO}_2\text{CF}_3)$ (0.36 g, 1.42 mmol) in diethyl ether at -30°C . The reaction mixture was allowed to attain ambient temperature on its own, stirred for 1.5 hours, and then filtered to remove all of the resulting precipitate. Colorless crystals were grown from this solution overnight at -10°C . Yield: 0.22 g (31%); MS (EI, 245°C): m/z 985 $[(\text{M}-15)^+]$; IR (nujol): 3270 (w), 1261 (m), 1905 (s), 807 (s), 667 (w), 599 (w) cm^{-1} .

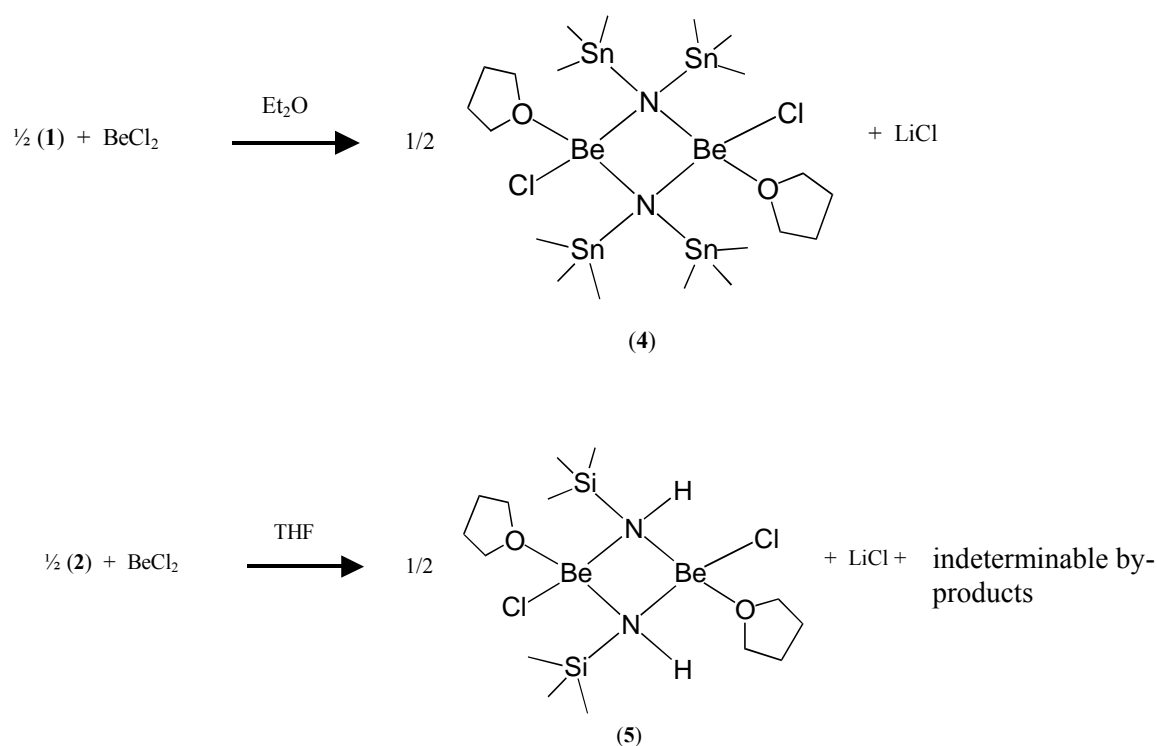
Crystal data for **6**. $\text{C}_{14}\text{H}_{36}\text{N}_2\text{O}_6\text{S}_2\text{F}_6\text{Be}_2\text{Sn}_4$: $M_r = 999.35 \text{ g cm}^{-3}$, crystal dimensions 0.46 x 0.20 x 0.20 mm, monoclinic, space group $P2(1)/c$, $a = 19.203(3)$, $b = 10.5666(17)$, $c = 18.032(3) \text{ \AA}$, $\alpha = 90^\circ$, $\beta = 116.219^\circ$; $V = 3282.4(9) \text{ \AA}^3$, $Z = 4$, $\rho_{\text{calcd}} = 2.022 \text{ g cm}^{-3}$, Siemens SMART CCD diffractometer, $1.18 \leq \theta \leq 28.68^\circ$, $\text{MoK}\alpha$ radiation ($\lambda = 0.71073 \text{ \AA}$), ω scans, $T = 193(2) \text{ K}$; of 20,193 measured reflections, 7,724 were independent and 6,197 observed with $I > 2\sigma(I)$, $-21 \leq h \leq 25$, $-13 \leq k \leq 13$, $-23 \leq l \leq 17$; $R_1 = 0.0366$, $wR_2 = 0.0907$, $GOF = 1.059$ for 349 parameters, $\Delta\rho_{\max} = 3.899 \text{ e}\text{\AA}^{-3}$. The structure was solved by direct methods (SHELXS-97) and refined by full-matrix least-squares procedures

(SHELXL-97), Lorentz polarization corrections and absorption correction (SADABS) were applied, $\mu = 0.3.197 \text{ mm}^{-1}$, min./max. transmission 0.5616/0.3216.

Results and Discussion

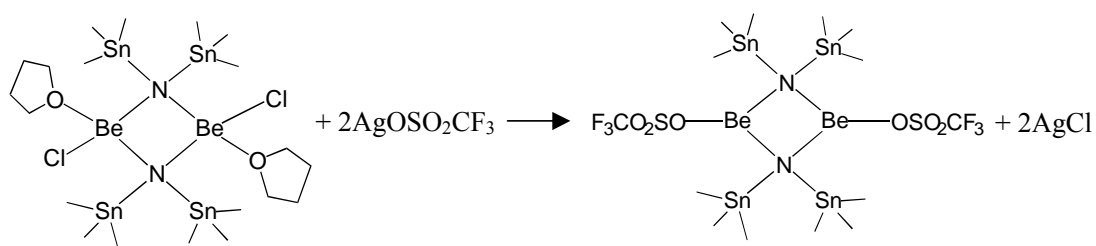
Synthesis

The synthesis of compounds **4** and **5**, shown in Scheme 2.2, was accomplished by reacting 2 equivalents of BeCl_2 with compounds **1** and **2**, respectively. After stirring overnight, the LiCl precipitate was filtered off and the products were recrystallized directly from the reaction solvent. Compound **4** was isolated in accordance with the expected reaction sequence, however, compound **5** was unexpectedly obtained (Scheme 2.2). Whether this complex formed due to the presence of moisture or because of an unanticipated reaction pathway is yet to be determined, as the reaction by-products could not be successfully characterized. The reaction of compound **3** with BeCl_2 led to indeterminable product mixtures.



Scheme 2.2. Synthesis of compounds **4-5**.

The synthesis of compound **6**, depicted in Scheme 2.3, was carried out via the reaction of compound **4** with two equivalents of silver(I)triflate. After stirring for one and a half hours at room temperature, the reaction mixture was filtered to remove the AgCl precipitate. The resulting beryllium dimer was recrystallized from diethyl ether at -10°C .



Scheme 2.3. Synthesis of compound **(6)**.

Characterization

Crystals of compounds **4-6** were analyzed by single crystal X-ray diffraction and the crystal structures of these compounds are given in Figures 2.5-2.7.

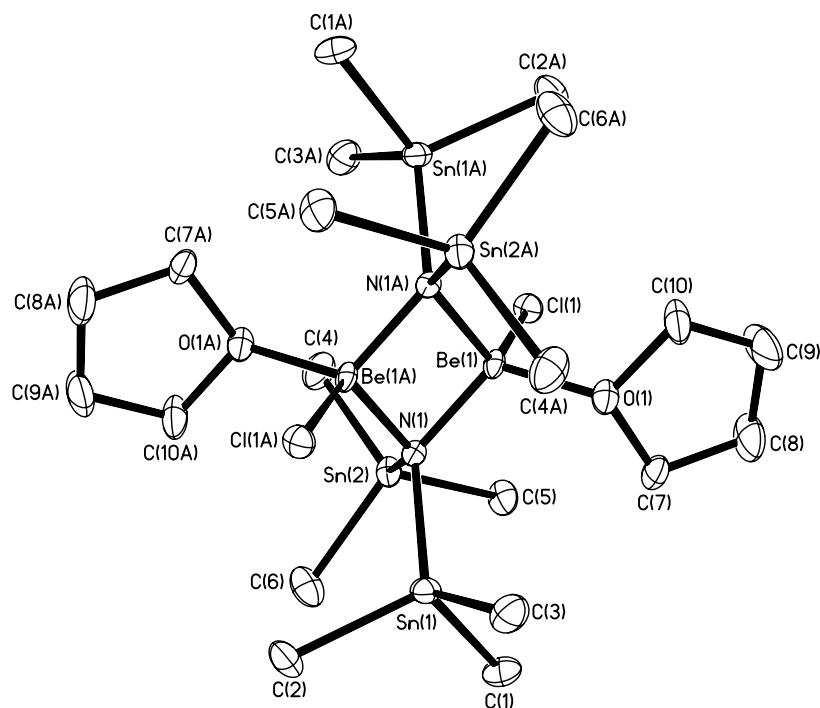


Figure 2.5. ORTEP plot representation (30% probability) with numbering scheme for compound **4**. Hydrogen atoms have been omitted for clarity.

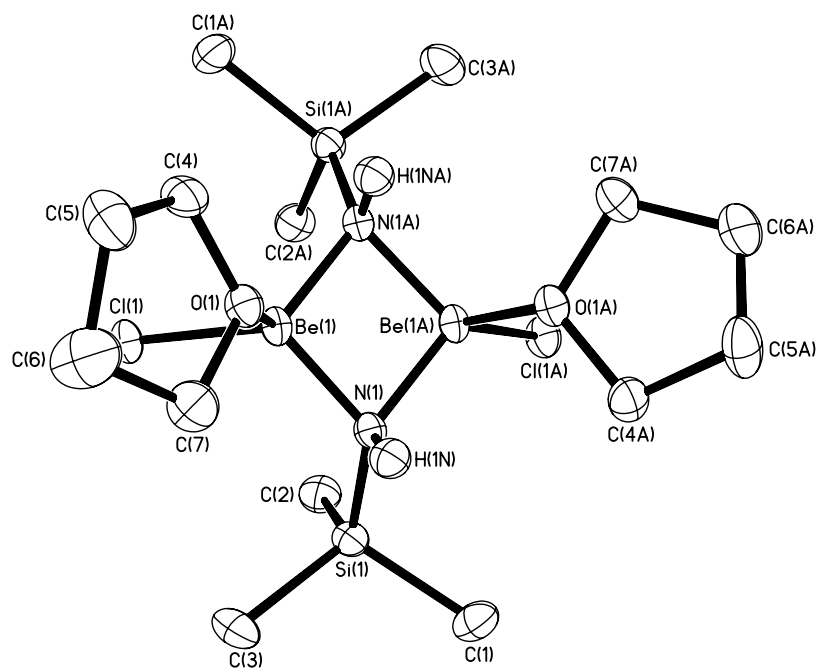


Figure 2.6. ORTEP plot representation (30% probability) with numbering scheme for compound **5**. Hydrogen atoms have been omitted for clarity.

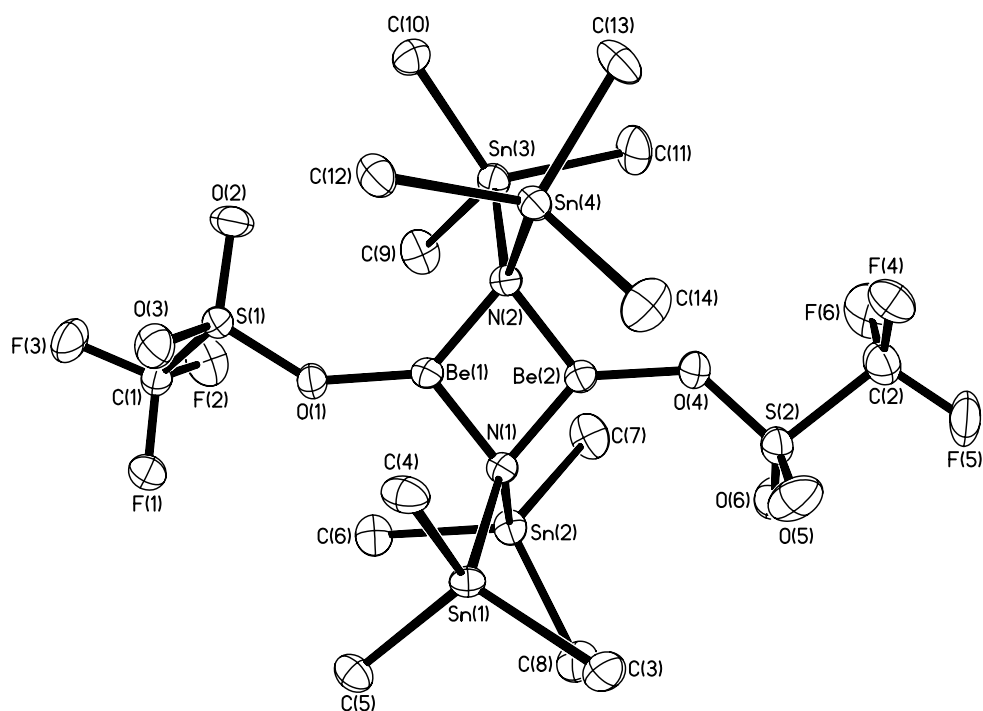


Figure 2.7. ORTEP plot representation (30% probability) with numbering scheme for compound **6**. Hydrogen atoms have been omitted for clarity.

All three complexes exist as beryllium dimers in the solid state, with the stannyl or silyl amide acting as a bridging ligand. Chloride ligands and THF molecules attached to the lithium metal centers complete the coordination sphere for **4** and **5**, whereas a triflate ligand completes the coordination sphere for **6**. A summary of the principal interatomic distances and angles for compounds **4-6** is provided in Table 2.2, and a complete list of all distances and angles can be found in Tables A.14, A.18, and A.22 respectively.

Table 2.2. Selected average interatomic distances (Å) and angles (degrees) for compounds **4-6**.

(4)	distance/angle	(5)	distance/angle	(6)	distance/angle
Sn-N	2.093(6)	Si-N	1.756(3)	Sn-N	2.116(4)
Be-N	1.722(10)	Be-N	1.707(6)	Be-N	1.646(7)
Be-O	1.718(10)	Be-O	1.703(5)	Be-O	1.550(7)
Be-Cl	2.072(9)	Be-Cl	2.026(5)	-	-
-	-	N-H	0.920	-	-
Be-N-Be	79.3(5)	Be-N-Be	80.9(3)	Be-N-Be	102.2(4)
N-Be-N	100.7(5)	N-Be-N	98.7(3)	N-Be-N	77.8(3)

Compounds **4-6** are structurally analogous, with all complexes possessing a central Be₂N₂ rhombus. Compound **6** is comprised of a more distorted rhombus, as shown by the Be-N-Be and N-Be-N angles listed in Table 2.2. This is likely due to the decreased steric hindrance observed in the three-coordinate beryllium centers of **6**. The beryllium-nitrogen interatomic distances in **4** and **5** are in agreement with the previously reported

beryllium dimer possessing four-coordinate beryllium centers $\{[{}^i\text{Pr}_2\text{NBe}(\text{BH}_4)]_2$, Be-N = 1.695 Å and $\}$.¹⁴ The Be-N interatomic distance in **6** is significantly shorter than found for **4** and **5**, due to the decreased coordination on the beryllium(II) metal centers. The Group 14 element-nitrogen interatomic distances were also in the expected range as determined in previous structures containing these bridging amide ligands $\{[(\text{Me}_3\text{Sn})_2\text{NLi}(\text{}^t\text{BuMeO})]_2$, Sn-N_{avg} = 2.093 Å and $[(\text{Me}_3\text{Si})_2\text{NLi}\cdot\text{Et}_2\text{O}]_2$, Si-N_{avg} = 1.705 Å $\}$.^{3,11} For compound **5**, the amino hydrogen was assigned from the electron density map, and its presence was verified by the 3300 cm⁻¹ stretching frequency in the FT-IR spectrum.

Compound **4** was also structurally characterized by multinuclear NMR techniques. The solution state ¹¹⁹Sn NMR spectrum contains a single resonance at 75.1 ppm, which is positioned slightly downfield compared to the single resonance at 63.3 ppm for compound **1**. This can be attributed to the fact that the dicationic beryllium metal centers attract more electron density from the nitrogen atoms, thus deshielding the tin atoms. There are also two additional weak resonances found between 50 and 60 ppm, indicating a dynamic behavior in solution. This is also observed in the ⁹Be solution state NMR, where a strong single resonance occurs at 13.71 ppm, in agreement with previous studies involving four-coordinate beryllium centers, as well as two additional weak resonances observed upfield from this signal. The occurrence of these additional signals upfield suggests a dynamic equilibrium between solvated and non-solvated solution species, or between monomeric and dimeric structures. In the solid-state ⁹Be NMR spectrum a single resonance was observed at approximately 0.3 ppm (Figure 2.8). This

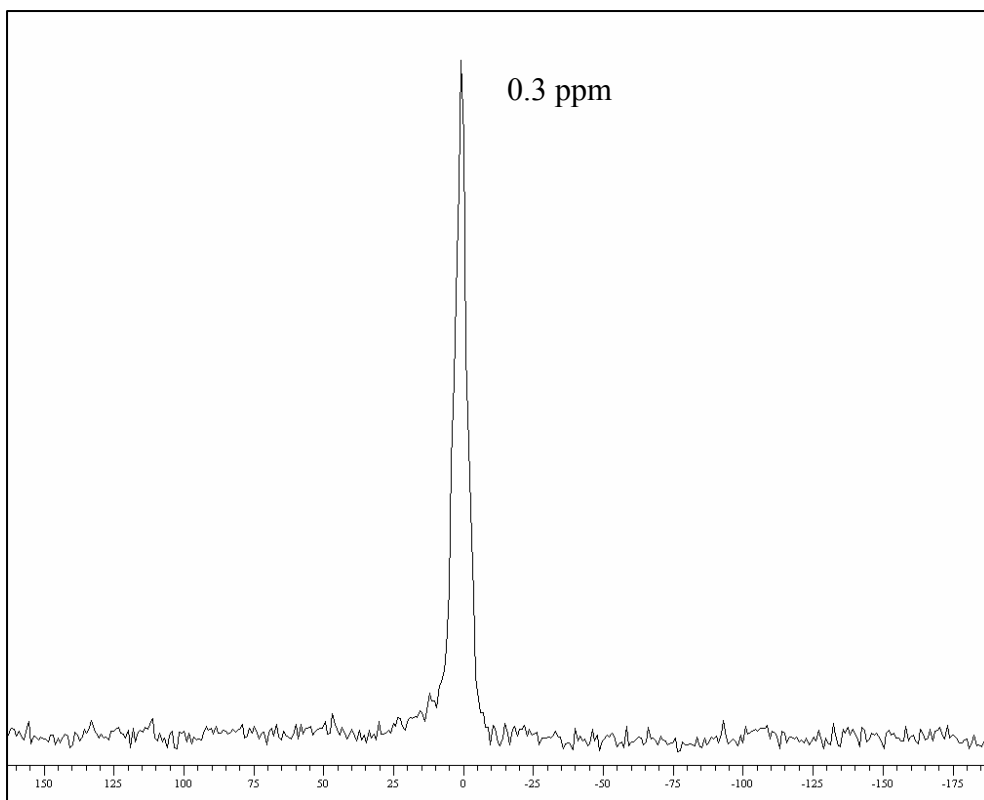


Figure 2.8. Solid state ^9Be NMR spectrum of compound **4** (chemical shift scale in ppm).

result substantiates the possibility of dynamic behavior in solution. Due to the limited yield of compounds **5** and **6**, further characterization via multinuclear NMR techniques was limited. However, the dimeric structure of **6** was confirmed by EI-MS techniques. The solid-state structure obtained for **4** via X-ray diffraction techniques was confirmed by the presence of a ($\text{M}-15^+$) molecular ion in the EI mass spectrum and by satisfactory elemental analyses.

Conclusion

In summary, the reaction of compounds **1** and **2** with BeCl₂ led to the synthesis and characterization of a new class of beryllium amides. Specifically, compound **4** represents the first structurally characterized example of a beryllium amide possessing stannyl substituents. Additionally, compound **4** was used as a synthon in the preparation of the triflate-coordinated beryllium dimer, **6**. This species opens up further potential exploration of this class of compounds via subsequent ligand exchange reactions.

References

- (1) Collum, D. B. *Acc. Chem. Res.* **1993**, 26, 227.
- (2) Chen, H.; Bartlett, R. A.; Dias, H. V. R.; Olmstead, M. M.; Power, P. P. *J. Am. Chem. Soc.* **1989**, 111, 4338.
- (3) Lappert, M. F.; Slade, M. J.; Singh, A.; Atwood, J. L.; Rogers, R. D.; Shakir, R. *J. Am. Chem. Soc.* **1983**, 105, 302.
- (4) Mootz, D.; Zinnius, A.; Bottcher, B. *Angew. Chem.* **1969**, 81, 398.
- (5) Veith, M.; Wieczorek, S.; Fries, K.; Huch, V. *Z. Anorg. Allg. Chem.* **2000**, 626, 1237.
- (6) Brauer, D. J.; Burger, H.; Liewald, G. R.; Wilke, J. *J. Organomet. Chem.* **1985**, 287, 305.
- (7) Pauer, F.; Power, P. P. In *Lithium Chemistry*; Schleyer, P. v. R., Ed.; John Wiley & Sons: New York, 1995, p 295.
- (8) Gregory, K.; Schleyer, P. R.; Snaith, R. *Adv. Inorg. Chem.* **1991**, 37, 47.
- (9) Lappert, M. F.; Power, P. P.; Sanger, A. R.; Srivastava, R. C. *Metal and Metalloid Amides: Syntheses, Structures, and Physical and Chemical Properties*; Ellis Horwood: Chichester, 1980.
- (10) Reiss, P.; Fenske, D. *Z. Anorg. Allg. Chem.* **2000**, 626, 1317.

- (11) Neumann, C.; Seifert, T.; Storch, W.; Vosteen, N.; Wrackmeyer, B. *Angew. Chem., Int. Ed.* **2001**, *40*, 3405-3407.
- (12) Lehn, W. H. *J. Amer. Chem. Soc.* **1964**, *86*, 305.
- (13) Rannenberg, M.; Hausen, H. D.; Weidlein, J. J. *Organomet. Chem* **1989**, *376*, C27-C30.
- (14) Noth, H.; Schlosser, D. *Eur. J. Inorg. Chem.* **2003**, 2245-2254.

CHAPTER 3

SYNTHESIS AND CHARACTERIZATION OF LUMINESCENT TETRAMERIC SILVER(I) AMIDES POSSESSING GROUP 14 SUBSTITUENTS: $[(\text{Me}_3\text{Si})_2\text{NAg}]_4$ and $[(\text{Me}_3\text{Sn})(\text{Me}_3\text{E})\text{NAg}]_4$ (E = Si, Ge, Sn)

Introduction

Silver(I) coordination compounds have garnered the attention of numerous researchers due to their potential use in sensor technology, application in drug treatment regimens, and their rich photophysical properties.¹ In addition, the nature of argentophilic, d^{10} - d^{10} interactions observed in polynuclear silver(I) complexes are of interest from a fundamental standpoint.²

Approximately eight years ago, Lappert and coworkers reported a planar, tetranuclear silver(I) amide possessing trimethylsilyl moieties.³ This compound was accessed through the use of the N-lithio bis(trimethylsilyl)amine precursor and was thought to have opened up an avenue leading to a new class of polynuclear silver complexes. However, until recent work by Rees and Bunge, no analogous silver(I) compounds have been reported.⁴ In addition, given the ability of $[(\text{Me}_3\text{Sn})_2\text{NLi}\cdot\text{THF}]_2$ (**1**) to undergo metathesis reactions with BeCl_2 , it is of interest to determine if similar reaction chemistry can take place with transition metals. Thus, the synthesis and characterization of a series of tetrameric silver(I) amide complexes possessing group 14 substituents, $[(\text{Me}_3\text{Si})_2\text{NAg}]_4$ (**10**) and $[(\text{Me}_3\text{Sn})(\text{Me}_3\text{E})\text{NAg}]_4$ {E = Si (**8**), Ge (**9**), Sn (**7**)} is described herein.

Experimental

All manipulations were carried out in a dry atmosphere glovebox or by standard Schlenk techniques. All solvents were dried over Na metal and were freshly distilled under an inert atmosphere prior to use. AgBr was purchased from Fisher and hexamethyldisilazane was purchased from Aldrich and used without further purification. 10M *n*BuLi was purchased from Aldrich and diluted with hexane. The concentration of the *n*BuLi solution was determined using the procedure reported by Gilman.⁵

$[(\text{Me}_3\text{Sn})_2\text{NLi}\bullet(\text{THF})]_2$, $[(\text{Me}_3\text{Sn})(\text{Me}_3\text{Si})\text{NLi}\bullet(\text{Et}_2\text{O})]_2$, and $[(\text{Me}_3\text{Sn})(\text{Me}_3\text{Ge})\text{NLi}\bullet(\text{Et}_2\text{O})]_2$ were prepared as described in Chapter 2. All NMR experiments were performed on a Bruker 400 MHz Spectrometer at 300K using C_6D_6 solvent that was distilled over CaH_2 and stored under argon. ^1H , ^{13}C , and ^{29}Si spectra were referenced to TMS. ^{119}Sn spectra were externally referenced to Me_4Sn . Elemental analyses were performed in triplicate on a Perkin Elmer Series II CHNS/O Analyzer 2400, FT-IR measurements were completed on a Bruker Equinox 55 Spectrometer, mass spectrometry analyses were recorded on a VG Instruments 70SE (Electron Impact ionization; 70eV), and UV/VIS measurements were carried out on a Perkin Elmer UV/VIS/NIR Lambda 19 Spectrometer. All fluorescence measurements were collected on a SPEX Fluorolog Spectrofluorometer equipped with a xenon arc lamp and single grating excitation monochromator. Excited-state lifetimes were measured with a time-correlated single photon counting fluorometer consisting of Photochemical Research Associates flashlamp and optics (PRA Model 510B high-voltage power supply, PRA Model 510B nanosecond lamp, and PRA Model 1200 sample box) and double

monochromators (Istruments SA, Inc., Model H10, on excitation, and Bausch and Lomb, No. 33-86-79, on emission).

Synthesis of [(Me₃Sn)₂NAg]₄ (7): A solution of [(Me₃Sn)₂NLi•(THF)]₂ (0.50 g, 0.59 mmol) in diethyl ether (40 mL) was added dropwise to a diethyl ether slurry of AgBr (0.22 g, 1.19 mmol) at −78°C. The reaction mixture was stirred overnight under an argon atmosphere under light exclusion. The solution was then allowed to attain ambient temperature on its own and it was stirred for an additional 2 hours. The resulting pale yellow solution contained a significant amount of colorless precipitate. The solvent was removed *in vacuo*, the solid residue extracted with 20 mL of hexane, and the resulting slurry filtered to give a clear, golden solution. Colorless crystals were grown from this solution overnight at −40°C. Yield: 0.44 g (83%); ¹H NMR (400 MHz, C₆D₆, 25°C, TMS): δ 0.45 (s, SnMe₃); ¹³C NMR (100.6 MHz, C₆D₆, 25°C, TMS): δ 1.03 (s, SnMe₃); ¹¹⁹Sn NMR (149.3 MHz, C₆D₆, 25°C, Me₄Sn): δ 100 (s, SnMe₃); MS (EI, 451°C): *m/z* 1796 [M⁺]; elemental analysis calculated (%) for C₂₄H₇₂N₄Sn₈Ag₄: C 16.03, H 4.04; found: C 16.39, H 4.18.

Crystal data for **7**. C₂₄H₇₂N₄Sn₈Ag₄: *M_r* = 1797.86 g cm^{−3}, crystal dimensions 0.476 x 0.272 x 0.136 mm, monoclinic, space group *P*2(1)/c, *a* = 18.355(3), *b* = 13.010(2) *c* = 23.107(4) Å, α = 90, β = 110.936°; *V* = 5153.7(15) Å³, *Z* = 4, ρ_{calcd} = 2.317 g cm^{−3}, Siemens SMART CCD diffractometer, 1.19 ≤ θ ≤ 28.75°, MoK_α radiation (λ = 0.71073 Å), ω scans, *T* = 193(2) K; of 27,333 measured reflections, 11,907 were independent and 10,280 observed with *I* > 2σ(*I*), −24 ≤ *h* ≤ 16, −17 ≤ *k* ≤ 12, −30 ≤ *l* ≤ 30; *R*₁ = 0.0617, *wR*₂ = 0.1601, GOF = 1.056 for 409 parameters, Δρ_{max} = 2.052 eÅ^{−3}. The structure was solved

by direct methods (SHELXS-97) and refined by full-matrix least-squares procedures (SHELXL-97), Lorentz polarization corrections and absorption correction (SADABS) were applied, $\mu = 5.303 \text{ mm}^{-1}$, min./max. transmission 0.5325/0.1869.

*Synthesis of $[(\text{Me}_3\text{Sn})(\text{Me}_3\text{Si})\text{NAg}]_4$ (**8**):* Compound **8** was prepared in an analogous fashion to compound **7** using $[(\text{Me}_3\text{Sn})(\text{Me}_3\text{Si})\text{NLi} \cdot (\text{Et}_2\text{O})]_2$ (0.50 g, 0.75 mmol) and AgBr (0.28 g, 1.50 mmol). Colorless crystals were grown from hexane overnight. Yield: 0.41 g (77%); ^1H NMR (400 MHz, C_6D_6 , 25°C, TMS): δ 0.47 (t, 36H, SiMe₃), 0.43 (t, 36H, SnMe₃); ^{13}C NMR (100.6 MHz, C_6D_6 , 25°C, TMS): δ 8.53 (s, SiMe₃), 0.34 (s, SnMe₃); ^{29}Si NMR (79 MHz, C_6D_6 , 25°C, Me₄Si): δ 8.21 (s, SiMe₃); ^{119}Sn NMR (149.3 MHz, C_6D_6 , 25°C, Me₄Sn): δ 75.0 (s, SnMe₃); elemental analysis calculated (%) for $\text{C}_{24}\text{H}_{72}\text{N}_4\text{Si}_4\text{Sn}_4\text{Ag}_4$: C 20.08, H 5.05, N 3.90; found: C 20.00, H 4.57, N 3.95.

Crystal data for **8**. $\text{C}_{24}\text{H}_{72}\text{N}_4\text{Si}_4\text{Sn}_4\text{Ag}_4$: $M_r = 1435.46 \text{ g cm}^{-3}$, crystal dimensions 0.15 x 0.13 x 0.11 mm, monoclinic, space group $C2/m$, $a = 20.708(5)$, $b = 14.095(3)$ $c = 9.550(2)$ Å, $\alpha = 90$, $\beta = 115.966^\circ$; $V = 2506.0(10) \text{ Å}^3$, $Z = 2$, $\rho_{\text{calcd}} = 1.902 \text{ g cm}^{-3}$, Siemens SMART CCD diffractometer, $1.81 \leq \theta \leq 28.65^\circ$, MoK α radiation ($\lambda = 0.71073$ Å), ω scans, $T = 193(2)$ K; of 7,823 measured reflections, 3,101 were independent and 2,267 observed with $I > 2\sigma(I)$, $-16 \leq h \leq 26$, $-16 \leq k \leq 18$, $-12 \leq l \leq 11$; $R_1 = 0.0558$, $wR_2 = 0.1608$, GOF = 1.107 for 99 parameters, $\Delta\rho_{\text{max}} = 2.120 \text{ e Å}^{-3}$. The structure was solved by direct methods (SHELXS-97) and refined by full-matrix least-squares procedures (SHELXL-97), Lorentz polarization corrections and absorption correction (SADABS) were applied, $\mu = 3.601 \text{ mm}^{-1}$, min./max. transmission 0.6907/0.6178.

Synthesis of [(Me₃Sn)(Me₃Ge)NAg]₄ (9): Compound **9** was prepared in an analogous fashion to compound **7** using [(Me₃Sn)(Me₃Ge)NLi•(Et₂O)]₂ (0.50 g, 0.65 mmol) and AgBr (0.24 g, 1.3 mmol). Colorless crystals were grown from hexane overnight. Yield: 0.38 g (73%); ¹H NMR (400 MHz, C₆D₆, 25°C, TMS): δ 0.55 (t, 36H, GeMe₃), 0.45 (t, 36H, SnMe₃); ¹³C NMR (100.6 MHz, C₆D₆, 25°C, TMS): δ 8.71 (s, GeMe₃), 0.49 (s, SnMe₃); ¹¹⁹Sn NMR (149.3 MHz, C₆D₆, 25°C, Me₄Sn): δ 84.9 (s, SnMe₃); elemental analysis calculated (%) for C₂₄H₇₂N₄Ge₄Sn₄Ag₄: C 17.87, H 4.50, N 3.47; found: C 17.88, H 4.49, N 4.22.

Crystal data for **9**. C₂₄H₇₂N₄Ge₄Sn₄Ag₄: *M_r* = 1613.46 g cm⁻³, crystal dimensions 0.31 x 0.10 x 0.10 mm, monoclinic, space group C2/c, *a* = 33.982(8), *b* = 14.182(3) *c* = 21.170(5) Å, α = 90, β = 94.761°; *V* = 10,167(4) Å³, *Z* = 8, ρ_{calcd} = 2.108 g cm⁻³, Siemens SMART CCD diffractometer, 1.20 ≤ θ ≤ 28.65°, MoK_α radiation (λ = 0.71073 Å), ω scans, *T* = 193(2) K; of 31,339 measured reflections, 12,011 were independent and 6,927 observed with *I* > 2σ(*I*), -31 ≤ *h* ≤ 45, -17 ≤ *k* ≤ 18, -28 ≤ *l* ≤ 27; *R*₁ = 0.0806, *wR*₂ = 0.2364, GOF = 1.075 for 409 parameters, Δρ_{max} = 4.900 eÅ⁻³. The structure was solved by direct methods (SHELXS-97) and refined by full-matrix least-squares procedures (SHELXL-97), Lorentz polarization corrections and absorption correction (SADABS) were applied, μ = 5.775 mm⁻¹, min./max. transmission 0.5904/0.2710.

Synthesis of [(Me₃Si)₂NAg]₄ (10): *N*-lithio bis(trimethylsilyl)amine was prepared by adding 3.10 mL of *n*BuLi (1.6 M solution in hexane) to a diethyl ether solution of (Me₃Si)₂NH (0.80 g, 4.9 mmol) at 0°C. The solution was allowed to attain ambient temperature on its own and it was subsequently stirred for 2 hours under an argon atmosphere. This solution was added dropwise to a diethyl ether slurry of AgBr (0.92 g,

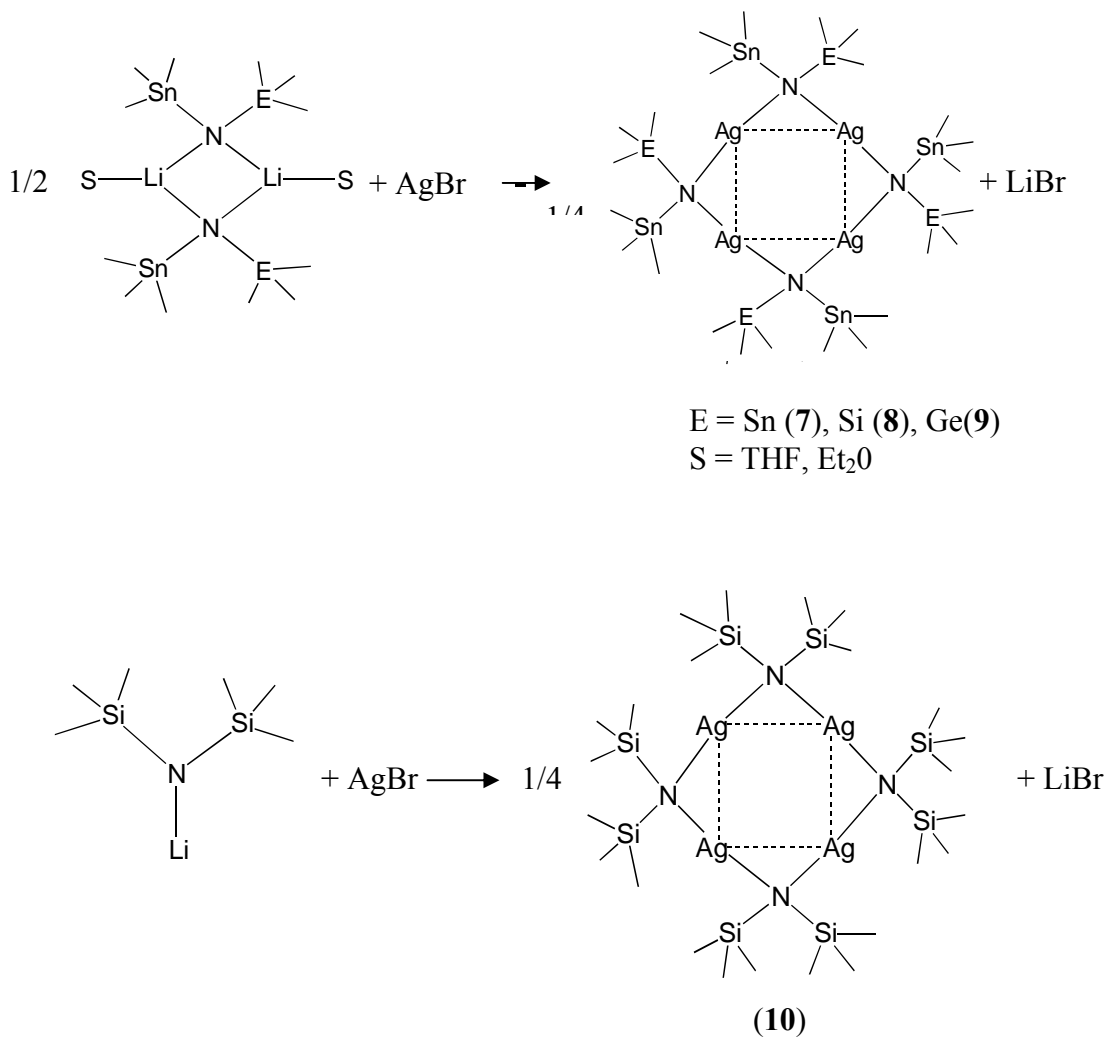
4.9 mmol) at -78°C and it was stirred overnight under an argon atmosphere under light exclusion. The reaction mixture was then allowed to attain ambient temperature and it was stirred for an additional 3 hours. The resulting pale yellow solution contained a significant amount of colorless precipitate. The solvent was removed *in vacuo*, the solid residue extracted with 30 mL of hexane, and the resulting slurry filtered to yield a clear, golden solution. Colorless crystals were grown overnight at -40°C . Yield: 0.33 g (66%); ^1H NMR (400 MHz, C_6D_6 , 25°C , TMS): δ 0.55 (s, SiMe_3); ^{13}C NMR (100.6 MHz, C_6D_6 , 25°C , TMS): δ 8.71 (s, SiMe_3); MS (EI, 267°C): m/z 1057 $[(\text{M}-15)^+]$. Crystal data for **10**. $\text{C}_{24}\text{H}_{72}\text{N}_4\text{Si}_8\text{Ag}_4$: $M_r = 1073.06 \text{ g cm}^{-3}$, crystal dimensions 0.25 x 0.14 x 0.10 mm, monoclinic, space group $P2_1/n$, $a = 9.2069(15)$, $b = 13.807(2)$, $c = 17.664(2) \text{ \AA}$, $\alpha = 90$, $\beta = 91.245^{\circ}$, $V = 2319.1(7) \text{ \AA}^3$, $Z = 2$, $\rho_{\text{calcd}} = 1.537 \text{ g cm}^{-3}$, Siemens SMART CCD diffractometer, $1.85 \leq \theta \leq 28.74^{\circ}$, $\text{MoK}\alpha$ radiation ($\lambda = 0.71073 \text{ \AA}$), ω scans, $T = 193(2) \text{ K}$; of 14,415 measured reflections, 5,483 were independent and 3,585 observed with $I > 2\sigma(I)$, $-10 \leq h \leq 12$, $-18 \leq k \leq 16$, $-23 \leq l \leq 24$; $R_1 = 0.0238$, $wR_2 = 0.0574$, GOF = 1.076 for 207 parameters, $\Delta\rho_{\text{max}} = 0.419 \text{ e\AA}^{-3}$. The structure was solved by direct methods (SHELXS-97) and refined by full-matrix least-squares procedures (SHELXL-97), Lorentz polarization corrections and absorption correction (SADABS) were applied, $\mu = 1.890 \text{ mm}^{-1}$, min./max. transmission 0.8306/0.6443.

Results and Discussion

Synthesis

The synthesis of compounds **7-9** is depicted in Schemes 3.1. Compounds **7-9** were prepared by adding an ether solution of the appropriate lithiated stannylamine

(compounds **1-3**) to an ether slurry of AgBr at -78°C . The reaction mixture was stirred overnight at this temperature before allowing to attain ambient temperature. The solvent was removed *in vacuo*, the solid residue extracted with hexane, and the LiBr precipitate filtered off. Colorless crystals were grown at -40°C . Compound **10** was synthesized in a similar fashion; however, the *N*-lithio bis(trimethylsilyl)amine was generated *in situ* before being reacted with AgBr.



Scheme 3.1. Synthesis of compounds **7-10**.

Characterization

Crystals of compounds **7-10** were analysed by single crystal X-ray diffraction and the crystal structures of these compounds are depicted in Figures 3.1-3.4.

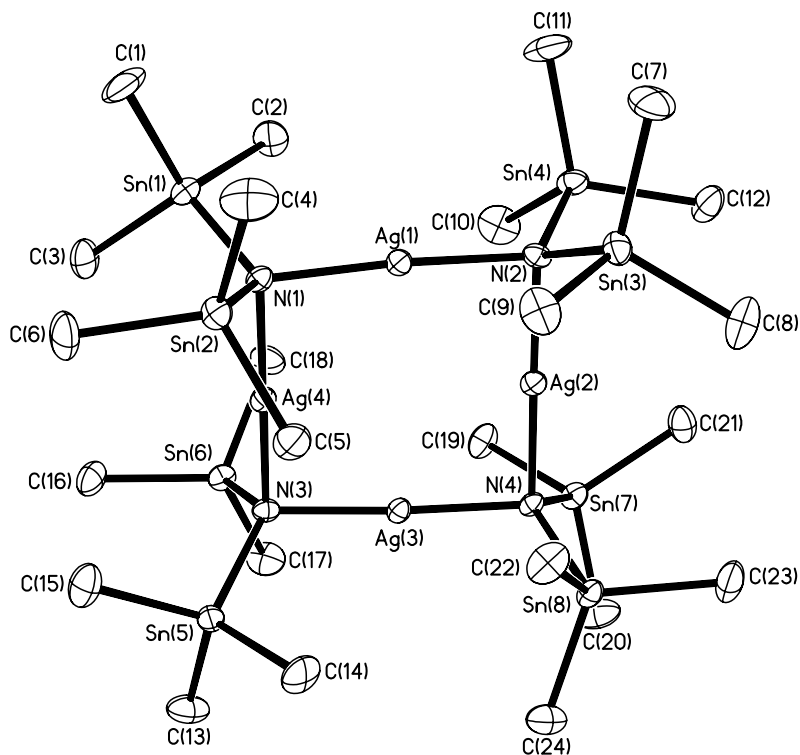


Figure 3.1. ORTEP plot representation (30% probability) with numbering scheme for compound **7**. Hydrogen atoms have been omitted for clarity.

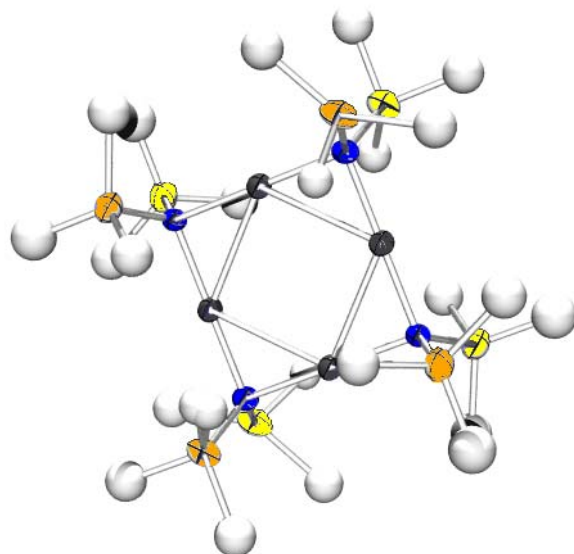


Figure 3.2. ORTEP plot representation (30% probability) for compound **8**. Hydrogen atoms have been omitted for clarity.

Sn ● N ● Ag ● Si ●

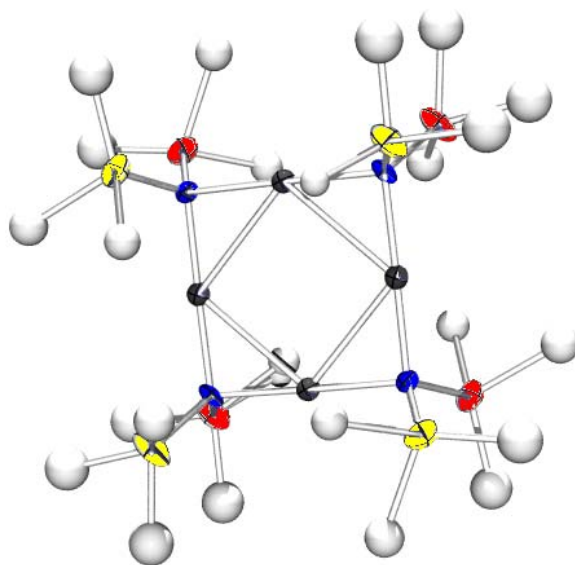


Figure 3.3. ORTEP plot representation (30% probability) for compound **9**. Hydrogen atoms have been omitted for clarity.

Sn ● N ● Ag ● Ge ●

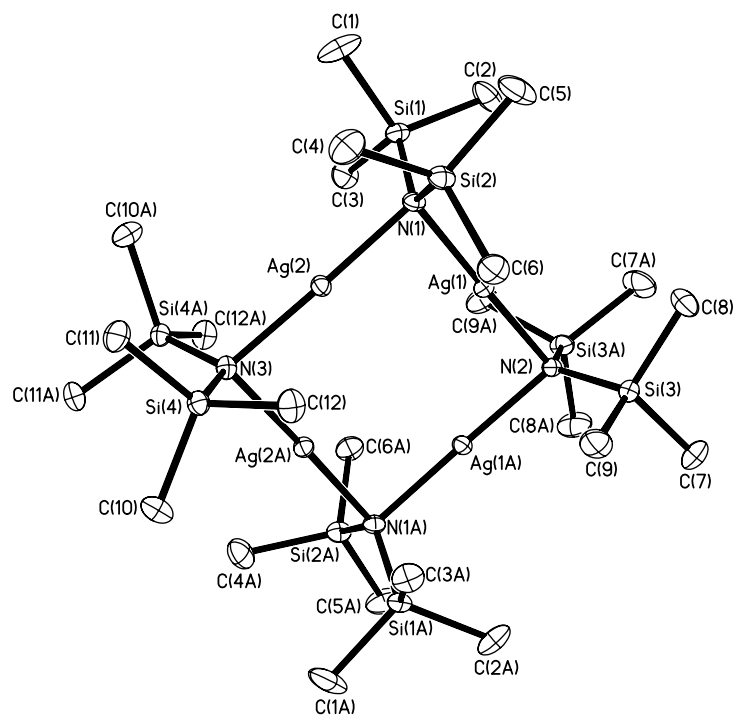


Figure 3.4. ORTEP plot representation (30% probability) with numbering scheme for compound **10**. Hydrogen atoms have been omitted for clarity.

All four complexes exist as tetramers in the solid state, comprised of a nearly planar Ag₄N₄ core, with each amido ligand bridging two silver metal centers. The predominant feature of these complexes are close interactions observed between silver(I) cations, found to be less than the sum of the van der Waals radii for Ag⁺ ions (< 3.4 Å). A summary of the principal interatomic distances and angles for compounds **7-10** is provided in Table 3.1 and a complete list of all distances and angles can be found in Tables A.26, A.30, A.33, and A.36, respectively.

Table 3.1. Selected average interatomic distances (Å) and angles (degrees) for compounds **7-10**.

(7)	Distance/ angle	(8)	Distance/ angle	(9)	Distance/ angle	(10)	Distance/ angle
Sn-N	2.053(6)	Sn/Si-N	1.959(6)	Sn/Ge-N	1.9562(6)	Si-N	1.747(15)
Ag-N	2.0994(6)	Ag-N	2.125(5)	Ag-N	2.1125(5)	Ag-N	2.145(2)
Ag-Ag	3.0024(8)	Ag-Ag	3.0026(14)	Ag-Ag	3.0112(10)	Ag-Ag	3.0087(6)
N-Ag-N	177.6(2)	N-Ag-N	179.7(2)	N-Ag-N	178.9(2)	N-Ag-N	178.76(7)
Ag-N-Ag-N	177.34	Ag-N-Ag-N	179.71	Ag-N-Ag-N	178.89	Ag-N-Ag-N	178.76

The Ag₄N₄ core is structurally analogous to the bis(trimethylsilyl)amido complex reported by Lappert *et al.*³ and to the more recent tetramethyl guanidine complexes reported in our laboratory.⁴ Compounds **7-10**, in a similar fashion to these previously reported structures, possess nearly planar metal-nitrogen cores (the Ag-N-Ag-N dihedral angles are summarized in Table 3.1) and nearly linear N-Ag-N angles.

Similar to the trend observed for the Li-N interatomic distance in compounds **1-3**, the Ag-N distance decreases with increasing molecular weight of the second amide

substituent (heavier Group 14 element). The Sn-N distances in compound **7** are observed to be in the expected range found for other trimethylstannyl amides.^{6,7} However, in compounds **8** and **9**, the tin atom was crystallographically indistinguishable from silicon and germanium atoms, respectively. In a similar fashion to compounds **2** and **3**, the observed Sn/Si- and Sn/Ge-N interatomic distances fall between the distances typically observed for Sn-N and Si-N or Ge-N. The presence of silicon and germanium in compounds **8** and **9** was verified by the ^{119}Sn NMR chemical shifts for the two compounds (Figure 3.5) and the elemental analyses.

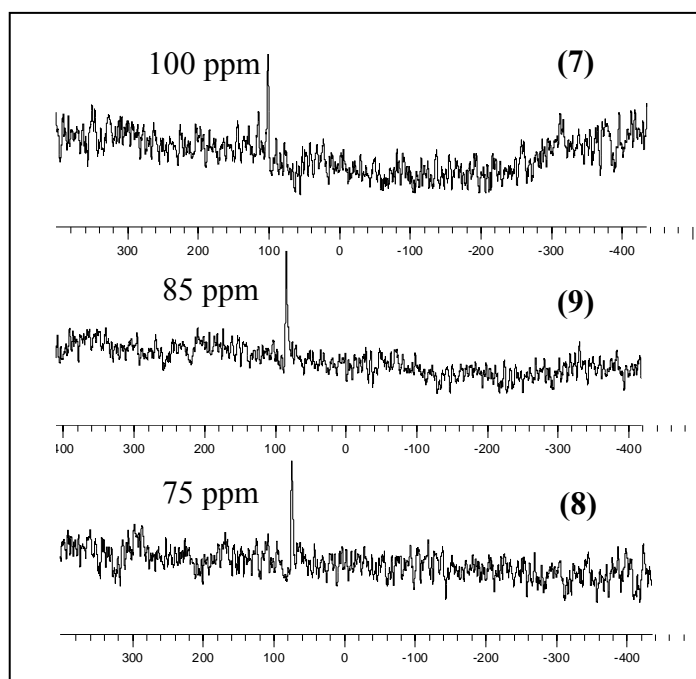


Figure 3.5. ^{119}Sn spectra for compounds **7-9** (chemical shift scale in ppm).

Perhaps the most notable feature of compounds **7-10** is the close contact observed for the silver(I) ions. As previously mentioned, the Ag-Ag distances are shorter than the

sum of the van der Waals radii, indicating the presence of a d^{10} - d^{10} closed shell interaction. This argentophilic interaction is believed to have a similar origin to commonly observed aurophilicity found in polynuclear gold(I) complexes. However, since the strength of the Ag^+ - Ag^+ closed shell interaction has been determined to be of a lesser magnitude than that for Au^+ - Au^+ (aurophilic interactions have been found to be of a similar energy as hydrogen bonds, whereas argentophilic contacts are about the same energy as standard van der Waals interactions), the occurrence of argentophilicity in silver complexes is less favored, and hence, less commonly observed.⁸

Theoretically, in the absence of $(n+1)s$ and $(n+1)p$ orbitals, the interaction between closed-shell d^{10} centers is repulsive in nature. However, mixing of the filled nd -orbitals with these empty orbitals derived from higher energy $[(n+1)s$ and $(n+1)p]$ results in metal-metal interactions. It is noted though, that the observation of short metal-metal contacts in such systems does not necessarily mean that a metal-metal bond exists, so the nature of the bridging ligands and their effect on the oligomerization of the metal centers needs to be taken into account. If indeed a metal-metal bond is formed, unique photophysical properties are often observed. In polynuclear silver(I) complexes, the origin of the emission has been assigned to $d\sigma^*$ - $p\sigma$, $d\sigma^*$ - s , and mixed-metal-centered, metal-to-ligand charge transfer (MLCT) transitions.² The absorption and emission spectra were obtained for compounds **7** and **8**, as well as the previously reported compound **10** with the aim of determining whether these compounds might provide an entry point for future studies on the nature of argentophilic, d^{10} - d^{10} interactions. The absorption, emission, and excitation spectra, along with the emission decay for compound **7** are shown in Figure 3.6. In addition, theoretical calculations were performed on a high

symmetry model of compound **7**, and graphical representations of the frontier orbitals for this model complex are illustrated in Figure 3.7 [The geometry of **7** was optimised using Density Functional Theory (DFT). The B3LYP method was employed with the LACVP* basis set. The model compound was found to have C_{2h} symmetry. The single point energy calculation used to generate the HOMO and LUMO surfaces was performed using the same method and basis set.]

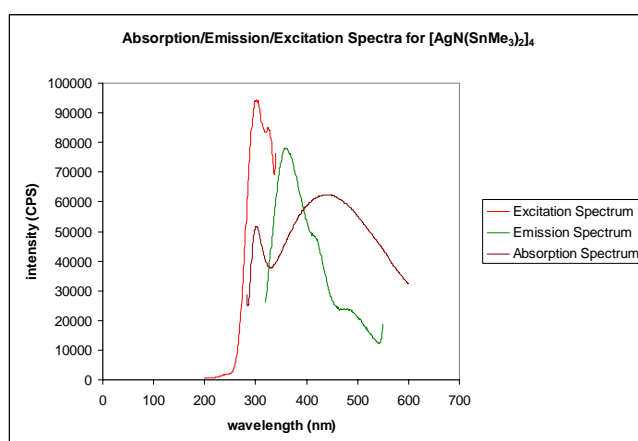


Figure 3.6.A. The UV/VIS absorption, emission (@ 300 nm), and excitation (@ 350 nm) spectra for compound **7** in hexane.

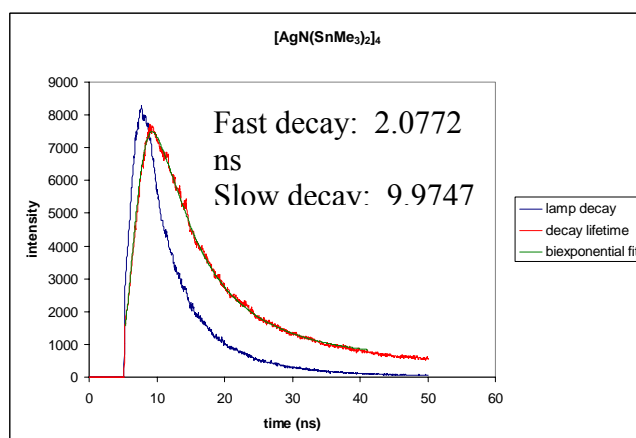
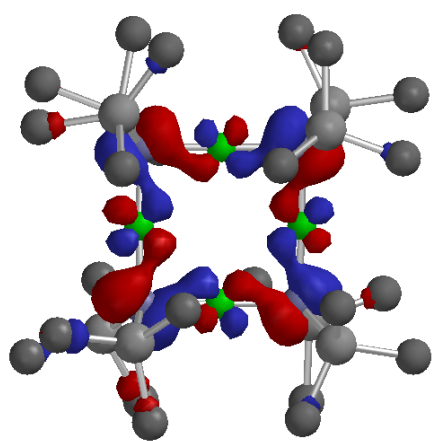
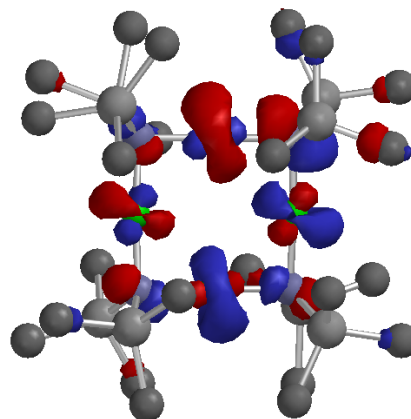


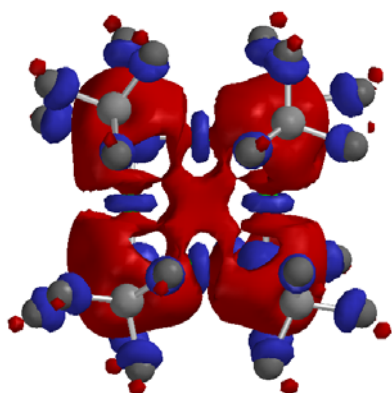
Figure 3.6.B. Emission decay for compound **7** in hexane (excitation @ 216 nm and emission @ 365).



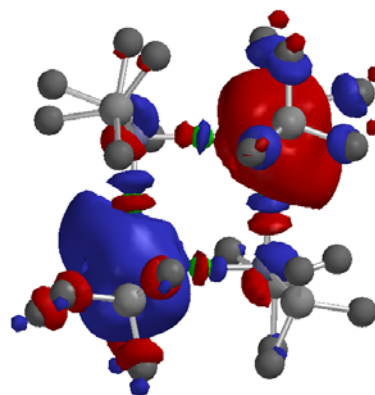
A



B



C



D

Figure 3.7. A: HOMO; B: HOMO(-1); C: LUMO; D: LUMO(-1) for compound **7** from DFT theoretical calculations.

As seen in Figure 3.6, compound **7** exhibits a sharp absorption at 298 nm, along with an additional broad absorption at 432 nm. Upon excitation at 300 nm, the complex intensely emitted at 365 nm and displayed vibronically structured bands located at 421 and 489 nm. The excitation spectrum was obtained by irradiating the complex at 365 nm and the maximum excitation peak was found at 305 nm. The emission decay was also collected and found to undergo biexponential decay, with the fast decay occurring in 2.0 ns and the slow decay in 9.9 ns. Photophysical studies were also performed for compounds **8** and **10**. Table 3.2 summarizes the results for compounds **7**, **8**, and **10**.

Table 3.2. UV/VIS absorption, emission, excitation, and decay lifetime for compounds **7**, **8**, and **10**.

	7	8	10
λ_{max} (nm)	298, 432	256, 438	265, 420
emission (nm)	(@ 300 nm) 365, 421, 489	(@ 266 nm) 378, 420,	(@ 297 nm) 365, 424, 491
excitation (nm)	(@ 365 nm) 305	(@ 365 nm) 306	(@ 360 nm) 308
lifetime (ns)	$\tau_1 = 2.0$ (fast)	$\tau_1 = 2.1$ (fast)	$\tau_1 = 2.0$ (fast)
excitation @ 315 nm	$\tau_2 = 9.9$ (slow)	$\tau_2 = 10.4$ (slow)	$\tau_2 = 9.7$ (slow)
emission @ 365 nm			

Though the spectroscopic results reported here do not conclusively indicate emission from a metal centered excited state, it is possible such a phenomenon is occurring in compounds **7**, **8**, and **10**. For compound **7**, the lower energy absorption band at 432 nm is likely due to a ligand-to-metal charge transfer (LMCT) and the higher energy band at 298

nm possibly arises from the population of a metal-centered excited state, expected to occur at higher energy than a LMCT transition. The potential for emission from metal-centered excited states is corroborated by the results of the theoretical calculations shown in Figure 3.7. The nature of the frontier orbitals indicates that there is indeed some electronic communication between the Ag^+ metal centers. This suggests that the emission may originate from excited states that are at least partially centered on the metal cations. However, more detailed photophysical studies, such as low temperature emission studies and the determination of the quantum yield, as well as excited state theoretical calculations would lend more insight into the nature of the emission processes observed in these tetranuclear complexes.

Conclusion

The planar, tetrameric silver-nitrogen core found in the silver(I) bis(trimethylsilyl)amide complex previously reported was believed to be a forerunner to a new class of silver amides.³ However, until recent work in our laboratory, no further progress in this area had been accomplished.⁴ This report extends the family of tetrameric amidosilver complexes via the use of homoleptic and heteroleptic lithiated stannyl amines. Compounds **7-9** were synthesized and fully characterized by single crystal X-ray diffraction experiments, as well as multinuclear NMR techniques. In addition, compounds **7**, **8**, and the previously reported compound **10** were analyzed by spectroscopic methods in an attempt to probe the nature of their photophysical properties. It was concluded that the close Ag-Ag interactions observed in these compounds result in emission that potentially originates from metal-centered excited states. More detailed

photophysical studies and excited state calculations, which would provide additional insight into the nature of the emission phenomena are warranted.

References

- (1) Yam, V. W. W.; Lo, K. K. W. *Chem. Soc. Rev.* **1999**, 28, 323-334.
- (2) Catalano, V. J.; Kar, H. M.; Garnas, J. *Angew. Chem. Int. Ed.* **1999**, 38, 1979-1982.
- (3) Hitchcock, P. B.; Lappert, M. F.; Pierssens, L. J. M. *Chem. Comm.* **1996**, 1189-1190.
- (4) Bunge, S. D.; Just, O.; Rees, W. S., Jr. In *The Molecular Design of Metal Amides*; Georgia Institute of Technology: Atlanta, 2001.
- (5) Gilman, H.; Cartledge, F. K. *J. Organometal. Chem.* **1964**, 2, 447.
- (6) Neumann, C.; Seifert, T.; Storch, W.; Vosteen, N.; Wrackmeyer, B. *Angew. Chem., Int. Ed.* **2001**, 40, 3405-3407.
- (7) Nutt, W. R.; Murray, K. J.; Gullick, J. M.; Odom, J. D.; Ding, Y.; Lebioda, L. *Organometallics* **1996**, 15, 1728.
- (8) Bardaji, M.; Laguna, A. *Eur. J. Inorg. Chem.* **2003**, 3069.

CHAPTER 4

SYNTHESIS AND STRUCTURAL DETERMINATION OF DIMERIC ZINC(II)

AND ZIRCONIUM(IV) AMIDES: $[\text{Zn}\{\text{N}(\text{SnMe}_3)_2\}(\text{Cl})_2\bullet\text{Li}(\text{Et}_2\text{O})_2]_2$ AND

$[(\text{C}_5\text{H}_5)_2\text{ZrNSnMe}_3]_2$

Introduction

Zinc and zirconium amides have previously been synthesized and employed as precursors in the MOCVD of zinc nitride¹ and atomic layer deposition (ALD) of zirconium oxide², respectively. In the scope of this work, the synthesis and structural characterization of zinc(II) and zirconium(IV) amides is desired in order to further explore the use of the lithiated bis(trimethylstannyl)amine as a synthon to new transition metal complexes. In addition, it is of interest to synthesize heterometallic zirconium-tin complexes that may be used as “same-source” precursors for ZTT via MOCVD.

The reaction of zinc and zirconium halides with *N*-lithio bis(trimethylstannyl)amine (**1**) was examined. The isolated metal amide dimers, $[\text{Zn}\{\text{N}(\text{SnMe}_3)_2\}(\text{Cl})_2\bullet\text{Li}(\text{Et}_2\text{O})_2]_2$ (**11**) and $[(\text{C}_5\text{H}_5)_2\text{ZrNSnMe}_3]_2$ (**12**) represent the first structurally characterized zinc amido and zirconium imido compounds possessing the trimethylstannyl moiety.

Experimental

All manipulations were carried out in a dry atmosphere glovebox or by standard Schlenk techniques. All solvents were dried over Na⁰ metal and were freshly distilled under an inert atmosphere prior to use. ZnCl_2 and $(\text{C}_5\text{H}_5)_2\text{ZrCl}_2$ reagents were purchased from

Alfa Aesar and used without further purification. $[(\text{Me}_3\text{Sn})_2\text{NLi}\bullet(\text{THF})]_2$ was prepared as described in Chapter 2.

*Synthesis of $[\text{Zn}\{\text{N}(\text{SnMe}_3)_2\}(\text{Cl})_2\bullet\text{Li}(\text{Et}_2\text{O})_2]_2$ (**11**):* A solution of $[(\text{Me}_3\text{Sn})_2\text{NLi}\bullet(\text{THF})]_2$ (1.00 g, 1.19 mmol) in diethyl ether (40 mL) was added to a diethyl ether slurry of ZnCl_2 (0.19 g, 2.38 mmol) in a dropwise fashion at 0°C . The reaction mixture was allowed to attain ambient temperature on its own whereby a colorless precipitate formed within 10 minutes. After stirring overnight under an argon atmosphere the reaction mixture was filtered and its volume subsequently reduced, *in vacuo*, to about 30 mL. Colorless crystals were grown at -40°C over a two-day period.

Crystal data for **11**. $\text{C}_{28}\text{H}_{76}\text{N}_2\text{O}_4\text{Cl}_4\text{Sn}_4\text{Zn}_2$: $M_r = 1266.09 \text{ g cm}^{-3}$, crystal dimensions 0.15 x 0.14 x 0.14 mm, triclinic, space group $P-1$, $a = 11.990(3)$, $b = 12.044(3)$, $c = 20.926(4)$ Å, $\alpha = 83.604(4)$, $\beta = 76.341(4)$, $\gamma = 61.753(4)^\circ$; $V = 2586.8(9) \text{ Å}^3$, $Z = 2$, $\rho_{\text{calcd}} = 1.625 \text{ g cm}^{-3}$, Siemens SMART CCD diffractometer, $1.00 \leq \theta \leq 25.05^\circ$. $\text{MoK}\alpha$ radiation ($\lambda = 0.71073 \text{ Å}$), ω scans, $T = 193(2) \text{ K}$; of 13,749 measured reflections, 9,092 were independent and 5,631 observed with $I > 2\sigma(I)$, $-14 \leq h \leq 10$, $-14 \leq k \leq 14$, $-24 \leq l \leq 22$; $R_1 = 0.0701$, $wR_2 = 0.1596$, $\text{GOF} = 1.029$ for 438 parameters, $\Delta\rho_{\text{max}} = 1.420 \text{ e Å}^{-3}$. The structure was solved by direct methods (SHELXS-97) and refined by full-matrix least-squares procedures (SHELXL-97), Lorentz polarization corrections and absorption correction (SADABS) were applied, $\mu = 3.047 \text{ mm}^{-1}$, min./max. transmission 0.6820/0.6528.

*Synthesis of [(C₅H₅)₂ZrNSnMe₃]₂ (**12**):* A solution of [(Me₃Sn)₂NLi•(THF)]₂ (1.00 g, 1.19 mmol) in diethyl ether (40 mL) was added to a diethyl ether slurry of (C₅H₅)₂ZrCl₂ (0.19 g, 2.38 mmol) in a dropwise fashion at 0°C. The reaction mixture was allowed to attain ambient temperature on its own whereby a colorless precipitate formed within 10 minutes. After stirring overnight under an argon atmosphere the reaction mixture was filtered and its volume reduced, *in vacuo*, to about 30 mL. Yellow crystals were grown at –80°C over a two-day period.

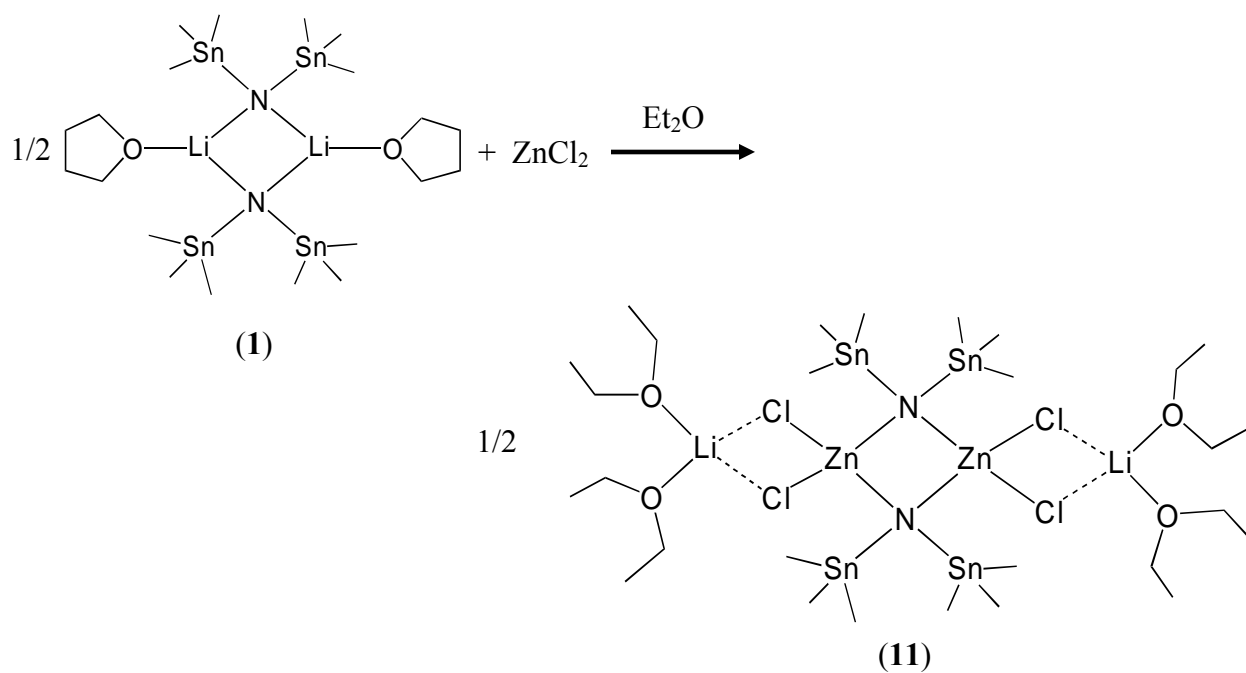
Crystal data for **12**. C₂₆H₃₈N₂Sn₂Zr₂: $M_r = 798.40 \text{ g cm}^{-3}$, crystal dimensions 0.34 x 0.20 x 0.07 mm, monoclinic, space group *P2(1)/n*, $a = 8.2519(5)$, $b = 16.2209(11)$, $c = 10.3432(7) \text{ Å}$, $\alpha = 90$, $\beta = 98.5650(10)^\circ$; $V = 1369.03(16) \text{ Å}^3$, $Z = 2$, $\rho_{\text{calcd}} = 1.937 \text{ g cm}^{-3}$, Siemens SMART CCD diffractometer, $2.35 \leq \theta \leq 28.80^\circ$. MoK α radiation ($\lambda = 0.71073 \text{ Å}$), ω scans, $T = 193(2) \text{ K}$; of 8,762 measured reflections, 3265 were independent and 2,137 observed with $I > 2\sigma(I)$, $-11 \leq h \leq 9$, $-20 \leq k \leq 19$, $-12 \leq l \leq 13$; $R_1 = 0.0406$, $wR_2 = 0.0935$, GOF = 0.964 for 161 parameters, $\Delta\rho_{\text{max}} = 0.969 \text{ eÅ}^{-3}$. The structure was solved by direct methods (SHELXS-97) and refined by full-matrix least-squares procedures (SHELXL-97), Lorentz polarization corrections and absorption correction (SADABS) were applied, $\mu = 2.560 \text{ mm}^{-1}$, min./max. transmission 0.8452/0.4765.

Results and Discussion

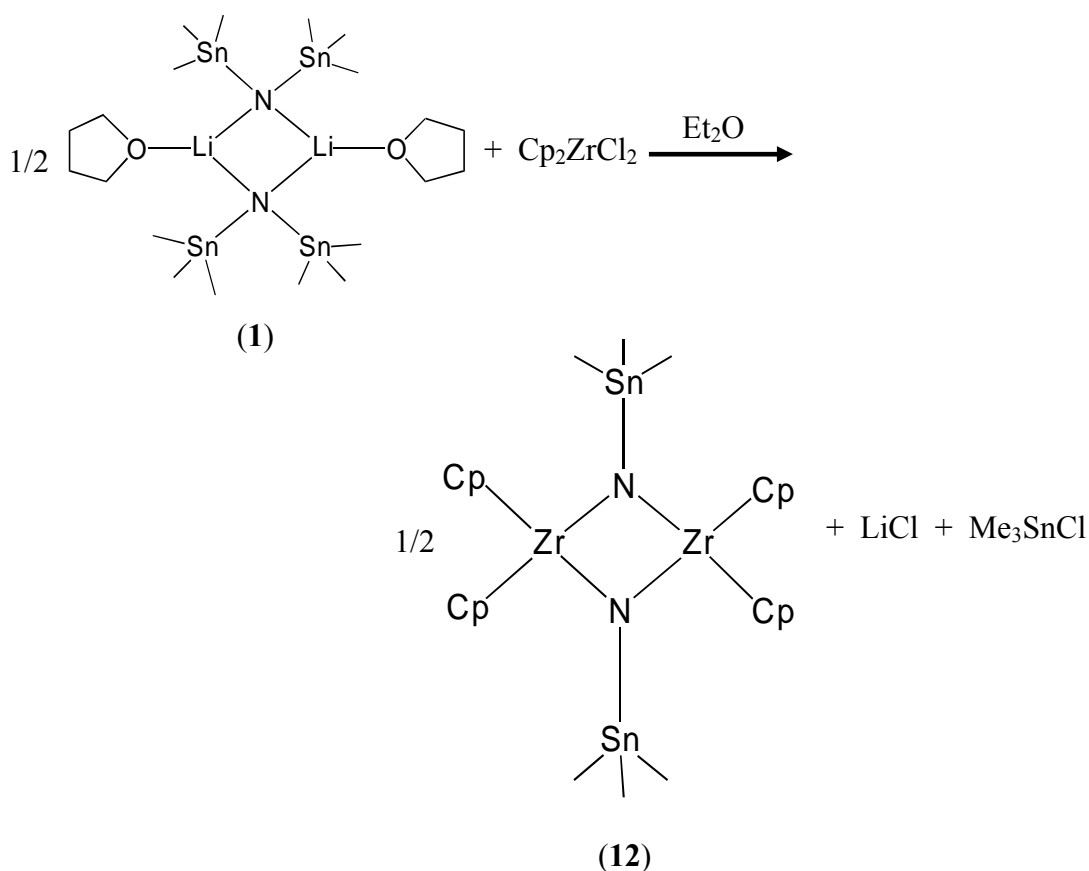
Synthesis

The synthesis of compounds **11** and **12** is illustrated in Schemes 4.1 and 4.2, respectively. Both complexes were prepared by reacting the appropriate metal halide starting material with 0.5 equivalents of **1**. The reaction mixtures were stirred overnight and the resulting

solutions were filtered. Crystals of each compound were obtained directly from the mother liquor (compound **11**: colorless crystals at -40°C ; compound **12**: yellow crystals at -80°C).



Scheme 4.1. Synthesis of compound **11**.



Scheme 4.2: Synthesis of compound **12**.

A comparison of the reactions in Schemes 4.1 and 4.2 to those discussed in Chapters 2 (**1** + BeCl₂) and 3 (**1** + AgBr) indicates that the metal chlorides react with the lithiated bis(trimethylstannyl)amine in a different fashion. In the case of Zn, instead of producing an equivalent of lithium halide and the corresponding oligomeric coordination complex possessing the bridging bis(stannyl)amide moiety, an “ate” complex forms that retains both chloride ligands in the coordination sphere. When the bis(cyclopentadienyl)zirconium dichloride is utilized, a metal dimer possessing a bridging stannylimide ligand is obtained. In addition, both lithium chloride and

trimethyltin chloride are formed as co-products. A potential explanation for the formation of compound **12** and trimethyltin chloride as a by-product is the increased lability of the Zr-Cl bond in Cp_2ZrCl_2 (Zr-Cl interatomic distance = 2.6 Å) in comparison to BeCl_2 and ZnCl_2 (Be-Cl interatomic distance = 2.2 Å and Zn-Cl interatomic distance = 2.2 Å). A literature search has concluded that no prior metathesis reaction involving the elimination of both LiCl and Me_3SnCl has been observed.

Characterization

The molecular structures of compounds **11** and **12**, determined by single crystal X-ray diffraction are depicted in Figures 4.1 and 4.2.

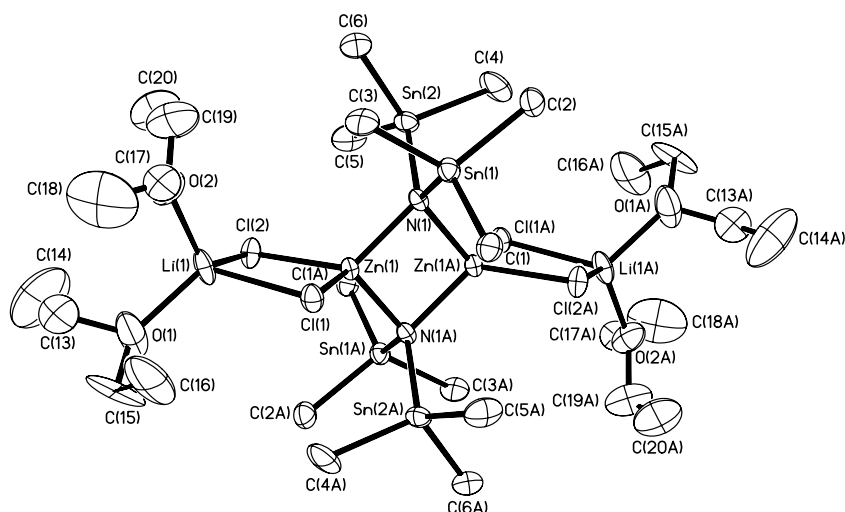


Figure 4.1. ORTEP plot representation (30% probability) with numbering scheme for compound **11**. Hydrogen atoms have been omitted for clarity.

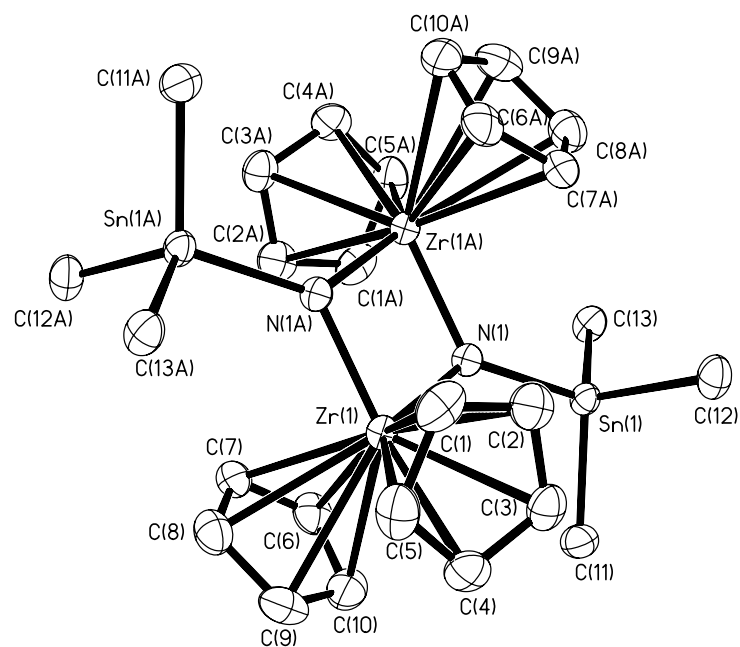


Figure 4.2. ORTEP plot representation (30% probability) with numbering scheme for compound **12**. Hydrogen atoms have been omitted for clarity.

Compounds **11** and **12** both exist as dimers in the solid state and are comprised of M_2N_2 rhomboid cores. Table 4.1 lists the pertinent interatomic distances and angles for **11** and **12**, and complete lists of all angles and distances for these two structures are located in Tables A.40 and A.44, respectively.

Table 4.1. Selected average interatomic distances (Å) and angles (degrees) for compounds **11** and **12**.

(11)	distance/angle	(12)	distance/angle
Sn-N	2.087(8)	Sn-N	2.047(4)
Zn-N	2.023(8)	Zr-N	2.059(4)
Zn-Cl	2.315(3)	Zr-C	2.603(6)
N-Zn-N	96.3(3)	N-Zr-N	80.95(17)
Zn-N-Zn	83.6(3)	Zr-N-Zr	99.05(17)

Compound **11** represents the first structurally characterized zinc amide “ate” complex. It possesses a dimeric Zn_2N_2 core, with bridging bis(stannylamide) ligands and terminal chloride ligands. The Sn-N interatomic distance is in the range observed for compounds **1**, **4**, and **6**, and the Zn-N distance is similar to that found previously in other zinc amide dimers $\{[ZnN[Si(CH_3)CH_2CH_2Si(CH_3)_2]]_2, Zn-N_{\text{bridging}} = 2.065 \text{ Å}\}^3$. As is expected in an “ate” complex, the Zn-Cl interatomic distance is longer than the predicted Zn-Cl distance in $ZnCl_2$ (approximately 2.2 Å). Additionally, the acute M-N-M and obtuse N-M-N angles are found in compounds **1-5** as well.

The dimeric compound **12** possesses zirconium(IV) metal centers bridged by trimethylstannyl imido units and terminally coordinated by cyclopentadienyl ligands. The Sn-N distance found in **12** is slightly shorter than in compounds **4**, **7**, and **11**, due to the fact that only one trimethylstannyl moiety is bound to the nitrogen. The observed Zr-N distance corresponds well with Zr-N distances found in other zirconium amide dimers $\{[\text{Cp}_2\text{ZrN}(\text{Ph}^t\text{Bu})]_2, \text{Zr-N} = 2.096 \text{ \AA}\}$.⁴ The obtuse M-N-M and the acute N-M-N angles are in contrast to the observed angles in compounds **1-5** and **11**. This likely can be attributed to the decreased steric hindrance around the bridging nitrogen.

Conclusions

The initial account on the synthesis and structural characterization of zinc and zirconium complexes containing stannylamine or stannylimine ligands is reported. In addition, both compounds exemplify the first zinc amide “ate” and the first metal amide complex synthesized via a metathesis reaction involving the elimination of LiCl and Me₃SnCl (**11** and **12**, respectively). The successful synthesis and characterization of compound **12** emphasizes the significance of **1** as a synthon to heterometallic coordination compounds that can potentially be employed as ZTT precursors in MOCVD processes.

References

- (1) Maile, E.; Devi, A.; Fischer, R. A. *Proceedings - Electrochemical Society* **2003**, 975.
- (2) Hausmann, D. M.; Kim, E.; Becker, J.; Gordon, R. G. *Chem. Mater.* **2002**, 14, 4350.
- (3) Just, O.; Gaul, D. A.; Rees, W. S., Jr. *Polyhedron* **2001**, 20, 815.

- (4) Walsh, P. J.; Hollander, F. J.; Bergman, R. G. *J. Am. Chem. Soc.* **1988**, *110*, 8729.

CHAPTER 5

DESIGN AND SYNTHESIS OF GROUP 14-NITROGEN HETEROCUBANES

SECTION A: SYNTHESIS AND CHARACTERIZATION OF A SERIES OF GROUP

14-NITROGEN HETEROCUBANES: $[M(\mu_3\text{-NSiMe}_3)]_4$ (M = Ge, Sn, Pb)

Introduction

After establishing that the reaction of $[(\text{Me}_3\text{Sn})_2\text{NLi}\bullet(\text{THF})]_2$ (**1**) with Cp_2ZrCl_2 yields both LiCl and Me_3SnCl as by-products (Chapter 4), it was of interest to determine whether dicationic metal species analogously generate LiCl and Me_3SnCl upon reaction with $[(\text{Me}_3\text{Sn})(\text{Me}_3\text{E})\text{NLi}\bullet\text{THF}]_2$ {E = Si(**2**), Ge(**3**), Sn(**1**)}, and if so, what type of oligomeric metal complex might be formed.

Since tin amides may be useful precursors in the MOCVD of ZTT,¹ initial experiments investigated the reaction of SnCl_2 with compound **2**. The results indicate that LiCl and Me_3SnCl do indeed form as by-products in the reaction, while a tetrameric tin-nitrogen heterocubane possessing exo-cube silicon moieties is generated as the primary product (see Scheme 5.1). Since the cubane structural motif has previously been used by Barron, *et al.*, in the molecular design of gallium sulfide precursors² for utilization in MOCVD processes, the utility of these tin-nitrogen cubanes in the MOCVD of ZTT needs to be explored. The implemented molecular design strategy sought to exhibit control over the identity of the divalent metal cation located in the cube, as well as the tetravalent atom bound to nitrogen in the exo-cube position. The exploration of this design concept will be summarized in this chapter, and specifically, this sub-chapter

explores the modification of the endo-cube metal, resulting in the synthesis and characterization of the three compounds, $[M(\mu_3\text{-NSiMe}_3)]_4$ [$M = \text{Sn}$ (**13**), Ge (**14**), Pb (**15**)]

Experimental

All manipulations were carried out in a dry atmosphere glovebox or by standard Schlenk techniques. All solvents were dried over Na° metal or P_2O_5 (CH_2Cl_2) and were freshly distilled under an inert atmosphere prior to use. SnCl_2 and PbCl_2 reagents were purchased from Alfa Aesar and used without further purification.

$[(\text{Me}_3\text{Sn})(\text{Me}_3\text{Si})\text{NLi}\cdot(\text{Et}_2\text{O})]_2$ was prepared as described in Chapter 2 and $\text{GeCl}_2\cdot(\text{dioxane})^3$ was prepared according to literature procedures. All NMR experiments were performed on a Bruker 400 MHz Spectrometer at 300K using C_6D_6 solvent that was distilled over CaH_2 and stored under argon. ^1H and ^{13}C spectra were referenced to TMS. ^{119}Sn spectra were externally referenced to Me_4Sn . Elemental analyses were performed in triplicate on a Perkin Elmer Series II CHNS/O Analyzer 2400, FT-IR measurements were performed on a Bruker Equinox 55 Spectrometer, mass spectrometry analyses were done on a VG Instruments 70SE (Electron Impact; 70eV), and UV/VIS measurements were performed on a Perkin Elmer UV/VIS/NIR Lambda 19 Spectrometer. All TGA experiments were performed on a Perkin Elmer 7/DX thermal analyser interfaced to a Perkin Elmer Thermal Analysis Controller (TAC). The instrument is housed in a dry atmosphere glovebox. Argon was used as the purge gas and all %weight vs. temperature profiles were done at a $10^\circ\text{C}/\text{min}$. temperature ramp under ambient pressure.

*Synthesis of $[Sn(\mu_3-NSiMe_3)]_4$ (**13**):* A sample of $[(Me_3Sn)(Me_3Si)NLi\bullet(Et_2O)]_2$ (0.75 g, 1.13 mmol) was dissolved in diethyl ether (40 mL) and the solution was added to a diethyl ether slurry of $SnCl_2$ (0.42 g, 2.26 mmol) in a dropwise fashion at 0°C. The reaction mixture was allowed to attain ambient temperature on its own and a colorless precipitate formed within 10 minutes. The solution was stirred overnight under an argon atmosphere and the reaction mixture was subsequently filtered through a Schlenk frit. The solvent was removed *in vacuo* and the orange solid residue was extracted with 15 mL of CH_2Cl_2 . Orange crystals were grown from this solution at -80°C over a two-day period. Yield: 0.15 g (33%); 1H NMR (400 MHz, C_6D_6 , 25°C, TMS): δ 0.26 (s, $SiCH_3$); ^{13}C NMR (100.6 MHz, C_6D_6 , 25°C, TMS): δ -0.06 (s, $SiCH_3$); ^{119}Sn NMR (149.3 MHz, C_6D_6 , 25°C, Me_4Sn): δ 782 (s); MS (EI, 174°C): m/z 824 $[M^+]$; IR (nujol): 1301 (m), 852 (s), 749 (m), 722 (m), 518 (m) cm^{-1} ; elemental analysis calculated (%) for $C_{12}H_{36}N_4Si_4Sn_4$: C 17.49, H 4.41; found: C 17.51, H 4.42.

Crystal data for **13**. $C_{12}H_{36}N_4Si_4Sn_4$: $M_r = 869.64 g\ cm^{-3}$, crystal dimensions 0.221 x 0.204 x 0.102 mm, monoclinic, space group $C2/m$, $a = 26.05(2)$, $b = 12.066(9)$, $c = 10.933(8)$ Å, $\alpha = 90$, $\beta = 110.176^\circ$; $V = 3225(4)$ Å³, $Z = 4$, $\rho_{calcd} = 1.791 g\ cm^{-3}$, Siemens SMART CCD diffractometer, $1.67 \leq \theta \leq 28.77^\circ$, $Mo_{K\alpha}$ radiation ($\lambda = 0.71073$ Å), ω scans, $T = 193(2)$ K; of 10,430 measured reflections, 4,037 were independent and 2,894 observed with $I > 2\sigma(I)$, $-28 \leq h \leq 33$, $-15 \leq k \leq 14$, $-14 \leq l \leq 9$; $R_1 = 0.0349$, $wR_2 = 0.0711$, GOF = 1.053 for 141 parameters, $\Delta\rho_{max} = 0.981 e\text{Å}^{-3}$. The structure was solved by direct methods (SHELXS-97) and refined by full-matrix least-squares procedures (SHELXL-97), Lorentz polarization corrections and absorption correction (SADABS) were applied, $\mu = 3.220 mm^{-1}$, min./max. transmission 0.7348/0.5364.

*Synthesis of $[Ge(\mu_3\text{-NSiMe}_3)]_4$ (**14**):* Compound **14** was prepared in an analogous fashion to compound **13** using $[(\text{Me}_3\text{Sn})(\text{Me}_3\text{Si})\text{NLi}\bullet(\text{Et}_2\text{O})]_2$ (0.80 g, 1.20 mmol) and GeCl_2 (0.34g, 2.41 mmol). Pale yellow crystals were grown from CH_2Cl_2 at -80°C over a two-day period. Yield: 0.11 g (29%); Pale yellow crystals decomposed at 190°C ; ^1H NMR (400 MHz, C_6D_6 , 25°C , TMS): δ 0.312 (s, SiCH_3); ^{13}C NMR (100.6 MHz, C_6D_6 , 25°C , TMS): δ -1.465 (s, SiCH_3); elemental analysis calculated (%) for $\text{C}_{12}\text{H}_{36}\text{N}_4\text{Ge}_4\text{Si}_4$: C 22.55, H 5.68, N 8.76, found: C 23.56, H 5.24, N 9.10.

Crystal data for **14**. $\text{C}_{15.5}\text{H}_{40}\text{N}_4\text{Ge}_4\text{Si}_4$: $M_r = 685.23 \text{ g cm}^{-3}$, crystal dimensions $0.56 \times 0.20 \times 0.17 \text{ mm}$, monoclinic, space group $C2/c$, $a = 25.748(5)$, $b = 11.878(2)$, $c = 21.478(4) \text{ \AA}$, $\alpha = 90$, $\beta = 110.690^\circ$; $V = 6145(2) \text{ \AA}^3$, $Z = 8$, $\rho_{\text{calcd}} = 1.481 \text{ g cm}^{-3}$, Siemens SMART CCD diffractometer, $1.69 \leq \theta \leq 28.70^\circ$, $\text{MoK}\alpha$ radiation ($\lambda = 0.71073 \text{ \AA}$), ω scans, $T = 193(2) \text{ K}$; of 18,078 measured reflections, 7,251 were independent and 5,531 observed with $I > 2\sigma(I)$, $-29 \leq h \leq 33$, $-14 \leq k \leq 15$, $-28 \leq l \leq 12$; $R_1 = 0.0506$, $wR_2 = 0.1330$, GOF = 1.057 for 269 parameters, $\Delta\rho_{\text{max}} = 1.412 \text{ e\AA}^{-3}$. The structure was solved by direct methods (SHELXS-97) and refined by full-matrix least-squares procedures (SHELXL-97), Lorentz polarization corrections and absorption correction (SADABS) were applied, $\mu = 4.041 \text{ mm}^{-1}$, min./max. transmission 0.5466/0.2102.

*Synthesis of $[Pb(\mu_3\text{-NSiMe}_3)]_4$ (**15**):* Compound **15** was prepared in an analogous fashion to compound **13** using $[(\text{Me}_3\text{Sn})(\text{Me}_3\text{Si})\text{NLi}\bullet(\text{Et}_2\text{O})]_2$ (0.75 g, 1.13 mmol) and PbCl_2 (0.63g, 2.26 mmol). Yellow crystals were grown from CH_2Cl_2 at -80°C over a two-day period. Yield: 0.25 g (38%); Yellow crystals decomposed at 225°C ; ^1H NMR (400 MHz, C_6D_6 , 25°C , TMS): δ 0.027 (s, SiCH_3); ^{13}C NMR (100.6 MHz, C_6D_6 , 25°C , TMS):

δ -0.389 (s, SiCH₃); MS (EI, 274°C): m/z 1178 [M⁺]; IR (nujol): 1255 (m), 1242 (m), 864 (m), 826 (s), 741 (m), 523 (m) cm⁻¹; elemental analysis calculated (%) for

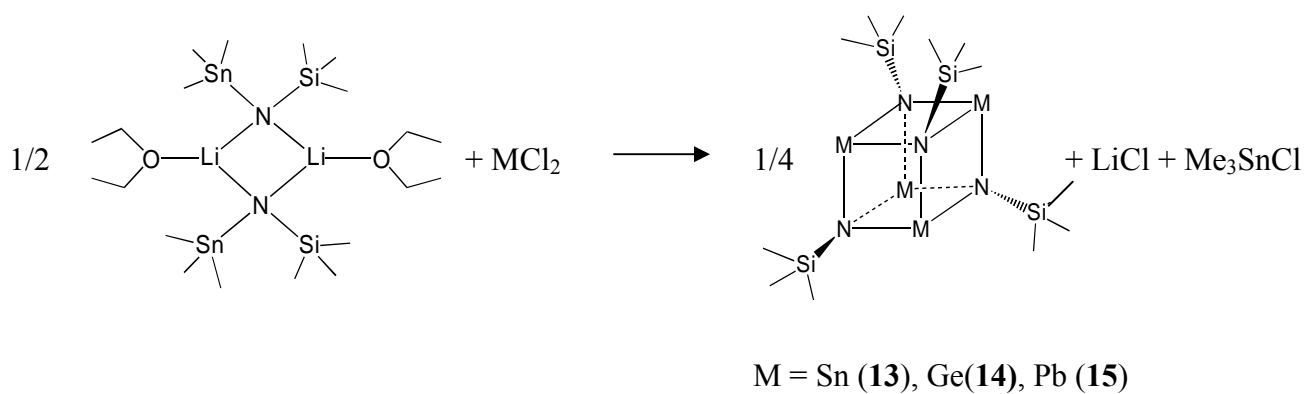
C₁₂H₃₆N₄Pb₄Si₄: C 12.24, H 3.08, N 4.76, found: C 12.19, H 3.09, N 4.89.

Crystal data for **15**. C₁₂H₃₆N₄Pb₄Si₄: M_r = 1177.57 g cm⁻³, crystal dimensions 0.459 x 0.408 x 0.170 mm, trigonal, space group $R\bar{3}$, a = 10.7447(8), c = 47.935(7) Å, α = 90, γ = 120°; V = 4792.6(9) Å³, Z = 6, ρ_{calcd} = 2.448 g cm⁻³, Siemens SMART CCD diffractometer, $2.23 \leq \theta \leq 28.74^\circ$, MoK α radiation (λ = 0.71073 Å), ω scans, T = 193(2) K; of 8,240 measured reflections, 2,473 were independent and 2,127 observed with $I > 2\sigma(I)$, $-14 \leq h \leq 11$, $-12 \leq k \leq 14$, $-54 \leq l \leq 63$; R_1 = 0.0507, wR_2 = 0.1426, GOF = 1.082 for 82 parameters, $\Delta\rho_{\text{max}}$ = 4.103 eÅ⁻³. The structure was solved by direct methods (SHELXS-97) and refined by full-matrix least-squares procedures (SHELXL-97), Lorentz polarization corrections and absorption correction (SADABS) were applied, μ = 21.167 mm⁻¹, min./max. transmission 0.1234/0.0368.

Results and Discussion

Synthesis

Compounds **13-15** were prepared analogously by reacting the appropriate divalent metal chloride with 0.5 equivalents of compound **2** (see Scheme 5.1). The reaction mixtures were stirred overnight at room temperature and then filtered to remove LiCl. The solvent was then removed, the solid product residues extracted with 15 mL of CH₂Cl₂, and crystals of each compound grown over a two-day period at -80°C.



Scheme 5.1. Synthesis of compounds **13-15**.

Characterization

Crystals of compounds **13-15** were each analyzed by a single crystal X-ray diffraction experiment. The results are shown in Figures 5.1-5.3.

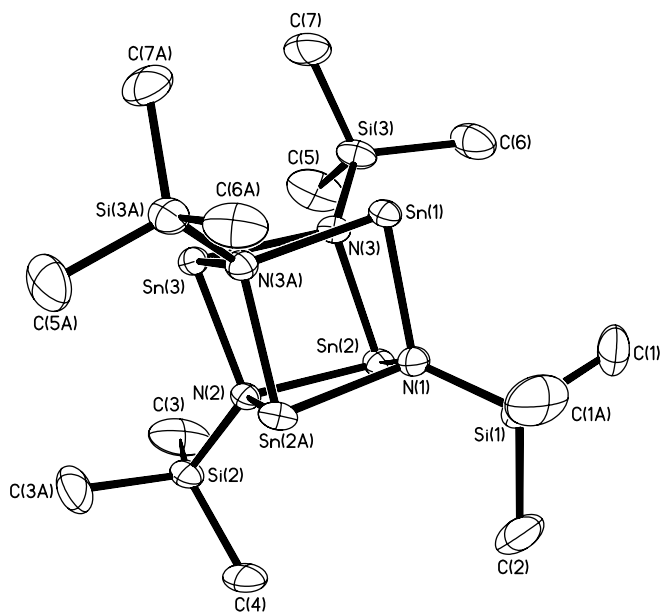


Figure 5.1. ORTEP plot representation (30% probability) with numbering scheme for compound **13**. Hydrogen atoms have been omitted for clarity.

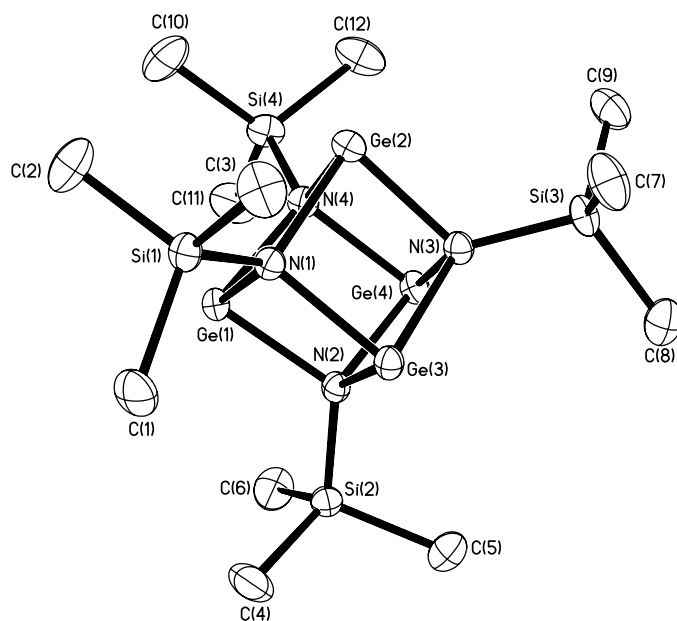


Figure 5.2. ORTEP plot representation (30% probability) with numbering scheme for compound **14**. Hydrogen atoms have been omitted for clarity.

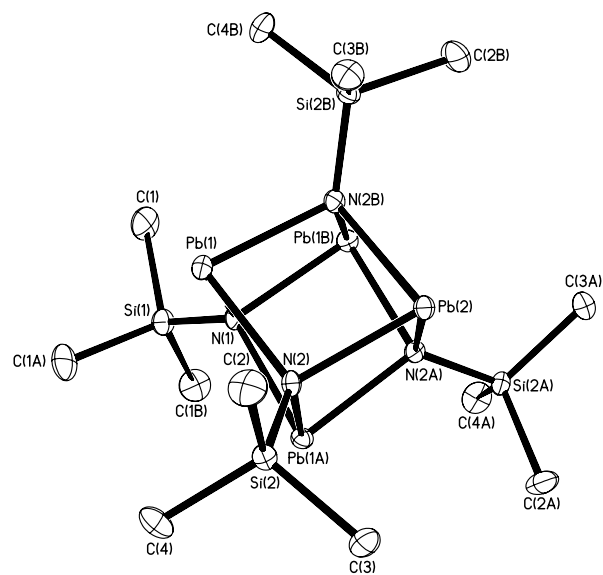


Figure 5.3. ORTEP plot representation (30% probability) with numbering scheme for compound **15**. Hydrogen atoms have been omitted for clarity.

All three complexes exist as tetramers in the solid state, with the trimethylsilyl imide units each bridging three divalent metal centers. A summary of the principal interatomic distances and angles for compounds **13-15** is provided in Table 5.1, and a complete list of all distances and angles can be found in Tables A.48, A.52, and A.56, respectively.

Table 5.1. Selected average interatomic distances (Å) and angles (degrees) for compounds **13-15**.

(13)	distance/angle	(14)	distance/angle	(15)	distance/angle
Si-N	1.733(5)	Si-N	1.742(3)	Si-N	1.704(11)
Sn-N	2.203(4)	Ge-N	2.013(3)	Pb-N	2.301(7)
Sn-N-Sn	97.26(14)	Ge-N-Ge	96.65(12)	Pb-N-Pb	97.4(3)
N-Sn-N	82.27(15)	N-GeN	84.06(6)	N-Pb-N	81.8(3)

Although the synthesis of compound **13** (via the reaction of **2** with SnCl₂) differs from the route employed by Veith, *et al.*, who reacted the cyclic diazastannylenes, Sn(^tBuN)₂SiMe₂, with the primary amine, Me₂SiNH₂,⁴ the results of single crystal X-ray diffraction studies are in both cases analogous.

Conversely, the incorporation of the trimethylsilyl moiety into germanium- or lead-nitrogen cubanes has to our knowledge not been reported to date. However, the configuration of the central M₄N₄ skeleton does not differ drastically from other Group 14-nitrogen cubane species described formerly. The M₄N₄ core for both **14** and **15** exhibits a distortion from a perfect cube, as evidenced by the average angles of 84.06° (N-Ge-N) and 96.65° (Ge-N-Ge) in **14**, as well as the average angles of 81.8° (N-Pb-N)

and 97.40° (Pb-N-Pb) in **15**. This type of distortion is common for similar Group 14-nitrogen cubanes. Comparison to compound **13** (average N-Sn-N = 83.12° and average Sn-N-Sn = 96.52°) indicates an increasing trend of distortion from perfect cube geometry from germanium to lead. This can be attributed to the decrease in sp-hybridization in the heavier tin and lead atoms. The average Ge-N and Pb-N interatomic distances of 2.013 Å in **14** and 2.304 Å in **15** are comparable to those found in previous reports: [GeN(C₆H₆)]₄, 2.019 Å;⁵ [PbN(C₆H₁₂)]₄, 2.303 Å;⁶ and [PbN(2,6-*i*-Pr₂C₆H₃)]₄, 2.337 Å.⁷ The distorted tetrahedral geometry about the silicon atoms in **14** and **15**, with average Si-N interatomic distances of 1.742 and 1.704 Å, respectively, is in agreement with previous structures containing the trimethylsilyl moiety in a similar chemical environment: (Me₃C)Al₂Li₂[μ₃-N(SiMe₃)]₄, Si-N_{avg} = 1.691 Å;⁸ [MeGa(μ₃-NSiMe₃)]₄, Si-N_{avg} = 1.727 Å;⁹ [MeIn(μ₃-NSiMe₃)]₂·[Li(Me₃Si)N-NH^tBu]₂, Si-N_{avg} = 1.743 Å.¹⁰

Since it is ultimately desired to utilize this class of compounds as MOCVD precursors, it was of utmost importance to determine whether these high molecular weight compounds possess sufficient volatility and vapor phase stability. The results of the thermogravimetric analysis (TGA) of compound **15** (Figure 5.4) indicate that complexes possessing this tetranuclear geometry exhibit sufficient volatility and vapor phase integrity for potential employment as MOCVD precursors.

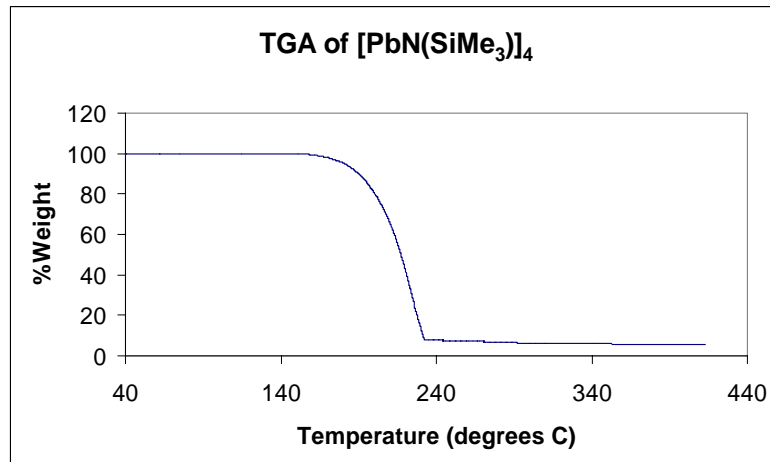


Figure 5.4. TGA plot of percent weight vs. temperature for compound **15**.

Conclusion

Compound **13**, previously synthesized and characterized by Veith, *et al.*, was prepared using a method that employed the heteroleptic stannylamide, [(Me₃Sn)(Me₃Si)NLi•Et₂O]₂ (**2**) as a starting material. This synthetic route was successfully extended to the congeners possessing germanium and lead. Compounds **14** and **15** are rare examples of Ge- and Pb-nitrogen heterocubanes and represent the first report of either class of compounds that contain the trimethylsilyl moiety. These results demonstrate the success of the molecular design strategy aimed at changing the identity of the endo-cube dicationic metal and indicate that the use of other lithiated stannylamides, such as [(Me₃Sn)₂NLi•Et₂O]₂ (**1**) and [(Me₃Sn)(Me₃Ge)NLi•Et₂O]₂ (**3**), may provide access to additional series of Group 14-nitrogen heterocubanes.

SECTION B: MOLECULAR DESIGN OF GROUP 14-NITROGEN

HETEROCUBANES - MODIFICATION OF THE EXO-CUBE SUBSTITUENT:



Introduction

Chapter 5 – Part A demonstrates the modification of the endo-cube dicationic metal by reacting the appropriate metal dichloride with the heteroleptic stannylamide, $[(\text{Me}_3\text{Sn})(\text{Me}_3\text{Si})\text{NLi}\cdot\text{Et}_2\text{O}]_2$ (**2**). This sub-chapter aims to arrive at a synthetic route that can exhibit control over the identity of the exo-cube substituent. Thus, the synthesis and characterization of the tin-nitrogen heterocubanes, $[\text{Sn}(\mu_3\text{-NGeMe}_3)]_4$ (**16**) and $[\text{Sn}(\mu_3\text{-NSnMe}_3)]_4$ (**17**) are described herein.

Experimental

All manipulations were carried out in a dry atmosphere glovebox or by standard Schlenk techniques. All solvents were dried over Na° metal or P_2O_5 (CH_2Cl_2) and were freshly distilled under an inert atmosphere prior to use. SnCl_2 was purchased from Alfa Aesar and used without further purification. $[(\text{Me}_3\text{Sn})_2\text{NLi}\cdot(\text{THF})]_2$ and $[(\text{Me}_3\text{Sn})(\text{Me}_3\text{Ge})\text{NLi}\cdot(\text{Et}_2\text{O})]_2$ were prepared as described in Chapter 2. All NMR experiments were performed on a Bruker 400 MHz Spectrometer at 300K using C_6D_6 solvent that was distilled over CaH_2 and stored under argon. ^1H and ^{13}C spectra were referenced to TMS. ^{119}Sn spectra were externally referenced to Me_4Sn . Elemental analyses were performed in triplicate on a Perkin Elmer Series II CHNS/O Analyzer

2400, FT-IR measurements were performed on a Bruker Equinox 55 Spectrometer, mass spectrometry analyses were done on a VG Instruments 70SE (Electron Impact; 70eV), and UV/VIS measurements were performed on a Perkin Elmer UV/VIS/NIR Lambda 19 Spectrometer. All TGA experiments were performed on a Perkin Elmer 7/DX thermal analyser interfaced to a Perkin Elmer Thermal Analysis Controller (TAC). The instrument is housed in a dry atmosphere glovebox. Argon was used as the purge gas and all %weight vs. temperature profiles were done at a 10°C/min. temperature ramp under ambient pressure.

*Synthesis of $[Sn(\mu_3-NGeMe_3)]_4$ (**16**):* Compound **16** was prepared in an analogous fashion to compound **13** using $[(Me_3Sn)(Me_3Ge)NLi\bullet(Et_2O)]_2$ (0.50 g, 0.66 mmol) and $SnCl_2$ (0.25 g, 1.33 mmol). Yellow crystals were grown from CH_2Cl_2 at $-80^\circ C$ over a two-day period. Yield: 0.07 g (21%); Yellow crystals decomposed at $250^\circ C$; 1H NMR (400 MHz, C_6D_6 , $25^\circ C$, TMS): δ 0.45 (s, $GeCH_3$); ^{13}C NMR (100.6 MHz, C_6D_6 , $25^\circ C$, TMS): δ 0.21 (s, $GeCH_3$); ^{119}Sn NMR (149.3 MHz, C_6D_6 , $25^\circ C$, Me_4Sn): δ 954 (s); MS (EI, $270^\circ C$): m/z 1002 $[M^+]$; IR (nujol): 1075 (m), 818 (m), 725 (m), 599(s), 563 (m), 515 (m) cm^{-1} ; elemental analysis calculated (%) for $C_{12}H_{36}N_4Sn_4Ge_4$: C 14.39, H 3.62, N 5.59, found: C 14.41, H 3.22, N 5.71.

Crystal data for **16**. $C_{12}H_{36}N_4Sn_4Ge_4$: $M_r = 1033.57$ g cm^{-3} , crystal dimensions 0.19 x 0.09 x 0.07 mm, monoclinic, space group $C2/c$, $a = 12.520(4)$, $b = 17.891(5)$, $c = 15.642(5)$ Å, $\alpha = 90$, $\beta = 107.536^\circ$; $V = 3341.1(17)$ Å³, $Z = 4$, $\rho_{calcd} = 2.055$ g cm^{-3} , Siemens SMART CCD diffractometer, $2.05 \leq \theta \leq 28.75^\circ$, $Mo_{K\alpha}$ radiation ($\lambda = 0.71073$ Å), ω scans, $T = 193(2)$ K; of 10,311 measured reflections, 3,989 were independent and

1,908 observed with $I > 2\sigma(I)$, $-8 \leq h \leq 16$, $-18 \leq k \leq 23$, $-21 \leq l \leq 19$; $R_1 = 0.0865$, $wR_2 = 0.2208$, GOF = 0.975 for 130 parameters, $\Delta\rho_{\max} = 4.388 \text{ e}\text{\AA}^{-3}$. The structure was solved by direct methods (SHELXS-97) and refined by full-matrix least-squares procedures (SHELXL-97), Lorentz polarization corrections and absorption correction (SADABS) were applied, $\mu = 6.497 \text{ mm}^{-1}$, min./max. transmission 0.6664/0.3763.

Synthesis of $[\text{Sn}(\mu_3\text{-NSnMe}_3)]_4$ (17): Compound **17** was prepared in an analogous fashion to compound **13** using $[(\text{Me}_3\text{Sn})_2\text{NLi}\cdot(\text{THF})]_2$ (0.50 g, 0.59 mmol) and SnCl_2 (0.22 g, 1.19 mmol). Orange crystals were grown from CH_2Cl_2 at -80°C over a two-day period. Yield: 0.18 g (51%); Orange crystals decomposed at 210°C ; ^1H NMR (400 MHz, C_6D_6 , 25°C , TMS): δ 0.29 (s, SnCH_3); ^{13}C NMR (100.6 MHz, C_6D_6 , 25°C , TMS): δ 1.36 (s, SnCH_3); ^{119}Sn NMR (149.3 MHz, C_6D_6 , 25°C , Me_4Sn): δ -40.4 (s, SnMe_3), 797.3 (s, $\text{Sn}(u_3\text{-N})$); MS (EI, 273°C): m/z 1188 $[\text{M}^+]$; IR (nujol): 1181 (w), 1033 (m), 721 (m), 663 (m), 529 (w) cm^{-1} ; elemental analysis calculated (%) for $\text{C}_{12}\text{H}_{36}\text{N}_4\text{Sn}_8$: C 12.15, H 3.06, N 4.72, found: C 11.96, H 2.78, N 3.96.

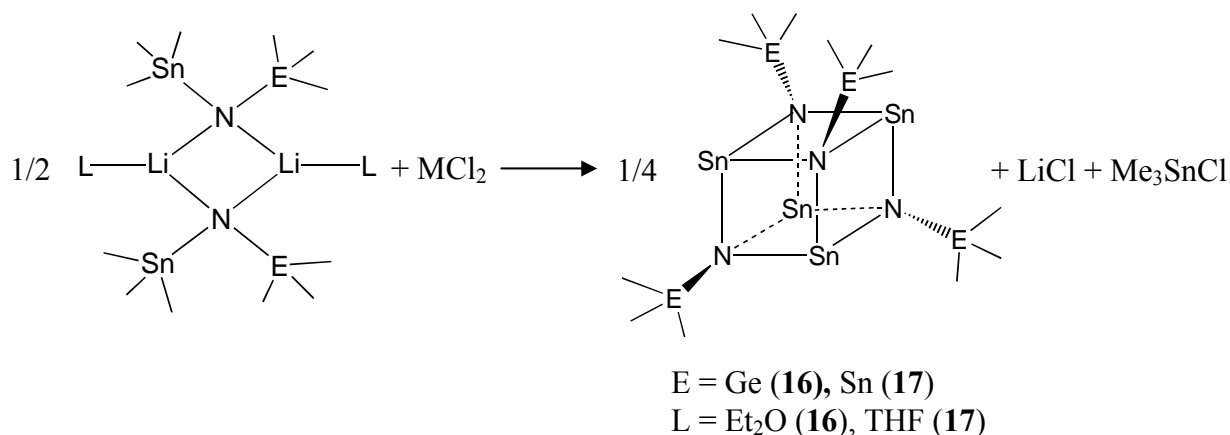
Crystal data for **17**. $\text{C}_{12}\text{H}_{36}\text{N}_4\text{Sn}_8$: $M_r = 1185.97 \text{ g cm}^{-3}$, crystal dimensions 0.14 x 0.10 x 0.10 mm, cubic, space group $I\bar{4}3m$, $a = 11.6106(14) \text{ \AA}$, $\alpha = 90^\circ$; $V = 1565.2(3) \text{ \AA}^3$, $Z = 2$, $\rho_{\text{calcd}} = 2.516 \text{ g cm}^{-3}$, Siemens SMART CCD diffractometer, $2.48 \leq \theta \leq 28.69^\circ$, $\text{MoK}\alpha$ radiation ($\lambda = 0.71073 \text{ \AA}$), ω scans, $T = 193(2) \text{ K}$; of 4,478 measured reflections, 405 were independent and 394 observed with $I > 2\sigma(I)$, $-15 \leq h \leq 15$, $-15 \leq k \leq 15$, $-8 \leq l \leq 15$; $R_1 = 0.0214$, $wR_2 = 0.0474$, GOF = 1.226 for 18 parameters, $\Delta\rho_{\max} = 0.915 \text{ e}\text{\AA}^{-3}$. The structure was solved by direct methods (SHELXS-97) and refined by full-matrix least-squares procedures (SHELXL-97), Lorentz polarization corrections and absorption

correction (SADABS) were applied, $\mu = 6.276 \text{ mm}^{-1}$, min./max. transmission 0.5669/0.4823.

Results and Discussion

Synthesis

Compounds **16** and **17** were prepared analogously by reacting the appropriate divalent metal chloride with 0.5 equivalents of compound **2** (see Scheme 5.2). The reaction mixtures were stirred overnight at room temperature and LiCl was filtered off. The solvent was then removed, the solid product residues extracted into about 15 mL of CH_2Cl_2 , and crystals of each compound were grown over a two-day period at -80°C .



Scheme 5.2. Synthesis of compounds **16-17**.

Characterization

Crystals of compounds **16** and **17** were each analyzed by a single crystal X-ray diffraction experiment. The results are shown in Figures 5.5 and 5.6.

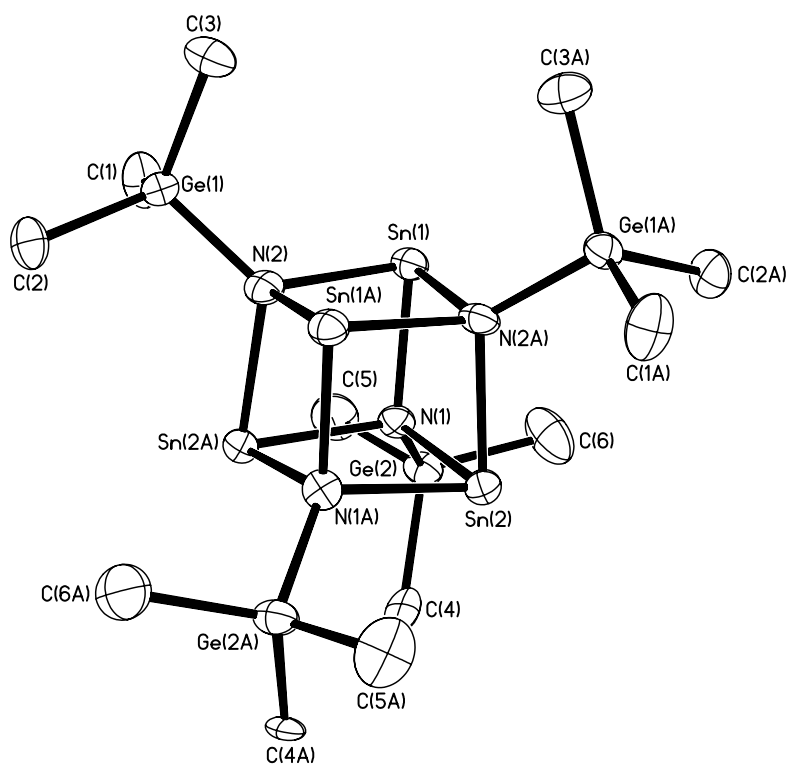


Figure 5.5. ORTEP plot representation (30% probability) with numbering scheme for compound **16**. Hydrogen atoms have been omitted for clarity.

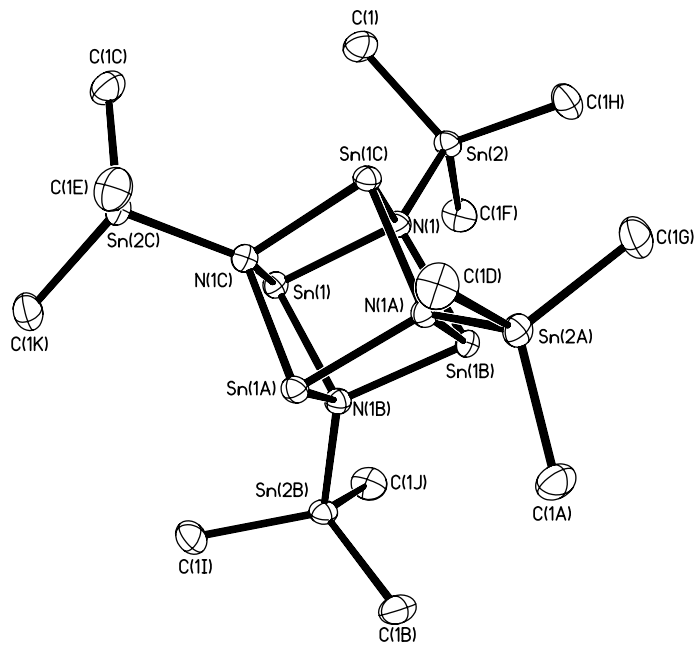


Figure 5.6. ORTEP plot representation (30% probability) with numbering scheme for compound **17**. Hydrogen atoms have been omitted for clarity.

Both complexes exist as tetramers in the solid state, with the trimethylstannyl and trimethylgermyl imide units each bridging three divalent metal centers. A summary of the principal interatomic distances and angles for compounds **16** and **17** is provided in Table 5.2, and a complete list of all distances and angles can be found in Tables A.60 and A.64, respectively.

Table 5.2. Selected average interatomic distances (Å) and angles (degrees) for compounds **16** and **17**.

(16)	distance/angle	(17)	distance/angle
Ge-N	1.860(12)	Sn-N	2.043(7)
Sn-N (endo-cube)	2.207(11)	Sn-N (endo-cube)	2.196(3)
Sn-N-Sn	97.2(4)	Sn-N-Sn	96.5(2)
N-Sn-N	82.27(4)	N-Sn-N	83.1(2)

The simultaneous interaction of nitrogen with Sn(II) and Ge(IV) metal centers observed in **16** is to our knowledge unique. In addition, this compound is the first Group 14-nitrogen heterocubane possessing exo-cube germanium. However, the configuration of the central Sn₄N₄ skeleton does not differ drastically from other tin-nitrogen cubane species previously reported in the literature. The Sn₄N₄ core exhibits a distortion from a perfect cube, as evidenced by the average N-Sn(1)-N angle of 82.27(4)° and the average Sn-N-Sn angle of 97.2(4)°. This distortion is commonplace in such Group 14-nitrogen cubanes, and was also observed in compounds **13-15**. The average Ge-N interatomic

distance [1.860(12) Å] is in agreement with previously reported values

$[(\text{Li}[\text{N}(\text{GeMe}_3)_2])_3, \text{Ge-N}_{\text{avg}} = 1.837 \text{ Å}]$.¹¹

The occurrence of the nitrogen-bridged Sn(II) and Sn(IV) centers observed in **17** is also believed to be unprecedented and the exo-cube trimethyltin moiety represents the heaviest exo-cube substituent in a Group 14-nitrogen cubane to date. The Sn₄N₄ core in **17** also exhibits distortion from a perfect cube, as evidenced by the average N-Sn(1)-N angle of 83.1(2)° and the average Sn-N-Sn angle of 96.5(2)°. This distortion is analogous to that observed in compounds **13-16**. The geometry about the tin(IV) atoms is distorted tetrahedral and the average Sn-N interatomic distance of 2.043(7) Å is in agreement with tin(IV)-nitrogen distances previously reported: SnBr[N(SiMe₃)₂]₃, 2.056(7) Å,¹² Sn(CH₃)(NR₂)₃, (R = C(CD₃)₂CH₃, Ar = 3,5-C₆H₃Me₂), 2.044(4) Å¹³ and Sn(NCPh₂)₄, 2.068(37) Å.¹⁴ The average Sn(II)-N interatomic distances in both **16** and **17** are similar to values found for other tin-nitrogen cubanes: [Sn(μ₃-NSiMe₃)]₄, 2.196(4) Å;⁴ [Sn(μ₃-N{4-MeOC₆H₄})]₄, 2.205(3) Å¹⁵ and [Sn(μ₃-N{2,6-ⁱPr₂C₆H₃})]₄, 2.227(8) Å.¹⁶

The tin-nitrogen heterocubanes, **13**, **16**, and **17** were also characterized by multinuclear NMR techniques. Specifically, the ¹¹⁹Sn NMR of these compounds aids in verifying the oxidation state of the tin(II) atoms located in the endo-cube position, and in the case of compound **17**, the oxidation state of the exo-cube trimethyl tin moiety. The positions of the ¹¹⁹Sn resonances for these compounds are summarized in Table 5.3. The endo-cube tin resonances for **13**, **16**, and **17** do not show any discernable trend, but do fall in the predicted range for tin(II) cations. The exo-cube tin resonance found in **17** is observed at higher field, expected for tin(IV) nuclei (see Figure 5.7).

Table 5.3. ^{119}Sn NMR resonances observed for compounds **13**, **16**, and **17**.

(13)	Resonance (ppm)	(16)	Resonance (ppm)	(17)	Resonance (ppm)
Endo-cube Sn(II)	782	Endo-cube Sn(II)	954	Endo-cube Sn(II)	797
Exo-cube Sn(IV)	-	-	-	-	-40

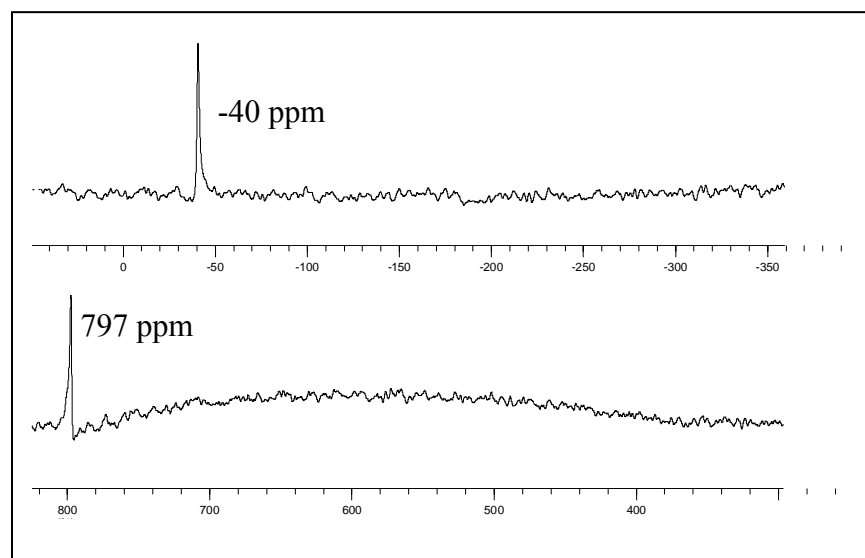


Figure 5.7. ^{119}Sn NMR spectrum of compound **17** (chemical shift scale in ppm).

The volatility of compound **17** was determined by TGA. The cubane species is volatile below 250°C, but appears to decompose at higher temperatures. The TGA plot of percent weight versus temperature is graphically depicted in Figure 5.8.

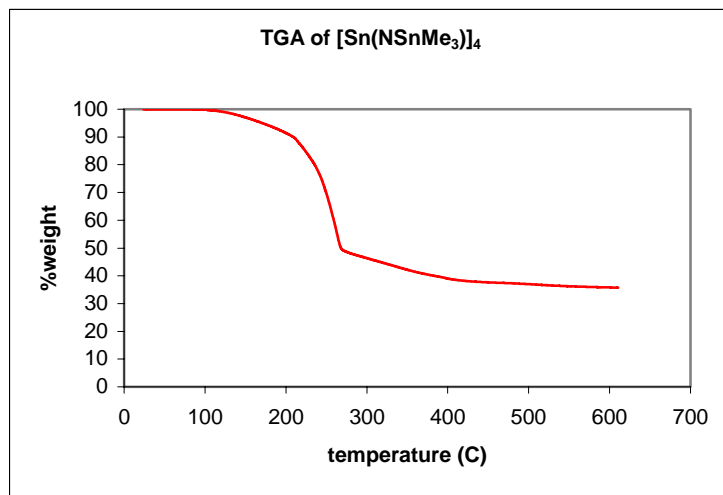


Figure 5.8. TGA plot of percent weight vs. temperature for compound **17**.

Conclusion

Since the molecular design of the endo-cube metal in Group 14-nitrogen heterocubanes was achieved in Chapter 5 – Part A, it was of interest to determine if the identity of the exo-cube substituent could also be controlled. Thus, this chapter describes the synthesis and characterization of the tin-nitrogen heterocubanes possessing exo-cube germanium and exo-cube tin, $[\text{Sn}(\mu_3\text{-NGeMe}_3)]_4$ (**16**) and $[\text{Sn}(\mu_3\text{-NSnMe}_3)]_4$ (**17**). The preparation of these compounds demonstrates that not only the endo-cube metal, but also the exo-cube heavy-atom substituent can be modified. In addition, compounds **16-17**, as well as

compound **13** are amenable to characterization via ^{119}Sn NMR and provide spectroscopic information on tin nuclei that are found in unusual coordination environments. The results reported here are encouraging in the respect that additional Group 14-nitrogen heterocubane species may be successfully synthesized and that the molecular design of this class of compounds may ultimately lead to precursors for the MOCVD of ZTT.

SECTION C: MOLECULAR DESIGN OF GROUP 14-NITROGEN
HETEROCUBANES - MODIFICATION OF BOTH THE EXO- AND ENDO-CUBE
SUBSTITUENT: $[M(\mu_3\text{-NGeMe}_3)]_4$ (M = Ge, Pb)

Introduction

The first two sub-chapters described the synthesis and characterization of a variety of Group 14-nitrogen heterocubanes. Chapter 5 – Part A demonstrated that the endo-cube metal could be altered by changing the metal dichloride used in the synthetic workup. Chapter 5 – Part B established that the exo-cube substituent could be modified by using a different lithiated stannylamine in the course of the synthesis. This chapter describes the procedures used to obtain analogous heterocubane species possessing both modified endo-cube dications and exo-cube substituents. Thus, the synthesis and characterization of $[\text{Ge}(\mu_3\text{-NGeMe}_3)]_4$ (**18**) and $[\text{Pb}(\mu_3\text{-NGeMe}_3)]_4$ (**19**) is described herein.

Experimental

All manipulations were carried out in a dry atmosphere glovebox or by standard Schlenk techniques. All solvents were dried over Na^o metal or P₂O₅ (CH₂Cl₂) and were freshly distilled under an inert atmosphere prior to use. SnCl₂ and PbCl₂ reagents were purchased from Alfa Aesar and used without further purification. $[(\text{Me}_3\text{Sn})_2\text{NLi}\bullet(\text{THF})]_2$, $[(\text{Me}_3\text{Sn})(\text{Me}_3\text{Si})\text{NLi}\bullet(\text{Et}_2\text{O})]_2$, and $[(\text{Me}_3\text{Sn})(\text{Me}_3\text{Ge})\text{NLi}\bullet(\text{Et}_2\text{O})]_2$ were prepared as described in Chapter 2. GeCl₂·(dioxane) was prepared according to literature procedures.³ All NMR experiments were performed on a Bruker 400 MHz Spectrometer at 300K using C₆D₆ solvent that was distilled over CaH₂ and stored under argon. ¹H, ¹³C,

and ^{29}Si spectra were referenced to TMS. ^{119}Sn and ^7Li spectra were externally referenced to Me_4Sn and LiBr respectively. Elemental analyses were performed in triplicate on a Perkin Elmer Series II CHNS/O Analyzer 2400, FT-IR measurements were performed on a Bruker Equinox 55 Spectrometer, mass spectrometry analyses were done on a VG Instruments 70SE (Electron Impact; 70eV), and UV/VIS measurements were performed on a Perkin Elmer UV/VIS/NIR Lambda 19 Spectrometer. All TGA experiments were performed on a Perkin Elmer 7/DX thermal analyser interfaced to a Perkin Elmer Thermal Analysis Controller (TAC). The instrument is housed in a dry atmosphere glovebox. Argon was used as the purge gas and all %weight vs. temperature profiles were done at a $10^\circ\text{C}/\text{min}$. temperature ramp under ambient pressure.

*Synthesis of $[\text{Ge}(\mu_3\text{-NGeMe}_3)]_4$ (**18**):* Compound **18** was prepared in an analogous fashion to compound **13** using $[(\text{Me}_3\text{Sn})(\text{Me}_3\text{Ge})\text{NLi}\bullet(\text{Et}_2\text{O})]_2$ (0.60 g, 0.80 mmol) and GeCl_2 (0.23 g, 1.60 mmol). Pale yellow crystals were grown from CH_2Cl_2 at -80°C over a two-day period. Yield: 0.05 g (15%); Pale yellow crystals decomposed at 265°C ; ^1H NMR (400 MHz, C_6D_6 , 25°C , TMS): δ 0.50 (s, GeCH_3); ^{13}C NMR (100.6 MHz, C_6D_6 , 25°C , TMS): δ -1.14 (s, GeCH_3); MS (EI, 274°C): m/z 820 $[\text{M}^+]$; IR (nujol): 1261 (m), 1231 (m), 1015 (s), 824 (m), 735 (m), 603 (m), 558 (m) cm^{-1} ; elemental analysis calculated (%) for $\text{C}_{12}\text{H}_{36}\text{N}_4\text{Ge}_8$: C 17.62, H 4.44, N 6.86, found: C 17.74, H 4.34, N 7.34.

Crystal data for **18**. $\text{C}_{12}\text{H}_{36}\text{N}_4\text{Ge}_8$: $M_r = 817.17 \text{ g cm}^{-3}$, crystal dimensions 0.17 x 0.14 x 0.10 mm, cubic, space group $I-43m$, $a = 11.2872(10) \text{ \AA}$, $\beta = 90^\circ$; $V = 1438.0(2) \text{ \AA}^3$, $Z = 2$, $\rho_{\text{calcd}} = 1.887 \text{ g cm}^{-3}$, Siemens SMART CCD diffractometer, $2.55 \leq \theta \leq 28.79^\circ$, $\text{MoK}\alpha$

radiation ($\lambda = 0.71073 \text{ \AA}$), ω scans, $T = 193(2) \text{ K}$; of 4,569 measured reflections, 369 were independent and 329 observed with $I > 2\sigma(I)$, $-14 \leq h \leq 15$, $-12 \leq k \leq 15$, $-15 \leq l \leq 14$; $R_1 = 0.0339$, $wR_2 = 0.0757$, $\text{GOF} = 1.047$ for 18 parameters, $\Delta\rho_{\text{max}} = 0.785 \text{ e\AA}^{-3}$. The structure was solved by direct methods (SHELXS-97) and refined by full-matrix least-squares procedures (SHELXL-97), Lorentz polarization corrections and absorption correction (SADABS) were applied, $\mu = 8.245 \text{ mm}^{-1}$, min./max. transmission 0.4868/0.3346.

*Synthesis of $[\text{Pb}(\mu_3\text{-NGeMe}_3)]_4$ (**19**):* Compound **19** was prepared in an analogous fashion to compound **13** using $[(\text{Me}_3\text{Sn})(\text{Me}_3\text{Ge})\text{NLi}\bullet(\text{Et}_2\text{O})]_2$ (0.50 g, 0.66 mmol) and PbCl_2 (0.37 g, 1.33 mmol). Yellow crystals were grown from CH_2Cl_2 at -80°C over a two-day period. Yield: 0.25 g (55%); Yellow crystals decomposed at 265°C ; ^1H NMR (400 MHz, C_6D_6 , 25°C , TMS): δ 0.19 (s, GeCH_3); ^{13}C NMR (100.6 MHz, C_6D_6 , 25°C , TMS): δ -1.02 (s, GeCH_3); MS (EI, 42°C): m/z 1356 $[\text{M}^+]$; IR (nujol): 1228 (m), 812 (m), 719 (m), 589(m), 531 (w) cm^{-1} ; elemental analysis calculated (%) for $\text{C}_{12}\text{H}_{36}\text{N}_4\text{Pb}_4\text{Ge}_4$: C 10.63, H 2.68, N 4.13, found: C 10.57, H 2.61, N 4.22.

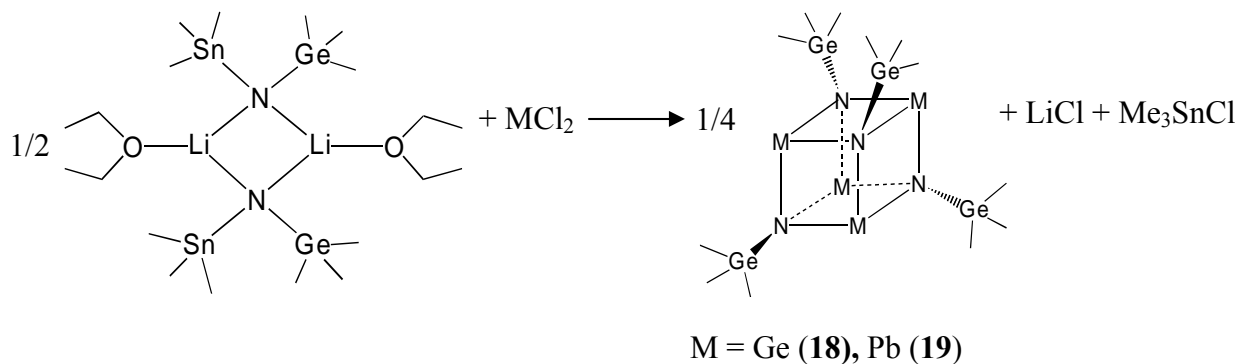
Crystal data for **19**. $M_r = 2674.85 \text{ g cm}^{-3}$, crystal dimensions 0.374 x 0.136 x 0.119 mm, cubic, space group $P-43n$, $a = 18.2282(14) \text{ \AA}$, $\alpha = 90^\circ$; $V = 6056.6(8) \text{ \AA}^3$, $Z = 4$, $\rho_{\text{calcd}} = 2.933 \text{ g cm}^{-3}$, Siemens SMART CCD diffractometer, $1.58 \leq \theta \leq 28.68^\circ$, $\text{MoK}\alpha$ radiation ($\lambda = 0.71073 \text{ \AA}$), ω scans, $T = 193(2) \text{ K}$; of 36,464 measured reflections, 2,561 were independent and 1,359 observed with $I > 2\sigma(I)$, $-21 \leq h \leq 23$, $-23 \leq k \leq 24$, $-14 \leq l \leq 23$; $R_1 = 0.0579$, $wR_2 = 0.1416$, $\text{GOF} = 0.974$ for 73 parameters, $\Delta\rho_{\text{max}} = 2.855 \text{ e\AA}^{-3}$. The structure was solved by direct methods (SHELXS-97) and refined by full-matrix least-

squares procedures (SHELXL-97), Lorentz polarization corrections and absorption correction (SADABS) were applied, $\mu = 26.067 \text{ mm}^{-1}$, min./max. transmission 0.5466/0.2102.

Results and Discussion

Synthesis

Compounds **18** and **19** were prepared analogously by reacting the appropriate divalent metal chloride with 0.5 equivalents of compound **3** (see Scheme 5.3). The reaction mixtures were stirred overnight at room temperature and LiCl was filtered off. The solvent was then removed, the solid product residues extracted into about 15 mL of CH_2Cl_2 , and crystals of each compound were grown over a two-day period at -80°C .



Scheme 5.3. Synthesis of compounds **18-19**.

Characterization

Crystals of compounds **18** and **19** were each analyzed by a single crystal X-ray diffraction experiment. The results are shown in Figures 5.9 and 5.10.

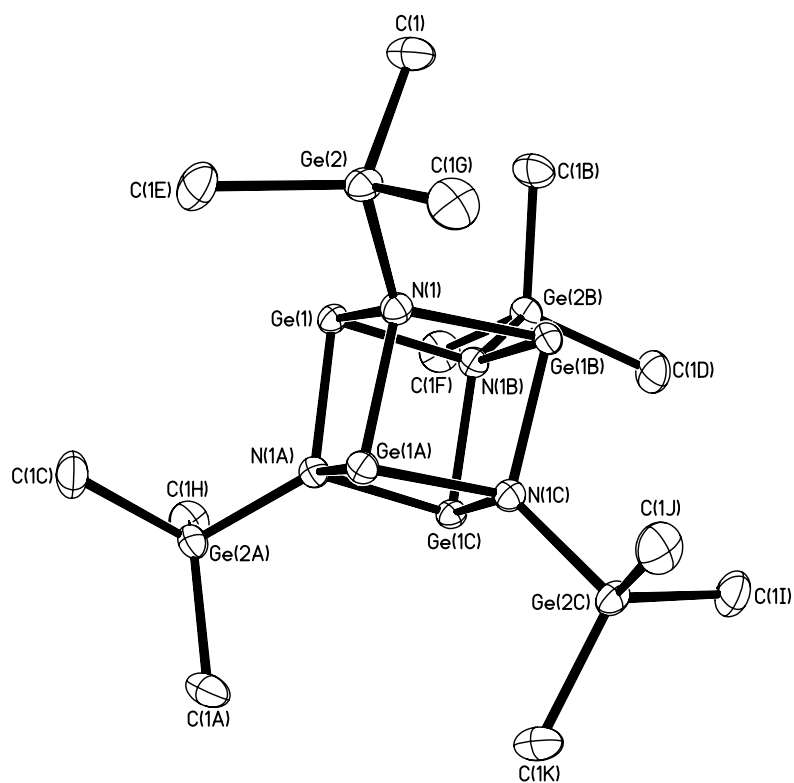


Figure 5.9. ORTEP plot representation (30% probability) with numbering scheme for compound **18**. Hydrogen atoms have been omitted for clarity.

Both complexes exist as tetramers in the solid state, with the trimethylgermyl imide units each bridging three divalent metal centers. A summary of the principal interatomic distances and angles for compounds **18** and **19** is provided in Table 5.4, and a complete list of all distances and angles can be found in Tables A.68 and A.72, respectively.

Table 5.4. Selected average interatomic distances (Å) and angles (degrees) for compounds **16**, **18**, and **19**.

(16)	distance/angle	(18)	distance/angle	(19)	distance/angle
Ge-N	1.860(12)	Ge-N	1.870(9)	Ge-N	1.850(2)
Sn-N (endo-cube)	2.207(11)	Ge-N (endo-cube)	2.002(4)	Pb-N (endo-cube)	2.293(14)
Sn-N-Sn	97.2(4)	Ge-N-Ge	95.7(3)	Pb-N-Pb	98.4(7)
N-Sn-N	82.27(4)	N-Ge-N	84.0(3)	N-Pb-N	80.9(7)

The molecular structure of compounds **18** and **19** were revealed by single-crystal X-ray diffraction techniques to be tetranuclear, based on a M_4N_4 architecture (Figure 5.6 and 5.7). Each nitrogen atom is four-coordinate, bridging three M(II) [M = Ge, Pb] metal centers and one germanium(IV) atom. The metal-nitrogen cage exhibits the typical distortion from perfect cube geometry, evidenced by the obtuse M-N-M angles and the acute N-M-N angles (see Table 5.4). The Ge(IV)-N interatomic distances of 1.870(9) Å and 1.850(2) Å (observed for **18** and **19**, respectively) are comparable to the previously reported value found in $(Li[N(GeMe_3)_2])_3$ [$Ge-N_{avg} = 1.837$ Å].¹¹ The endo-cube M-N interatomic distances (M = Ge, Pb) also fall in the expected range observed in previous

Group 14-nitrogen heterocubanes: **18** [Ge-N = 2.002 Å]; [GeN(C₆H₆)₄] [Ge-N_{avg} = 2.023 Å];⁵ **19** [Pb-N = 2.293 Å]; [PbN(C₆H₁₂)₄] [Pb-N = 2.303 Å]⁶ and [PbN(2,6-*i*-Pr₂C₆H₃)₄] [Pb-N = 2.337 Å].⁷

Compounds **18** and **19**, along with compound **16** comprise an additional series of Group 14-nitrogen heterocubanes. Similar to the series of structures consisting of compounds **13-15**, the distortion in the M₄N₄ core observed in **16**, **18**, and **19** increases as the molecular weight of the Group 14 element increases (see Table 5.4). The occurrence of this phenomenon was previously discussed in Chapter 5 – Part A.

The volatility of compound **19** was determined by TGA. The cubane species is volatile below 300°C, but appears to decompose at higher temperatures. The TGA plot of percent weight versus temperature is graphically depicted in Figure 5.11.

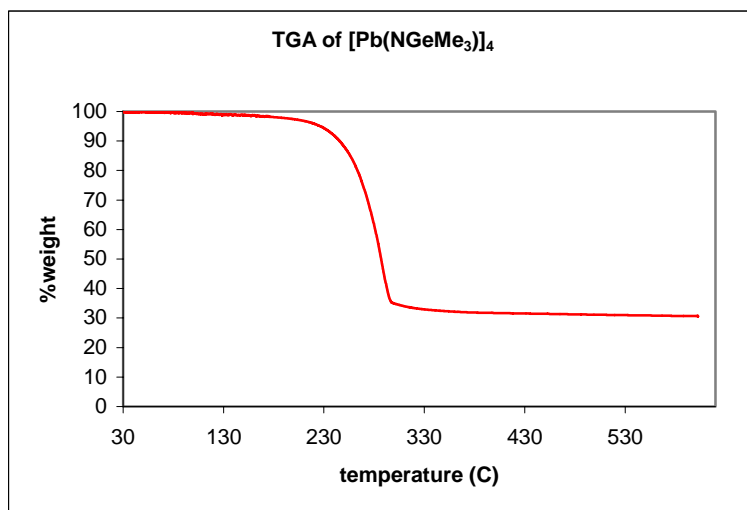


Figure 5.11. TGA plot of percent weight vs. temperature for compound **19**.

Conclusion

The first three sections of this chapter have discussed the use of both the homoleptic lithiated bis(stannylamine) (**1**) and heteroleptic lithiated stannylamines [(**2**) and (**3**)] as precursors to Group 14-nitrogen heterocubanes. The successful molecular design of these compounds, accomplished by varying the endo-cube metal and exo-cube substituent has been demonstrated and the culmination of this design approach is described in this sub-chapter via the synthesis and characterization of **18** and **19**. The ultimate goal of extending this design motif to include titanium and zirconium cations for the preparation of ZTT precursors will be explored in the final section of this chapter.

SECTION D: REACTION OF TIN-NITROGEN OXO OCUBANES WITH TETRAKIS

TITANIUM ALKOXIDES: $\text{Sn}_6(\mu_3\text{-O})_4(\mu_3\text{-O}^i\text{Pr})_4$ AND $\text{Sn}_6(\mu_3\text{-O})_4(\mu_3\text{-O}^t\text{Bu})_4$

Introduction

The first three sections of this chapter were devoted to exploring the use of lithiated stannylamines as precursors in the synthesis of Group 14-nitrogen heterocubanes and the subsequent molecular design of this class of compounds. Ideally, the incorporation of titanium or zirconium into either the endo-cube dication or exo-cube tetracation positions could potentially lead to MOCVD precursors for ZTT. However, dicationic titanium and zirconium are not synthetically useful species. In addition, trimethyl titanium chloride and trimethyl zirconium chloride reagents required to model the reactions described in the earlier sections of this chapter are not sufficiently stable at ambient conditions. Hence, an alternative design strategy is needed. The mixed-metal aminoalkoxide species previously reported by Veith, *et al.*, $(^i\text{PrO})_4\text{Ti}[\text{OPb}_4(\text{N}^t\text{Bu})_3]$ ¹⁷ proved to be a model complex for a potential mixed-metal aminoalkoxide possessing tin and titanium. This sub-chapter describes the synthesis of the previously reported oxo cubane, $[\text{Sn}_4(\text{N}^t\text{Bu})_3\text{O}]$ (**20**)¹⁸ and its reaction with tetrakis(alkoxide) titanium(IV) reagents. These reactions resulted in the isolation of the tin-oxygen cage structures $\text{Sn}_6(\mu_3\text{-O})_4(\mu_3\text{-O}^i\text{Pr})_4$ (**21**) and $\text{Sn}_6(\mu_3\text{-O})_4(\mu_3\text{-O}^t\text{Bu})_4$ (**22**). The synthesis and structural characterization of these compounds is described herein.

Experimental

All manipulations were carried out in a dry atmosphere glovebox or by standard Schlenk techniques. All solvents were dried over Na^o metal and were freshly distilled under an inert atmosphere prior to use. Ti(O^tBu)₄ was purchased from Alfa Aesar and t-butylamine was purchased from Aldrich and both were used without further purification. Sn(NMe₂)₂ was prepared according to literature procedures.¹⁹ Elemental analyses were performed in triplicate on a Perkin Elmer Series II CHNS/O Analyzer 2400 and FT-IR measurements were performed on a Bruker Equinox 55 Spectrometer.

Synthesis of Sn₄O(N^tBu)₃•CH₃CN (20): Tertiary-butyl amine (0.43 g, 5.9 mmol) was added dropwise to a THF (25 mL) solution of Sn(NMe₂)₂ (1.21 g, 5.9 mmol) at room temperature and stirred for 2 hours. An acetonitrile (10 mL) solution of H₂O (0.023 mL, 1.28 mmol) was then added dropwise, *in situ*, to the reaction mixture at −78°C. The solution was allowed to attain ambient temperature on its own, stirred for an additional 2 hours, and subsequently filtered through a Schlenk frit. Finally, all volatile material was removed *in vacuo* and a bright yellow powder was isolated. Yield: 0.168 g (15%); IR (nujol): 2359 (w), 1377 (m), 1021 (m), 799 (m) cm^{−1}; elemental analysis calculated (%) for C₁₄H₃₀N₄OSn₄: C 22.57, H 4.06, N 7.52, found: C 22.46, H 4.37, N 7.33.

Synthesis of Sn₆(μ₃-O)₄(μ₃-OⁱPr)₄ (21): Compound **20** (0.168 g, 0.24 mmol) was dispersed in hexane (20 mL) and to this was added a hexane solution of Ti(OⁱPr)₄ (0.068 g, 0.24 mmol) at room temperature. The reaction mixture was stirred overnight under an

argon atmosphere and the solution was filtered through a Schlenk frit. Yellow crystals were grown overnight at -40°C .

Crystal data for **21**. $\text{C}_{12}\text{H}_{28}\text{O}_8\text{Sn}_6$: $M_r = 1012.48 \text{ g cm}^{-3}$, crystal dimensions $0.14 \times 0.12 \times 0.10 \text{ mm}$, tetragonal, space group $I4(1)/a$, $a = 11.6029(10)$, $c = 18.017(3) \text{ \AA}$, $\alpha = 90^{\circ}$; $V = 2435.6(5) \text{ \AA}^3$, $Z = 4$, $\rho_{\text{calcd}} = 2.773 \text{ g cm}^{-3}$, Siemens SMART CCD diffractometer, $2.09 \leq \theta \leq 28.66^{\circ}$, $\text{MoK}\alpha$ radiation ($\lambda = 0.71073 \text{ \AA}$), ω scans, $T = 193(2) \text{ K}$; of 6755 measured reflections, 1482 were independent and 987 observed with $I > 2\sigma(I)$, $-15 \leq h \leq 14$, $-11 \leq k \leq 15$, $-24 \leq l \leq 22$; $R_1 = 0.0283$, $wR_2 = 0.0582$, $\text{GOF} = 1.086$ for 66 parameters, $\Delta\rho_{\text{max}} = 0.619 \text{ e\AA}^{-3}$. The structure was solved by direct methods (SHELXS-97) and refined by full-matrix least-squares procedures (SHELXL-97), Lorentz polarization corrections and absorption correction (SADABS) were applied, $\mu = 6.114 \text{ mm}^{-1}$, min./max. transmission 0.5744/0.4902.

*Synthesis of $\text{Sn}_6(\mu_3\text{-O})_4(\mu_3\text{-O}^t\text{Bu})_4$ (**22**):* Compound **20** (0.168 g, 0.24 mmol) was dispersed in hexane (20 mL) and to this was added a hexane solution of $\text{Ti}(\text{O}^t\text{Bu})_4$ (0.082 g, 0.24 mmol) at room temperature. The reaction mixture was stirred overnight under an argon atmosphere and the solution was filtered through a Schlenk frit. Yellow crystals were grown overnight at -80°C .

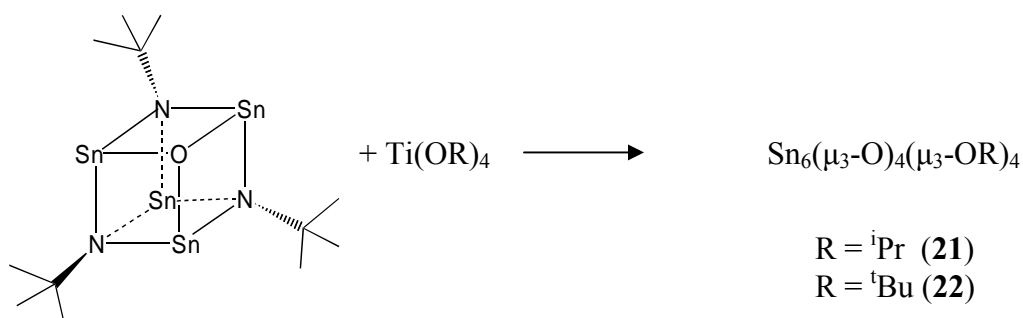
Crystal data for **22**. $\text{C}_{16}\text{H}_{36}\text{O}_8\text{Sn}_6$: $M_r = 1068.59 \text{ g cm}^{-3}$, crystal dimensions $0.31 \times 0.15 \times 0.14 \text{ mm}$, orthorhombic, space group $Pnma$, $a = 10.296(3)$, $b = 16.486(4)$, $c = 17.871(4) \text{ \AA}$, $\alpha = 90^{\circ}$; $V = 3033.5(13) \text{ \AA}^3$, $Z = 4$, $\rho_{\text{calcd}} = 2.340 \text{ g cm}^{-3}$, Siemens SMART CCD diffractometer, $1.68 \leq \theta \leq 28.96^{\circ}$, $\text{MoK}\alpha$ radiation ($\lambda = 0.71073 \text{ \AA}$), ω scans, $T = 193(2) \text{ K}$; of 8628 measured reflections, 3517 were independent and 2974 observed with $I >$

$2\sigma(I)$, $-5 \leq h \leq 13$, $-17 \leq k \leq 19$, $-23 \leq l \leq 23$; $R_1 = 0.0743$, $wR_2 = 0.1966$, $\text{GOF} = 1.028$ for 163 parameters, $\Delta\rho_{\text{max}} = 5.254 \text{ e}\text{\AA}^{-3}$. The structure was solved by direct methods (SHELXS-97) and refined by full-matrix least-squares procedures (SHELXL-97), Lorentz polarization corrections and absorption correction (SADABS) were applied, $\mu = 4.895 \text{ mm}^{-1}$, min./max. transmission 0.5557/0.3158.

Results and Discussion

Synthesis

Compound **20** was synthesized as previously reported by Wright and coworkers.¹⁸ The synthesis of compounds **21** and **22** is shown in Scheme 5.4. Both compounds were prepared by carefully adding a hexane solution of the appropriate tetrakis titanium alkoxide to an equimolar amount of compound **20** at room temperature. The reaction mixture was stirred overnight and filtered to afford a clear, yellow solution. Yellow crystals of compounds **21** and **22** were grown from the hexane reaction solution overnight at -40°C and -80°C , respectively.



Scheme 5.4. Synthesis of compounds **21-22**.

Characterization

Crystals of compounds **21** and **22** were each analyzed by a single crystal X-ray diffraction experiment. The results are shown in Figures 5.12 and 5.13.

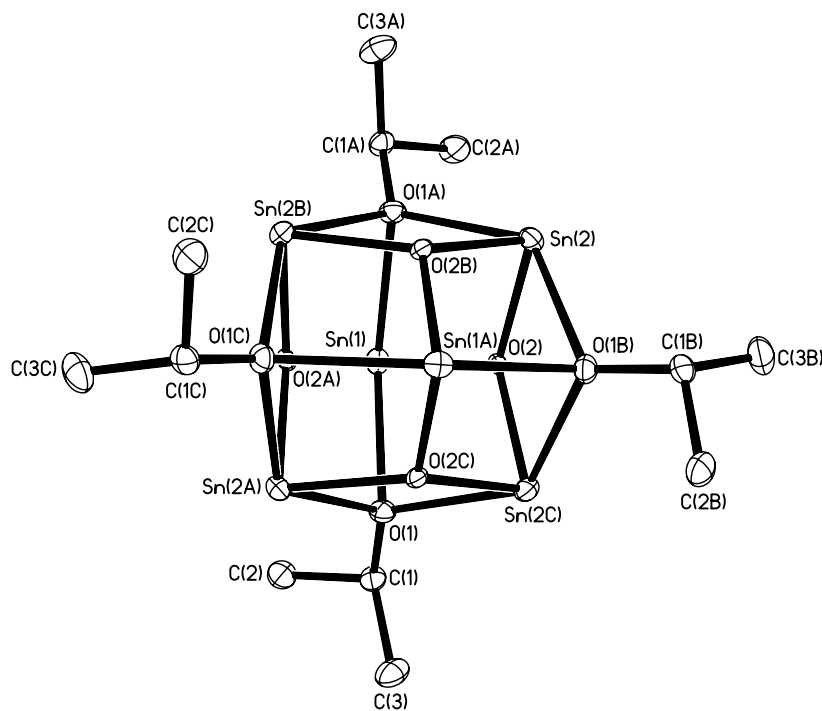


Figure 5.12. ORTEP plot representation (30% probability) with numbering scheme for compound **21**. Hydrogen atoms have been omitted for clarity.

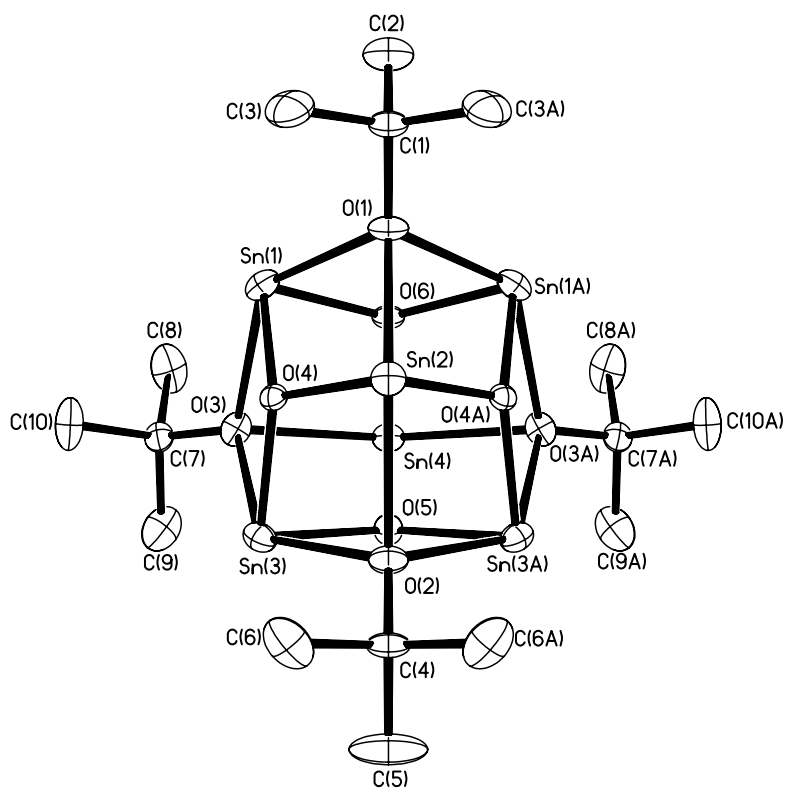


Figure 5.13. ORTEP plot representation (30% probability) with numbering scheme for compound **22**. Hydrogen atoms have been omitted for clarity.

Instead of obtaining the expected bimetallic aminoalkoxides, $(^i\text{PrO})_4\text{Ti}[\text{OSn}_4(\text{N}^t\text{Bu})_3]$ or $(^t\text{BuO})_4\text{Ti}[\text{OSn}_4(\text{N}^t\text{Bu})_3]$, the hexameric tin species **21** and **22** were isolated. It is noted that due to the limited yields of compound **20**, extensive characterization of this intermediate beyond elemental analysis was not carried out. Given this fact, the identity of **20** as depicted in Scheme 5.4 cannot be reported here with complete confidence. Thus, an explanation for the unanticipated formation of **21** and **22** cannot be formulated without obtaining additional data.

As seen in Figures 5.12 and 5.13, these compounds are comprised of tin hexamers, with each tin(II) metal center being coordinated by two $(\mu_3\text{-O})^{-2}$ and two $(\mu_3\text{-O}^t\text{Bu})^{-1}$ ligands. The structures can best be described as being comprised of two $[\text{Sn}_2(\mu_2\text{-O})(\mu_2\text{-OR})]$ dimers that are bridged by two Sn^{+2} cations, two O^{-2} atoms, and two RO^{-1} ligands. These types of structures are not unprecedented, as compound **21**²⁰ and the analogous compounds $\text{Sn}_6(\mu_3\text{-O})_4(\mu_3\text{-OC}_5\text{H}_{11})_4$ ²¹ and $\text{Sn}_6(\mu_3\text{-O})_4(\mu_3\text{-OCH}_3)_4$ ²² have been previously synthesized and structurally characterized. However, these three species were synthesized via a different pathway than that reported here in this sub-chapter. The pertinent interatomic distances for **21** and **22** are listed in Table 5.5 and all of the interatomic distances and angles can be found in Tables A.76 and A.80, respectively. The Sn-O and Sn-OR distances are within the range observed in the structural analogues previously reported (see Table 5.6).

Table 5.5. Selected average interatomic distances (Å) and angles (degrees) for compounds **21** and **22**.

(21)	distance	(22)	distance
Sn-O	2.082(3)	Sn-O	2.074(8)
Sn-O ⁱ Pr	2.393(3)	Sn-O ^t Bu	2.393(8)

Table 5.6. Selected average interatomic distances (Å) and angles (degrees) for compounds Sn₆(u₃-O)₄(u₃-OCH₃)₄ and Sn₆(u₃-O)₄(u₃-OC₅H₁₁)₄.

Sn ₆ (u ₃ -O) ₄ (u ₃ -OCH ₃) ₄	distance	Sn ₆ (u ₃ -O) ₄ (u ₃ -OC ₅ H ₁₁) ₄	distance
Sn-O	2.067	Sn-O	2.083
Sn-OR	2.379	Sn-OR	2.447

Conclusion

In an attempt to prepare bi-metallic aminoalkoxides, the oxocubane species **20** was reacted with tetrakis(alkoxide) titanium(IV). Aminoalkoxides of this type would potentially serve as useful precursors in the MOCVD of ZTT. However, instead of obtaining tin-titanium heterometallic aminoalkoxides, the hexameric tin species **21** and **22** were produced. Such species will not likely show utility in MOCVD applications. Thus, alternative synthetic routes to tin-titanium heterometallic compounds will be pursued in future chapters.

References

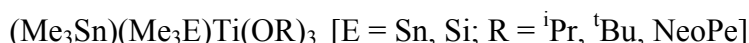
- (1) Just, O.; Rees, W. S., Jr. In *Adv. Mater. Opt. Electron.*, 2000; Vol. 10, p 213.
- (2) Schulz, S.; Gillan, E. G.; Ross, J. L.; Rogers, L. M.; Rogers, R. D.; Barron, A. R. In *Organometallics*, 1996; Vol. 15, pp 4880-4883.
- (3) Fjeldberg, T.; Haaland, A.; Schilling, B. E. R.; Lappert, M. F.; Thorne, A. J. *J. Chem. Soc., Dalton Trans.* **1986**, 8, 1551-1560.
- (4) Veith, M.; Opsolder, M.; Zimmer, M.; Huch, V. In *Eur. J. Inorg. Chem.*, 2000; Vol. 6, pp 1143-1146.
- (5) Grigsby, W. J.; Hascall, T.; Ellison, J.; Olmstead, M. M.; Power, P. P. *Inorg. Chem.* **1996**, 35, 3254-3261.
- (6) Allan, R. E.; Beswick, M. A.; Davies, M. K.; Raithby, P. R.; Steiner, A.; Wright, D. S. *J. Organomet. Chem.* **1998**, 550, 71-76.
- (7) Chen, H.; Bartlett, R. A.; Dias, H. V. R.; Olmstead, M. M.; Power, P. P. *Inorg. Chem.* **1991**, 30, 3390-3394.
- (8) Uhl, W.; Molter, J.; Koch, R. *Aluminum/lithium amide with trimethyl silyl units*, 1999.
- (9) Kuhner, S.; Kuhnle, R.; Hausen, H. D.; Weidlein, J. In *Z. Anorg. Allg. Chem.*, 1997; Vol. 623, pp 25-34.
- (10) Noth, H.; Seifert, T. In *Eur. J. Inorg. Chem.*, 2002, pp 602-612.
- (11) Rannenber, M.; Hausen, H. D.; Weidlein, J. *J. Organomet. Chem.* **1989**, 376, C27-C30.
- (12) Lappert, M. F.; Misra, M. C.; Onyszchuk, M.; Rowe, R. S.; Power, P. P.; Slade, M. J. In *J. Organomet. Chem.*, 1987; Vol. 330, pp 31-46.
- (13) Laplaza, C. E.; Davis, W. M.; Cummins, C. In *Organometallics*, 1995; Vol. 14, pp 577-580.
- (14) Alcock, N. W.; Pierce-Butler, M. In *J. Chem. Soc., Dalton Trans.*, 1975, pp 2469-2476.
- (15) Bashall, A.; Feeder, N.; Harron, E. A.; McPartlin, M.; Mosquera, M. E. G.; Saez, D.; Wright, D. S. In *J. Chem. Soc., Dalton Trans.*, 2000, pp 4104-4111.
- (16) Chen, H.; Bartlett, R. A.; Dias, H. V. R.; Olmstead, M. M.; Power, P. P. In *Inorg. Chem.*, 1991; Vol. 30, pp 3390-3394.

- (17) Papiernik, R.; Hubert-Pfalzgraf, L. G.; Veith, M.; Volker, H., Eds. *Ti-Pb aminoalkoxide*, 1997; Vol. 130.
- (18) Galan, B.; Mosquera, M. E. G.; Palmer, J. S.; Raithby, P. R.; Wright, D. S. In *J. Chem. Soc., Dalton Trans.*, 1999, pp 1043-1044.
- (19) Olmstead, M. M.; Power, P. P. "Sn(NMe₂)₂," 1984.
- (20) Sasaki, Y.; Miyazawa, N. In *Kin. Daigaku Rik. Kenk. Hokoku*, 1992; Vol. 28, p 237.
- (21) Boyle, T. J.; Alam, T. M.; Rodriguez, M. A.; Zechmann, C. A. In *Inorg. Chem.*, 2002; Vol. 41, p 2574.
- (22) Harrison, P. G.; Haylett, B. J.; King, T. J. In *Chem. Commun.*, 1978, p 112.

CHAPTER 6

THE MOCVD OF ZTT VIA THE USE OF TIN-TITANIUM ALKOXIDE-AMIDES

SECTION A: SYNTHESIS AND CHARACTERIZATION OF HETEROMETALLIC ALKOXIDE-AMIDES FOR USE AS PRECURSORS IN THE CVD OF ZTT:



Introduction

As was discussed in Chapter 1, decreasing dimensions in integrated circuit (IC) design have driven the need for high dielectric constant (high- k) materials to replace SiO_2 ($k \sim 4$) as the gate oxide. For various reasons, particularly integration issues, the replacement of SiO_2 as the gate oxide material proves to be extraordinarily difficult. Although several binary metal oxide, oxynitride, and silicate compounds have been studied as alternative gate oxide materials, only few can meet all of the rigorous demands placed upon high- k dielectrics in silicon-based devices. Specifically, it is of great importance to find gate oxide materials that display sufficiently low leakage currents, which aids in decreasing the overall power consumption of the device.^{1,2}

A recent entry into the group of potential alternative dielectric materials is zirconium-tin-titanate (ZTT). High- k ZTT films were initially prepared via Magnetron sputtering by van Dover, *et al.*, and the results of their work suggested that this material may be a viable candidate for use in CMOS devices.³ More recently, MOCVD has been used by Senzaki, *et al.*, as well as researchers in our laboratory, to fabricate thin films of

ZTT.^{4,5} In a recent report, ZTT thin films were made by using a solvent-free precursor mixture comprised of $\text{Zr}(\text{O}^t\text{Bu})_4$, $\text{Sn}(\text{O}^t\text{Bu})_4$, and $\text{Ti}(\text{O}^t\text{Bu})_4$.⁴ The precursor was transported to a cold-walled reactor via a direct liquid injection system and then introduced onto the heated silicon substrate by a vaporizer. ZTT thin films were grown between 350°C and 390°C and as-deposited materials were found to have dielectric constants ranging from 20-27.⁵

It is believed that properties of metal oxide films, such as dielectric constant, are governed by the ratio of metal cations present in the final material, and control over the cation ratio in the final film can be achieved by manipulating the nature of the precursors. Thus, it is of interest to design an alternative precursor system for the MOCVD of ZTT, with the ultimate aim being the increase of the dielectric constant and reduction of the leakage current. One approach is to synthesize heterometallic precursors possessing two or more of the metals of interest. If the ratio of metal cations is fixed in the precursor molecule, then better control of the cations in the final material can be achieved.⁶

As described earlier in this work, the lithiated stannylamine, $[(\text{Me}_3\text{Sn})_2\text{NLi}\cdot\text{THF}]$ can be used in the synthesis of heterometallic coordination compounds. Hence, the reactions of both homoleptic $[(\text{Me}_3\text{Sn})_2\text{NLi}\cdot\text{THF}]$ and heteroleptic $[(\text{Me}_3\text{Sn})(\text{Me}_3\text{Si})\text{NLi}\cdot\text{Et}_2\text{O}]$ lithiated stannylamines with tris(alkoxide)titanium(IV) chloride species were carried out and resulted in the production of the heterometallic alkoxide-amides $(\text{Me}_3\text{Sn})_2\text{NTi}(\text{O}^i\text{Pr})_3$ (**23**), $(\text{Me}_3\text{Sn})_2\text{NTi}(\text{O}^t\text{Bu})_3$ (**24**), $(\text{Me}_3\text{Sn})(\text{Me}_3\text{Si})\text{NTi}(\text{O}^i\text{Pr})_3$ (**25**), and $(\text{Me}_3\text{Sn})_2\text{NTi}(\text{OC}_5\text{H}_{11})_3$ (**27**). Details of the synthesis and characterization of this series of compounds are described herein.

Experimental

All manipulations were carried out in a dry atmosphere glovebox or by standard Schlenk techniques. All solvents were dried over Na⁰ metal and were freshly distilled under an inert atmosphere prior to use. (ⁱPrO)₃TiCl was purchased from Alfa Aesar and used without further purification. [(Me₃Sn)₂NLi•(THF)]₂ and [(Me₃Sn)(Me₃Si)NLi•(Et₂O)]₂ were prepared as described in Chapter 2. (ⁱBuO)₃TiCl was prepared according to literature procedures.⁷ All NMR experiments were performed on a Bruker 400 MHz Spectrometer at 300K using C₆D₆ solvent that was distilled over CaH₂ and stored under argon. ¹H, ¹³C, and ²⁹Si spectra were referenced to TMS. ¹¹⁹Sn spectra were externally referenced to Me₄Sn. All elemental analyses were performed in triplicate on a Perkin Elmer Series II CHNS/O Analyzer 2400. All FT-IR measurements were performed on a Bruker Equinox 55 Spectrometer. All mass spectrometry analyses were done on a VG Instruments 70SE (Electron Impact; 70eV). All TGA experiments were performed on a Perkin Elmer 7/DX thermal analyser interfaced to a Perkin Elmer Thermal Analysis Controller (TAC). The instrument is housed in a dry atmosphere glovebox. Argon was used as the purge gas and all %weight vs. temperature profiles were done at a 10°C/min. temperature ramp under ambient pressure.

Synthesis of (Me₃Sn)₂NTi(OⁱPr)₃ (23): A diethyl ether (30 mL) solution of [(Me₃Sn)₂NLi•(THF)]₂ (2.00 g, 2.38 mmol) was added dropwise to a diethyl ether slurry of (ⁱPrO)₃TiCl (1.24 g, 4.76 mmol) at 0°C. The reaction mixture was allowed to attain ambient temperature on its own and a colorless precipitate formed within 15 minutes.

The reaction was stirred overnight under an argon atmosphere and was filtered through a Schlenk frit, resulting in a clear yellow solution. The solvent was removed from the filtrate *in vacuo* and the residual oil was distilled under vacuum (70-75°C, 0.01 Torr) to give a colorless liquid. Yield: 1.52 g (57%); ^1H NMR (400 MHz, C_6D_6 , 25°C, TMS): δ 0.27 (d, 18 H, SnCH_3), 1.23 (d, 18 H, CH_3), 1.01 (m, 3 H, CH); ^{13}C NMR (100.6 MHz, C_6D_6 , 25°C, TMS): δ -3.55 (d, SnCH_3), 26.90 (d, CH_3), 75.00 (d, CH), ^{119}Sn NMR (149.3 MHz, C_6D_6 , 25°C, Me_4Sn): δ 78.0 (d, SnCH_3); MS (EI, 110°C): m/z 551 [(M-15) $^+$]; elemental analysis calculated (%) for $\text{C}_{15}\text{H}_{39}\text{NO}_3\text{Sn}_2\text{Ti}$: C 31.79, H 6.94, N 2.47, found: C 31.30, H 7.05, N 2.80.

Synthesis of $(\text{Me}_3\text{Sn})_2\text{NTi}(\text{O}^i\text{Bu})_3$ (24): Compound **24** was prepared in an analogous fashion to compound **23** using $[(\text{Me}_3\text{Sn})_2\text{NLi}\cdot(\text{THF})]_2$ (2.00 g, 2.38 mmol) and $(^i\text{BuO})_3\text{TiCl}$ (1.44 g, 4.76 mmol). The product was distilled (75-80°C, 0.01 Torr) to produce a colorless liquid. Yield: 1.69 g (58%); ^1H NMR (400 MHz, C_6D_6 , 25°C, TMS): δ 0.21 (s, 18 H, SnCH_3), 1.35 (s, 27 H, CH_3); ^{13}C NMR (100.6 MHz, C_6D_6 , 25°C, TMS): δ -1.49 (s, SnCH_3), 32.46 (s, CH_3), 79.99 (s, $\text{C}(\text{CH}_3)_3$), ^{119}Sn NMR (149.3 MHz, C_6D_6 , 25°C, Me_4Sn): δ 89.8 (s, SnCH_3); elemental analysis calculated (%) for $\text{C}_{18}\text{H}_{45}\text{NO}_3\text{Sn}_2\text{Ti}$: C 35.51, H 7.45, N 2.30, found: C 35.32, H 7.44, N 2.46.

Synthesis of $(\text{Me}_3\text{Sn})(\text{Me}_3\text{Si})\text{NTi}(\text{O}^i\text{Pr})_3$ (25): Compound **25** as prepared in an analogous fashion to compound **23** using $[(\text{Me}_3\text{Sn})(\text{Me}_3\text{Si})\text{NLi}\cdot(\text{Et}_2\text{O})]_2$ (2.00 g, 3.07 mmol) and $(^i\text{PrO})_3\text{TiCl}$ (1.60 g, 6.14 mmol). The product was isolated as a yellow oil after removal of solvent under vacuum. Yield: 1.55 g (54%); ^1H NMR (400 MHz, C_6D_6 , 25°C, TMS):

δ 0.15 (d, 9 H, SiCH₃), 0.34 (d, 9 H, SnCH₃), 1.12 (m, 18 H, CH₃), 4.47 (m, 3 H, CH); ¹³C NMR (100.6 MHz, C₆D₆, 25°C, TMS): δ -1.78 (s, SiCH₃), 4.78 (s, SnCH₃), 26.7 (s, CH₃), 76.3 (s, CH); ¹¹⁹Sn NMR (149.3 MHz, C₆D₆, 25°C, Me₄Sn): δ 66.7 (s, SnCH₃), ²⁹Si NMR (79 MHz, C₆D₆, 25°C, Me₄Si): δ 5.53 (s, SiMe₃); elemental analysis calculated (%) for C₁₅H₃₉NO₃SnSiTi: C 37.84, H 8.26, N 2.94, found: C 38.24, H 8.82, N 3.42.

Synthesis of (C₅H₁₁O)₃TiCl (26): A toluene solution of TiCl₄ (1.91 g, 4.8 mmol) was added dropwise at room temperature to a toluene (30 mL) solution of (C₅H₁₁O)₄Ti (0.30 g, 1.6 mmol). The reaction mixture was then brought to reflux and stirred overnight in an argon atmosphere. All volatile materials were subsequently removed *in vacuo* and a colorless solid was isolated. Attempts to grow crystals of this material were not successful. Yield: 1.21 g (55%); elemental analysis calculated (%) for C₁₅H₃₃O₃ClTi: C 52.26, H 9.65, found: C 51.34, H 9.67.

Synthesis of (Me₃Sn)₂NTi(OC₅H₁₁)₃ (27): A diethyl ether (30 mL) solution of [(Me₃Sn)₂NLi•(THF)]₂ (0.87 g, 2.00 mmol) was added dropwise to a diethyl ether slurry of **26** (0.64 g, 2.00 mmol) at 0°C. The reaction mixture was allowed to attain ambient temperature on its own and a colorless precipitate formed within 15 minutes. The reaction was stirred overnight under an argon atmosphere and was filtered through a Schlenk frit, resulting in a clear yellow solution. Finally, the solvent was removed from the filtrate *in vacuo*, resulting in the isolation of a yellow oil. Yield: 0.75 g (59%); ¹H NMR (400 MHz, C₆D₆, 25°C, TMS): δ 0.41 (s, 18 H, SnCH₃), 1.01 (s, 27 H, CH₃), 4.08

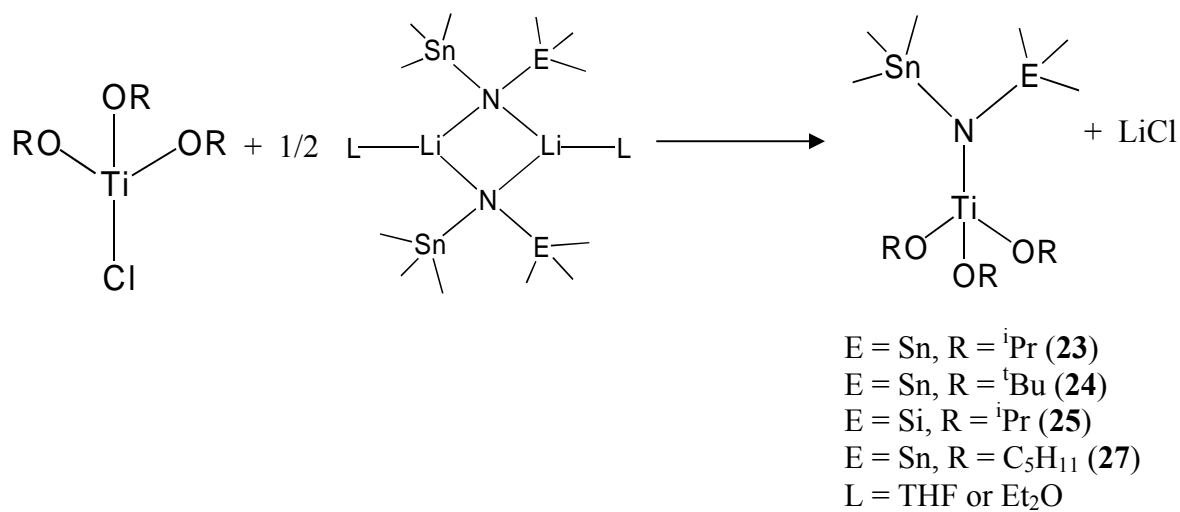
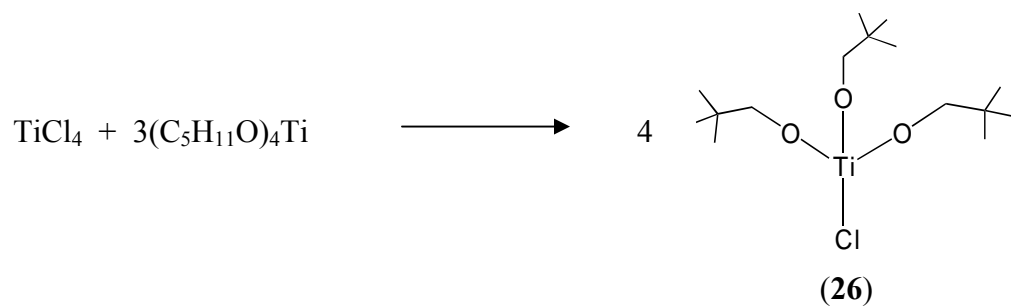
(s, 6 H); ^{13}C NMR (100.6 MHz, C_6D_6 , 25°C, TMS): δ -1.78 (s, SnCH_3), 26.61 (s, CH_3), 34.26 (s, -C-), 85.67 (s, $-\text{CH}_2-$); ^{119}Sn NMR (149.3 MHz, C_6D_6 , 25°C, Me_4Sn): δ 70.3 (s, SnCH_3); elemental analysis calculated (%) for $\text{C}_{21}\text{H}_{51}\text{NO}_3\text{Sn}_2\text{Ti}$: C 38.75, H 7.90, N 2.15, found: C 38.07, H 8.07, N 2.62.

Results and Discussion

Synthesis

Tris(alkoxide)titanium(IV) chlorides can be prepared by the comproportionation reaction between titanium tetrachloride and titanium tetrakis alkoxides. For the purposes of this work, the isopropyl derivative was purchased, the tertiarybutyl congener synthesized according to previous literature reports,⁷ and the neopentoxide species (**26**) prepared by the method depicted in Scheme 6.1. Compound **26** was obtained by the reaction of one equivalent of titanium tetrachloride with three equivalents of tetrakis(neopentoxide)titanium(IV) in a refluxing solution of toluene. After stirring overnight under reflux, the volatile materials were removed *in vacuo* and a colorless solid material was isolated.

Compounds **23-25** and **27** were analogously prepared by reacting each tris(alkoxide)titanium(IV) chloride with 0.5 equivalents of the appropriate lithiated stannylamine (see Scheme 6.1). The reaction mixture was stirred overnight at room temperature and the resulting LiCl precipitate was filtered off. The solvent was then distilled off at ambient pressure, and the final liquid product was either distilled under vacuum (compounds **23-24**) or dried under reduced pressure (compounds **25** and **27**).



Scheme 6.1. Synthesis of compounds **23-27**.

Characterization

The structures of compounds **23-27**, depicted in Scheme 6.1, are consistent with the multinuclear NMR and elemental analysis data. Since **23** and **24** are distillable liquids exhibiting significant volatility, it can be surmised that these species exist as monomers in the liquid state. Empirical evidence to support this notion is found in the mass spectrum of compound **23**. A molecular ion peak $[(M-15)^+]$ is observed in the electron impact (EI) mass spectrum at $m/z = 551$, the mass of the monomeric congener after the loss of one methyl fragment. The mass spectra obtained for compounds **24** and **25** gave inconclusive results. In solution, compounds **23** and **25** potentially undergo a dynamic conversion from monomer to dimer, evidenced by the splitting of the $\text{Sn}(\text{CH}_3)_3$ methyl peaks in the ^1H NMR. However, variable temperature ^1H NMR of compound **23** shows no coalescence of these peaks at higher temperatures (Figure 6.1). One possible explanation for the splitting of these peaks may be due to a difference in symmetry between compounds **23** and **25** and compound **24**.

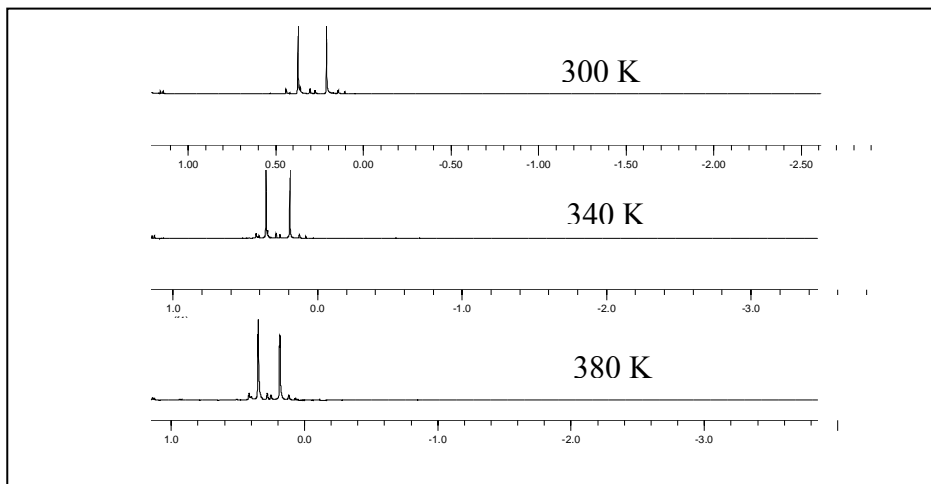


Figure 6.1. Variable temperature ^1H NMR of compound **23**: $-\text{Sn}(\text{CH}_3)_2$ peaks shown (chemical shift scale in ppm).

The thermal properties of compounds **23-25** were examined by thermogravimetric analysis (TGA). The results of these analyses are summarized in Figure 6.2. All three compounds show significant volatility below 200°C at atmospheric pressure. Compounds **23** and **24** exhibit single-step mass losses with residual percent weight values below 10%. Compound **25** also shows a single-step mass loss, but appears to undergo decomposition when approximately 20% of the sample mass remains. A qualitative comparison of the TGA plots indicates a trend of increasing volatility for the alkoxide-amides in the order: **24** > **23** > **25**. An explanation for this trend can be found in the steric bulk present on all three complexes. Compound **24**, having two trimethyl stannyl moieties bound to nitrogen and three tert-butoxides bound to titanium, has the most steric protection around the titanium metal center, thereby limiting intermolecular interactions and increasing its volatility. Compound **23**, with two trimethyl stannyl moieties bound to nitrogen and three iso-propoxides bound to titanium, effectively has less steric protection than **24**. Finally, compound **25**, with one trimethyl stannyl and one trimethyl silyl group bound to nitrogen, along with three iso-propoxides bound to titanium effectively has less steric protection than **23**.

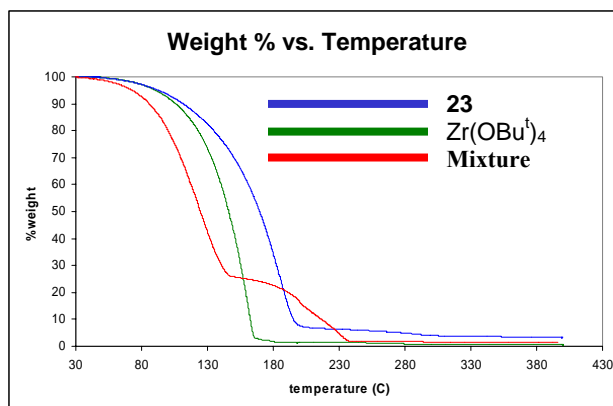
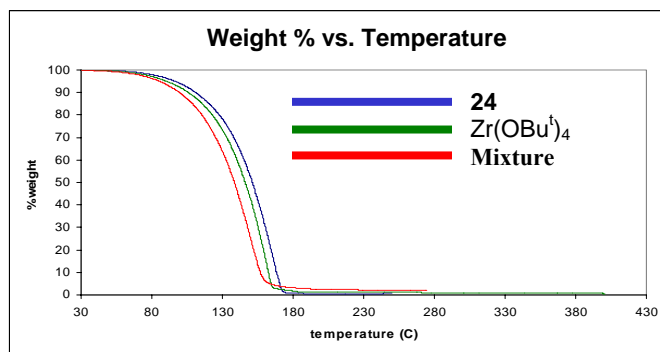
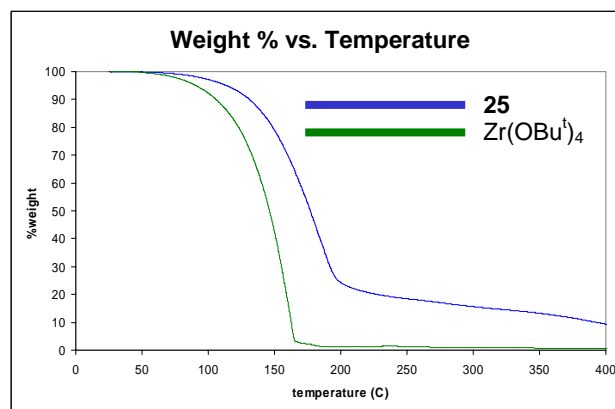


Figure 6.2.A. TGA plots of compound **23**, $\text{Zr}(\text{OBu}^t)_4$, and a mixture of the two species.



A



B

Figure 6.2.B. TGA plot of A: compound **24**, $\text{Zr}(\text{OBu}^t)_4$, and a mixture of the two species B: compound **25** and $\text{Zr}(\text{OBu}^t)_4$.

Since it was desired to deposit ZTT films using compounds **1-3** in combination with $\text{Zr}(\text{OBu}^t)_4$, the TGA profile of zirconium tert-butoxide is also provided in Figure 6.2. Separate TGA experiments for compounds **23-25** are plotted adjacent to the $\text{Zr}(\text{OBu}^t)_4$ TG curve. It is evident that compound **24** closely matches zirconium tert-butoxide in volatility. In addition, equimolar mixtures of $\text{Zr}(\text{OBu}^t)_4$ with compounds **23** and **24** were analyzed. It can be seen in Figure 6.2 that the mixture with **24** gives a single-step mass loss, whereas the mixture with **23** gives a two-step mass loss. Whether the two-step mass loss observed in the latter case is caused by interaction of the aminoalkoxide with $\text{Zr}(\text{OBu}^t)_4$, or because **23** has slightly lower volatility remains to be determined. Based on the thermal analyses, compounds **23-25** appear to be viable candidates for utilization in conjunction with $\text{Zr}(\text{OBu}^t)_4$ in the MOCVD of ZTT.

Conclusion

The synthesis and characterization of a series of heterometallic alkoxide-amides (compounds **23-26** and **27**) possessing both tin and titanium has been carried out in an attempt to prepare MOCVD precursors of ZTT containing more than one of the desired cations. During the course of this study, it was found that compounds **23-25** possess similar volatilities to $\text{Zr}(\text{OBu}^t)_4$, making the combination of these compounds a viable precursor cocktail for the MOCVD of ZTT.

SECTION B: CVD OF ZTT USING BIS(TRIMETHYLSTANNYL)AMIDE TITANIUM(IV) TRIS(ALKOXIDES)

Introduction

In Chapter 6 – Part A the series of heterometallic alkoxide-amides, $(\text{Me}_3\text{Sn})_2\text{NTi}(\text{O}^i\text{Pr})_3$ (**23**), $(\text{Me}_3\text{Sn})_2\text{NTi}(\text{O}^t\text{Bu})_3$ (**24**), and $(\text{Me}_3\text{Sn})(\text{Me}_3\text{Si})\text{NTi}(\text{O}^i\text{Pr})_3$ (**25**) were found to be viable precursors for the MOCVD of ZTT. This conclusion was based on the thermogravimetric analysis of **23-25** and $\text{Zr}(\text{O}^t\text{Bu})_4$, which have subsequently been employed in tandem in the MOCVD of ZTT. The deposition of ZTT thin films and their characterization via X-ray Photoelectron Spectroscopy (XPS) and Scanning Electron Microscopy (SEM) is described herein.

Experimental

All depositions were performed with a low-pressure, hot-walled tube furnace reactor, which is schematically depicted in Figure 6.2. Ultra high purity nitrogen and oxygen gases were purchased from AirGas and used without further scrubbing. The system is comprised of a quartz tube (2 cm internal diameter), housed in a Lindberg Blue M Furnace, which is interfaced with a MKS Instruments Type 631 Baratron Pressure Transducer (with MKS Instruments Type 250 Controller and Readout) and Welch 5 vacuum pump. The precursor delivery line is interfaced with two MKS Instruments Mass-Flo[®] gas flow controllers, one that controls the flow of nitrogen carrier gas into the precursor reservoir, and another that controls the flow of oxygen into the reactor chamber. For all depositions, a silicon wafer (approximately 1.5 cm x 1.5 cm) was

placed in a 10% aqueous HF solution for 5 minutes. The wafer was dried by evaporation, placed on a porcelain base, and then inserted into the quartz tube furnace. At this point, the furnace was placed under vacuum and the detachable precursor reservoir was taken into a dry atmosphere glovebox. The precursors were weighed into glass vials and loaded into the reservoir, the reservoir valves closed, and the entire apparatus transported and attached to the reactor. Once the furnace, precursor delivery lines, and precursor reservoir were brought to the appropriate temperature, the carrier gas and oxygen gas were turned on and the valves to the precursor reservoir opened. The experimental conditions for each deposition are summarized in Table 6.1.

ZTT thin films: Films **1-5** were analyzed as deposited. All SEM pictures were obtained on a Leo 1530 thermally assisted FEG scanning electron microscope. All X-ray Photoelectron Spectroscopy (XPS) measurements were performed on a PHI 1600/3057 with a standard aluminum x-ray source. The atomic concentration of the films deposition in runs 1-5 are summarized in Table 6.2.

Results and Discussion

A schematic of the MOCVD system is depicted in Figure 6.3 and the experimental conditions for each deposition are summarized in Table 6.1. To avoid decomposition, the precursors were loaded into a vial and sealed in the detachable reservoir inside a dry atmosphere glovebox. Then, the reservoir was attached to the reactor while still under argon. Once the desired temperature of the reservoir was attained, the nitrogen carrier gas and oxygen gas were turned on and the reservoir opened up to the system. Once the deposition was complete, the wafer was allowed to slowly reach ambient temperature

while under a nitrogen atmosphere and then stored in a vacuum desiccator until further characterization was carried out. Experiments 1 and 3 used a physical mixture of the amidoalkoxide and zirconium tert-butoxide liquids, and experiments 2, 4, and 5 were performed using separate vials for each precursor.

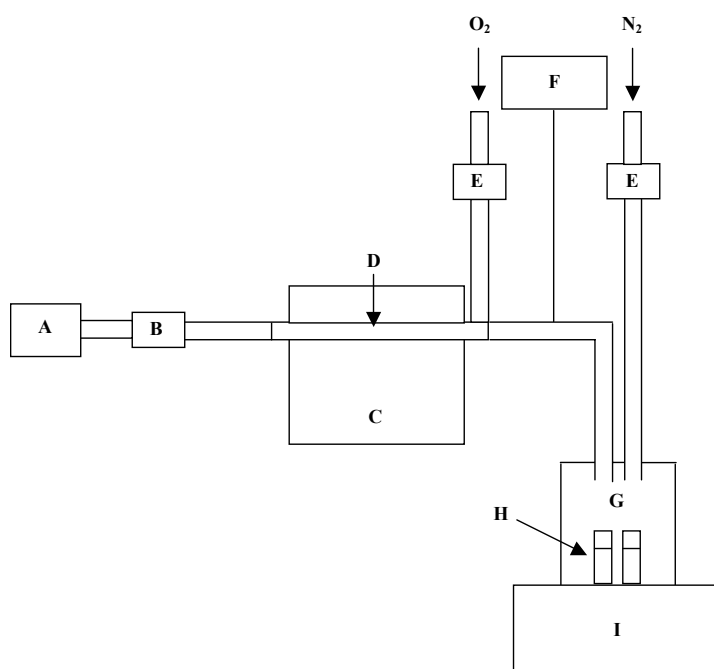


Figure 6.3. Schematic of MOCVD reactor (A: vacuum pump B: pressure transducer C: furnace D: quartz tube E: gas flow controllers F: precursor delivery line temperature controller G: detachable precursor reservoir H: vials containing liquid precursor I: heating plate).

Table 6.1. Experimental conditions for the MOCVD of ZTT using precursors **23-25** and $\text{Zr}(\text{OBU})_4$.

deposition	precursor system	precursor reservoir temp.	delivery line temp.	furnace temp.	pressure	carrier gas flow	oxygen gas flow	deposition time
experiment 1	23 (0.2g)/ $\text{Zr}(\text{OPr}^i)_4$ (0.2g) mixed	70°C	100- 120°C	430°C	6.4 Torr	200 sccm	100 sccm	30 min.
experiment 2	23 (0.2g)/ $\text{Zr}(\text{OPr}^i)_4$ (0.2g) separate	75°C	100- 120°C	430°C	5.5 Torr	200 sccm	100 sccm	30 min.
experiment 3	24 (0.1g)/ $\text{Zr}(\text{OPr}^i)_4$ (0.1g) mixed	55°C	100- 120°C	430°C	6.5 Torr	200 sccm	100 sccm	30 min.
experiment 4	24 (0.2g)/ $\text{Zr}(\text{OPr}^i)_4$ (0.2g) separate	60°C	100- 120°C	430°C	6.2 Torr	200 sccm	100 sccm	30 min.
experiment 5	25 (0.1g)/ $\text{Zr}(\text{OPr}^i)_4$ (0.1g) separate	65°C	100- 120°C	430°C	6.4 Torr	200 sccm	100 sccm	30 min.

X-ray photoelectron spectroscopy (XPS) was performed on the films obtained from MOCVD experiments 1-5. High resolution spectra were recorded and the atomic concentration, as well as the molar composition of each film is summarized in Table 6.2. All compositional data is relevant only for the film surface due to the fact that ion sputtering was not available at the time of analysis. The films obtained from experiments 1-3, and 5 lacked the presence of zirconium in the film. However, films from experiments 1, 3, and 5 showed the presence of both tin and titanium, indicating that the aminoalkoxide precursor delivered the cations to the substrate. Experiment 4 gave the

most encouraging results in that all three metals were found to be in the oxide material, suggesting that the compound **24** is best suited to be used along with $\text{Zr}(\text{O}^i\text{Bu})_4$ in the MOCVD of ZTT. Whether the lack of zirconium in films 1-3 and 5 is due to precursor incompatibility or limitations in the MOCVD reactor system has not been determined at this time. All films exhibited carbon contamination (ranging from 17-24%), however it is possible that this arises from ambient carbon sources. XPS spectra need to be obtained after plasma sputtering to determine the sub-surface atomic content.

Table 6.2. Atomic concentration and molar composition of ZTT films calculated from high resolution XPS measurements.

film	%Zr3d	%Sn3d5	%Ti2p	%O1s	%C1s	molar composition
experiment 1	0.00	2.10	17.55	44.80	20.22	$\text{Sn}_{0.02}\text{Ti}_{0.37}\text{O}_{2.80}$
experiment 2	0.00	23.88	0.00	52.87	23.25	$\text{Sn}_{0.20}\text{O}_{3.31}$
experiment 3	0.00	12.23	9.27	53.80	24.69	$\text{Sn}_{0.10}\text{Ti}_{0.19}\text{O}_{3.36}$
experiment 4	8.85	13.73	2.18	53.81	21.41	$\text{Zr}_{0.97}\text{Sn}_{0.12}\text{Ti}_{0.05}\text{O}_{3.33}$
experiment 5	0.00	8.67	13.94	59.72	17.67	$\text{Sn}_{0.07}\text{Ti}_{0.29}\text{O}_{3.73}$

The ZTT thin films were also characterized by SEM (micrographs of films 1 and 4 are shown in Figure 6.4). All films possessed smooth surfaces comprised of regularly arrayed, homogeneous crystallites. The size of the crystallites varied between films, and ranged in size from about 20 nm to 200 nm. Some of the films contained larger, heterogeneous particles that could have been ablated contaminants from the reactor wall.

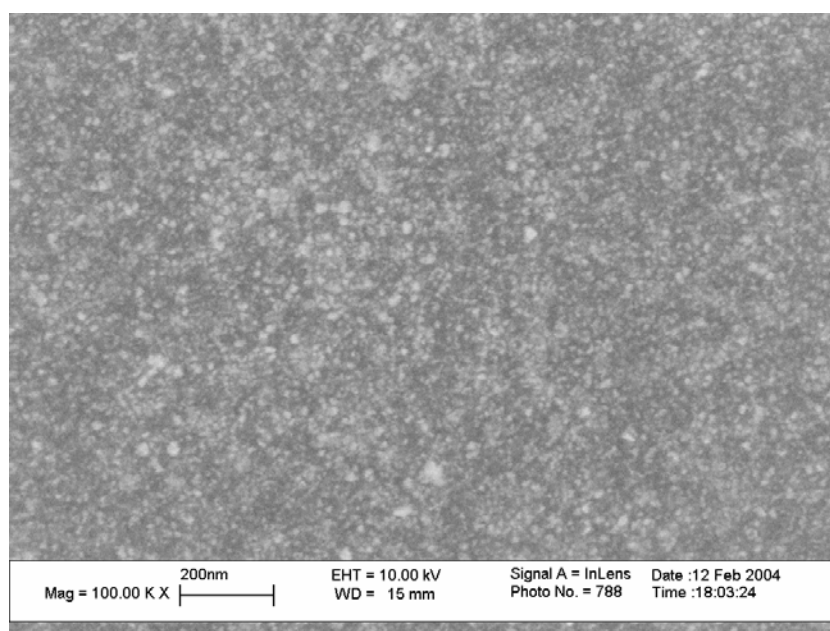
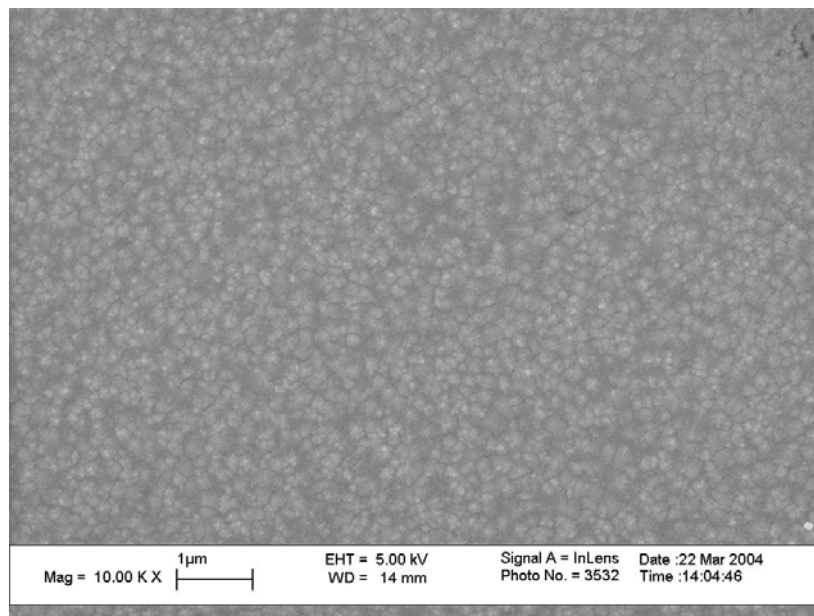


Figure 6.4.A. SEM picture of film from experiment 1.



B

Figure 6.4.B. SEM picture of film from experiment 4.

Conclusion

Compounds **23-25** were found to be viable MOCVD precursors based on thermogravimetric analyses and were subsequently utilized, in conjunction with $\text{Zr}(\text{O}^t\text{Bu})_4$ in the fabrication of metal oxide thin films via the use of a low-pressure, hot-walled tube furnace reactor. The as-deposited films were analyzed by high resolution XPS and SEM. Initial results suggest the synthesized alkoxide-amides are adequate in delivering tin and titanium cations to the substrate surface. The precursor cocktail comprised of separate sources of compound **2** and $\text{Zr}(\text{O}^t\text{Bu})_4$ resulted in a film that contained an oxide material containing all three metals in the molar ratio, $\text{Zr}_{0.97}\text{Sn}_{0.12}\text{Ti}_{0.05}\text{O}_{3.33}$. Based on these results, further investigation into the use of

compounds **23-25** as precursors for ZTT and optimization of the deposition conditions is warranted.

References

- (1) Buchanan, D. A. *IBM J. Res. Develop.* **1999**, *43*, 245-264.
- (2) Bersuker, G.; Zeitzoff, P.; Brown, G.; Huff, H. R. *Materials Today* **2004**, *7*, 26-33.
- (3) Dover, R. B. v.; Schneemeyer, L. F. *IEEE Electron Device Letters* **1998**, *19*, 329-331.
- (4) Senzaki, Y.; Alers, G. B.; Hochberg, A. K.; Roberts, D. A.; Norman, J. A. T.; Fleming, R. M.; Krautter, H. *Eletrochem. Solid-State Lett.* **2000**, *9*, 435-436.
- (5) Mays, E. L.; Hess, D. W.; Rees, W. S., Jr. *Journal of Crystal Growth* **2004**, *261*, 309-315.
- (6) Afzaal, M.; Croch, D.; Malik, M. A.; Motevalli, M.; O'Brien, P.; Park, J. H.; Woolins, J. D. *Eur. J. Inorg. Chem.* **2004**, 171-177.
- (7) Selent, D.; Pickardt, J.; Claus, P. *J. Organomet. Chem.* **1994**, *468*, 131-138.

CHAPTER 7

CONCLUSIONS AND FUTURE WORK

The attempt to synthesize molecular precursors for use in the MOCVD of ZTT has led to the isolation of a variety of coordination compounds possessing stannylamine ligands. Specifically, a series of dimeric beryllium and tetrameric silver amides, two series of Group 14-nitrogen heterocubanes, zinc and zirconium dimeric amido complexes, and a new class of heterometallic titanium alkoxides, all coordinated by stannylamine moieties were prepared and characterized.

The significance of the results reported herein lies on two fronts. First, the extension of the coordination chemistry of stannylamines, a field that has remained relatively unexplored, has been successfully carried out. Second, a novel route to volatile heterometallic alkoxide-amides containing tin(IV) cations was discovered.

Regarding the former case, the library of complexes possessing stannylamines was expanded in this work via the use of lithiated stannylamines. Amido transfer reagents of this nature were previously uncharacterized and limited in the synthesis of metal amides to the copper tetramer reported by Fenske and coworkers. Thus, the synthetic work reported in this dissertation has described the isolation and full characterization of lithiated stannylamines and documented initial reactions of these complexes with selected main group and transition metal halides. Future work in this area would lie primarily in synthesis. It would be of general interest from an inorganic synthetic chemistry standpoint to explore the reactions of the lithiated stannylamines reported in this dissertation with the full gamut of metals found in the periodic table and

compare the properties of the resulting complexes with any analogous alkyl- and silylamide congeners.

In regards to the latter case, tin-titanium alkoxide-amides were synthesized via the reaction of lithiated stannylamines with tris(alkoxide) titanium(IV)chloride species. Initial TGA studies revealed that these complexes exhibit the volatility and vapor phase integrity necessary for MOCVD applications. Therefore, these precursors were subsequently employed in tandem with $\text{Zr}(\text{O}^t\text{Bu})_4$ in preliminary MOCVD experiments and were found to be viable candidates for the deposition of ZTT. With respect to the goals of this dissertation, that is the design and synthesis of ZTT MOCVD precursors, and to application in the materials industry, the results reported in Chapter 6 are most important. Future research related to this work can be encompassed by two major areas. First, a materials chemistry project could be pursued with the aim of carefully characterizing the alkoxide-amide/ $\text{Zr}(\text{O}^t\text{Bu})_4$ precursor cocktail and optimizing the MOCVD conditions in the preparation of ZTT thin films. Comparison of the film properties with those obtained by Senzaki, *et al.* and Rees *et al.* would shed light on the ultimate utility of the alkoxide-amide species as ZTT precursors. Second, a synthetic chemistry project could be initiated to investigate the extension of the heterometallic alkoxide-amide synthesis to other mixed metal systems possessing tin(IV) cations. The successful completion of this undertaking would potentially provide a convenient route to a variety of heterometallic oxide materials and could have an impact on the industrial fabrication of tin oxide materials.

To conclude this dissertation, the library of known stannylamide coordination complexes has been substantially increased, and the route employed to obtain them may

provide access to an even larger library of such compounds. Additionally, the lithiated stannylamines reported here were used to synthesize novel heterometallic alkoxide-amides that were found to exhibit adequate volatility and vapor phase integrity for use in MOCVD processes. This class of compounds may ultimately result in an improved precursor system for the deposition of ZTT films and the synthetic pathway used to procure these alkoxide-amides has the potential to lead to a variety of new heterometallic coordination complexes.

References:

- (1) Reiss, P.; Fenske, D.Z. *Anorg. Allg. Chem.* **2000**, 626, 1317.
- (2) Senzaki, Y.; Alers, G.B.; Hochberg, A.K. Roberts, D.A.; Norman, J.A.T.; Fleming, R.M.; Krautter, H. *Electrochem. Solid-State Lett.* **2000**, 9, 435-436.
- (3) Mays, E.L.; Hess, D.W.; Rees, W.S., Jr. *Journal of Crystal Growth.* **2004**, 261, 309-315.

APPENDIX A
CRYSTALLOGRAPHIC TABLES

Table A.1. Atomic Coordinates ($\times 10^4$) and Equivalent Isotropic Displacement Parameters ($\text{\AA}^2 \times 10^3$) for $\text{C}_{20}\text{H}_{52}\text{N}_2\text{O}_2\text{Li}_2\text{Sn}_4$ (**1**).

Atom	x	y	z	U(eq)
Sn(1)	3571(1)	-970(1)	-1025(1)	58(1)
N(1)	5000	0	-1629(5)	52(3)
C(1)	3041(16)	86(19)	-2(6)	149(7)
C(2)	4163(12)	-2440(40)	-897(9)	229(15)
C(3)	1800(13)	-1070(20)	-1700(10)	157(9)
C(4)	7950(20)	-2620(20)	-3110(9)	182(11)
C(5)	8870(20)	-3490(20)	-2850(11)	147(7)
O(1)	7179(7)	-2179(7)	-2500	100(4)
Li(1)	5830(14)	-830(14)	-2500	51(5)

Table A.2. Interatomic Distances (Å) and Angles (°) for C₂₀H₅₂N₂O₂Li₂Sn₄ (**1**).

Sn(1)-C(2)	1.59(3)	C(3)-Sn(1)-C(1)	107.0(7)
Sn(1)-N(1)	2.022(4)	C(2)-Sn(1)-Li(1)#1	123.8(7)
Sn(1)-C(3)	2.129(16)	N(1)-Sn(1)-Li(1)#1	34.6(3)
Sn(1)-C(1)	2.160(12)	C(3)-Sn(1)-Li(1)#1	73.9(4)
Sn(1)-Li(1)#1	3.223(5)	C(1)-Sn(1)-Li(1)#1	117.2(5)
N(1)-Li(1)#1	1.935(14)	Li(1)#1-N(1)-Li(1)	74.1(10)
N(1)-Li(1)	1.935(14)	Li(1)#1-N(1)-Sn(1)#1	121.22(15)
N(1)-Sn(1)#1	2.022(4)	Li(1)-N(1)-Sn(1)#1	109.0(2)
C(4)-C(5)	1.34(2)	Li(1)#1-N(1)-Sn(1)	109.0(2)
C(4)-O(1)	1.396(13)	Li(1)-N(1)-Sn(1)	121.22(15)
C(5)-C(5)#2	1.35(3)	Sn(1)#1-N(1)-Sn(1)	116.1(4)
O(1)-C(4)#2	1.396(13)	C(5)-C(4)-O(1)	108.1(15)
O(1)-Li(1)	1.90(2)	C(4)-C(5)-C(5)#2	107.8(12)
Li(1)-N(1)#3	1.935(14)	C(4)-O(1)-C(4)#2	104.9(15)
Li(1)-Li(1)#1	2.33(4)	C(4)-O(1)-Li(1)	127.5(7)
Li(1)-Sn(1)#1	3.223(5)	C(4)#2-O(1)-Li(1)	127.5(7)
Li(1)-Sn(1)#3	3.223(5)	O(1)-Li(1)-N(1)#3	127.0(5)
C(2)-Sn(1)-N(1)	104.7(7)	O(1)-Li(1)-N(1)	127.0(5)
C(2)-Sn(1)-C(3)	110.1(8)	N(1)#3-Li(1)-N(1)	105.9(10)
N(1)-Sn(1)-C(3)	107.7(4)	O(1)-Li(1)-Li(1)#1	180.0
C(2)-Sn(1)-C(1)	114.6(7)	N(1)#3-Li(1)-Li(1)#1	53.0(5)
N(1)-Sn(1)-C(1)	120.6(5)	N(1)-Li(1)-Li(1)#1	53.0(5)

O(1)-Li(1)-Sn(1)#1	105.2(3)	Li(1)#1-Li(1)-Sn(1)#3	74.8(3)
N(1)#3-Li(1)-Sn(1)#1	119.3(7)	Sn(1)#1-Li(1)-Sn(1)#3	149.7(7)
N(1)-Li(1)-Sn(1)#1	36.38(7)	O(1)-Li(1)-Sn(1)#3	105.2(3)
Li(1)#1-Li(1)-Sn(1)#1	74.8(3)	N(1)#3-Li(1)-Sn(1)#3	36.38(7)

Table A.3. Anisotropic displacement parameters ($\text{\AA}^2 \times 10^3$) for $\text{C}_{20}\text{H}_{52}\text{N}_2\text{O}_2\text{Li}_2\text{Sn}_4$ (**1**).

Atom	U11	U22	U33	U23	U13	U12
Sn(1)	67(1)	64(1)	43(1)	9(1)	7(1)	0(1)
N(1)	61(7)	66(7)	28(4)	0	0	27(5)
C(1)	213(19)	35(14)	98(9)	-27(10)	110(11)	-45(16)
C(2)	31(6)	550(40)	103(11)	-128(19)	-21(7)	45(15)
C(3)	47(7)	260(20)	166(15)	132(15)	9(8)	-22(10)
C(4)	200(20)	210(20)	128(13)	-35(14)	46(14)	173(18)
C(5)	124(16)	150(19)	170(20)	4(14)	39(14)	31(12)
O(1)	99(6)	99(6)	103(9)	-6(6)	-6(6)	58(8)
Li(1)	55(8)	55(8)	43(9)	-14(7)	-14(7)	18(10)

Table A.4. Hydrogen coordinates ($\times 10^4$) and isotropic displacement parameters ($\text{\AA}^2 \times 10^3$) for $\text{C}_{20}\text{H}_{52}\text{N}_2\text{O}_2\text{Li}_2\text{Sn}_4$ (**1**).

Atom	x	y	z	U(eq)
H(1A)	3515	-296	411	223
H(1B)	2100	9	82	223
H(1C)	3276	1009	-51	223
H(2A)	4242	-2887	-1369	343
H(2B)	3575	-2937	-579	343
H(2C)	5024	-2378	-668	343
H(3A)	1975	-680	-2180	236
H(3B)	1096	-586	-1459	236
H(3C)	1540	-1981	-1762	236
H(4A)	7392	-3044	-3474	218
H(4B)	8385	-1875	-3343	218
H(5A)	9734	-3079	-2833	176
H(5B)	8922	-4255	-3172	176

Table A.5. Atomic Coordinates ($\times 10^4$) and Equivalent Isotropic Displacement Parameters ($\text{\AA}^2 \times 10^3$) for $\text{C}_{20}\text{H}_{52}\text{N}_2\text{O}_2\text{Li}_2\text{Si}_2\text{Sn}_2$ (**2**).

Atom	x	y	z	U(eq)
Sn(1)	1413(1)	4046(1)	1050(1)	44(1)
Si(1)	1413(1)	4046(1)	1050(1)	44(1)
N(1)	0	5000	1595(3)	51(1)
C(1)	3075(8)	3965(8)	1703(4)	94(2)
C(2)	854(7)	2165(9)	767(5)	102(3)
C(3)	1951(7)	5069(8)	77(3)	81(2)
C(4)	2699(9)	7950(10)	1826(4)	107(3)
C(5)	3020(20)	9275(14)	1929(9)	334(17)
Li(1)	874(9)	5874(9)	2500	56(3)
O(1)	2262(4)	7262(4)	2500	71(2)

Table A.6. Interatomic Distances (Å) and Angles (°) for C₂₀H₅₂N₂O₂Li₂Si₂Sn₂ (**2**).

Sn(1)-N(1)	1.919(3)	Sn(1)#1-N(1)-Sn(1)	120.8(3)
Sn(1)-Li(1)	3.138(4)	Si(1)#1-N(1)-Li(1)	119.50(11)
Sn(1)-Li(1)#1	3.374(6)	Sn(1)#1-N(1)-Li(1)	119.50(11)
N(1)-Si(1)#1	1.919(3)	Sn(1)-N(1)-Li(1)	106.91(15)
N(1)-Sn(1)#1	1.919(3)	Si(1)#1-N(1)-Li(1)#1	106.91(15)
N(1)-Li(1)	1.987(9)	Sn(1)#1-N(1)-Li(1)#1	106.91(15)
N(1)-Li(1)#1	1.987(9)	Sn(1)-N(1)-Li(1)#1	119.50(11)
C(4)-C(5)	1.346(14)	Li(1)-N(1)-Li(1)#1	75.0(6)
C(4)-O(1)	1.418(7)	C(5)-C(4)-O(1)	114.6(9)
Li(1)-O(1)	1.921(14)	O(1)-Li(1)-N(1)	127.5(3)
Li(1)-N(1)#2	1.987(9)	O(1)-Li(1)-N(1)#2	127.5(3)
Li(1)-Li(1)#1	2.42(3)	N(1)-Li(1)-N(1)#2	105.0(6)
Li(1)-Si(1)#2	3.138(4)	O(1)-Li(1)-Li(1)#1	180.0(7)
Li(1)-Sn(1)#2	3.138(4)	N(1)-Li(1)-Li(1)#1	52.5(3)
Li(1)-Sn(1)#1	3.374(6)	N(1)#2-Li(1)-Li(1)#1	52.5(3)
Li(1)-Sn(1)#3	3.374(6)	O(1)-Li(1)-Si(1)#2	106.5(2)
O(1)-C(4)#2	1.418(7)	N(1)-Li(1)-Si(1)#2	117.7(4)
N(1)-Sn(1)-Li(1)	37.29(19)	N(1)#2-Li(1)-Si(1)#2	35.80(5)
N(1)-Sn(1)-Li(1)#1	30.84(15)	Li(1)#1-Li(1)-Si(1)#2	73.5(2)
Li(1)-Sn(1)-Li(1)#1	43.4(4)	O(1)-Li(1)-Sn(1)#2	106.5(2)
Si(1)#1-N(1)-Sn(1)#1	0.00(3)	N(1)-Li(1)-Sn(1)#2	117.7(4)
Si(1)#1-N(1)-Sn(1)	120.8(3)	N(1)#2-Li(1)-Sn(1)#2	35.80(5)

Li(1)#1-Li(1)-Sn(1)#2	73.5(2)	Sn(1)#2-Li(1)-Sn(1)#1	102.7(2)
Si(1)#2-Li(1)-Sn(1)#2	0.000(14)	Sn(1)-Li(1)-Sn(1)#1	61.52(10)
O(1)-Li(1)-Sn(1)	106.5(2)	O(1)-Li(1)-Sn(1)#3	116.92(19)
N(1)-Li(1)-Sn(1)	35.80(5)	N(1)-Li(1)-Sn(1)#3	108.5(4)
N(1)#2-Li(1)-Sn(1)	117.7(4)	N(1)#2-Li(1)-Sn(1)#3	29.67(4)
Li(1)#1-Li(1)-Sn(1)	73.5(2)	Li(1)#1-Li(1)-Sn(1)#3	63.08(19)
Si(1)#2-Li(1)-Sn(1)	146.9(4)	Si(1)#2-Li(1)-Sn(1)#3	61.52(10)
Sn(1)#2-Li(1)-Sn(1)	146.9(4)	Sn(1)#2-Li(1)-Sn(1)#3	61.52(10)
O(1)-Li(1)-Sn(1)#1	116.92(19)	Sn(1)-Li(1)-Sn(1)#3	102.7(2)
N(1)-Li(1)-Sn(1)#1	29.67(4)	Sn(1)#1-Li(1)-Sn(1)#3	126.2(4)
N(1)#2-Li(1)-Sn(1)#1	108.5(4)	C(4)#2-O(1)-C(4)	113.5(7)
Li(1)#1-Li(1)-Sn(1)#1	63.08(19)	C(4)#2-O(1)-Li(1)	123.3(3)
Si(1)#2-Li(1)-Sn(1)#1	102.7(2)	C(4)-O(1)-Li(1)	123.3(3)

Table A.7. Anisotropic displacement parameters ($\text{\AA}^2 \times 10^3$) for $\text{C}_{20}\text{H}_{52}\text{N}_2\text{O}_2\text{Li}_2\text{Si}_2\text{Sn}_2$ (**2**).

Atom	U11	U22	U33	U23	U13	U12
Sn(1)	44(1)	51(1)	36(1)	-6(1)	5(1)	1(1)
Si(1)	44(1)	51(1)	36(1)	-6(1)	5(1)	1(1)
N(1)	41(3)	48(3)	64(4)	0	0	4(2)
C(1)	99(5)	118(6)	65(4)	-17(4)	5(4)	-16(4)
C(2)	73(5)	124(7)	109(6)	-42(5)	13(4)	1(4)
C(3)	89(5)	91(5)	63(3)	2(3)	26(3)	2(4)
C(4)	103(6)	141(7)	75(4)	19(5)	0(4)	-63(5)
C(5)	630(40)	119(10)	253(18)	-70(12)	290(20)	-148(18)
Li(1)	51(4)	51(4)	66(8)	-5(4)	5(4)	1(5)
O(1)	74(2)	74(2)	63(3)	-8(2)	8(2)	-26(3)

Table A.8. Hydrogen coordinates ($\times 10^4$) and isotropic displacement parameters ($\text{\AA}^2 \times 10^3$) for $\text{C}_{20}\text{H}_{52}\text{N}_2\text{O}_2\text{Li}_2\text{Si}_2\text{Sn}_2$ (**2**).

Atom	x	y	z	U(eq)
H(1A)	3355	4866	1831	190(30)
H(1B)	3786	3517	1430	190(30)
H(1C)	2878	3473	2160	190(30)
H(2A)	440	1735	1198	140(20)
H(2B)	1635	1658	614	140(20)
H(2C)	219	2201	355	140(20)
H(3A)	1188	5119	-259	136(18)
H(3B)	2677	4599	-171	136(18)
H(3C)	2240	5966	207	136(18)
H(4A)	3476	7490	1627	620(120)
H(4B)	1994	7890	1452	620(120)
H(5A)	2451	9825	1611	550(110)
H(5B)	3948	9419	1797	550(110)
H(5C)	2878	9515	2452	550(110)

Table A.9. Atomic Coordinates ($\times 10^4$) and Equivalent Isotropic Displacement Parameters ($\text{\AA}^2 \times 10^3$) for $\text{C}_{20}\text{H}_{56}\text{N}_2\text{O}_2\text{Li}_2\text{Ge}_2\text{Sn}_2$ (**3**).

Atom	x	y	z	U(eq)
Ge(1)	5916(1)	1383(1)	8964(1)	37(1)
Sn(1)	5916(1)	1383(1)	8964(1)	37(1)
N(1)	5000	0	8388(3)	31(1)
C(1)	6061(7)	3077(7)	8309(4)	59(2)
C(2)	4897(8)	1960(7)	9928(3)	60(2)
C(3)	7827(8)	819(7)	9255(4)	68(2)
C(4)	2131(7)	2787(7)	8171(4)	62(2)
C(5)	651(10)	2673(16)	8184(7)	135(5)
O(1)	2725(3)	2275(3)	7500	43(1)
Li(1)	4126(8)	874(8)	7500	31(2)

Table A.10. Interatomic Distances (Å) and Angles (°) for C₂₀H₅₂N₂O₂Li₂Ge₂Sn₂ (**3**).

Ge(1)-N(1)	1.915(3)	N(1)-Ge(1)-C(2)	114.1(2)
Ge(1)-C(3)	2.015(8)	C(3)-Ge(1)-C(2)	108.3(3)
Ge(1)-C(1)	2.026(6)	C(1)-Ge(1)-C(2)	106.4(3)
Ge(1)-C(2)	2.051(6)	N(1)-Ge(1)-Li(1)	36.42(16)
Ge(1)-Li(1)	3.162(3)	C(3)-Ge(1)-Li(1)	132.7(3)
N(1)-Sn(1)#1	1.915(3)	C(1)-Ge(1)-Li(1)	72.6(2)
N(1)-Ge(1)#1	1.915(3)	C(2)-Ge(1)-Li(1)	116.9(3)
N(1)-Li(1)	1.980(8)	Ge(1)-N(1)-Sn(1)#1	115.8(3)
N(1)-Li(1)#1	1.980(8)	Ge(1)-N(1)-Ge(1)#1	115.8(3)
C(4)-O(1)	1.412(7)	Sn(1)#1-N(1)-Ge(1)#1	0.00(3)
C(4)-C(5)	1.451(12)	Ge(1)-N(1)-Li(1)	108.54(13)
O(1)-C(4)#2	1.412(7)	Sn(1)#1-N(1)-Li(1)	121.61(9)
O(1)-Li(1)	1.937(12)	Ge(1)#1-N(1)-Li(1)	121.61(9)
Li(1)-N(1)#3	1.980(8)	Ge(1)-N(1)-Li(1)#1	121.61(9)
Li(1)-Li(1)#1	2.42(2)	Sn(1)#1-N(1)-Li(1)#1	108.54(13)
Li(1)-Sn(1)#2	3.162(3)	Ge(1)#1-N(1)-Li(1)#1	108.54(13)
Li(1)-Ge(1)#2	3.162(3)	Li(1)-N(1)-Li(1)#1	75.3(5)
Li(1)-Sn(1)#3	3.401(5)	O(1)-C(4)-C(5)	113.4(7)
Li(1)-Sn(1)#1	3.401(5)	C(4)#2-O(1)-C(4)	114.4(6)
N(1)-Ge(1)-C(3)	112.07(19)	C(4)#2-O(1)-Li(1)	122.8(3)
N(1)-Ge(1)-C(1)	107.9(2)	C(4)-O(1)-Li(1)	122.8(3)
C(3)-Ge(1)-C(1)	107.7(3)	O(1)-Li(1)-N(1)#3	127.6(3)

O(1)-Li(1)-N(1)	127.6(3)	Sn(1)#2-Li(1)-Ge(1)	147.5(4)
N(1)#3-Li(1)-N(1)	104.7(5)	Ge(1)#2-Li(1)-Ge(1)	147.5(4)
O(1)-Li(1)-Li(1)#1	180.0(6)	O(1)-Li(1)-Sn(1)#3	116.79(16)
N(1)#3-Li(1)-Li(1)#1	52.4(3)	N(1)#3-Li(1)-Sn(1)#3	28.66(3)
N(1)-Li(1)-Li(1)#1	52.4(3)	N(1)-Li(1)-Sn(1)#3	109.1(4)
O(1)-Li(1)-Sn(1)#2	106.27(18)	Li(1)#1-Li(1)-Sn(1)#3	63.21(16)
N(1)#3-Li(1)-Sn(1)#2	35.04(5)	Sn(1)#2-Li(1)-Sn(1)#3	59.11(8)
N(1)-Li(1)-Sn(1)#2	118.5(4)	Ge(1)#2-Li(1)-Sn(1)#3	59.11(8)
Li(1)#1-Li(1)-Sn(1)#2	73.73(18)	Ge(1)-Li(1)-Sn(1)#3	105.12(18)
O(1)-Li(1)-Ge(1)#2	106.27(18)	O(1)-Li(1)-Sn(1)#1	116.79(16)
N(1)#3-Li(1)-Ge(1)#2	35.04(5)	N(1)#3-Li(1)-Sn(1)#1	109.1(4)
N(1)-Li(1)-Ge(1)#2	118.5(4)	N(1)-Li(1)-Sn(1)#1	28.66(3)
Li(1)#1-Li(1)-Ge(1)#2	73.73(18)	Li(1)#1-Li(1)-Sn(1)#1	63.21(16)
Sn(1)#2-Li(1)-Ge(1)#2	0.000(18)	Sn(1)#2-Li(1)-Sn(1)#1	105.12(18)
O(1)-Li(1)-Ge(1)	106.27(18)	Ge(1)#2-Li(1)-Sn(1)#1	105.12(18)
N(1)#3-Li(1)-Ge(1)	118.5(4)	Ge(1)-Li(1)-Sn(1)#1	59.11(8)
N(1)-Li(1)-Ge(1)	35.04(5)	Sn(1)#3-Li(1)-Sn(1)#1	126.4(3)
Li(1)#1-Li(1)-Ge(1)	73.73(18)		

Table A.11. Anisotropic displacement parameters ($\text{\AA}^2 \times 10^3$) for $\text{C}_{20}\text{H}_{52}\text{N}_2\text{O}_2\text{Li}_2\text{Ge}_2\text{Sn}_2$ (**3**).

Atom	U11	U22	U33	U23	U13	U12
Ge(1)	46(1)	34(1)	31(1)	-3(1)	-2(1)	-3(1)
Sn(1)	46(1)	34(1)	31(1)	-3(1)	-2(1)	-3(1)
N(1)	35(3)	34(3)	24(2)	0	0	-6(2)
C(1)	78(4)	47(3)	53(4)	5(3)	-2(3)	-9(3)
C(2)	69(4)	64(4)	49(3)	-22(3)	10(3)	-6(4)
C(3)	76(5)	59(4)	68(4)	-6(3)	-20(4)	-4(3)
C(4)	67(4)	65(4)	54(4)	-10(3)	10(3)	14(3)
C(5)	93(7)	178(12)	135(10)	-71(10)	6(7)	5(7)
O(1)	47(2)	47(2)	34(3)	1(2)	1(2)	11(2)
Li(1)	32(3)	32(3)	29(5)	-10(3)	-10(3)	5(4)

Table A.12. Hydrogen coordinates ($\times 10^4$) and isotropic displacement parameters ($\text{\AA}^2 \times 10^3$) for $\text{C}_{20}\text{H}_{52}\text{N}_2\text{O}_2\text{Li}_2\text{Ge}_2\text{Sn}_2$ (**3**).

Atom	x	y	z	U(eq)
H(1A)	5247	3601	8355	160(30)
H(1B)	6184	2815	7796	160(30)
H(1C)	6820	3610	8469	160(30)
H(2A)	4937	1241	10289	114(19)
H(2B)	3969	2151	9808	114(19)
H(2C)	5313	2756	10132	114(19)
H(3A)	8323	573	8813	100(18)
H(3B)	7786	59	9589	100(18)
H(3C)	8273	1560	9500	100(18)
H(4A)	2376	3722	8226	190(40)
H(4B)	2496	2303	8591	190(40)
H(5A)	391	1774	8040	250(50)
H(5B)	267	3314	7840	250(50)
H(5C)	327	2856	8681	250(50)

Table A.13. Atomic Coordinates ($\times 10^4$) and Equivalent Isotropic Displacement Parameters ($\text{\AA}^2 \times 10^3$) for $\text{C}_{20}\text{H}_{52}\text{N}_2\text{O}_2\text{Cl}_2\text{Be}_2\text{Sn}_4$ (**4**).

Atom	x	y	z	U(eq)
Sn(1)	5101(1)	222(1)	2371(1)	31(1)
Sn(2)	7648(1)	104(1)	4804(1)	29(1)
Cl(1)	3437(2)	-1422(1)	3346(2)	31(1)
N(1)	5704(5)	91(4)	4271(5)	21(1)
O(1)	4320(5)	1884(4)	4585(5)	32(1)
Be(1)	5144(7)	815(6)	5231(8)	23(2)
C(1)	6287(9)	1321(8)	1857(9)	48(2)
C(2)	5279(10)	-1183(7)	1488(9)	51(2)
C(3)	3274(8)	793(8)	1525(8)	45(2)
C(4)	8543(8)	-688(8)	6454(9)	49(2)
C(5)	8434(8)	1611(7)	4906(9)	41(2)
C(6)	8260(8)	-670(8)	3433(10)	49(2)
C(7)	4893(8)	2609(6)	3963(8)	40(2)
C(8)	4812(11)	3622(8)	4467(13)	65(3)
C(9)	4073(17)	3526(9)	5271(15)	91(5)
C(10)	3705(9)	2478(7)	5299(11)	53(3)

Table A.14. Interatomic Distances (Å) and Angles (°) for C₂₀H₅₂N₂O₂Cl₂Be₂Sn₄ (**4**).

Sn(1)-N(1)	2.092(6)	C(3)-Sn(1)-C(2)	107.5(4)
Sn(1)-C(3)	2.132(9)	N(1)-Sn(1)-C(1)	107.9(3)
Sn(1)-C(2)	2.136(9)	C(3)-Sn(1)-C(1)	103.7(4)
Sn(1)-C(1)	2.166(9)	C(2)-Sn(1)-C(1)	106.5(4)
Sn(2)-N(1)	2.094(5)	N(1)-Sn(2)-C(4)	115.5(3)
Sn(2)-C(4)	2.130(9)	N(1)-Sn(2)-C(5)	113.8(3)
Sn(2)-C(5)	2.148(8)	C(4)-Sn(2)-C(5)	108.6(4)
Sn(2)-C(6)	2.157(9)	N(1)-Sn(2)-C(6)	108.8(3)
Cl(1)-Be(1)#1	2.072(9)	C(4)-Sn(2)-C(6)	104.7(4)
N(1)-Be(1)	1.715(10)	C(5)-Sn(2)-C(6)	104.5(4)
N(1)-Be(1)#1	1.726(10)	Be(1)-N(1)-Be(1)#1	79.3(5)
O(1)-C(10)	1.452(10)	Be(1)-N(1)-Sn(1)	124.2(4)
O(1)-C(7)	1.452(9)	Be(1)#1-N(1)-Sn(1)	111.4(4)
O(1)-Be(1)	1.718(10)	Be(1)-N(1)-Sn(2)	111.4(4)
Be(1)-N(1)#1	1.726(10)	Be(1)#1-N(1)-Sn(2)	123.2(4)
Be(1)-Cl(1)#1	2.072(9)	Sn(1)-N(1)-Sn(2)	106.7(2)
Be(1)-Be(1)#1	2.195(17)	C(10)-O(1)-C(7)	106.9(6)
C(7)-C(8)	1.459(13)	C(10)-O(1)-Be(1)	118.6(6)
C(8)-C(9)	1.427(17)	C(7)-O(1)-Be(1)	118.7(5)
C(9)-C(10)	1.434(13)	N(1)-Be(1)-O(1)	115.2(6)
N(1)-Sn(1)-C(3)	118.0(3)	N(1)-Be(1)-N(1)#1	100.7(5)
N(1)-Sn(1)-C(2)	112.3(3)	O(1)-Be(1)-N(1)#1	114.7(5)

N(1)-Be(1)-Cl(1)#1	111.9(4)	Cl(1)#1-Be(1)-Be(1)#1	125.8(6)
O(1)-Be(1)-Cl(1)#1	102.7(5)	O(1)-C(7)-C(8)	107.8(8)
N(1)#1-Be(1)-Cl(1)#1	112.0(5)	C(9)-C(8)-C(7)	107.3(9)
N(1)-Be(1)-Be(1)#1	50.6(4)	C(8)-C(9)-C(10)	109.2(9)
O(1)-Be(1)-Be(1)#1	131.5(7)	C(9)-C(10)-O(1)	107.8(8)
N(1)#1-Be(1)-Be(1)#1	50.2(4)		

Table A.15. Anisotropic displacement parameters ($\text{\AA}^2 \times 10^3$) for $\text{C}_{20}\text{H}_{52}\text{N}_2\text{O}_2\text{Cl}_2\text{Be}_2\text{Sn}_4$ (**4**).

Atom	U11	U22	U33	U23	U13	U12
Sn(1)	38(1)	30(1)	27(1)	-1(1)	15(1)	-4(1)
Sn(2)	24(1)	24(1)	43(1)	0(1)	15(1)	-2(1)
Cl(1)	31(1)	29(1)	33(1)	-5(1)	9(1)	-8(1)
N(1)	17(2)	21(3)	26(2)	3(2)	7(2)	1(2)
O(1)	29(3)	23(3)	46(3)	2(2)	15(2)	1(2)
Be(1)	21(4)	15(4)	35(4)	3(3)	11(3)	-2(3)
C(1)	58(6)	51(6)	46(5)	11(4)	34(4)	-4(4)
C(2)	71(6)	39(5)	48(5)	-17(4)	27(5)	-2(4)
C(3)	47(5)	44(5)	41(4)	7(4)	7(4)	1(4)
C(4)	37(4)	45(5)	64(6)	16(4)	15(4)	9(4)
C(5)	37(4)	31(4)	60(5)	-5(4)	22(4)	-13(3)
C(6)	35(4)	48(5)	71(6)	-17(5)	26(4)	-2(4)
C(7)	52(5)	24(4)	49(5)	9(3)	22(4)	2(3)
C(8)	79(8)	24(5)	107(9)	-4(5)	53(7)	-9(4)
C(9)	161(14)	27(5)	124(12)	-24(6)	103(12)	-20(7)
C(10)	56(6)	23(4)	96(8)	1(4)	49(6)	4(4)

Table A.16. Hydrogen coordinates ($\times 10^4$) and isotropic displacement parameters ($\text{\AA}^2 \times 10^3$) for $\text{C}_{20}\text{H}_{52}\text{N}_2\text{O}_2\text{Cl}_2\text{Be}_2\text{Sn}_4$ (**4**).

Atom	x	y	z	U(eq)
H(1A)	6715	1718	2548	120(30)
H(1B)	5796	1758	1238	120(30)
H(1C)	6872	969	1559	120(30)
H(2A)	5625	-1690	2085	140(40)
H(2B)	5807	-1083	994	140(40)
H(2C)	4484	-1399	993	140(40)
H(3A)	2683	333	1671	56(18)
H(3B)	3138	855	673	56(18)
H(3C)	3188	1445	1856	56(18)
H(4A)	8763	-215	7111	100(30)
H(4B)	9270	-1015	6386	100(30)
H(4C)	7994	-1187	6601	100(30)
H(5A)	7793	2092	4561	190(60)
H(5B)	9024	1625	4468	190(60)
H(5C)	8832	1782	5735	190(60)
H(6A)	7998	-1364	3378	60(19)
H(6B)	9140	-643	3649	60(19)
H(6C)	7911	-344	2668	60(19)
H(7A)	4472	2603	3113	60(20)
H(7B)	5736	2431	4084	60(20)
H(8A)	5618	3865	4898	150(60)

H(8B)	4440	4092	3831	150(60)
H(9A)	3358	3949	4997	180(70)
H(9B)	4537	3742	6066	180(70)
H(10A)	2830	2417	4965	70(20)
H(10B)	3940	2236	6115	70(20)

Table A.17. Atomic Coordinates ($\times 10^4$) and Equivalent Isotropic Displacement Parameters ($\text{\AA}^2 \times 10^3$) for $\text{C}_{14}\text{H}_{36}\text{Be}_2\text{F}_6\text{N}_2\text{O}_6\text{S}_2\text{Sn}_4$ (**5**).

Atom	x	y	z	U(eq)
Sn(1)	4126(1)	8849(1)	841(1)	32(1)
Sn(2)	3030(1)	10547(1)	1622(1)	38(1)
Sn(3)	1133(1)	11474(1)	-1287(1)	38(1)
Sn(4)	1912(1)	9001(1)	-1959(1)	33(1)
S(1)	3510(1)	12711(1)	-816(1)	34(1)
S(2)	1747(1)	7152(1)	536(1)	47(1)
Be(1)	2864(3)	10677(6)	-254(3)	29(1)
Be(2)	2208(4)	9227(6)	-117(4)	32(1)
N(1)	3053(2)	9766(4)	555(2)	29(1)
N(2)	2025(2)	10115(4)	-935(2)	29(1)
O(1)	3413(2)	11734(3)	-276(2)	39(1)
O(2)	2795(2)	13143(4)	-1450(2)	54(1)
O(3)	4119(2)	12398(4)	-1027(2)	51(1)
O(4)	1643(2)	8238(4)	-48(2)	45(1)
O(5)	2266(3)	6184(5)	509(3)	73(1)
O(6)	1805(3)	7571(4)	1304(2)	60(1)
C(1)	3885(3)	14010(5)	-68(3)	43(1)
C(2)	809(4)	6420(6)	-1(4)	56(2)
C(3)	4157(4)	7014(5)	1343(4)	51(1)
C(4)	4168(3)	8742(6)	-320(3)	47(1)

C(5)	5010(3)	10055(5)	1691(3)	43(1)
C(6)	3594(4)	12345(6)	1833(3)	50(1)
C(7)	1834(4)	10747(7)	1359(4)	59(2)
C(8)	3609(4)	9224(6)	2600(3)	57(2)
C(9)	1552(4)	12939(5)	-372(4)	56(2)
C(10)	951(3)	12220(6)	-2455(4)	53(2)
C(11)	157(3)	10516(6)	-1279(5)	61(2)
C(12)	2594(3)	9943(6)	-2457(3)	48(1)
C(13)	699(3)	8882(6)	-2793(4)	54(2)
C(14)	2260(4)	7134(5)	-1487(4)	60(2)
F(1)	4525(2)	13656(3)	583(2)	55(1)
F(2)	3362(2)	14364(3)	180(2)	66(1)
F(3)	4053(2)	14989(3)	-413(2)	65(1)
F(4)	690(2)	6043(4)	-751(2)	72(1)
F(5)	804(3)	5386(4)	421(3)	76(1)
F(6)	249(2)	7240(5)	-66(3)	93(2)

Table A.18. Interatomic Distances (Å) and Angles (°) for C₁₄H₃₆Be₂F₆N₂O₆S₂Sn₄ (**5**).

Sn(1)-N(1)	2.124(4)	S(2)-O(4)	1.509(4)
Sn(1)-C(3)	2.129(5)	S(2)-C(2)	1.799(6)
Sn(1)-C(4)	2.133(5)	Be(1)-O(1)	1.549(7)
Sn(1)-C(5)	2.135(5)	Be(1)-N(2)	1.645(7)
Sn(2)-N(1)	2.113(4)	Be(1)-N(1)	1.649(7)
Sn(2)-C(6)	2.136(6)	Be(1)-Be(2)	2.067(9)
Sn(2)-C(8)	2.137(6)	Be(2)-O(4)	1.551(7)
Sn(2)-C(7)	2.141(6)	Be(2)-N(1)	1.639(7)
Sn(3)-N(2)	2.107(4)	Be(2)-N(2)	1.650(7)
Sn(3)-C(10)	2.128(6)	C(1)-F(3)	1.318(6)
Sn(3)-C(11)	2.135(6)	C(1)-F(2)	1.321(7)
Sn(3)-C(9)	2.143(6)	C(1)-F(1)	1.324(6)
Sn(4)-N(2)	2.119(4)	C(2)-F(4)	1.330(8)
Sn(4)-C(12)	2.132(5)	C(2)-F(5)	1.334(7)
Sn(4)-C(14)	2.135(6)	C(2)-F(6)	1.346(8)
Sn(4)-C(13)	2.146(5)	N(1)-Sn(1)-C(3)	111.1(2)
S(1)-O(3)	1.419(4)	N(1)-Sn(1)-C(4)	103.80(17)
S(1)-O(2)	1.420(4)	C(3)-Sn(1)-C(4)	111.3(2)
S(1)-O(1)	1.487(4)	N(1)-Sn(1)-C(5)	106.27(18)
S(1)-C(1)	1.834(5)	C(3)-Sn(1)-C(5)	112.0(2)
S(2)-O(6)	1.412(4)	C(4)-Sn(1)-C(5)	111.9(2)
S(2)-O(5)	1.444(5)	N(1)-Sn(2)-C(6)	107.27(18)

N(1)-Sn(2)-C(8)	106.5(2)	O(6)-S(2)-O(5)	120.0(3)
C(6)-Sn(2)-C(8)	113.4(2)	O(6)-S(2)-O(4)	112.0(3)
N(1)-Sn(2)-C(7)	106.8(2)	O(5)-S(2)-O(4)	113.3(3)
C(6)-Sn(2)-C(7)	111.2(3)	O(6)-S(2)-C(2)	106.8(3)
C(8)-Sn(2)-C(7)	111.3(3)	O(5)-S(2)-C(2)	102.7(3)
N(2)-Sn(3)-C(10)	107.9(2)	O(4)-S(2)-C(2)	99.1(3)
N(2)-Sn(3)-C(11)	106.0(2)	O(1)-Be(1)-N(2)	134.0(4)
C(10)-Sn(3)-C(11)	114.9(3)	O(1)-Be(1)-N(1)	123.9(4)
N(2)-Sn(3)-C(9)	106.33(19)	N(2)-Be(1)-N(1)	102.1(4)
C(10)-Sn(3)-C(9)	109.6(3)	O(1)-Be(1)-Be(2)	174.7(4)
C(11)-Sn(3)-C(9)	111.7(3)	N(2)-Be(1)-Be(2)	51.3(3)
N(2)-Sn(4)-C(12)	105.17(18)	N(1)-Be(1)-Be(2)	50.9(3)
N(2)-Sn(4)-C(14)	105.81(19)	O(4)-Be(2)-N(1)	132.4(4)
C(12)-Sn(4)-C(14)	117.1(3)	O(4)-Be(2)-N(2)	125.1(4)
N(2)-Sn(4)-C(13)	107.75(19)	N(1)-Be(2)-N(2)	102.3(4)
C(12)-Sn(4)-C(13)	114.3(2)	O(4)-Be(2)-Be(1)	173.9(5)
C(14)-Sn(4)-C(13)	106.1(3)	N(1)-Be(2)-Be(1)	51.3(3)
O(3)-S(1)-O(2)	118.6(3)	N(2)-Be(2)-Be(1)	51.0(3)
O(3)-S(1)-O(1)	111.7(2)	Be(2)-N(1)-Be(1)	77.9(3)
O(2)-S(1)-O(1)	113.2(2)	Be(2)-N(1)-Sn(2)	113.4(3)
O(3)-S(1)-C(1)	105.7(3)	Be(1)-N(1)-Sn(2)	119.5(3)
O(2)-S(1)-C(1)	106.1(3)	Be(2)-N(1)-Sn(1)	123.9(3)
O(1)-S(1)-C(1)	99.2(2)	Be(1)-N(1)-Sn(1)	107.0(3)

Sn(2)-N(1)-Sn(1)	111.43(16)	F(3)-C(1)-S(1)	109.8(4)
Be(1)-N(2)-Be(2)	77.7(3)	F(2)-C(1)-S(1)	110.5(4)
Be(1)-N(2)-Sn(3)	112.2(3)	F(1)-C(1)-S(1)	110.5(4)
Be(2)-N(2)-Sn(3)	118.7(3)	F(4)-C(2)-F(5)	107.1(5)
Be(1)-N(2)-Sn(4)	122.7(3)	F(4)-C(2)-F(6)	109.4(5)
Be(2)-N(2)-Sn(4)	111.2(3)	F(5)-C(2)-F(6)	111.8(6)
Sn(3)-N(2)-Sn(4)	111.04(16)	F(4)-C(2)-S(2)	110.9(4)
S(1)-O(1)-Be(1)	143.3(3)	F(5)-C(2)-S(2)	107.6(4)
S(2)-O(4)-Be(2)	133.3(3)	F(6)-C(2)-S(2)	110.0(5)
F(3)-C(1)-F(2)	108.6(5)	F(2)-C(1)-F(1)	109.0(5)

Table A.19. Anisotropic displacement parameters ($\text{\AA}^2 \times 10^3$) for $\text{C}_{14}\text{H}_{36}\text{Be}_2\text{F}_6\text{N}_2\text{O}_6\text{S}_2\text{Sn}_4$ (**5**).

Atom	U11	U22	U33	U23	U13	U12
Sn(1)	33(1)	35(1)	26(1)	-1(1)	11(1)	2(1)
Sn(2)	44(1)	44(1)	31(1)	-8(1)	22(1)	-6(1)
Sn(3)	29(1)	37(1)	47(1)	4(1)	18(1)	5(1)
Sn(4)	31(1)	40(1)	29(1)	-4(1)	15(1)	-4(1)
S(1)	34(1)	36(1)	31(1)	1(1)	12(1)	-5(1)
S(2)	46(1)	51(1)	41(1)	3(1)	17(1)	-15(1)
Be(1)	31(3)	34(3)	24(2)	-3(2)	15(2)	1(2)
Be(2)	34(3)	34(3)	30(3)	-1(2)	16(2)	0(2)
N(1)	30(2)	35(2)	26(2)	-2(2)	16(2)	0(2)
N(2)	28(2)	33(2)	29(2)	1(2)	15(2)	3(2)
O(1)	40(2)	42(2)	35(2)	-1(2)	15(2)	-13(2)
O(2)	43(2)	53(2)	43(2)	4(2)	-2(2)	-1(2)
O(3)	53(2)	64(3)	47(2)	-3(2)	31(2)	-5(2)
O(4)	44(2)	47(2)	44(2)	5(2)	19(2)	-11(2)
O(5)	58(3)	87(3)	88(3)	39(3)	45(3)	33(3)
O(6)	86(3)	54(2)	37(2)	-7(2)	25(2)	-13(2)
C(1)	47(3)	41(3)	38(3)	1(2)	18(2)	-10(2)
C(2)	47(3)	61(4)	60(4)	-2(3)	23(3)	-13(3)
C(3)	52(3)	42(3)	53(3)	7(3)	18(3)	5(3)
C(4)	37(3)	69(4)	34(2)	-2(2)	15(2)	6(3)
C(5)	35(3)	54(3)	40(3)	-8(2)	18(2)	-3(2)

C(6)	62(4)	51(3)	44(3)	-14(3)	30(3)	-8(3)
C(7)	56(4)	69(4)	70(4)	-14(3)	43(3)	-4(3)
C(8)	75(4)	68(4)	32(3)	0(3)	27(3)	-8(3)
C(9)	54(4)	42(3)	77(4)	-12(3)	35(3)	5(3)
C(10)	45(3)	54(3)	53(3)	18(3)	15(3)	3(3)
C(11)	40(3)	61(4)	99(5)	7(4)	45(3)	2(3)
C(12)	43(3)	73(4)	35(2)	-11(3)	24(2)	-18(3)
C(13)	33(3)	76(4)	50(3)	-20(3)	17(2)	-15(3)
C(14)	86(5)	42(3)	62(4)	-3(3)	43(3)	9(3)
F(1)	49(2)	62(2)	39(2)	-1(2)	8(1)	-16(2)
F(2)	71(2)	56(2)	78(2)	-23(2)	41(2)	-7(2)
F(3)	87(3)	45(2)	57(2)	6(2)	25(2)	-23(2)
F(4)	75(3)	73(3)	47(2)	-17(2)	7(2)	-21(2)
F(5)	91(3)	53(2)	88(3)	2(2)	44(2)	-32(2)
F(6)	51(2)	102(4)	134(4)	11(3)	50(3)	15(2)

Table A.20. Hydrogen coordinates ($\times 10^4$) and isotropic displacement parameters ($\text{\AA}^2 \times 10^3$) for $\text{C}_{14}\text{H}_{36}\text{Be}_2\text{F}_6\text{N}_2\text{O}_6\text{S}_2\text{Sn}_4$ (**5**).

Atom	x	y	z	U(eq)
H(3A)	4287	7085	1914	77(13)
H(3B)	4536	6512	1276	77(13)
H(3C)	3662	6626	1062	77(13)
H(4A)	3807	8126	-658	88(15)
H(4B)	4676	8511	-233	88(15)
H(4C)	4039	9544	-585	88(15)
H(5A)	4921	10899	1488	73(13)
H(5B)	5503	9778	1751	73(13)
H(5C)	4999	10026	2213	73(13)
H(6A)	3973	12332	1630	104(17)
H(6B)	3838	12519	2410	104(17)
H(6C)	3221	12984	1555	104(17)
H(7A)	1518	10619	785	140(20)
H(7B)	1747	11574	1509	140(20)
H(7C)	1705	10138	1667	140(20)
H(8A)	3440	8391	2405	93(15)
H(8B)	3490	9408	3047	93(15)
H(8C)	4153	9284	2782	93(15)
H(9A)	2089	12813	-27	109(18)
H(9B)	1275	12914	-47	109(18)
H(9C)	1477	13738	-637	109(18)

H(10A)	1297	11824	-2630	78(13)
H(10B)	1044	13106	-2407	78(13)
H(10C)	431	12063	-2849	78(13)
H(11A)	-249	10476	-1826	120(20)
H(11B)	-19	10964	-937	120(20)
H(11C)	304	9683	-1071	120(20)
H(12A)	2721	10768	-2228	116(19)
H(12B)	2307	10001	-3040	116(19)
H(12C)	3057	9477	-2324	116(19)
H(13A)	414	8691	-2490	93(15)
H(13B)	619	8234	-3187	93(15)
H(13C)	527	9668	-3069	93(15)
H(14A)	2721	7177	-982	101(17)
H(14B)	2356	6649	-1877	101(17)
H(14C)	1860	6747	-1394	101(17)

Table A.21. Atomic Coordinates ($\times 10^4$) and Equivalent Isotropic Displacement Parameters ($\text{\AA}^2 \times 10^3$) for $\text{C}_{14}\text{H}_{36}\text{N}_2\text{O}_2\text{Cl}_2\text{Be}_2\text{Si}_2$ (**6**).

Atom	x	y	z	U(eq)
Cl(1)	9804(1)	2564(1)	810(1)	41(1)
Si(1)	12064(1)	231(1)	1108(1)	35(1)
N(1)	12373(3)	1444(3)	562(2)	30(1)
O(1)	11992(2)	3872(2)	545(1)	35(1)
Be(1)	11405(4)	2536(4)	336(3)	31(1)
C(1)	13384(4)	-761(4)	1144(3)	53(1)
C(2)	10779(4)	-624(4)	784(2)	47(1)
C(3)	11760(5)	737(4)	2031(2)	53(1)
C(4)	11472(5)	4919(4)	242(2)	46(1)
C(5)	11762(5)	5904(4)	750(3)	62(2)
C(6)	11918(7)	5288(5)	1448(4)	85(2)
C(7)	12338(5)	4106(4)	1282(2)	53(1)

Table A.22. Interatomic Distances (Å) and Angles (°) for C₁₄H₃₆N₂O₂Cl₂Be₂Si₂ (**6**).

Cl(1)-Be(1)	2.026(5)	Be(1)#1-N(1)-Si(1)	125.8(2)
Si(1)-N(1)	1.756(3)	Be(1)-N(1)-Si(1)	125.9(2)
Si(1)-C(2)	1.856(5)	C(4)-O(1)-C(7)	109.6(3)
Si(1)-C(3)	1.865(4)	C(4)-O(1)-Be(1)	118.8(3)
Si(1)-C(1)	1.876(5)	C(7)-O(1)-Be(1)	119.0(3)
N(1)-Be(1)#1	1.704(6)	O(1)-Be(1)-N(1)#1	108.5(3)
N(1)-Be(1)	1.711(6)	O(1)-Be(1)-N(1)	109.7(3)
O(1)-C(4)	1.445(5)	N(1)#1-Be(1)-N(1)	98.7(3)
O(1)-C(7)	1.470(5)	O(1)-Be(1)-Cl(1)	103.6(3)
O(1)-Be(1)	1.703(5)	N(1)#1-Be(1)-Cl(1)	117.6(3)
Be(1)-N(1)#1	1.704(6)	N(1)-Be(1)-Cl(1)	118.5(3)
Be(1)-Be(1)#1	2.215(10)	O(1)-Be(1)-Be(1)#1	114.95(18)
C(4)-C(5)	1.509(6)	N(1)#1-Be(1)-Be(1)#1	49.7(2)
C(5)-C(6)	1.501(8)	N(1)-Be(1)-Be(1)#1	49.4(2)
C(6)-C(7)	1.459(7)	Cl(1)-Be(1)-Be(1)#1	141.42(14)
N(1)-Si(1)-C(2)	111.93(18)	O(1)-C(4)-C(5)	105.6(4)
N(1)-Si(1)-C(3)	110.08(19)	C(6)-C(5)-C(4)	103.7(4)
C(2)-Si(1)-C(3)	108.9(2)	C(7)-C(6)-C(5)	106.2(5)
N(1)-Si(1)-C(1)	109.4(2)	C(6)-C(7)-O(1)	106.4(4)
C(2)-Si(1)-C(1)	109.0(2)		
C(3)-Si(1)-C(1)	107.4(2)		
Be(1)#1-N(1)-Be(1)	80.9(3)		

Table A.23. Anisotropic displacement parameters ($\text{\AA}^2 \times 10^3$) for $\text{C}_{14}\text{H}_{36}\text{N}_2\text{O}_2\text{Cl}_2\text{Be}_2\text{Si}_2$ (**6**).

Atom	U11	U22	U33	U23	U13	U12
Cl(1)	33(1)	48(1)	41(1)	-5(1)	12(1)	0(1)
Si(1)	41(1)	31(1)	33(1)	0(1)	1(1)	-1(1)
N(1)	31(2)	28(2)	30(2)	-4(1)	3(1)	-1(1)
O(1)	39(2)	32(1)	36(1)	-6(1)	3(1)	-3(1)
Be(1)	30(2)	30(2)	32(3)	-6(2)	6(2)	-1(2)
C(1)	55(3)	44(3)	59(3)	1(2)	-11(2)	11(2)
C(2)	52(3)	39(2)	48(3)	5(2)	0(2)	-3(2)
C(3)	69(3)	56(3)	34(2)	5(2)	5(2)	-6(2)
C(4)	67(3)	32(2)	40(2)	5(2)	8(2)	1(2)
C(5)	93(4)	34(3)	59(3)	-7(2)	25(3)	-9(2)
C(6)	128(6)	52(3)	76(4)	-27(3)	-36(4)	13(4)
C(7)	59(3)	52(3)	48(3)	-15(2)	-10(2)	-1(2)

Table A.24. Hydrogen coordinates ($\times 10^4$) and isotropic displacement parameters ($\text{\AA}^2 \times 10^3$) for $\text{C}_{14}\text{H}_{36}\text{N}_2\text{O}_2\text{Cl}_2\text{Be}_2\text{Si}_2$ (**6**).

Atom	x	y	z	U(eq)
HN1	13033	1805	743	40(12)
H(1A)	13538	-1072	681	66(9)
H(1B)	13235	-1397	1467	66(9)
H(1C)	14056	-320	1304	66(9)
H(2A)	10109	-114	744	63(9)
H(2B)	10607	-1247	1112	63(9)
H(2C)	10958	-954	328	63(9)
H(3A)	12379	1253	2184	58(9)
H(3B)	11720	68	2341	58(9)
H(3C)	11023	1151	2043	58(9)
H(4A)	10635	4829	196	54(10)
H(4B)	11799	5076	-218	54(10)
H(5A)	12472	6301	611	130(20)
H(5B)	11132	6466	772	130(20)
H(6A)	12480	5698	1736	150(30)
H(6B)	11183	5251	1698	150(30)
H(7A)	11991	3545	1592	62(11)
H(7B)	13170	4065	1331	62(11)

Table A.25. Atomic Coordinates ($\times 10^4$) and Equivalent Isotropic Displacement Parameters ($\text{\AA}^2 \times 10^3$) for $\text{C}_{24}\text{H}_{72}\text{N}_4\text{Sn}_8\text{Ag}_4$ (**7**).

Atom	x	y	z	U(eq)
Ag(1)	2333(1)	8695(1)	1587(1)	26(1)
Ag(2)	2633(1)	10457(1)	2477(1)	26(1)
Ag(3)	2654(1)	9076(1)	3529(1)	26(1)
Ag(4)	2319(1)	7321(1)	2638(1)	26(1)
Sn(1)	2876(1)	6141(1)	1561(1)	33(1)
Sn(2)	913(1)	6783(1)	1291(1)	33(1)
Sn(3)	1627(1)	11040(1)	951(1)	37(1)
Sn(4)	3660(1)	10677(1)	1576(1)	37(1)
Sn(5)	1683(1)	7011(1)	3868(1)	31(1)
Sn(6)	3660(1)	6854(1)	4053(1)	30(1)
Sn(7)	3758(1)	11300(1)	3935(1)	31(1)
Sn(8)	1703(1)	11372(1)	3377(1)	31(1)
N(1)	2080(3)	7144(5)	1676(3)	26(1)
N(2)	2567(3)	10270(5)	1553(3)	27(1)
N(3)	2583(3)	7485(5)	3597(3)	27(1)
N(4)	2710(3)	10658(5)	3400(3)	25(1)
C(1)	2408(9)	5391(10)	670(5)	69(4)
C(2)	3893(5)	7008(8)	1640(5)	51(2)
C(3)	3148(6)	4995(7)	2258(5)	51(2)
C(4)	443(7)	7037(12)	309(5)	68(3)

C(5)	316(5)	7756(8)	1719(5)	47(2)
C(6)	781(7)	5199(8)	1478(6)	60(3)
C(7)	1760(10)	11177(11)	70(5)	82(5)
C(8)	1544(7)	12529(8)	1295(6)	68(3)
C(9)	600(6)	10191(9)	863(5)	54(2)
C(10)	4490(6)	9936(11)	2366(5)	65(3)
C(11)	3874(7)	10168(11)	775(5)	69(3)
C(12)	3699(7)	12332(8)	1633(7)	64(3)
C(13)	2105(6)	6822(10)	4859(4)	57(3)
C(14)	783(6)	8137(8)	3593(6)	58(3)
C(15)	1260(6)	5569(8)	3453(5)	56(3)
C(16)	3555(6)	5231(7)	4114(4)	49(2)
C(17)	4149(6)	7501(9)	4963(4)	55(3)
C(18)	4378(6)	7238(8)	3527(5)	51(2)
C(19)	4617(5)	10131(7)	4102(4)	44(2)
C(20)	3661(6)	11828(10)	4783(5)	60(3)
C(21)	4010(6)	12547(7)	3435(5)	49(2)
C(22)	781(6)	10708(9)	2613(5)	52(2)
C(23)	1822(6)	12983(7)	3248(6)	57(3)
C(24)	1509(6)	11071(9)	4213(5)	53(2)

Table A.26. Interatomic Distances (Å) and Angles (°) for C₂₄H₇₂N₄Sn₈Ag₄ (**7**).

Ag(1)-N(1)	2.097(6)	Sn(3)-C(8)	2.121(11)
Ag(1)-N(2)	2.102(6)	Sn(3)-C(9)	2.131(10)
Ag(1)-Ag(2)	2.9967(8)	Sn(3)-C(7)	2.143(10)
Ag(1)-Ag(4)	3.0224(8)	Sn(4)-N(2)	2.056(6)
Ag(2)-N(4)	2.103(6)	Sn(4)-C(11)	2.131(9)
Ag(2)-N(2)	3.0111(8)	Sn(4)-C(10)	2.145(12)
Ag(2)-Sn(4)	3.2820(8)	Sn(4)-C(12)	2.157(10)
Ag(3)-N(3)	2.084(6)	Sn(5)-N(3)	2.058(6)
Ag(3)-N(4)	2.087(6)	Sn(5)-C(15)	2.124(10)
Ag(3)-Ag(4)	2.9880(8)	Sn(5)-C(14)	2.128(9)
Ag(4)-N(3)	2.105(6)	Sn(5)-C(13)	2.153(9)
Ag(4)-N(1)	2.118(6)	Sn(6)-N(3)	2.050(6)
Ag(4)-Sn(2)	3.3306(8)	Sn(6)-C(16)	2.129(9)
Sn(1)-N(1)	2.045(6)	Sn(6)-C(17)	2.141(9)
Sn(1)-C(3)	2.119(9)	Sn(6)-C(18)	2.147(9)
Sn(1)-C(2)	2.132(9)	Sn(7)-N(4)	2.056(6)
Sn(1)-C(1)	2.160(10)	Sn(7)-C(19)	2.125(8)
Sn(2)-N(1)	2.060(6)	Sn(7)-C(21)	2.136(10)
Sn(2)-C(5)	2.135(9)	Sn(7)-C(20)	2.143(9)
Sn(2)-C(6)	2.136(10)	Sn(8)-N(4)	2.051(6)
Sn(2)-C(4)	2.146(10)	Sn(8)-C(24)	2.122(9)
Sn(3)-N(2)	2.050(6)	Sn(8)-C(23)	2.140(10)

Sn(8)-C(22)	2.142(9)	N(3)-Ag(4)-N(1)	178.7(2)
N(1)-Ag(1)-N(2)	176.0(2)	N(3)-Ag(4)-Ag(3)	44.22(17)
N(1)-Ag(1)-Ag(2)	131.43(16)	N(1)-Ag(4)-Ag(3)	136.10(17)
N(2)-Ag(1)-Ag(2)	44.72(16)	N(3)-Ag(4)-Ag(1)	136.19(18)
N(1)-Ag(1)-Ag(4)	44.47(16)	N(1)-Ag(4)-Ag(1)	43.91(17)
N(2)-Ag(1)-Ag(4)	131.85(16)	Ag(3)-Ag(4)-Ag(1)	92.46(2)
Ag(2)-Ag(1)-Ag(4)	87.32(2)	N(3)-Ag(4)-Sn(2)	144.61(16)
N(4)-Ag(2)-N(2)	179.2(2)	N(1)-Ag(4)-Sn(2)	36.53(16)
N(4)-Ag(2)-Ag(1)	136.09(17)	Ag(3)-Ag(4)-Sn(2)	134.78(2)
N(2)-Ag(2)-Ag(1)	44.53(17)	Ag(1)-Ag(4)-Sn(2)	66.418(19)
N(4)-Ag(2)-Ag(3)	43.83(17)	N(1)-Sn(1)-C(3)	109.6(3)
N(2)-Ag(2)-Ag(3)	136.72(18)	N(1)-Sn(1)-C(2)	107.2(3)
Ag(1)-Ag(2)-Ag(3)	92.51(2)	C(3)-Sn(1)-C(2)	110.2(4)
N(4)-Ag(2)-Sn(4)	141.90(16)	N(1)-Sn(1)-C(1)	110.7(4)
N(2)-Ag(2)-Sn(4)	37.43(16)	C(3)-Sn(1)-C(1)	108.2(5)
Ag(1)-Ag(2)-Sn(4)	68.771(19)	C(2)-Sn(1)-C(1)	111.0(5)
Ag(3)-Ag(2)-Sn(4)	136.00(2)	N(1)-Sn(2)-C(5)	107.0(3)
N(3)-Ag(3)-N(4)	176.4(2)	N(1)-Sn(2)-C(6)	108.0(4)
N(3)-Ag(3)-Ag(4)	44.77(16)	C(5)-Sn(2)-C(6)	111.4(4)
N(4)-Ag(3)-Ag(4)	131.60(15)	N(1)-Sn(2)-C(4)	112.6(4)
N(3)-Ag(3)-Ag(2)	132.14(16)	C(5)-Sn(2)-C(4)	108.6(5)
N(4)-Ag(3)-Ag(2)	44.27(15)	C(6)-Sn(2)-C(4)	109.3(5)
Ag(4)-Ag(3)-Ag(2)	87.69(2)	N(1)-Sn(2)-Ag(4)	37.75(16)

C(5)-Sn(2)-Ag(4)	78.3(3)	C(15)-Sn(5)-C(13)	108.3(5)
C(6)-Sn(2)-Ag(4)	96.9(3)	C(14)-Sn(5)-C(13)	110.0(4)
C(4)-Sn(2)-Ag(4)	147.1(4)	N(3)-Sn(6)-C(16)	109.7(3)
N(2)-Sn(3)-C(8)	110.3(4)	N(3)-Sn(6)-C(17)	109.6(4)
N(2)-Sn(3)-C(9)	108.2(3)	C(16)-Sn(6)-C(17)	110.0(4)
C(8)-Sn(3)-C(9)	109.2(5)	N(3)-Sn(6)-C(18)	106.9(3)
N(2)-Sn(3)-C(7)	109.3(4)	C(16)-Sn(6)-C(18)	110.9(4)
C(8)-Sn(3)-C(7)	109.2(6)	C(17)-Sn(6)-C(18)	109.7(4)
C(9)-Sn(3)-C(7)	110.5(6)	N(4)-Sn(7)-C(19)	107.0(3)
N(2)-Sn(4)-C(11)	112.3(4)	N(4)-Sn(7)-C(21)	108.7(3)
N(2)-Sn(4)-C(10)	107.2(4)	C(19)-Sn(7)-C(21)	110.6(4)
C(11)-Sn(4)-C(10)	107.7(5)	N(4)-Sn(7)-C(20)	108.3(3)
N(2)-Sn(4)-C(12)	105.6(3)	C(19)-Sn(7)-C(20)	111.2(4)
C(11)-Sn(4)-C(12)	110.5(5)	C(21)-Sn(7)-C(20)	110.9(5)
C(10)-Sn(4)-C(12)	113.5(5)	N(4)-Sn(8)-C(24)	109.6(3)
N(2)-Sn(4)-Ag(2)	38.57(16)	N(4)-Sn(8)-C(23)	108.2(3)
C(11)-Sn(4)-Ag(2)	148.2(4)	C(24)-Sn(8)-C(23)	111.4(5)
C(10)-Sn(4)-Ag(2)	79.3(3)	N(4)-Sn(8)-C(22)	106.1(3)
C(12)-Sn(4)-Ag(2)	93.6(3)	C(24)-Sn(8)-C(22)	109.6(4)
N(3)-Sn(5)-C(15)	109.3(4)	C(23)-Sn(8)-C(22)	111.7(4)
N(3)-Sn(5)-C(14)	109.0(4)	Sn(1)-N(1)-Sn(2)	118.7(3)
C(15)-Sn(5)-C(14)	110.7(4)	Sn(1)-N(1)-Ag(1)	114.1(3)
N(3)-Sn(5)-C(13)	109.5(3)	Sn(2)-N(1)-Ag(1)	114.1(3)

Sn(1)-N(1)-Ag(4)	108.4(3)	Sn(5)-N(3)-Ag(3)	113.6(3)
Sn(2)-N(1)-Ag(4)	105.7(3)	Sn(6)-N(3)-Ag(4)	108.5(3)
Ag(1)-N(1)-Ag(4)	91.6(2)	Sn(5)-N(3)-Ag(4)	112.5(3)
Sn(3)-N(2)-Sn(4)	118.0(3)	Ag(3)-N(3)-Ag(4)	91.0(2)
Sn(3)-N(2)-Ag(1)	111.6(3)	Sn(8)-N(4)-Sn(7)	118.2(3)
Sn(4)-N(2)-Ag(1)	117.4(3)	Sn(8)-N(4)-Ag(3)	111.1(3)
Sn(3)-N(2)-Ag(2)	111.1(3)	Sn(7)-N(4)-Ag(3)	113.5(3)
Sn(4)-N(2)-Ag(2)	104.0(3)	Sn(8)-N(4)-Ag(2)	107.2(3)
Ag(1)-N(2)-Ag(2)	90.7(2)	Sn(7)-N(4)-Ag(2)	111.7(3)
Sn(6)-N(3)-Sn(5)	117.1(3)	Ag(3)-N(4)-Ag(2)	91.9(2)
Sn(6)-N(3)-Ag(3)	111.2(3)		

Table A.27. Anisotropic displacement parameters ($\text{\AA}^2 \times 10^3$) for $\text{C}_{24}\text{H}_{72}\text{N}_4\text{Sn}_8\text{Ag}_4$ (7).

Atom	U11	U22	U33	U23	U13	U12
Ag(1)	23(1)	26(1)	29(1)	-2(1)	10(1)	-3(1)
Ag(2)	23(1)	27(1)	29(1)	-3(1)	10(1)	-2(1)
Ag(3)	23(1)	24(1)	29(1)	-2(1)	9(1)	1(1)
Ag(4)	23(1)	26(1)	28(1)	-2(1)	9(1)	0(1)
Sn(1)	36(1)	32(1)	35(1)	-6(1)	15(1)	4(1)
Sn(2)	26(1)	35(1)	38(1)	-6(1)	9(1)	-8(1)
Sn(3)	41(1)	32(1)	36(1)	5(1)	11(1)	1(1)
Sn(4)	35(1)	40(1)	42(1)	-11(1)	23(1)	-11(1)
Sn(5)	27(1)	29(1)	41(1)	3(1)	17(1)	3(1)
Sn(6)	24(1)	34(1)	31(1)	0(1)	7(1)	4(1)
Sn(7)	26(1)	33(1)	33(1)	-8(1)	7(1)	-3(1)
Sn(8)	28(1)	28(1)	38(1)	-4(1)	13(1)	3(1)
N(1)	23(3)	27(3)	29(3)	-3(2)	9(2)	2(2)
N(2)	23(3)	33(3)	29(3)	2(2)	13(2)	-1(2)
N(3)	23(3)	32(3)	26(3)	0(2)	10(2)	3(2)
N(4)	23(3)	24(3)	27(3)	-7(2)	9(2)	-2(2)
C(1)	103(10)	60(7)	45(5)	-23(5)	27(6)	17(6)
C(2)	33(4)	53(6)	73(7)	4(5)	28(4)	3(4)
C(3)	54(6)	31(5)	64(6)	11(4)	18(4)	11(4)
C(4)	49(6)	106(10)	36(5)	-11(5)	-1(4)	-5(6)
C(5)	39(5)	47(5)	62(6)	-11(4)	24(4)	-7(4)

C(6)	54(6)	34(5)	94(8)	-3(5)	28(6)	-14(4)
C(7)	125(12)	89(10)	44(6)	28(6)	44(7)	41(9)
C(8)	65(7)	38(5)	87(9)	-8(5)	11(6)	10(5)
C(9)	42(5)	57(6)	50(5)	5(4)	0(4)	-8(4)
C(10)	42(5)	83(9)	62(6)	2(6)	10(5)	-4(5)
C(11)	75(8)	87(9)	64(7)	-31(6)	49(6)	-9(7)
C(12)	69(7)	34(5)	119(10)	-19(6)	69(7)	-17(5)
C(13)	59(6)	79(8)	37(4)	11(5)	24(4)	15(5)
C(14)	40(5)	52(6)	89(8)	1(5)	31(5)	22(4)
C(15)	49(6)	42(5)	70(7)	-12(5)	11(5)	-5(4)
C(16)	63(6)	35(5)	45(5)	2(4)	13(4)	14(4)
C(17)	48(5)	75(7)	33(4)	-13(4)	3(4)	-15(5)
C(18)	38(5)	60(6)	66(6)	5(5)	33(4)	-4(4)
C(19)	31(4)	40(5)	50(5)	-6(4)	1(3)	9(3)
C(20)	46(5)	88(9)	48(5)	-34(5)	17(4)	-15(5)
C(21)	39(5)	39(5)	66(6)	8(4)	16(4)	-4(4)
C(22)	34(4)	61(6)	48(5)	-14(4)	-1(4)	4(4)
C(23)	48(5)	30(5)	96(8)	-1(5)	31(5)	5(4)
C(24)	53(6)	69(7)	44(5)	1(5)	25(4)	5(5)

Table A.28. Hydrogen coordinates ($\times 10^4$) and isotropic displacement parameters ($\text{\AA}^2 \times 10^3$) for $\text{C}_{24}\text{H}_{72}\text{N}_4\text{Sn}_8\text{Ag}_4$ (**7**).

Atom	x	y	z	U(eq)
H(1A)	2072	4848	690	90(30)
H(1B)	2824	5120	563	90(30)
H(1C)	2123	5874	365	90(30)
H(2A)	3745	7624	1406	56(18)
H(2B)	4220	6614	1485	56(18)
H(2C)	4168	7172	2062	56(18)
H(3A)	3372	5308	2653	70(20)
H(3B)	3509	4522	2198	70(20)
H(3C)	2686	4642	2234	70(20)
H(4A)	673	7635	211	90(30)
H(4B)	-106	7128	179	90(30)
H(4C)	554	6460	102	90(30)
H(5A)	149	7363	1995	70(20)
H(5B)	-125	8054	1410	70(20)
H(5C)	658	8285	1943	70(20)
H(6A)	902	4784	1186	120(40)
H(6B)	258	5074	1445	120(40)
H(6C)	1124	5035	1884	120(40)
H(7A)	2209	11579	113	180(60)
H(7B)	1312	11499	-217	180(60)
H(7C)	1819	10512	-79	180(60)

H(8A)	1594	12482	1718	120(40)
H(8B)	1052	12822	1062	120(40)
H(8C)	1949	12952	1261	120(40)
H(9A)	564	9609	606	110(30)
H(9B)	155	10616	684	110(30)
H(9C)	623	9969	1261	110(30)
H(10A)	4313	9263	2406	170(50)
H(10B)	4546	10321	2729	170(50)
H(10C)	4980	9895	2314	170(50)
H(11A)	4130	9521	857	240(80)
H(11B)	4195	10654	673	240(80)
H(11C)	3393	10103	438	240(80)
H(12A)	3458	12615	1230	130(40)
H(12B)	4226	12553	1801	130(40)
H(12C)	3429	12558	1892	130(40)
H(13A)	2536	6362	4981	100(30)
H(13B)	1700	6552	4980	100(30)
H(13C)	2266	7470	5053	100(30)
H(14A)	999	8794	3734	150(50)
H(14B)	401	7976	3768	150(50)
H(14C)	548	8143	3154	150(50)
H(15A)	1251	5564	3039	85
H(15B)	747	5462	3451	85

H(15C)	1593	5037	3682	85
H(16A)	3120	5077	4231	70(20)
H(16B)	4016	4964	4415	70(20)
H(16C)	3480	4929	3723	70(20)
H(17A)	4552	7969	4976	90(30)
H(17B)	4357	6967	5256	90(30)
H(17C)	3754	7854	5059	90(30)
H(18A)	4207	6863	3149	100(30)
H(18B)	4905	7066	3759	100(30)
H(18C)	4340	7953	3440	100(30)
H(19A)	4608	9710	4435	90(30)
H(19B)	5117	10437	4205	90(30)
H(19C)	4510	9723	3740	90(30)
H(20A)	3261	12332	4694	60(20)
H(20B)	4142	12121	5038	60(20)
H(20C)	3536	11266	4992	60(20)
H(21A)	4149	12284	3104	110(30)
H(21B)	4431	12938	3705	110(30)
H(21C)	3562	12972	3271	110(30)
H(22A)	853	9985	2611	210(70)
H(22B)	787	10992	2236	210(70)
H(22C)	294	10851	2654	210(70)
H(23A)	2100	13294	3637	140(40)

H(23B)	1319	13286	3075	140(40)
H(23C)	2100	13084	2976	140(40)
H(24A)	1491	10350	4269	130(40)
H(24B)	1028	11370	4192	130(40)
H(24C)	1921	11359	4551	130(40)

Table A.29. Atomic Coordinates ($\times 10^4$) and Equivalent Isotropic Displacement Parameters ($\text{\AA}^2 \times 10^3$) for $\text{C}_{24}\text{H}_{72}\text{N}_4\text{Si}_4\text{Sn}_4\text{Ag}_4$ (**8**).

Atom	x	y	z	U(eq)
Ag(1)	4236(1)	1062(1)	8759(1)	33(1)
Sn(1)	4659(1)	2812(1)	11330(1)	49(1)
Si(1)	4659(1)	2812(1)	11330(1)	49(1)
Sn(2)	3286(1)	0	5356(1)	46(1)
Si(2)	3286(1)	0	5356(1)	46(1)
Sn(3)	2658(1)	0	8123(1)	48(1)
Si(3)	2658(1)	0	8123(1)	48(1)
N(1)	5000	2134(5)	10000	34(2)
N(2)	3474(4)	0	7534(10)	36(2)
C(1)	5324(18)	3760(20)	12470(40)	105(8)
C(1A)	5557(11)	3253(15)	13240(20)	69(5)
C(2)	3648(14)	3300(19)	9850(30)	89(7)
C(2A)	4035(12)	3874(14)	10190(30)	68(5)
C(3)	4590(15)	1880(17)	12740(30)	82(6)
C(3A)	4151(12)	1892(16)	12060(30)	72(5)
C(4)	4250(20)	80(130)	5320(40)	69(17)
C(4A)	4150(20)	-380(30)	5280(40)	40(9)
C(5)	3039(13)	1456(16)	4590(30)	77(6)
C(5A)	2612(14)	962(17)	4170(30)	86(7)
C(6)	2308(13)	1416(17)	7740(30)	83(6)

C(6A)	1907(17)	840(20)	6710(30)	109(9)
C(7)	3040(20)	270(30)	10150(50)	55(12)
C(7A)	3000(20)	-330(30)	10560(50)	58(12)

Table A.30. Interatomic Distances (Å) and Angles (°) for C₂₄H₇₂N₄Si₄Sn₄Ag₄ (**8**).

Ag(1)-N(2)	2.118(5)	Sn(2)-Ag(1)#1	3.3281(12)
Ag(1)-N(1)	2.132(5)	Sn(3)-C(7)#	1.78(4)
Ag(1)-Ag(1)#1	2.9949(11)	Sn(3)-C(7)	1.78(4)
Ag(1)-Ag(1)#2	3.0104(11)	Sn(3)-C(6A)#1	1.95(3)
Ag(1)-Sn(1)	3.3151(11)	Sn(3)-C(6A)	1.95(3)
Ag(1)-Sn(2)	3.3281(12)	Sn(3)-N(2)	2.000(8)
Sn(1)-C(1)	1.88(3)	Sn(3)-C(6)	2.10(2)
Sn(1)-C(3)	1.93(2)	Sn(3)-C(6)#1	2.10(2)
Sn(1)-N(1)	1.952(4)	Sn(3)-C(7A)#1	2.16(5)
Sn(1)-C(2A)	1.97(2)	Sn(3)-C(7A)	2.16(5)
Sn(1)-C(3A)	2.05(2)	N(1)-Si(1)#2	1.952(4)
Sn(1)-C(2)	2.07(3)	N(1)-Sn(1)#2	1.952(4)
Sn(2)-C(4A)#1	1.91(4)	N(1)-Ag(1)#2	2.132(5)
Sn(2)-C(4A)	1.91(4)	N(2)-Ag(1)#1	2.118(5)
Sn(2)-C(5A)#1	1.92(2)	C(1)-C(1A)	0.98(3)
Sn(2)-C(5A)	1.92(2)	C(2)-C(2A)	1.08(3)
Sn(2)-N(2)	1.940(9)	C(3)-C(3A)	0.86(3)
Sn(2)-C(4)#1	2.03(4)	C(4)-C(4)#1	0.2(4)
Sn(2)-C(4)	2.03(4)	C(4)-C(4A)#1	0.47(17)
Sn(2)-C(5)#1	2.16(2)	C(4)-C(4A)	0.69(17)
Sn(2)-C(5)	2.16(2)	C(4A)-C(4)#1	0.47(17)

C(4A)-C(4A)#1	1.08(8)	C(1)-Sn(1)-C(3)	109.7(13)
C(5)-C(5A)	1.06(3)	C(1)-Sn(1)-N(1)	109.9(10)
C(6)-C(6A)	1.27(3)	C(3)-Sn(1)-N(1)	106.2(7)
C(7)-C(7A)#1	0.43(6)	C(1)-Sn(1)-C(2A)	85.3(12)
C(7)-C(7)#1	0.75(7)	C(3)-Sn(1)-C(2A)	132.3(10)
C(7)-C(7A)	0.94(4)	N(1)-Sn(1)-C(2A)	110.5(7)
C(7A)-C(7)#1	0.43(6)	C(1)-Sn(1)-C(3A)	129.0(12)
C(7A)-C(7A)#1	0.93(8)	C(3)-Sn(1)-C(3A)	25.3(8)
N(2)-Ag(1)-N(1)	179.7(2)	N(1)-Sn(1)-C(3A)	107.9(7)
N(2)-Ag(1)-Ag(1)#1	45.00(14)	C(2A)-Sn(1)-C(3A)	111.8(10)
N(1)-Ag(1)-Ag(1)#1	135.09(14)	C(1)-Sn(1)-C(1A)	28.6(10)
N(2)-Ag(1)-Ag(1)#2	135.00(14)	C(3)-Sn(1)-C(1A)	84.3(10)
N(1)-Ag(1)-Ag(1)#2	45.09(14)	N(1)-Sn(1)-C(1A)	106.4(6)
Ag(1)#1-Ag(1)-Ag(1)#2	90.0	C(2A)-Sn(1)-C(1A)	112.5(9)
N(2)-Ag(1)-Sn(1)	145.8(2)	C(3A)-Sn(1)-C(1A)	107.5(9)
N(1)-Ag(1)-Sn(1)	33.95(6)	C(1)-Sn(1)-C(2)	115.2(12)
Ag(1)#1-Ag(1)-Sn(1)	138.052(19)	C(3)-Sn(1)-C(2)	110.0(11)
Ag(1)#2-Ag(1)-Sn(1)	64.60(2)	N(1)-Sn(1)-C(2)	105.3(7)
N(2)-Ag(1)-Sn(2)	33.2(2)	C(2A)-Sn(1)-C(2)	31.0(8)
N(1)-Ag(1)-Sn(2)	147.03(6)	C(3A)-Sn(1)-C(2)	85.6(10)
Ag(1)#1-Ag(1)-Sn(2)	63.260(14)	C(1A)-Sn(1)-C(2)	139.6(10)
Ag(1)#2-Ag(1)-Sn(2)	137.48(3)	C(1)-Sn(1)-Ag(1)	147.5(10)
Sn(1)-Ag(1)-Sn(2)	155.41(2)	C(3)-Sn(1)-Ag(1)	86.3(7)

N(1)-Sn(1)-Ag(1)	37.59(12)	C(5A)-Sn(2)-C(4)	115(4)
C(2A)-Sn(1)-Ag(1)	105.0(6)	N(2)-Sn(2)-C(4)	106.5(11)
C(3A)-Sn(1)-Ag(1)	76.3(6)	C(4)#1-Sn(2)-C(4)	7(10)
C(1A)-Sn(1)-Ag(1)	136.6(6)	C(4A)#1-Sn(2)-C(5)#1	110.1(13)
C(2)-Sn(1)-Ag(1)	83.1(7)	C(4A)-Sn(2)-C(5)#1	78.8(13)
C(4A)#1-Sn(2)-C(4A)	33(2)	C(5A)#1-Sn(2)-C(5)#1	29.2(8)
C(4A)#1-Sn(2)-C(5A)#1	129.1(13)	C(5A)-Sn(2)-C(5)#1	117.8(11)
C(4A)-Sn(2)-C(5A)#1	103.3(13)	N(2)-Sn(2)-C(5)#1	105.6(6)
C(4A)#1-Sn(2)-C(5A)	103.3(13)	C(4)#1-Sn(2)-C(5)#1	92(5)
C(4A)-Sn(2)-C(5A)	129.1(13)	C(4)-Sn(2)-C(5)#1	98(5)
C(5A)#1-Sn(2)-C(5A)	89.9(16)	C(4A)#1-Sn(2)-C(5)	78.8(13)
C(4A)#1-Sn(2)-N(2)	106.8(11)	C(4A)-Sn(2)-C(5)	110.1(13)
C(4A)-Sn(2)-N(2)	106.8(11)	C(5A)#1-Sn(2)-C(5)	117.8(11)
C(5A)#1-Sn(2)-N(2)	112.8(8)	C(5A)-Sn(2)-C(5)	29.2(8)
C(5A)-Sn(2)-N(2)	112.8(8)	N(2)-Sn(2)-C(5)	105.6(6)
C(4A)#1-Sn(2)-C(4)#1	20(5)	C(4)#1-Sn(2)-C(5)	98(5)
C(4A)-Sn(2)-C(4)#1	13(6)	C(4)-Sn(2)-C(5)	92(5)
C(5A)#1-Sn(2)-C(4)#1	115(4)	C(5)#1-Sn(2)-C(5)	143.1(12)
C(5A)-Sn(2)-C(4)#1	120(4)	C(4A)#1-Sn(2)-Ag(1)	75.2(11)
N(2)-Sn(2)-C(4)#1	106.5(11)	C(4A)-Sn(2)-Ag(1)	90.0(10)
C(4A)#1-Sn(2)-C(4)	13(6)	C(5A)#1-Sn(2)-Ag(1)	149.4(8)
C(4A)-Sn(2)-C(4)	20(5)	C(5A)-Sn(2)-Ag(1)	103.0(8)
C(5A)#1-Sn(2)-C(4)	120(4)	N(2)-Sn(2)-Ag(1)	36.69(15)

C(4)#1-Sn(2)-Ag(1)	83(3)	C(6A)-Sn(3)-N(2)	108.7(10)
C(4)-Sn(2)-Ag(1)	80(3)	C(7)#1-Sn(3)-C(6)	110.0(14)
C(5)#1-Sn(2)-Ag(1)	135.1(6)	C(7)-Sn(3)-C(6)	86.7(14)
C(5)-Sn(2)-Ag(1)	81.6(6)	C(6A)#1-Sn(3)-C(6)	110.1(12)
C(4A)#1-Sn(2)-Ag(1)#1	90.0(10)	C(6A)-Sn(3)-C(6)	36.3(10)
C(4A)-Sn(2)-Ag(1)#1	75.2(11)	N(2)-Sn(3)-C(6)	102.8(6)
C(5A)#1-Sn(2)-Ag(1)#1	103.0(8)	C(7)#1-Sn(3)-C(6)#1	86.7(14)
C(5A)-Sn(2)-Ag(1)#1	149.4(8)	C(7)-Sn(3)-C(6)#1	110.0(14)
N(2)-Sn(2)-Ag(1)#1	36.69(15)	C(6A)#1-Sn(3)-C(6)#1	36.3(10)
C(4)#1-Sn(2)-Ag(1)#1	80(3)	C(6A)-Sn(3)-C(6)#1	110.1(12)
C(4)-Sn(2)-Ag(1)#1	83(3)	N(2)-Sn(3)-C(6)#1	102.8(6)
C(5)#1-Sn(2)-Ag(1)#1	81.6(6)	C(6)-Sn(3)-C(6)#1	143.7(13)
C(5)-Sn(2)-Ag(1)#1	135.1(6)	C(7)#1-Sn(3)-C(7A)#1	25.3(11)
Ag(1)-Sn(2)-Ag(1)#1	53.48(3)	C(7)-Sn(3)-C(7A)#1	6(2)
C(7)#1-Sn(3)-C(7)	24(2)	C(6A)#1-Sn(3)-C(7A)#1	131.5(15)
C(7)#1-Sn(3)-C(6A)#1	117.6(15)	C(6A)-Sn(3)-C(7A)#1	113.8(15)
C(7)-Sn(3)-C(6A)#1	135.9(16)	N(2)-Sn(3)-C(7A)#1	112.4(12)
C(7)#1-Sn(3)-C(6A)	135.9(16)	C(6)-Sn(3)-C(7A)#1	84.7(13)
C(7)-Sn(3)-C(6A)	117.6(15)	C(6)#1-Sn(3)-C(7A)#1	108.4(13)
C(6A)#1-Sn(3)-C(6A)	74.5(18)	C(7)#1-Sn(3)-C(7A)	6(2)
C(7)#1-Sn(3)-N(2)	106.5(13)	C(7)-Sn(3)-C(7A)	25.3(11)
C(7)-Sn(3)-N(2)	106.5(13)	C(6A)#1-Sn(3)-C(7A)	113.8(15)
C(6A)#1-Sn(3)-N(2)	108.7(10)	C(6A)-Sn(3)-C(7A)	131.5(15)

N(2)-Sn(3)-C(7A)	112.4(12)	C(2)-C(2A)-Sn(1)	79.5(17)
C(6)-Sn(3)-C(7A)	108.4(13)	C(3A)-C(3)-Sn(1)	80(2)
C(6)#1-Sn(3)-C(7A)	84.7(13)	C(3)-C(3A)-Sn(1)	74(2)
C(7A)#1-Sn(3)-C(7A)	25(2)	C(4)#1-C(4)-C(4A)#1	155(10)
Si(1)#2-N(1)-Sn(1)#2	0.00(4)	C(4)#1-C(4)-C(4A)	17(5)
Si(1)#2-N(1)-Sn(1)	121.4(4)	C(4A)#1-C(4)-C(4A)	138(10)
Sn(1)#2-N(1)-Sn(1)	121.4(4)	C(4)#1-C(4)-Sn(2)	87(5)
Si(1)#2-N(1)-Ag(1)	112.14(8)	C(4A)#1-C(4)-Sn(2)	69(10)
Sn(1)#2-N(1)-Ag(1)	112.14(8)	C(4A)-C(4)-Sn(2)	70(7)
Sn(1)-N(1)-Ag(1)	108.46(8)	C(4)#1-C(4A)-C(4)	8(10)
Si(1)#2-N(1)-Ag(1)#2	108.46(8)	C(4)#1-C(4A)-C(4A)#1	25(10)
Sn(1)#2-N(1)-Ag(1)#2	108.46(8)	C(4)-C(4A)-C(4A)#1	17(5)
Sn(1)-N(1)-Ag(1)#2	112.14(8)	C(4)#1-C(4A)-Sn(2)	98(10)
Ag(1)-N(1)-Ag(1)#2	89.8(3)	C(4)-C(4A)-Sn(2)	90(6)
Sn(2)-N(2)-Sn(3)	120.2(4)	C(4A)#1-C(4A)-Sn(2)	73.5(11)
Sn(2)-N(2)-Ag(1)	110.1(3)	C(5A)-C(5)-Sn(2)	62.6(18)
Sn(3)-N(2)-Ag(1)	111.2(3)	C(5)-C(5A)-Sn(2)	88(2)
Sn(2)-N(2)-Ag(1)#1	110.1(3)	C(6A)-C(6)-Sn(3)	65.3(17)
Sn(3)-N(2)-Ag(1)#1	111.2(3)	C(6)-C(6A)-Sn(3)	78.3(19)
Ag(1)-N(2)-Ag(1)#1	90.0(3)	C(7A)#1-C(7)-C(7)#1	102(9)
C(1A)-C(1)-Sn(1)	85(2)	C(7A)#1-C(7)-C(7A)	75(10)
C(1)-C(1A)-Sn(1)	6(2)	C(7)#1-C(7)-C(7A)	27(3)
C(2A)-C(2)-Sn(1)	69.4(17)	C(7A)#1-C(7)-Sn(3)	149(10)

C(7)#1-C(7)-Sn(3)	77.8(12)	C(7)#1-C(7A)-Sn(3)	25(9)
C(7A)-C(7)-Sn(3)	101(4)	C(7A)#1-C(7A)-Sn(3)	77.6(11)
C(7)#1-C(7A)-C(7A)#1	78(9)	C(7)-C(7A)-Sn(3)	54(3)
C(7)#1-C(7A)-C(7)	51(9)		
C(7A)#1-C(7A)-C(7)	27(3)		

Table A.31. Anisotropic displacement parameters ($\text{\AA}^2 \times 10^3$) for $\text{C}_{24}\text{H}_{72}\text{N}_4\text{Si}_4\text{Sn}_4\text{Ag}_4$ (**8**).

Atom	U11	U22	U33	U23	U13	U12
Ag(1)	32(1)	30(1)	38(1)	0(1)	16(1)	0(1)
Sn(1)	57(1)	38(1)	50(1)	-1(1)	22(1)	5(1)
Si(1)	57(1)	38(1)	50(1)	-1(1)	22(1)	5(1)
Sn(2)	37(1)	64(1)	35(1)	0	14(1)	0
Si(2)	37(1)	64(1)	35(1)	0	14(1)	0
Sn(3)	25(1)	77(1)	41(1)	0	14(1)	0
Si(3)	25(1)	77(1)	41(1)	0	14(1)	0
N(1)	26(4)	31(4)	37(4)	0	7(3)	0
N(2)	24(4)	36(4)	43(4)	0	11(3)	0

Table A.32. Atomic Coordinates ($\times 10^4$) and Equivalent Isotropic Displacement Parameters ($\text{\AA}^2 \times 10^3$) for $\text{C}_{24}\text{H}_{72}\text{N}_4\text{Ge}_4\text{Sn}_4\text{Ag}_4$ (**9**).

Atom	x	y	z	U(eq)
Ag(1)	763(1)	1057(1)	6255(1)	26(1)
Sn(1)	338(1)	2808(1)	3704(1)	40(1)
Ge(1)	338(1)	2808(1)	3704(1)	40(1)
Sn(2)	2346(1)	0	6954(1)	48(1)
Ge(2)	2346(1)	0	6954(1)	48(1)
Sn(3)	1712(1)	0	9614(1)	44(1)
Ge(3)	1712(1)	0	9614(1)	44(1)
N(1)	0	2092(5)	5000	29(2)
N(2)	1521(4)	0	7479(9)	27(2)
C(1)	996(14)	3853(16)	4880(30)	69(6)
C(1A)	1397(12)	3331(16)	5260(20)	64(5)
C(2)	-275(15)	3898(17)	2630(30)	80(7)
C(2A)	-577(11)	3274(15)	1780(20)	57(5)
C(3)	843(11)	1864(14)	2870(20)	52(4)
C(3A)	420(12)	1966(14)	2150(30)	58(5)
C(4)	2691(14)	1525(18)	7270(30)	77(7)
C(4A)	3138(16)	818(19)	8340(30)	87(8)
C(5)	2031(19)	0	4650(40)	67(9)
C(5A)	1988(14)	-440(18)	4650(30)	14(4)
C(6)	730(30)	190(40)	9610(50)	50(17)

C(6A)	880(20)	-270(30)	9870(50)	32(11)
C(7)	2412(16)	940(20)	10800(30)	87(8)
C(7A)	2039(13)	1394(17)	10450(30)	65(6)

Table A.33. Interatomic Distances (Å) and Angles (°) for C₂₄H₇₂N₄Ge₄Sn₄Ag₄ (**9**).

Ag(1)-N(1)	2.107(5)	Sn(3)-C(6A)#1	1.90(4)
Ag(1)-N(2)	2.118(5)	Sn(3)-N(2)	1.912(8)
Ag(1)-Ag(1)#1	2.9992(11)	Sn(3)-C(7)	1.93(3)
Ag(1)-Ag(1)#2	3.0233(10)	Sn(3)-C(7)#1	1.93(3)
Ag(1)-Sn(3)	3.3122(11)	Sn(3)-C(6)	2.06(5)
Ag(1)-Sn(1)	3.3265(9)	Sn(3)-C(6)#1	2.06(5)
Sn(1)-N(1)	1.961(4)	Sn(3)-C(7A)#1	2.13(2)
Sn(1)-C(3A)	1.98(2)	Sn(3)-C(7A)	2.13(2)
Sn(1)-C(2)	1.98(3)	Sn(3)-Ag(1)#1	3.3122(11)
Sn(1)-C(1)	2.00(2)	N(1)-Ge(1)#2	1.961(4)
Sn(1)-C(3)	2.07(2)	N(1)-Sn(1)#2	1.961(4)
Sn(1)-C(2A)	2.09(2)	N(1)-Ag(1)#2	2.107(5)
Sn(1)-C(1A)	2.18(2)	N(2)-Ag(1)#1	2.118(5)
Sn(2)-C(4A)	1.98(3)	C(1)-C(1A)	1.05(3)
Sn(2)-C(4A)#1	1.98(3)	C(2)-C(2A)	1.18(3)
Sn(2)-N(2)	1.986(8)	C(3)-C(3A)	0.86(2)
Sn(2)-C(5)	2.02(4)	C(4)-C(4A)	1.44(4)
Sn(2)-C(5A)	2.09(2)	C(5)-C(5A)	0.63(3)
Sn(2)-C(5A)#1	2.09(2)	C(5)-C(5A)#1	0.63(3)
Sn(2)-C(4)	2.26(3)	C(5A)-C(5A)#1	1.25(5)
Sn(2)-C(4)#1	2.26(3)	C(6)-C(6A)#1	0.32(7)
Sn(3)-C(6A)	1.90(4)	C(6)-C(6)#1	0.55(12)

C(6)-C(6A)	0.72(5)	C(3A)-Sn(1)-C(1)	127.7(10)
C(6A)-C(6)#1	0.32(7)	C(2)-Sn(1)-C(1)	80.7(11)
C(6A)-C(6A)#1	0.76(8)	N(1)-Sn(1)-C(3)	107.2(6)
C(7)-C(7A)	0.95(3)	C(3A)-Sn(1)-C(3)	24.4(7)
N(1)-Ag(1)-N(2)	178.9(2)	C(2)-Sn(1)-C(3)	128.4(10)
N(1)-Ag(1)-Ag(1)#1	134.16(14)	C(1)-Sn(1)-C(3)	111.3(10)
N(2)-Ag(1)-Ag(1)#1	44.91(15)	N(1)-Sn(1)-C(2A)	106.8(6)
N(1)-Ag(1)-Ag(1)#2	44.16(14)	C(3A)-Sn(1)-C(2A)	82.4(9)
N(2)-Ag(1)-Ag(1)#2	134.91(15)	C(2)-Sn(1)-C(2A)	33.5(9)
Ag(1)#1-Ag(1)-Ag(1)#2	90.0	C(1)-Sn(1)-C(2A)	113.3(9)
N(1)-Ag(1)-Sn(3)	148.15(6)	C(3)-Sn(1)-C(2A)	106.2(8)
N(2)-Ag(1)-Sn(3)	32.8(2)	N(1)-Sn(1)-C(1A)	105.9(6)
Ag(1)#1-Ag(1)-Sn(3)	63.079(12)	C(3A)-Sn(1)-C(1A)	109.3(9)
Ag(1)#2-Ag(1)-Sn(3)	138.11(3)	C(2)-Sn(1)-C(1A)	108.4(10)
N(1)-Ag(1)-Sn(1)	33.71(6)	C(1)-Sn(1)-C(1A)	28.8(8)
N(2)-Ag(1)-Sn(1)	146.1(2)	C(3)-Sn(1)-C(1A)	87.5(8)
Ag(1)#1-Ag(1)-Sn(1)	138.301(16)	C(2A)-Sn(1)-C(1A)	138.7(9)
Ag(1)#2-Ag(1)-Sn(1)	64.251(18)	N(1)-Sn(1)-Ag(1)	36.62(12)
Sn(3)-Ag(1)-Sn(1)	155.33(2)	C(3A)-Sn(1)-Ag(1)	91.4(6)
N(1)-Sn(1)-C(3A)	110.0(6)	C(2)-Sn(1)-Ag(1)	150.5(8)
N(1)-Sn(1)-C(2)	114.3(8)	C(1)-Sn(1)-Ag(1)	104.0(7)
C(3A)-Sn(1)-C(2)	108.9(10)	C(3)-Sn(1)-Ag(1)	77.7(5)
N(1)-Sn(1)-C(1)	111.8(7)	C(2A)-Sn(1)-Ag(1)	137.1(6)

C(1A)-Sn(1)-Ag(1)	83.4(6)	C(4A)#1-Sn(2)-C(4)#1	39.2(10)
C(4A)-Sn(2)-C(4A)#1	71.9(16)	N(2)-Sn(2)-C(4)#1	102.9(6)
C(4A)-Sn(2)-N(2)	112.5(9)	C(5)-Sn(2)-C(4)#1	94.6(7)
C(4A)#1-Sn(2)-N(2)	112.5(9)	C(5A)-Sn(2)-C(4)#1	78.6(9)
C(4A)-Sn(2)-C(5)	120.9(11)	C(5A)#1-Sn(2)-C(4)#1	111.9(9)
C(4A)#1-Sn(2)-C(5)	120.9(11)	C(4)-Sn(2)-C(4)#1	146.8(13)
N(2)-Sn(2)-C(5)	112.4(11)	C(6A)-Sn(3)-C(6A)#1	23(3)
C(4A)-Sn(2)-C(5A)	133.8(11)	C(6A)-Sn(3)-N(2)	111.7(14)
C(4A)#1-Sn(2)-C(5A)	110.0(11)	C(6A)#1-Sn(3)-N(2)	111.7(14)
N(2)-Sn(2)-C(5A)	108.9(7)	C(6A)-Sn(3)-C(7)	123.8(16)
C(5)-Sn(2)-C(5A)	17.5(7)	C(6A)#1-Sn(3)-C(7)	106.4(16)
C(4A)-Sn(2)-C(5A)#1	110.0(11)	N(2)-Sn(3)-C(7)	112.3(9)
C(4A)#1-Sn(2)-C(5A)#1	133.8(11)	C(6A)-Sn(3)-C(7)#1	106.4(15)
N(2)-Sn(2)-C(5A)#1	108.9(7)	C(6A)#1-Sn(3)-C(7)#1	123.8(16)
C(5)-Sn(2)-C(5A)#1	17.5(7)	N(2)-Sn(3)-C(7)#1	112.3(8)
C(5A)-Sn(2)-C(5A)#1	34.7(14)	C(7)-Sn(3)-C(7)#1	87.1(18)
C(4A)-Sn(2)-C(4)	39.2(10)	C(6A)-Sn(3)-C(6)	20.4(15)
C(4A)#1-Sn(2)-C(4)	110.5(11)	C(6A)#1-Sn(3)-C(6)	8(2)
N(2)-Sn(2)-C(4)	102.9(6)	N(2)-Sn(3)-C(6)	105.0(14)
C(5)-Sn(2)-C(4)	94.6(7)	C(7)-Sn(3)-C(6)	113.5(17)
C(5A)-Sn(2)-C(4)	111.9(9)	C(7)#1-Sn(3)-C(6)	125.7(19)
C(5A)#1-Sn(2)-C(4)	78.6(9)	C(6A)-Sn(3)-C(6)#1	8(2)
C(4A)-Sn(2)-C(4)#1	110.5(11)	C(6A)#1-Sn(3)-C(6)#1	20.4(15)

N(2)-Sn(3)-C(6)#1	105.0(14)	C(7)#1-Sn(3)-Ag(1)#1	103.6(9)
C(7)-Sn(3)-C(6)#1	125.7(19)	C(6)-Sn(3)-Ag(1)#1	83.9(13)
C(7)#1-Sn(3)-C(6)#1	113.5(17)	C(6)#1-Sn(3)-Ag(1)#1	76.8(15)
C(6)-Sn(3)-C(6)#1	15(3)	C(7A)#1-Sn(3)-Ag(1)#1	84.3(6)
C(6A)-Sn(3)-C(7A)#1	85.6(14)	C(7A)-Sn(3)-Ag(1)#1	137.9(6)
C(6A)#1-Sn(3)-C(7A)#1	107.1(14)	C(6A)-Sn(3)-Ag(1)	91.8(13)
N(2)-Sn(3)-C(7A)#1	106.6(6)	C(6A)#1-Sn(3)-Ag(1)	81.4(13)
C(7)-Sn(3)-C(7A)#1	112.6(13)	N(2)-Sn(3)-Ag(1)	36.80(15)
C(7)#1-Sn(3)-C(7A)#1	26.5(9)	C(7)-Sn(3)-Ag(1)	103.6(9)
C(6)-Sn(3)-C(7A)#1	106.1(18)	C(7)#1-Sn(3)-Ag(1)	149.1(8)
C(6)#1-Sn(3)-C(7A)#1	91.6(17)	C(6)-Sn(3)-Ag(1)	76.8(15)
C(6A)-Sn(3)-C(7A)	107.1(14)	C(6)#1-Sn(3)-Ag(1)	83.9(13)
C(6A)#1-Sn(3)-C(7A)	85.6(14)	C(7A)#1-Sn(3)-Ag(1)	137.9(6)
N(2)-Sn(3)-C(7A)	106.6(6)	C(7A)-Sn(3)-Ag(1)	84.3(6)
C(7)-Sn(3)-C(7A)	26.5(9)	Ag(1)#1-Sn(3)-Ag(1)	53.84(2)
C(7)#1-Sn(3)-C(7A)	112.6(13)	Sn(1)-N(1)-Ge(1)#2	117.6(4)
C(6)-Sn(3)-C(7A)	91.6(17)	Sn(1)-N(1)-Sn(1)#2	117.6(4)
C(6)#1-Sn(3)-C(7A)	106.1(18)	Ge(1)#2-N(1)-Sn(1)#2	0.00(4)
C(7A)#1-Sn(3)-C(7A)	136.4(13)	Sn(1)-N(1)-Ag(1)#2	112.66(7)
C(6A)-Sn(3)-Ag(1)#1	81.4(13)	Ge(1)#2-N(1)-Ag(1)#2	109.67(6)
C(6A)#1-Sn(3)-Ag(1)#1	91.8(13)	Sn(1)#2-N(1)-Ag(1)#2	109.67(6)
N(2)-Sn(3)-Ag(1)#1	36.80(15)	Sn(1)-N(1)-Ag(1)	109.67(6)
C(7)-Sn(3)-Ag(1)#1	149.1(8)	Ge(1)#2-N(1)-Ag(1)	112.66(7)

Sn(1)#2-N(1)-Ag(1)	112.66(7)	C(5)-C(5A)-C(5A)#1	8(5)
Ag(1)#2-N(1)-Ag(1)	91.7(3)	C(5)-C(5A)-Sn(2)	74(5)
Sn(3)-N(2)-Sn(2)	118.6(4)	C(5A)#1-C(5A)-Sn(2)	72.7(7)
Sn(3)-N(2)-Ag(1)#1	110.4(3)	C(6A)#1-C(6)-C(6)#1	109(10)
Sn(2)-N(2)-Ag(1)#1	111.8(3)	C(6A)#1-C(6)-C(6A)	84(10)
Sn(3)-N(2)-Ag(1)	110.4(3)	C(6)#1-C(6)-C(6A)	25(5)
Sn(2)-N(2)-Ag(1)	111.8(3)	C(6A)#1-C(6)-Sn(3)	56(10)
Ag(1)#1-N(2)-Ag(1)	90.2(3)	C(6)#1-C(6)-Sn(3)	82.3(16)
C(1A)-C(1)-Sn(1)	85.1(18)	C(6A)-C(6)-Sn(3)	67(7)
C(1)-C(1A)-Sn(1)	66.1(17)	C(6)#1-C(6A)-C(6)	47(10)
C(2A)-C(2)-Sn(1)	78.5(16)	C(6)#1-C(6A)-C(6A)#1	71(10)
C(2)-C(2A)-Sn(1)	68.0(16)	C(6)-C(6A)-C(6A)#1	25(5)
C(3A)-C(3)-Sn(1)	72(2)	C(6)#1-C(6A)-Sn(3)	116(10)
C(3)-C(3A)-Sn(1)	83(2)	C(6)-C(6A)-Sn(3)	92(7)
C(4A)-C(4)-Sn(2)	59.9(14)	C(6A)#1-C(6A)-Sn(3)	78.5(13)
C(4)-C(4A)-Sn(2)	81.0(17)	C(7A)-C(7)-Sn(3)	89(2)
C(5A)-C(5)-C(5A)#1	163(10)	C(7)-C(7A)-Sn(3)	65(2)
C(5A)-C(5)-Sn(2)	88(5)		
C(5A)#1-C(5)-Sn(2)	88(5)		

Table A.34. Anisotropic displacement parameters ($\text{\AA}^2 \times 10^3$) for $\text{C}_{24}\text{H}_{72}\text{N}_4\text{Ge}_4\text{Sn}_4\text{Ag}_4$ (**9**).

Atom	U11	U22	U33	U23	U13	U12
Ag(1)	25(1)	24(1)	28(1)	0(1)	10(1)	-1(1)
Sn(1)	51(1)	31(1)	38(1)	6(1)	20(1)	-4(1)
Ge(1)	51(1)	31(1)	38(1)	6(1)	20(1)	-4(1)
Sn(2)	24(1)	87(1)	33(1)	0	14(1)	0
Ge(2)	24(1)	87(1)	33(1)	0	14(1)	0
Sn(3)	29(1)	72(1)	28(1)	0	10(1)	0
Ge(3)	29(1)	72(1)	28(1)	0	10(1)	0
N(1)	26(5)	18(4)	34(5)	0	6(4)	0
N(2)	13(4)	38(5)	29(4)	0	10(3)	0

Table A.35. Atomic Coordinates ($\times 10^4$) and Equivalent Isotropic Displacement Parameters ($\text{\AA}^2 \times 10^3$) for $\text{C}_{24}\text{H}_{72}\text{N}_4\text{Si}_4\text{Ag}_4$ (**10**).

Atom	x	y	z	U(eq)
Ag(1)	8025(1)	3568(1)	1719(1)	22(1)
Ag(2)	8032(1)	1408(1)	1724(1)	22(1)
Si(1)	10426(1)	2555(1)	792(1)	26(1)
Si(2)	7303(1)	2391(1)	195(1)	27(1)
Si(3)	5978(1)	5276(1)	2145(1)	31(1)
Si(4)	5907(1)	-304(1)	2232(1)	24(1)
N(1)	8557(2)	2490(1)	924(1)	21(1)
N(2)	7500	4664(2)	2500	22(1)
N(3)	7500	301(2)	2500	22(1)
C(1)	11050(3)	1691(3)	79(2)	56(1)
C(2)	10996(3)	3810(2)	523(2)	47(1)
C(3)	11423(3)	2245(2)	1656(2)	36(1)
C(4)	7191(3)	1118(2)	-145(2)	47(1)
C(5)	7787(3)	3183(3)	-592(2)	50(1)
C(6)	5447(3)	2762(2)	484(2)	37(1)
C(7)	5442(4)	6313(2)	2744(2)	56(1)
C(8)	6318(3)	5743(2)	1200(2)	48(1)
C(9)	4388(3)	4443(2)	2080(2)	45(1)
C(10)	4900(3)	-770(2)	3041(2)	38(1)
C(11)	6284(3)	-1349(2)	1613(2)	37(1)

C(12)	4653(3)	525(2)	1721(2)	34(1)
-------	---------	--------	---------	-------

Table A.36. Interatomic Distances (Å) and Angles (°) for C₂₄H₇₂N₄Si₄Ag₄ (**10**).

Ag(1)-N(2)	2.141(2)	Si(4)-C(10)	1.874(3)
Ag(1)-N(1)	2.1425(19)	N(2)-Si(3)#1	1.7487(15)
Ag(1)-Ag(2)	2.9822(6)	N(2)-Ag(1)#1	2.141(2)
Ag(1)-Ag(1)#1	3.0282(6)	N(3)-Si(4)#1	1.7485(15)
Ag(2)-N(3)	2.146(2)	N(3)-Ag(2)#1	2.146(2)
Ag(2)-N(1)	2.1512(19)	N(2)-Ag(1)-N(1)	179.01(7)
Ag(2)-Ag(2)#1	3.0158(6)	N(2)-Ag(1)-Ag(2)	134.87(5)
Si(1)-N(1)	1.745(2)	N(1)-Ag(1)-Ag(2)	46.13(5)
Si(1)-C(3)	1.858(3)	N(2)-Ag(1)-Ag(1)#1	44.99(5)
Si(1)-C(1)	1.865(3)	N(1)-Ag(1)-Ag(1)#1	136.01(5)
Si(1)-C(2)	1.879(3)	Ag(2)-Ag(1)-Ag(1)#1	89.879(5)
Si(2)-N(1)	1.748(2)	N(3)-Ag(2)-N(1)	178.51(7)
Si(2)-C(5)	1.866(3)	N(3)-Ag(2)-Ag(1)	135.49(5)
Si(2)-C(4)	1.867(3)	N(1)-Ag(2)-Ag(1)	45.89(5)
Si(2)-C(6)	1.871(3)	N(3)-Ag(2)-Ag(2)#1	45.37(5)
Si(3)-N(2)	1.7487(15)	N(1)-Ag(2)-Ag(2)#1	136.00(5)
Si(3)-C(9)	1.864(3)	Ag(1)-Ag(2)-Ag(2)#1	90.119(5)
Si(3)-C(7)	1.872(3)	N(1)-Si(1)-C(3)	109.93(11)
Si(3)-C(8)	1.874(3)	N(1)-Si(1)-C(1)	112.57(13)
Si(4)-N(3)	1.7485(15)	C(3)-Si(1)-C(1)	106.94(15)
Si(4)-C(12)	1.863(3)	N(1)-Si(1)-C(2)	111.43(12)
Si(4)-C(11)	1.869(3)	C(3)-Si(1)-C(2)	107.33(14)

C(1)-Si(1)-C(2)	108.41(15)	C(11)-Si(4)-C(10)	108.20(13)
N(1)-Si(2)-C(5)	112.05(12)	Si(1)-N(1)-Si(2)	122.37(11)
N(1)-Si(2)-C(4)	110.95(12)	Si(1)-N(1)-Ag(1)	107.40(10)
C(5)-Si(2)-C(4)	107.92(14)	Si(2)-N(1)-Ag(1)	114.37(10)
N(1)-Si(2)-C(6)	110.91(12)	Si(1)-N(1)-Ag(2)	111.50(10)
C(5)-Si(2)-C(6)	106.94(14)	Si(2)-N(1)-Ag(2)	107.94(10)
C(4)-Si(2)-C(6)	107.87(14)	Ag(1)-N(1)-Ag(2)	87.98(7)
N(2)-Si(3)-C(9)	110.30(13)	Si(3)#1-N(2)-Si(3)	122.14(17)
N(2)-Si(3)-C(7)	111.89(14)	Si(3)#1-N(2)-Ag(1)	113.45(4)
C(9)-Si(3)-C(7)	106.96(15)	Si(3)-N(2)-Ag(1)	106.62(4)
N(2)-Si(3)-C(8)	111.03(10)	Si(3)#1-N(2)-Ag(1)#1	106.62(4)
C(9)-Si(3)-C(8)	107.48(15)	Si(3)-N(2)-Ag(1)#1	113.45(4)
C(7)-Si(3)-C(8)	109.00(15)	Ag(1)-N(2)-Ag(1)#1	90.03(11)
N(3)-Si(4)-C(12)	110.68(12)	Si(4)-N(3)-Si(4)#1	122.87(17)
N(3)-Si(4)-C(11)	111.88(11)	Si(4)-N(3)-Ag(2)#1	108.82(4)
C(12)-Si(4)-C(11)	107.05(13)	Si(4)#1-N(3)-Ag(2)#1	110.98(4)
N(3)-Si(4)-C(10)	111.73(10)	Si(4)-N(3)-Ag(2)	110.98(4)
C(12)-Si(4)-C(10)	107.07(13)	Si(4)#1-N(3)-Ag(2)	108.82(4)
		Ag(2)#1-N(3)-Ag(2)	89.26(11)

Table A.37. Anisotropic displacement parameters ($\text{\AA}^2 \times 10^3$) for $\text{C}_{24}\text{H}_{72}\text{N}_4\text{Si}_4\text{Ag}_4$ (**10**).

Atom	U11	U22	U33	U23	U13	U12
Ag(1)	23(1)	20(1)	22(1)	-1(1)	3(1)	2(1)
Ag(2)	25(1)	20(1)	20(1)	2(1)	0(1)	0(1)
Si(1)	22(1)	32(1)	23(1)	-2(1)	4(1)	2(1)
Si(2)	26(1)	36(1)	20(1)	2(1)	-2(1)	1(1)
Si(3)	32(1)	26(1)	35(1)	6(1)	10(1)	8(1)
Si(4)	26(1)	21(1)	26(1)	-1(1)	-1(1)	-2(1)
N(1)	22(1)	25(1)	17(1)	3(1)	1(1)	1(1)
N(2)	25(2)	17(2)	24(2)	0	9(1)	0
N(3)	25(2)	20(2)	21(2)	0	-2(1)	0
C(1)	37(2)	83(3)	49(2)	-27(2)	7(2)	10(2)
C(2)	36(2)	53(2)	50(2)	21(2)	1(2)	-11(2)
C(3)	27(2)	41(2)	41(2)	5(1)	-3(1)	4(1)
C(4)	48(2)	53(2)	38(2)	-14(2)	-9(1)	-1(2)
C(5)	43(2)	75(3)	31(2)	18(2)	-2(1)	-1(2)
C(6)	30(2)	43(2)	37(2)	5(1)	-3(1)	2(1)
C(7)	60(2)	41(2)	67(3)	2(2)	25(2)	20(2)
C(8)	49(2)	48(2)	48(2)	20(2)	9(2)	11(2)
C(9)	30(2)	56(2)	48(2)	12(2)	5(1)	5(2)
C(10)	36(2)	40(2)	37(2)	4(1)	2(1)	-5(1)
C(11)	43(2)	28(2)	40(2)	-7(1)	-4(1)	-3(1)

C(12)	34(2)	33(2)	37(2)	1(1)	-7(1)	-1(1)
-------	-------	-------	-------	------	-------	-------

Table A.38. Hydrogen coordinates ($\times 10^4$) and isotropic displacement parameters ($\text{\AA}^2 \times 10^3$) for $\text{C}_{24}\text{H}_{72}\text{N}_4\text{Si}_8\text{Ag}_4$ (**10**).

Atom	x	y	z	U(eq)
H(1A)	10773	1052	207	84(8)
H(1B)	12078	1725	47	84(8)
H(1C)	10618	1857	-382	84(8)
H(2A)	10521	3985	75	82(7)
H(2B)	12018	3826	463	82(7)
H(2C)	10736	4255	896	82(7)
H(3A)	11007	2585	2053	70(7)
H(3B)	12414	2425	1617	70(7)
H(3C)	11358	1568	1741	70(7)
H(4A)	8087	943	-358	74(7)
H(4B)	6431	1067	-503	74(7)
H(4C)	7000	696	252	74(7)
H(5A)	7858	3835	-431	63(6)
H(5B)	7057	3133	-966	63(6)
H(5C)	8693	2982	-780	63(6)
H(6A)	5196	2415	912	59(6)
H(6B)	4762	2622	101	59(6)
H(6C)	5439	3437	584	59(6)
H(7A)	5214	6076	3216	82(7)
H(7B)	4616	6628	2533	82(7)
H(7C)	6225	6759	2785	82(7)

H(8A)	7056	6224	1222	86(8)
H(8B)	5449	6017	1000	86(8)
H(8C)	6621	5224	897	86(8)
H(9A)	4677	3848	1866	56(6)
H(9B)	3644	4731	1785	56(6)
H(9C)	4033	4326	2557	56(6)
H(10A)	5459	-1261	3279	53(5)
H(10B)	3994	-1033	2880	53(5)
H(10C)	4737	-254	3373	53(5)
H(11A)	6691	-1117	1173	59(6)
H(11B)	5403	-1681	1502	59(6)
H(11C)	6949	-1779	1850	59(6)
H(12A)	4554	1112	1987	49(5)
H(12B)	3729	226	1662	49(5)
H(12C)	5036	662	1253	49(5)

Table A.39. Atomic Coordinates ($\times 10^4$) and Equivalent Isotropic Displacement Parameters ($\text{\AA}^2 \times 10^3$) for $\text{C}_{28}\text{H}_{76}\text{N}_2\text{O}_4\text{Cl}_4\text{Sn}_4\text{Zn}_2$ (**11**).

Atom	x	y	z	U(eq)
Sn(1)	2396(1)	5556(1)	4881(1)	38(1)
Sn(2)	-368(1)	7027(1)	6018(1)	43(1)
Sn(3)	-1999(1)	8739(1)	10070(1)	44(1)
Sn(4)	-2937(1)	8342(1)	8752(1)	43(1)
Zn(1)	543(1)	4019(1)	5396(1)	32(1)
Zn(2)	-4952(1)	11020(1)	9682(1)	31(1)
Cl(1)	2630(3)	2374(3)	5131(1)	44(1)
Cl(2)	-97(3)	3323(3)	6418(1)	50(1)
Cl(3)	-4358(4)	12515(3)	9825(2)	59(1)
Cl(4)	-5479(3)	11698(3)	8653(1)	44(1)
N(1)	569(8)	5700(8)	5265(4)	33(2)
N(2)	-3621(9)	9203(8)	9676(4)	37(2)
C(1)	3358(12)	4592(12)	3977(5)	47(3)
C(2)	2175(14)	7423(12)	4681(6)	59(4)
C(3)	3662(12)	4608(12)	5563(6)	55(4)
C(4)	-1029(16)	8893(12)	5628(8)	81(5)
C(5)	-1886(14)	6845(15)	6699(6)	71(4)
C(6)	950(15)	6809(13)	6633(6)	65(4)
C(7)	-2342(14)	9838(14)	10871(6)	65(4)
C(8)	-589(15)	9045(16)	9318(7)	77(5)

C(9)	-1236(14)	6823(13)	10389(7)	73(4)
C(10)	-1336(16)	6484(12)	8771(7)	77(5)
C(11)	-2221(14)	9412(14)	8049(6)	67(4)
C(12)	-4338(14)	8073(13)	8434(6)	65(4)
Li(1)	2120(20)	1758(18)	6240(12)	58(6)
Li(2)	-5250(20)	6830(20)	11252(11)	62(7)
O(1)	2269(14)	48(10)	6373(6)	119(5)
C(13)	2550(80)	-630(80)	6990(40)	110(30)
C(13')	1090(30)	-30(30)	6976(18)	137(11)
C(14)	1410(40)	-280(40)	7514(13)	270(20)
C(15)	2820(40)	-1010(30)	6044(19)	119(19)
C(15')	3830(50)	-1240(50)	5440(20)	73(13)
C(16)	3960(60)	-860(40)	5610(40)	150(30)
C(16')	3810(90)	-1600(90)	5860(50)	230(40)
O(2)	3041(10)	1975(10)	6789(5)	83(3)
C(17)	4700(40)	1320(40)	6466(17)	84(10)
C(17')	4190(50)	810(50)	6980(20)	133(16)
C(18)	5280(30)	280(30)	6668(18)	201(15)
C(19)	2710(30)	2990(30)	7224(12)	169(12)
C(20)	1640(20)	3370(20)	7680(11)	130(9)
O(3)	-3911(11)	5089(9)	11277(5)	77(3)
C(21')	-2650(60)	4540(60)	10870(30)	170(20)
C(21)	-3610(30)	4190(30)	10749(15)	68(8)

C(22)	-2580(20)	4170(20)	10205(11)	132(8)
C(23)	-4230(60)	4030(60)	11500(30)	170(20)
C(23')	-2980(40)	4660(40)	11660(20)	112(13)
C(24)	-3340(40)	3640(40)	12120(20)	269(19)
O(4)	-6789(12)	6873(14)	11841(6)	109(4)
C(25)	-7220(20)	7200(20)	12534(10)	126(9)
C(26)	-6250(20)	7250(20)	12802(9)	121(8)
C(27)	-7560(40)	6080(30)	11570(17)	236(19)
C(28)	-8300(30)	7140(30)	11490(16)	214(18)

Table A.40. Interatomic Distances (Å) and Angles (°) for C₂₈H₇₆N₂O₄Cl₄Sn₄Zn₂ (**11**).

Sn(1)-N(1)	2.078(8)	Zn(2)-N(2)	2.006(9)
Sn(1)-C(1)	2.108(11)	Zn(2)-N(2)#2	2.018(8)
Sn(1)-C(2)	2.140(12)	Zn(2)-Cl(3)	2.297(3)
Sn(1)-C(3)	2.159(12)	Zn(2)-Cl(4)	2.339(3)
Sn(2)-N(1)	2.079(8)	Zn(2)-Zn(2)#2	2.698(2)
Sn(2)-C(5)	2.116(13)	Zn(2)-Li(2)#2	3.134(18)
Sn(2)-C(4)	2.134(13)	Cl(1)-Li(1)	2.38(2)
Sn(2)-C(6)	2.171(14)	Cl(2)-Li(1)	2.39(2)
Sn(3)-C(7)	2.094(13)	Cl(3)-Li(2)#2	2.38(2)
Sn(3)-N(2)	2.097(10)	Cl(4)-Li(2)#2	2.36(2)
Sn(3)-C(9)	2.135(14)	N(1)-Zn(1)#1	2.036(9)
Sn(3)-C(8)	2.162(13)	N(2)-Zn(2)#2	2.018(8)
Sn(4)-N(2)	2.094(8)	Li(1)-O(2)	1.88(3)
Sn(4)-C(12)	2.113(14)	Li(1)-O(1)	1.97(2)
Sn(4)-C(11)	2.141(12)	Li(2)-O(4)	1.95(2)
Sn(4)-C(10)	2.155(14)	Li(2)-O(3)	1.95(3)
Zn(1)-N(1)	2.027(8)	Li(2)-Cl(4)#2	2.36(2)
Zn(1)-N(1)#1	2.036(9)	Li(2)-Cl(3)#2	2.38(2)
Zn(1)-Cl(2)	2.301(3)	Li(2)-Zn(2)#2	3.134(18)
Zn(1)-Cl(1)	2.322(3)	O(1)-C(15)	1.31(3)
Zn(1)-Zn(1)#1	2.695(2)	O(1)-C(13)	1.47(9)
Zn(1)-Li(1)	3.12(2)	O(1)-C(13')	1.69(4)

C(13)-C(14)	1.45(8)	C(21')-C(23')	1.61(7)
C(13)-C(13')	1.56(9)	C(21)-C(22)	1.46(3)
C(13)-C(15)	2.00(9)	C(21)-C(23)	1.60(6)
C(13')-C(14)	1.23(4)	C(23)-C(24)	1.76(6)
C(15)-C(16')	1.05(9)	C(23')-C(24)	1.63(5)
C(15)-C(15')	1.48(5)	O(4)-C(25)	1.45(2)
C(15)-C(16)	1.52(7)	O(4)-C(27)	1.82(4)
C(15')-C(16)	0.70(7)	C(25)-C(26)	1.43(3)
C(15')-C(16')	0.94(9)	C(27)-C(28)	1.18(3)
C(16)-C(16')	1.05(9)	N(1)-Sn(1)-C(1)	115.6(4)
O(2)-C(19)	1.45(3)	N(1)-Sn(1)-C(2)	107.8(4)
O(2)-C(17')	1.53(6)	C(1)-Sn(1)-C(2)	105.0(5)
O(2)-C(17)	1.74(4)	N(1)-Sn(1)-C(3)	110.8(4)
C(17)-C(18)	1.19(4)	C(1)-Sn(1)-C(3)	106.8(5)
C(17)-C(17')	1.35(5)	C(2)-Sn(1)-C(3)	110.8(5)
C(17')-C(18)	1.20(5)	N(1)-Sn(2)-C(5)	114.7(5)
C(19)-C(20)	1.32(3)	N(1)-Sn(2)-C(4)	110.8(5)
O(3)-C(23')	1.40(5)	C(5)-Sn(2)-C(4)	110.8(6)
O(3)-C(21')	1.42(6)	N(1)-Sn(2)-C(6)	110.7(4)
O(3)-C(23)	1.49(6)	C(5)-Sn(2)-C(6)	102.8(5)
O(3)-C(21)	1.50(3)	C(4)-Sn(2)-C(6)	106.5(6)
C(21')-C(22)	1.48(6)	C(7)-Sn(3)-N(2)	115.3(4)
C(21')-C(21)	1.48(7)	C(7)-Sn(3)-C(9)	107.2(6)

N(2)-Sn(3)-C(9)	109.4(5)	Cl(1)-Zn(1)-Li(1)	49.3(4)
C(7)-Sn(3)-C(8)	105.4(6)	Zn(1)#1-Zn(1)-Li(1)	172.9(4)
N(2)-Sn(3)-C(8)	108.2(5)	N(2)-Zn(2)-N(2)#2	95.8(4)
C(9)-Sn(3)-C(8)	111.4(6)	N(2)-Zn(2)-Cl(3)	117.8(3)
N(2)-Sn(4)-C(12)	113.0(4)	N(2)#2-Zn(2)-Cl(3)	122.4(3)
N(2)-Sn(4)-C(11)	109.7(4)	N(2)-Zn(2)-Cl(4)	112.3(3)
C(12)-Sn(4)-C(11)	111.1(6)	N(2)#2-Zn(2)-Cl(4)	111.8(3)
N(2)-Sn(4)-C(10)	110.9(5)	Cl(3)-Zn(2)-Cl(4)	97.44(11)
C(12)-Sn(4)-C(10)	105.2(6)	N(2)-Zn(2)-Zn(2)#2	48.1(2)
C(11)-Sn(4)-C(10)	106.6(6)	N(2)#2-Zn(2)-Zn(2)#2	47.7(3)
N(1)-Zn(1)-N(1)#1	96.9(3)	Cl(3)-Zn(2)-Zn(2)#2	138.40(11)
N(1)-Zn(1)-Cl(2)	122.1(3)	Cl(4)-Zn(2)-Zn(2)#2	124.11(10)
N(1)#1-Zn(1)-Cl(2)	115.6(2)	N(2)-Zn(2)-Li(2)#2	127.4(5)
N(1)-Zn(1)-Cl(1)	110.4(3)	N(2)#2-Zn(2)-Li(2)#2	135.9(5)
N(1)#1-Zn(1)-Cl(1)	114.3(3)	Cl(3)-Zn(2)-Li(2)#2	49.2(5)
Cl(2)-Zn(1)-Cl(1)	98.36(11)	Cl(4)-Zn(2)-Li(2)#2	48.4(5)
N(1)-Zn(1)-Zn(1)#1	48.6(3)	Zn(2)#2-Zn(2)-Li(2)#2	171.3(4)
N(1)#1-Zn(1)-Zn(1)#1	48.3(2)	Zn(1)-Cl(1)-Li(1)	83.1(5)
Cl(2)-Zn(1)-Zn(1)#1	136.63(11)	Zn(1)-Cl(2)-Li(1)	83.4(5)
Cl(1)-Zn(1)-Zn(1)#1	124.97(10)	Zn(2)-Cl(3)-Li(2)#2	84.0(5)
N(1)-Zn(1)-Li(1)	126.9(5)	Zn(2)-Cl(4)-Li(2)#2	83.7(6)
N(1)#1-Zn(1)-Li(1)	135.7(5)	Zn(1)-N(1)-Zn(1)#1	83.1(3)
Cl(2)-Zn(1)-Li(1)	49.5(4)	Zn(1)-N(1)-Sn(1)	114.0(4)

Zn(1)#1-N(1)-Sn(1)	116.3(4)	O(4)-Li(2)-Cl(3)#2	110.3(13)
Zn(1)-N(1)-Sn(2)	120.0(4)	O(3)-Li(2)-Cl(3)#2	112.6(11)
Zn(1)#1-N(1)-Sn(2)	112.9(4)	Cl(4)#2-Li(2)-Cl(3)#2	94.6(6)
Sn(1)-N(1)-Sn(2)	108.9(4)	O(4)-Li(2)-Zn(2)#2	127.4(11)
Zn(2)-N(2)-Zn(2)#2	84.2(4)	O(3)-Li(2)-Zn(2)#2	127.2(9)
Zn(2)-N(2)-Sn(4)	114.0(4)	Cl(4)#2-Li(2)-Zn(2)#2	47.9(3)
Zn(2)#2-N(2)-Sn(4)	118.9(4)	Cl(3)#2-Li(2)-Zn(2)#2	46.8(3)
Zn(2)-N(2)-Sn(3)	118.1(4)	C(15)-O(1)-C(13)	92(4)
Zn(2)#2-N(2)-Sn(3)	113.5(4)	C(15)-O(1)-C(13')	106.1(18)
Sn(4)-N(2)-Sn(3)	107.2(4)	C(13)-O(1)-C(13')	59(3)
O(2)-Li(1)-O(1)	109.0(11)	C(15)-O(1)-Li(1)	138.1(17)
O(2)-Li(1)-Cl(1)	112.8(11)	C(13)-O(1)-Li(1)	120(3)
O(1)-Li(1)-Cl(1)	116.5(12)	C(13')-O(1)-Li(1)	113.5(15)
O(2)-Li(1)-Cl(2)	112.6(11)	C(14)-C(13)-O(1)	113(6)
O(1)-Li(1)-Cl(2)	111.0(11)	C(14)-C(13)-C(13')	48(3)
Cl(1)-Li(1)-Cl(2)	94.3(7)	O(1)-C(13)-C(13')	68(4)
O(2)-Li(1)-Zn(1)	119.5(9)	C(14)-C(13)-C(15)	130(6)
O(1)-Li(1)-Zn(1)	131.4(12)	O(1)-C(13)-C(15)	41(3)
Cl(1)-Li(1)-Zn(1)	47.6(4)	C(13')-C(13)-C(15)	84(4)
Cl(2)-Li(1)-Zn(1)	47.1(4)	C(14)-C(13')-C(13)	61(4)
O(4)-Li(2)-O(3)	104.9(10)	C(14)-C(13')-O(1)	112(3)
O(4)-Li(2)-Cl(4)#2	121.4(12)	C(13)-C(13')-O(1)	54(3)
O(3)-Li(2)-Cl(4)#2	112.9(12)	C(13')-C(14)-C(13)	70(4)

C(16')-C(15)-O(1)	130(7)	C(17')-O(2)-Li(1)	118(2)
C(16')-C(15)-C(15')	39(5)	C(17)-O(2)-Li(1)	113.3(14)
O(1)-C(15)-C(15')	122(3)	C(18)-C(17)-C(17')	56(3)
C(16')-C(15)-C(16)	44(5)	C(18)-C(17)-O(2)	112(3)
O(1)-C(15)-C(16)	98(3)	C(17')-C(17)-O(2)	57(3)
C(15')-C(15)-C(16)	27(3)	C(18)-C(17')-C(17)	56(3)
C(16')-C(15)-C(13)	110(8)	C(18)-C(17')-O(2)	128(4)
O(1)-C(15)-C(13)	47(3)	C(17)-C(17')-O(2)	74(3)
C(15')-C(15)-C(13)	138(4)	C(17)-C(18)-C(17')	68(3)
C(16)-C(15)-C(13)	113(4)	C(20)-C(19)-O(2)	119(3)
C(16)-C(15')-C(16')	78(8)	C(23')-O(3)-C(21')	70(3)
C(16)-C(15')-C(15)	80(8)	C(23')-O(3)-C(23)	92(3)
C(16')-C(15')-C(15)	45(6)	C(21')-O(3)-C(23)	106(3)
C(15')-C(16)-C(16')	61(7)	C(23')-O(3)-C(21)	114(2)
C(15')-C(16)-C(15)	73(8)	C(21')-O(3)-C(21)	61(3)
C(16')-C(16)-C(15)	44(6)	C(23)-O(3)-C(21)	65(2)
C(15')-C(16')-C(16)	41(6)	C(23')-O(3)-Li(2)	124(2)
C(15')-C(16')-C(15)	96(9)	C(21')-O(3)-Li(2)	127(3)
C(16)-C(16')-C(15)	93(9)	C(23)-O(3)-Li(2)	122(3)
C(19)-O(2)-C(17')	108(2)	C(21)-O(3)-Li(2)	119.9(15)
C(19)-O(2)-C(17)	107.1(19)	O(3)-C(21')-C(22)	115(4)
C(17')-O(2)-C(17)	48(2)	O(3)-C(21')-C(21)	62(3)
C(19)-O(2)-Li(1)	132.1(16)	C(22)-C(21')-C(21)	59(3)

O(3)-C(21')-C(23')	55(3)	O(3)-C(23)-C(24)	91(3)
C(22)-C(21')-C(23')	161(5)	C(21)-C(23)-C(24)	122(4)
C(21)-C(21')-C(23')	103(4)	O(3)-C(23')-C(21')	56(3)
C(22)-C(21)-C(21')	60(3)	O(3)-C(23')-C(24)	100(3)
C(22)-C(21)-O(3)	111(2)	C(21')-C(23')-C(24)	120(4)
C(21')-C(21)-O(3)	57(3)	C(23')-C(24)-C(23)	75(3)
C(22)-C(21)-C(23)	155(3)	C(25)-O(4)-C(27)	114.4(17)
C(21')-C(21)-C(23)	98(4)	C(25)-O(4)-Li(2)	126.5(15)
O(3)-C(21)-C(23)	57(2)	C(27)-O(4)-Li(2)	117.3(17)
C(21)-C(22)-C(21')	60(3)	C(26)-C(25)-O(4)	112.9(15)
O(3)-C(23)-C(21)	58(2)	C(28)-C(27)-O(4)	80(3)

Table A.41. Anisotropic displacement parameters ($\text{\AA}^2 \times 10^3$) for $\text{C}_{28}\text{H}_{76}\text{N}_2\text{O}_4\text{Cl}_4\text{Sn}_4\text{Zn}_2$ (**11**).

Atom	U11	U22	U33	U23	U13	U12
Sn(1)	39(1)	42(1)	39(1)	6(1)	-8(1)	-23(1)
Sn(2)	48(1)	34(1)	44(1)	-8(1)	-5(1)	-16(1)
Sn(3)	35(1)	45(1)	50(1)	5(1)	-11(1)	-17(1)
Sn(4)	48(1)	38(1)	36(1)	-6(1)	2(1)	-17(1)
Zn(1)	32(1)	27(1)	33(1)	6(1)	-7(1)	-12(1)
Zn(2)	38(1)	29(1)	29(1)	5(1)	-6(1)	-18(1)
Cl(1)	38(2)	34(2)	43(2)	5(1)	-4(1)	-8(1)
Cl(2)	45(2)	57(2)	40(2)	18(2)	-7(1)	-21(2)
Cl(3)	97(3)	54(2)	58(2)	17(2)	-34(2)	-56(2)
Cl(4)	54(2)	51(2)	32(2)	12(1)	-13(1)	-29(2)
N(1)	33(5)	23(5)	37(5)	2(4)	-2(4)	-12(4)
N(2)	51(6)	32(5)	32(5)	-3(4)	0(4)	-24(5)
C(1)	44(8)	53(8)	43(7)	4(6)	-6(6)	-23(7)
C(2)	71(10)	65(9)	54(8)	17(7)	-19(7)	-44(8)
C(3)	38(8)	65(9)	70(9)	-3(7)	-19(7)	-27(7)
C(4)	93(13)	29(8)	107(13)	-8(8)	-14(10)	-18(8)
C(5)	57(9)	94(12)	58(9)	-29(8)	15(7)	-37(9)
C(6)	80(11)	62(9)	57(8)	-12(7)	-13(8)	-33(9)
C(7)	60(10)	80(11)	65(9)	3(8)	-34(8)	-31(9)
C(8)	63(10)	92(12)	79(11)	4(9)	-6(8)	-43(10)
C(9)	58(10)	56(9)	69(10)	3(8)	-6(8)	-2(8)

C(10)	94(12)	41(8)	63(9)	-18(7)	-7(9)	-7(9)
C(11)	74(10)	81(11)	34(7)	-15(7)	16(7)	-38(9)
C(12)	63(10)	66(10)	52(8)	-21(7)	-2(7)	-18(8)
Li(1)	46(13)	26(11)	78(15)	21(10)	-10(11)	-2(10)
Li(2)	68(16)	54(14)	61(14)	17(11)	18(12)	-43(13)
O(1)	158(13)	55(7)	90(9)	11(7)	22(8)	-29(8)
C(14)	320(50)	380(60)	72(18)	-20(30)	0(20)	-150(50)
C(15)	120(30)	70(20)	150(30)	-100(20)	120(30)	-70(20)
C(16)	160(50)	60(30)	160(50)	-40(30)	60(40)	-30(30)
O(2)	72(7)	77(7)	75(7)	-5(6)	-36(6)	-5(6)
C(18)	86(18)	140(30)	300(40)	-90(30)	0(20)	18(17)
C(19)	240(40)	170(30)	120(20)	-40(20)	-40(20)	-100(30)
C(20)	89(16)	150(20)	115(17)	-47(16)	-4(13)	-31(16)
O(3)	85(8)	46(6)	98(8)	8(6)	-30(7)	-27(6)
C(22)	111(18)	170(20)	132(18)	-45(16)	17(14)	-83(17)
O(4)	89(9)	160(13)	100(9)	46(9)	-13(7)	-88(10)
C(25)	106(17)	160(20)	103(16)	40(14)	32(13)	-85(16)
C(26)	125(19)	200(20)	77(13)	33(13)	-5(12)	-118(19)
C(27)	290(50)	130(30)	220(40)	0(30)	-140(30)	0(30)
C(28)	160(30)	120(20)	210(30)	20(20)	10(20)	30(20)

Table A.42. Hydrogen coordinates ($\times 10^4$) and isotropic displacement parameters ($\text{\AA}^2 \times 10^3$) for $\text{C}_{28}\text{H}_{76}\text{N}_2\text{O}_4\text{Cl}_4\text{Sn}_4\text{Zn}_2$ (**11**).

Atom	x	y	z	U(eq)
H(1A)	3493	3739	4032	40(18)
H(1B)	4178	4595	3834	40(18)
H(1C)	2839	5005	3654	40(18)
H(2A)	1813	7744	4296	50(20)
H(2B)	3005	7404	4607	50(20)
H(2C)	1607	7958	5049	50(20)
H(3A)	3699	5222	5801	80(30)
H(3B)	4515	4063	5324	80(30)
H(3C)	3335	4118	5865	80(30)
H(4A)	-524	8871	5194	80(30)
H(4B)	-936	9412	5907	80(30)
H(4C)	-1923	9235	5607	80(30)
H(5A)	-2651	7216	6518	100(30)
H(5B)	-2060	7269	7101	100(30)
H(5C)	-1636	5969	6787	100(30)
H(6A)	1389	5941	6758	100(30)
H(6B)	470	7319	7021	100(30)
H(6C)	1574	7071	6393	100(30)
H(7A)	-2768	10714	10759	60(20)
H(7B)	-1533	9639	10979	60(20)
H(7C)	-2881	9664	11243	60(20)

H(8A)	-162	8365	9006	100(30)
H(8B)	38	9079	9517	100(30)
H(8C)	-1018	9826	9097	100(30)
H(9A)	-1782	6479	10331	100(30)
H(9B)	-1205	6784	10846	100(30)
H(9C)	-379	6345	10135	100(30)
H(10A)	-571	6552	8773	90(30)
H(10B)	-1193	6022	8389	90(30)
H(10C)	-1531	6050	9160	90(30)
H(11A)	-2372	10157	8255	100(30)
H(11B)	-2662	9647	7690	100(30)
H(11C)	-1309	8911	7886	100(30)
H(12A)	-4800	7790	8796	80(30)
H(12B)	-3917	7453	8090	80(30)
H(12C)	-4935	8855	8270	80(30)

Table A.43. Atomic Coordinates ($\times 10^4$) and Equivalent Isotropic Displacement Parameters ($\text{\AA}^2 \times 10^3$) for $\text{C}_{26}\text{H}_{38}\text{N}_2\text{Sn}_2\text{Zr}_2$ (**12**).

Atom	x	y	z	U(eq)
Sn(1)	6936(1)	1621(1)	3866(1)	36(1)
Zr(1)	5741(1)	227(1)	6439(1)	33(1)
C(1)	3279(8)	844(4)	7334(7)	58(2)
C(2)	3742(8)	1449(4)	6562(7)	58(2)
C(3)	5278(9)	1755(4)	7134(6)	53(2)
C(4)	5714(8)	1339(4)	8278(6)	53(2)
C(5)	4485(9)	766(4)	8422(7)	62(2)
C(6)	8610(7)	-357(4)	6481(8)	56(2)
C(7)	7727(7)	-1012(4)	6832(6)	50(2)
C(8)	7328(8)	-878(4)	8051(7)	58(2)
C(9)	8005(9)	-139(5)	8497(8)	64(2)
C(10)	8769(8)	203(4)	7499(8)	64(2)
C(11)	9133(7)	1918(4)	5148(6)	54(2)
C(12)	5360(8)	2679(4)	3854(6)	54(2)
C(13)	7428(7)	1366(4)	1925(5)	46(1)
N(1)	5873(5)	604(2)	4559(4)	34(1)

Table A.44. Interatomic Distances (Å) and Angles (°) for C₂₆H₃₈N₂Sn₂Zr₂ (**12**).

Sn(1)-N(1)	2.047(4)	C(6)-C(10)	1.382(10)
Sn(1)-C(11)	2.136(6)	C(7)-C(8)	1.367(9)
Sn(1)-C(13)	2.146(6)	C(8)-C(9)	1.373(9)
Sn(1)-C(12)	2.152(6)	C(9)-C(10)	1.402(10)
Zr(1)-N(1)	2.057(4)	N(1)-Zr(1)#1	2.060(4)
Zr(1)-N(1)#1	2.060(4)	N(1)-Sn(1)-C(11)	109.4(2)
Zr(1)-C(6)	2.545(6)	N(1)-Sn(1)-C(13)	108.85(19)
Zr(1)-C(1)	2.559(6)	C(11)-Sn(1)-C(13)	111.3(2)
Zr(1)-C(10)	2.576(6)	N(1)-Sn(1)-C(12)	110.8(2)
Zr(1)-C(5)	2.584(7)	C(11)-Sn(1)-C(12)	106.3(2)
Zr(1)-C(7)	2.586(6)	C(13)-Sn(1)-C(12)	110.3(2)
Zr(1)-C(2)	2.595(6)	N(1)-Zr(1)-N(1)#1	80.95(17)
Zr(1)-C(4)	2.625(6)	N(1)-Zr(1)-C(6)	87.0(2)
Zr(1)-C(3)	2.626(6)	N(1)#1-Zr(1)-C(6)	107.20(19)
Zr(1)-C(8)	2.657(6)	N(1)-Zr(1)-C(1)	112.5(2)
Zr(1)-C(9)	2.682(7)	N(1)#1-Zr(1)-C(1)	87.06(19)
C(1)-C(2)	1.356(9)	C(6)-Zr(1)-C(1)	157.8(2)
C(1)-C(5)	1.392(9)	N(1)-Zr(1)-C(10)	102.8(2)
C(2)-C(3)	1.408(9)	N(1)#1-Zr(1)-C(10)	135.8(2)
C(3)-C(4)	1.363(9)	C(6)-Zr(1)-C(10)	31.3(2)
C(4)-C(5)	1.400(9)	C(1)-Zr(1)-C(10)	128.6(3)
C(6)-C(7)	1.367(9)	N(1)-Zr(1)-C(5)	137.17(19)

N(1)#1-Zr(1)-C(5)	108.3(2)	C(7)-Zr(1)-C(4)	119.6(2)
C(6)-Zr(1)-C(5)	126.5(2)	C(2)-Zr(1)-C(4)	50.6(2)
C(1)-Zr(1)-C(5)	31.4(2)	N(1)-Zr(1)-C(3)	90.47(19)
C(10)-Zr(1)-C(5)	98.4(3)	N(1)#1-Zr(1)-C(3)	130.21(19)
N(1)-Zr(1)-C(7)	104.98(19)	C(6)-Zr(1)-C(3)	121.3(2)
N(1)#1-Zr(1)-C(7)	85.30(18)	C(1)-Zr(1)-C(3)	51.4(2)
C(6)-Zr(1)-C(7)	30.9(2)	C(10)-Zr(1)-C(3)	93.9(2)
C(1)-Zr(1)-C(7)	140.0(2)	C(5)-Zr(1)-C(3)	51.0(2)
C(10)-Zr(1)-C(7)	50.9(2)	C(7)-Zr(1)-C(3)	143.6(2)
C(5)-Zr(1)-C(7)	117.2(2)	C(2)-Zr(1)-C(3)	31.3(2)
N(1)-Zr(1)-C(2)	86.7(2)	C(4)-Zr(1)-C(3)	30.09(19)
N(1)#1-Zr(1)-C(2)	99.00(19)	N(1)-Zr(1)-C(8)	134.7(2)
C(6)-Zr(1)-C(2)	151.7(2)	N(1)#1-Zr(1)-C(8)	95.42(19)
C(1)-Zr(1)-C(2)	30.5(2)	C(6)-Zr(1)-C(8)	50.8(2)
C(10)-Zr(1)-C(2)	125.0(2)	C(1)-Zr(1)-C(8)	112.4(2)
C(5)-Zr(1)-C(2)	50.9(2)	C(10)-Zr(1)-C(8)	50.7(2)
C(7)-Zr(1)-C(2)	168.1(2)	C(5)-Zr(1)-C(8)	87.1(2)
N(1)-Zr(1)-C(4)	119.20(19)	C(7)-Zr(1)-C(8)	30.2(2)
N(1)#1-Zr(1)-C(4)	137.57(19)	C(2)-Zr(1)-C(8)	137.9(2)
C(6)-Zr(1)-C(4)	110.6(2)	C(4)-Zr(1)-C(8)	93.8(2)
C(1)-Zr(1)-C(4)	51.4(2)	C(3)-Zr(1)-C(8)	122.9(2)
C(10)-Zr(1)-C(4)	79.3(2)	N(1)-Zr(1)-C(9)	133.4(2)
C(5)-Zr(1)-C(4)	31.2(2)	N(1)#1-Zr(1)-C(9)	125.1(2)

C(6)-Zr(1)-C(9)	50.7(2)	C(1)-C(5)-C(4)	107.2(6)
C(1)-Zr(1)-C(9)	107.2(2)	C(1)-C(5)-Zr(1)	73.3(4)
C(10)-Zr(1)-C(9)	30.8(2)	C(4)-C(5)-Zr(1)	76.0(4)
C(5)-Zr(1)-C(9)	76.1(2)	C(7)-C(6)-C(10)	107.6(7)
C(7)-Zr(1)-C(9)	49.7(2)	C(7)-C(6)-Zr(1)	76.2(4)
C(2)-Zr(1)-C(9)	120.2(2)	C(10)-C(6)-Zr(1)	75.6(4)
C(4)-Zr(1)-C(9)	69.9(2)	C(8)-C(7)-C(6)	109.5(6)
C(3)-Zr(1)-C(9)	96.0(2)	C(8)-C(7)-Zr(1)	77.8(4)
C(8)-Zr(1)-C(9)	29.8(2)	C(6)-C(7)-Zr(1)	72.9(3)
C(2)-C(1)-C(5)	108.2(6)	C(7)-C(8)-C(9)	107.8(6)
C(2)-C(1)-Zr(1)	76.2(4)	C(7)-C(8)-Zr(1)	72.0(4)
C(5)-C(1)-Zr(1)	75.3(4)	C(9)-C(8)-Zr(1)	76.1(4)
C(1)-C(2)-C(3)	108.8(6)	C(8)-C(9)-C(10)	107.7(7)
C(1)-C(2)-Zr(1)	73.3(4)	C(8)-C(9)-Zr(1)	74.1(4)
C(3)-C(2)-Zr(1)	75.6(4)	C(10)-C(9)-Zr(1)	70.4(4)
C(4)-C(3)-C(2)	107.1(6)	C(6)-C(10)-C(9)	107.4(7)
C(4)-C(3)-Zr(1)	74.9(4)	C(6)-C(10)-Zr(1)	73.1(4)
C(2)-C(3)-Zr(1)	73.1(3)	C(9)-C(10)-Zr(1)	78.8(4)
C(3)-C(4)-C(5)	108.6(6)	Sn(1)-N(1)-Zr(1)	131.0(2)
C(3)-C(4)-Zr(1)	75.0(4)	Sn(1)-N(1)-Zr(1)#1	129.1(2)
C(5)-C(4)-Zr(1)	72.8(4)	Zr(1)-N(1)-Zr(1)#1	99.05(17)

Table A.45. Anisotropic displacement parameters ($\text{\AA}^2 \times 10^3$) for $\text{C}_{26}\text{H}_{38}\text{N}_2\text{Sn}_2\text{Zr}_2$ (**12**).

Atom	U11	U22	U33	U23	U13	U12
Sn(1)	43(1)	34(1)	34(1)	2(1)	9(1)	-5(1)
Zr(1)	35(1)	31(1)	34(1)	-1(1)	11(1)	0(1)
C(1)	50(4)	50(4)	80(5)	-24(4)	26(4)	1(3)
C(2)	59(4)	50(4)	64(5)	-14(3)	9(4)	18(3)
C(3)	67(4)	41(3)	52(4)	-8(3)	18(3)	3(3)
C(4)	63(4)	56(4)	42(4)	-13(3)	8(3)	3(3)
C(5)	90(5)	54(4)	49(4)	4(3)	31(4)	4(4)
C(6)	39(3)	58(4)	71(5)	5(3)	8(3)	14(3)
C(7)	50(4)	44(3)	53(4)	2(3)	-2(3)	6(3)
C(8)	52(4)	60(4)	62(5)	16(3)	10(3)	0(3)
C(9)	59(4)	81(5)	48(4)	-4(4)	-7(3)	10(4)
C(10)	41(4)	53(4)	94(6)	0(4)	-6(4)	2(3)
C(11)	56(4)	54(4)	49(4)	1(3)	1(3)	-12(3)
C(12)	73(4)	41(3)	51(4)	6(3)	16(3)	-2(3)
C(13)	58(4)	46(3)	38(3)	0(3)	19(3)	-9(3)
N(1)	33(2)	34(2)	35(2)	1(2)	9(2)	-1(2)

Table A.46. Hydrogen coordinates ($\times 10^4$) and isotropic displacement parameters ($\text{\AA}^2 \times 10^3$) for $\text{C}_{26}\text{H}_{38}\text{N}_2\text{Sn}_2\text{Zr}_2$ (**12**).

Atom	x	y	z	U(eq)
H(1)	2291	525	7161	56(18)
H(2)	3123	1638	5757	110(30)
H(3)	5902	2178	6785	90(30)
H(4)	6699	1425	8884	60(20)
H(5)	4476	389	9136	80(20)
H(6)	9042	-298	5674	130(40)
H(7)	7432	-1491	6304	80(20)
H(8)	6688	-1237	8513	90(30)
H(9)	7963	100	9340	220(60)
H(10)	9304	729	7519	270(70)
H(11A)	8859	2168	5929	80(13)
H(11B)	9775	2295	4720	80(13)
H(11C)	9752	1424	5372	80(13)
H(12A)	4479	2635	3139	118(18)
H(12B)	5978	3170	3756	118(18)
H(12C)	4921	2703	4662	118(18)
H(13A)	8522	1155	1968	121(18)
H(13B)	7323	1865	1419	121(18)
H(13C)	6660	965	1521	121(18)

Table A.47. Atomic Coordinates ($\times 10^4$) and Equivalent Isotropic Displacement Parameters ($\text{\AA}^2 \times 10^3$) for $\text{C}_{12}\text{H}_{36}\text{N}_4\text{Si}_4\text{Sn}_4$ (**13**).

Atom	x	y	z	U(eq)
Sn(1)	833(1)	0	702(1)	36(1)
Sn(2)	122(1)	370(1)	552(1)	40(1)
Sn(3)	1966(1)	0	972(1)	38(1)
Si(1)	1143(1)	0	0008(2)	65(1)
Si(2)	3095(1)	0	737(2)	43(1)
Si(3)	1216(1)	381(1)	526(1)	49(1)
N(1)	1397(2)	0	738(5)	39(1)
N(2)	2385(2)	0	095(4)	34(1)
N(3)	1432(1)	202(3)	468(3)	36(1)
C(1)	724(3)	250(7)	887(6)	113(3)
C(2)	1723(4)	0	1583(7)	94(3)
C(3)	3347(2)	278(6)	186(7)	103(3)
C(4)	3327(3)	0	0531(7)	64(2)
C(5)	1811(3)	242(5)	613(7)	93(2)
C(6)	755(2)	197(5)	155(6)	76(2)
C(7)	833(2)	967(5)	812(4)	74(2)
C(8)	5000(2)	38(5)	0000(4)	51(4)
C(9)	4934(2)	0(5)	036(4)	48(3)
C(10)	4965(2)	989(5)	0950(4)	78(4)
C(11)	5167(2)	0(4)	2492(4)	113(8)

C(12)	4983(2)	0(4)	11805(4)	65(4)
C(13)	5118(2)	1019(5)	10534(4)	52(5)

Table A.48. Interatomic Distances (Å) and Angles (°) for C₁₂H₃₆N₄Si₄Sn₄ (**13**).

Sn(1)-N(1)	2.205(5)	N(2)-Sn(2)#1	2.203(3)
Sn(1)-N(3)	2.208(4)	C(8)-C(13)	0.5669
Sn(1)-N(3)#1	2.208(4)	C(8)-C(13)#2	0.567(9)
Sn(2)-N(1)	2.198(4)	C(8)-C(10)	1.0752
Sn(2)-N(2)	2.203(3)	C(8)-C(10)#2	1.075(10)
Sn(2)-N(3)	2.204(4)	C(8)-C(9)#3	1.515(12)
Sn(3)-N(2)	2.198(5)	C(8)-C(9)	1.5146
Sn(3)-N(3)#1	2.204(4)	C(9)-C(12)#3	1.015(10)
Sn(3)-N(3)	2.204(4)	C(9)-C(10)#2	1.221(2)
Si(1)-N(1)	1.731(5)	C(9)-C(10)#3	1.222(10)
Si(1)-C(1)#1	1.841(7)	C(9)-C(13)#2	1.339(4)
Si(1)-C(1)	1.841(7)	C(9)-C(13)#3	1.339(12)
Si(1)-C(2)	1.857(8)	C(9)-C(8)#3	1.515(11)
Si(2)-N(2)	1.735(5)	C(9)-C(11)#3	1.599(10)
Si(2)-C(4)	1.842(7)	C(9)-C(13)	1.9701
Si(2)-C(3)#1	1.857(6)	C(9)-C(13)#1	1.970(7)
Si(2)-C(3)	1.857(6)	C(9)-C(9)#3	2.014(10)
Si(3)-N(3)	1.732(4)	C(10)-C(13)	0.7007
Si(3)-C(5)	1.842(6)	C(10)-C(9)#3	1.222(10)
Si(3)-C(6)	1.858(6)	C(10)-C(12)	1.5068
Si(3)-C(7)	1.862(5)	C(10)-C(13)#2	1.562(10)
N(1)-Sn(2)#1	2.198(4)	C(10)-C(11)	1.9829

C(11)-C(12)	0.7389	C(1)#1-Si(1)-C(2)	109.8(3)
C(11)-C(9)#3	1.599(10)	C(1)-Si(1)-C(2)	109.8(3)
C(11)-C(10)#1	1.983(6)	N(2)-Si(2)-C(4)	110.1(3)
C(12)-C(9)#3	1.015(11)	N(2)-Si(2)-C(3)#1	108.4(2)
C(12)-C(10)#1	1.507(8)	C(4)-Si(2)-C(3)#1	108.8(3)
C(12)-C(13)	1.9749	N(2)-Si(2)-C(3)	108.4(2)
C(12)-C(13)#1	1.975(6)	C(4)-Si(2)-C(3)	108.8(3)
C(13)-C(13)#2	1.117(9)	C(3)#1-Si(2)-C(3)	112.3(5)
C(13)-C(9)#3	1.339(12)	N(3)-Si(3)-C(5)	109.7(2)
C(13)-C(10)#2	1.562(10)	N(3)-Si(3)-C(6)	109.5(2)
N(1)-Sn(1)-N(3)	82.28(13)	C(5)-Si(3)-C(6)	108.8(3)
N(1)-Sn(1)-N(3)#1	82.28(13)	N(3)-Si(3)-C(7)	109.2(2)
N(3)-Sn(1)-N(3)#1	82.08(19)	C(5)-Si(3)-C(7)	110.6(3)
N(1)-Sn(2)-N(2)	82.19(15)	C(6)-Si(3)-C(7)	109.0(2)
N(1)-Sn(2)-N(3)	82.51(16)	Si(1)-N(1)-Sn(2)	119.72(16)
N(2)-Sn(2)-N(3)	82.17(15)	Si(1)-N(1)-Sn(2)#1	119.72(16)
N(2)-Sn(3)-N(3)#1	82.31(13)	Sn(2)-N(1)-Sn(2)#1	97.5(2)
N(2)-Sn(3)-N(3)	82.31(13)	Si(1)-N(1)-Sn(1)	120.3(3)
N(3)#1-Sn(3)-N(3)	82.29(19)	Sn(2)-N(1)-Sn(1)	97.22(16)
N(1)-Si(1)-C(1)#1	108.9(3)	Sn(2)#1-N(1)-Sn(1)	97.22(16)
N(1)-Si(1)-C(1)	108.9(3)	Si(2)-N(2)-Sn(3)	119.9(3)
C(1)#1-Si(1)-C(1)	110.1(5)	Si(2)-N(2)-Sn(2)#1	119.90(15)
N(1)-Si(1)-C(2)	109.3(4)	Sn(3)-N(2)-Sn(2)#1	97.36(14)

Si(2)-N(2)-Sn(2)	119.90(15)	C(9)#3-C(8)-C(9)	83.3(3)
Sn(3)-N(2)-Sn(2)	97.36(14)	C(12)#3-C(9)-C(10)#2	84.2(9)
Sn(2)#1-N(2)-Sn(2)	97.2(2)	C(12)#3-C(9)-C(10)#3	84.1(6)
Si(3)-N(3)-Sn(3)	119.86(19)	C(10)#2-C(9)-C(10)#3	155.4(9)
Si(3)-N(3)-Sn(2)	119.50(19)	C(12)#3-C(9)-C(13)#2	113.4(8)
Sn(3)-N(3)-Sn(2)	97.17(13)	C(10)#2-C(9)-C(13)#2	31.34(8)
Si(3)-N(3)-Sn(1)	120.68(18)	C(10)#3-C(9)-C(13)#2	160.1(8)
Sn(3)-N(3)-Sn(1)	97.36(15)	C(12)#3-C(9)-C(13)#3	113.3(8)
Sn(2)-N(3)-Sn(1)	96.94(14)	C(10)#2-C(9)-C(13)#3	160.1(8)
C(13)-C(8)-C(13)#2	160.14(17)	C(10)#3-C(9)-C(13)#3	31.3(3)
C(13)-C(8)-C(10)	36.0	C(13)#2-C(9)-C(13)#3	133.3(8)
C(13)#2-C(8)-C(10)	142.1(10)	C(12)#3-C(9)-C(8)#3	128.4(8)
C(13)-C(8)-C(10)#2	142.1(4)	C(10)#2-C(9)-C(8)#3	138.5(7)
C(13)#2-C(8)-C(10)#2	36.0(7)	C(10)#3-C(9)-C(8)#3	44.7(4)
C(10)-C(8)-C(10)#2	173.37(6)	C(13)#2-C(9)-C(8)#3	116.3(7)
C(13)-C(8)-C(9)#3	61.4(3)	C(13)#3-C(9)-C(8)#3	21.81(18)
C(13)#2-C(8)-C(9)#3	137.5(6)	C(12)#3-C(9)-C(8)	128.4(6)
C(10)-C(8)-C(9)#3	53.0(3)	C(10)#2-C(9)-C(8)	44.7(5)
C(10)#2-C(8)-C(9)#3	133.4(4)	C(10)#3-C(9)-C(8)	138.5(4)
C(13)-C(8)-C(9)	137.5	C(13)#2-C(9)-C(8)	21.8(4)
C(13)#2-C(8)-C(9)	61.3(4)	C(13)#3-C(9)-C(8)	116.3(4)
C(10)-C(8)-C(9)	133.4	C(8)#3-C(9)-C(8)	96.7(3)
C(10)#2-C(8)-C(9)	53.04(10)	C(12)#3-C(9)-C(11)#3	20.5(2)

C(10)#2-C(9)-C(11)#3	88.3(7)	C(12)#3-C(9)-C(9)#3	159.1(8)
C(10)#3-C(9)-C(11)#3	88.3(5)	C(10)#2-C(9)-C(9)#3	91.6(5)
C(13)#2-C(9)-C(11)#3	111.5(6)	C(10)#3-C(9)-C(9)#3	91.6(6)
C(13)#3-C(9)-C(11)#3	111.5(6)	C(13)#2-C(9)-C(9)#3	68.6(4)
C(8)#3-C(9)-C(11)#3	131.7(7)	C(13)#3-C(9)-C(9)#3	68.6(5)
C(8)-C(9)-C(11)#3	131.7(4)	C(8)#3-C(9)-C(9)#3	48.3(3)
C(12)#3-C(9)-C(13)	133.3(6)	C(8)-C(9)-C(9)#3	48.3(3)
C(10)#2-C(9)-C(13)	52.4(5)	C(11)#3-C(9)-C(9)#3	179.6(6)
C(10)#3-C(9)-C(13)	127.6(4)	C(13)-C(9)-C(9)#3	39.3(3)
C(13)#2-C(9)-C(13)	33.0(4)	C(13)#1-C(9)-C(9)#3	39.24(7)
C(13)#3-C(9)-C(13)	107.8(4)	C(13)-C(10)-C(8)	28.4
C(8)#3-C(9)-C(13)	87.2(3)	C(13)-C(10)-C(9)#3	83.6(6)
C(8)-C(9)-C(13)	11.2	C(8)-C(10)-C(9)#3	82.3(5)
C(11)#3-C(9)-C(13)	140.7(4)	C(13)-C(10)-C(12)	122.6
C(12)#3-C(9)-C(13)#1	133.3(8)	C(8)-C(10)-C(12)	124.0
C(10)#2-C(9)-C(13)#1	127.6(4)	C(9)#3-C(10)-C(12)	42.1(5)
C(10)#3-C(9)-C(13)#1	52.4(6)	C(13)-C(10)-C(13)#2	39.8(3)
C(13)#2-C(9)-C(13)#1	107.8(4)	C(8)-C(10)-C(13)#2	12.9(3)
C(13)#3-C(9)-C(13)#1	33.0(4)	C(9)#3-C(10)-C(13)#2	89.3(5)
C(8)#3-C(9)-C(13)#1	11.2(3)	C(12)-C(10)-C(13)#2	128.8
C(8)-C(9)-C(13)#1	87.2(3)	C(13)-C(10)-C(11)	122.5
C(11)#3-C(9)-C(13)#1	140.7(6)	C(8)-C(10)-C(11)	134.4
C(13)-C(9)-C(13)#1	77.2(3)	C(9)#3-C(10)-C(11)	53.7(5)

C(12)-C(10)-C(11)	18.8	C(8)-C(13)-C(10)	115.6
C(13)#2-C(10)-C(11)	142.95(9)	C(8)-C(13)-C(13)#2	9.9
C(12)-C(11)-C(9)#3	28.7(4)	C(10)-C(13)-C(13)#2	116.6(5)
C(12)-C(11)-C(10)	41.1	C(8)-C(13)-C(9)#3	96.8(4)
C(9)#3-C(11)-C(10)	38.0(4)	C(10)-C(13)-C(9)#3	65.1(4)
C(12)-C(11)-C(10)#1	41.1(2)	C(13)#2-C(13)-C(9)#3	106.3(4)
C(9)#3-C(11)-C(10)#1	38.00(19)	C(8)-C(13)-C(10)#2	25.0(3)
C(10)-C(11)-C(10)#1	74.0(3)	C(10)-C(13)-C(10)#2	140.0(3)
C(11)-C(12)-C(9)#3	130.8(5)	C(13)#2-C(13)-C(10)#2	23.6(2)
C(11)-C(12)-C(10)	120.1	C(9)#3-C(13)-C(10)#2	110.4(4)
C(9)#3-C(12)-C(10)	53.8(6)	C(8)-C(13)-C(9)	31.3
C(11)-C(12)-C(10)#1	120.06(18)	C(10)-C(13)-C(9)	118.5
C(9)#3-C(12)-C(10)#1	53.7(4)	C(13)#2-C(13)-C(9)	40.69(16)
C(10)-C(12)-C(10)#1	104.8(3)	C(9)#3-C(13)-C(9)	72.2(4)
C(11)-C(12)-C(13)	120.3	C(10)#2-C(13)-C(9)	38.31(8)
C(9)#3-C(12)-C(13)	38.5(6)	C(8)-C(13)-C(12)	117.0
C(10)-C(12)-C(13)	17.4	C(10)-C(13)-C(12)	40.0
C(10)#1-C(12)-C(13)	91.8(3)	C(13)#2-C(13)-C(12)	124.7(3)
C(11)-C(12)-C(13)#1	120.26(12)	C(9)#3-C(13)-C(12)	28.2(4)
C(9)#3-C(12)-C(13)#1	38.5(4)	C(10)#2-C(13)-C(12)	136.24(14)
C(10)-C(12)-C(13)#1	91.8(3)	C(9)-C(13)-C(12)	98.3
C(10)#1-C(12)-C(13)#1	17.4		
C(13)-C(12)-C(13)#1	77.0(3)		

Table A.49. Anisotropic displacement parameters ($\text{\AA}^2 \times 10^3$) for $\text{C}_{12}\text{H}_{36}\text{N}_4\text{Si}_4\text{Sn}_4$ (**13**).

Atom	U11	U22	U33	U23	U13	U12
Sn(1)	26(1)	44(1)	33(1)	0	5(1)	0
Sn(2)	34(1)	41(1)	38(1)	-8(1)	3(1)	0(1)
Sn(3)	32(1)	49(1)	31(1)	0	10(1)	0
Si(1)	39(1)	123(2)	35(1)	0	15(1)	0
Si(2)	26(1)	56(1)	41(1)	0	3(1)	0
Si(3)	45(1)	40(1)	52(1)	12(1)	3(1)	2(1)
N(1)	33(3)	50(3)	32(3)	0	10(2)	0
N(2)	25(3)	42(3)	33(3)	0	6(2)	0
N(3)	34(2)	35(2)	35(2)	4(2)	6(2)	-1(2)
C(1)	76(5)	193(9)	79(5)	-42(5)	36(4)	32(5)
C(2)	91(7)	154(10)	36(5)	0	19(5)	0
C(3)	47(4)	144(7)	101(5)	49(5)	4(3)	-33(4)
C(4)	46(4)	84(6)	44(4)	0	-8(3)	0
C(5)	80(5)	65(4)	121(6)	43(4)	17(4)	-13(4)
C(6)	73(4)	55(4)	79(4)	-8(3)	-1(3)	19(3)
C(7)	76(4)	82(4)	51(4)	22(3)	5(3)	14(3)

Table A.50. Hydrogen coordinates ($\times 10^4$) and isotropic displacement parameters ($\text{\AA}^2 \times 10^3$) for $\text{C}_{12}\text{H}_{36}\text{N}_4\text{Si}_4\text{Sn}_4$ (**13**).

Atom	x	y	z	U(eq)
H(1A)	929	1887	9832	94(13)
H(1B)	620	1305	10637	94(13)
H(1C)	405	1205	9130	94(13)
H(2A)	1893	-708	11722	70(20)
H(2B)	1591	161	12271	70(20)
H(2C)	1982	547	11560	70(20)
H(3A)	3219	1299	7261	160(20)
H(3B)	3736	1281	8509	160(20)
H(3C)	3216	1910	8507	160(20)
H(4A)	3258	705	10829	90(20)
H(4B)	3708	-152	10872	90(20)
H(4C)	3135	-553	10817	90(20)
H(5A)	1983	3497	6480	115(15)
H(5B)	1693	3859	5045	115(15)
H(5C)	2063	2814	5357	115(15)
H(6A)	443	2765	6102	104(13)
H(6B)	642	3850	5648	104(13)
H(6C)	944	3394	7038	104(13)
H(7A)	1080	1652	3439	124(15)
H(7B)	664	2601	3324	124(15)
H(7C)	562	1437	3798	124(15)

Table A.51. Atomic Coordinates ($\times 10^4$) and Equivalent Isotropic Displacement Parameters ($\text{\AA}^2 \times 10^3$) for $\text{C}_{12}\text{H}_{36}\text{N}_4\text{Ge}_4\text{Si}_4$ (**14**).

Atom	x	y	z	U(eq)
Ge(1)	1946(1)	5100(1)	3065(1)	30(1)
Ge(2)	1926(1)	3699(1)	4206(1)	31(1)
Ge(3)	1895(1)	6203(1)	4291(1)	30(1)
Ge(4)	911(1)	4962(1)	3389(1)	32(1)
Si(1)	3077(1)	5077(1)	4379(1)	33(1)
Si(2)	1210(1)	7391(1)	2859(1)	37(1)
Si(3)	1161(1)	4756(1)	4990(1)	38(1)
Si(4)	1245(1)	2742(1)	2711(1)	40(1)
N(1)	2355(1)	5022(2)	4053(2)	29(1)
N(2)	1442(1)	6157(2)	3316(1)	30(1)
N(3)	1419(1)	4890(2)	4344(2)	30(1)
N(4)	1464(1)	3894(2)	3236(1)	32(1)
C(1)	3294(2)	6506(4)	4219(2)	55(1)
C(2)	3361(2)	3994(4)	3967(2)	62(1)
C(3)	3322(2)	4818(4)	5286(2)	56(1)
C(4)	1817(2)	8316(4)	2964(3)	65(1)
C(5)	730(2)	8118(4)	3200(2)	53(1)
C(6)	852(2)	7017(4)	1968(2)	61(1)
C(7)	1749(2)	4774(4)	5791(2)	61(1)
C(8)	677(2)	5939(4)	4945(2)	57(1)

C(9)	776(2)	3400(4)	4875(2)	55(1)
C(10)	1859(2)	1928(4)	2721(3)	74(2)
C(11)	851(2)	3271(4)	1860(2)	65(1)
C(12)	792(2)	1845(4)	3015(2)	64(1)
C(13)	4913(4)	5128(7)	4472(5)	42(2)
C(13A)	4832(5)	5224(9)	3737(7)	74(3)
C(14)	4857(3)	6088(7)	4806(5)	37(2)
C(14A)	4922(5)	5969(13)	4502(8)	89(4)
C(15)	4907(4)	5992(8)	5496(5)	54(2)
C(15A)	4956(4)	5938(9)	5150(6)	55(2)
C(16)	4981(6)	5001(9)	4147(8)	74(3)

Table A.52. Interatomic Distances (Å) and Angles (°) for C₁₂H₃₆N₄Ge₄Si₄ (**14**).

Ge(1)-N(1)	2.010(3)	Si(3)-C(8)	1.858(4)
Ge(1)-N(2)	2.013(3)	Si(3)-C(9)	1.862(4)
Ge(1)-N(4)	2.013(3)	Si(4)-N(4)	1.735(3)
Ge(2)-N(1)	2.014(3)	Si(4)-C(10)	1.849(5)
Ge(2)-N(4)	2.015(3)	Si(4)-C(11)	1.859(5)
Ge(2)-N(3)	2.016(3)	Si(4)-C(12)	1.861(4)
Ge(3)-N(2)	2.006(3)	C(13)-C(16)	0.792(15)
Ge(3)-N(3)	2.012(3)	C(13)-C(14A)	1.000(14)
Ge(3)-N(1)	2.015(3)	C(13)-C(14)	1.382(12)
Ge(4)-N(3)	2.007(3)	C(13)-C(15)#1	1.403(13)
Ge(4)-N(2)	2.013(3)	C(13)-C(15A)#1	1.478(13)
Ge(4)-N(4)	2.018(3)	C(13)-C(13A)	1.521(16)
Si(1)-N(1)	1.740(3)	C(13)-C(15A)	1.717(14)
Si(1)-C(3)	1.848(5)	C(13A)-C(16)	0.868(17)
Si(1)-C(2)	1.853(4)	C(13A)-C(14A)	1.81(2)
Si(1)-C(1)	1.856(4)	C(14)-C(15A)	0.713(12)
Si(2)-N(2)	1.748(3)	C(14)-C(14A)	0.743(14)
Si(2)-C(4)	1.857(5)	C(14)-C(15)	1.445(13)
Si(2)-C(5)	1.858(4)	C(14)-C(16)	2.024(16)
Si(2)-C(6)	1.861(4)	C(14A)-C(15A)	1.364(17)
Si(3)-N(3)	1.745(3)	C(14A)-C(16)	1.417(19)
Si(3)-C(7)	1.847(5)	C(15)-C(15A)	0.798(12)

C(15)-C(16)#1	1.381(15)	C(2)-Si(1)-C(1)	110.6(2)
C(15)-C(13)#1	1.403(13)	N(2)-Si(2)-C(4)	108.86(18)
C(15A)-C(13)#1	1.478(13)	N(2)-Si(2)-C(5)	108.07(18)
C(15A)-C(16)#1	1.838(19)	C(4)-Si(2)-C(5)	109.0(2)
C(16)-C(15)#1	1.381(15)	N(2)-Si(2)-C(6)	108.93(19)
C(16)-C(15A)#1	1.838(19)	C(4)-Si(2)-C(6)	110.8(2)
N(1)-Ge(1)-N(2)	83.84(12)	C(5)-Si(2)-C(6)	111.1(2)
N(1)-Ge(1)-N(4)	84.36(11)	N(3)-Si(3)-C(7)	108.8(2)
N(2)-Ge(1)-N(4)	84.07(13)	N(3)-Si(3)-C(8)	109.04(18)
N(1)-Ge(2)-N(4)	84.22(12)	C(7)-Si(3)-C(8)	110.8(2)
N(1)-Ge(2)-N(3)	84.13(11)	N(3)-Si(3)-C(9)	107.93(18)
N(4)-Ge(2)-N(3)	83.96(13)	C(7)-Si(3)-C(9)	110.9(2)
N(2)-Ge(3)-N(3)	83.99(13)	C(8)-Si(3)-C(9)	109.4(2)
N(2)-Ge(3)-N(1)	83.90(12)	N(4)-Si(4)-C(10)	108.94(19)
N(3)-Ge(3)-N(1)	84.22(11)	N(4)-Si(4)-C(11)	108.17(19)
N(3)-Ge(4)-N(2)	83.95(11)	C(10)-Si(4)-C(11)	110.8(3)
N(3)-Ge(4)-N(4)	84.12(11)	N(4)-Si(4)-C(12)	108.86(19)
N(2)-Ge(4)-N(4)	83.96(13)	C(10)-Si(4)-C(12)	109.7(2)
N(1)-Si(1)-C(3)	109.7(2)	C(11)-Si(4)-C(12)	110.3(2)
N(1)-Si(1)-C(2)	109.09(17)	Si(1)-N(1)-Ge(1)	120.64(17)
C(3)-Si(1)-C(2)	110.0(2)	Si(1)-N(1)-Ge(2)	122.22(15)
N(1)-Si(1)-C(1)	107.91(16)	Ge(1)-N(1)-Ge(2)	95.46(12)
C(3)-Si(1)-C(1)	109.6(2)	Si(1)-N(1)-Ge(3)	120.76(15)

Ge(1)-N(1)-Ge(3)	95.78(13)	C(16)-C(13)-C(15)#1	71.9(12)
Ge(2)-N(1)-Ge(3)	95.52(13)	C(14A)-C(13)-C(15)#1	160.7(13)
Si(2)-N(2)-Ge(3)	121.38(16)	C(14)-C(13)-C(15)#1	148.2(10)
Si(2)-N(2)-Ge(4)	121.94(15)	C(16)-C(13)-C(15A)#1	103.9(14)
Ge(3)-N(2)-Ge(4)	95.72(12)	C(14A)-C(13)-C(15A)#1	145.5(14)
Si(2)-N(2)-Ge(1)	119.78(15)	C(14)-C(13)-C(15A)#1	117.9(9)
Ge(3)-N(2)-Ge(1)	95.94(12)	C(15)#1-C(13)-C(15A)#1	32.0(5)
Ge(4)-N(2)-Ge(1)	95.76(12)	C(16)-C(13)-C(13A)	24.8(12)
Si(3)-N(3)-Ge(4)	121.59(17)	C(14A)-C(13)-C(13A)	89.1(12)
Si(3)-N(3)-Ge(3)	121.75(16)	C(14)-C(13)-C(13A)	118.4(8)
Ge(4)-N(3)-Ge(3)	95.71(13)	C(15)#1-C(13)-C(13A)	92.5(8)
Si(3)-N(3)-Ge(2)	120.05(16)	C(15A)#1-C(13)-C(13A)	123.7(9)
Ge(4)-N(3)-Ge(2)	95.83(13)	C(16)-C(13)-C(15A)	152.5(15)
Ge(3)-N(3)-Ge(2)	95.52(13)	C(14A)-C(13)-C(15A)	52.6(10)
Si(4)-N(4)-Ge(1)	121.49(16)	C(14)-C(13)-C(15A)	23.6(5)
Si(4)-N(4)-Ge(2)	121.30(16)	C(15)#1-C(13)-C(15A)	124.6(8)
Ge(1)-N(4)-Ge(2)	95.35(11)	C(15A)#1-C(13)-C(15A)	94.6(7)
Si(4)-N(4)-Ge(4)	121.01(15)	C(13A)-C(13)-C(15A)	141.5(8)
Ge(1)-N(4)-Ge(4)	95.61(12)	C(16)-C(13A)-C(13)	22.5(11)
Ge(2)-N(4)-Ge(4)	95.55(12)	C(16)-C(13A)-C(14A)	50.2(12)
C(16)-C(13)-C(14A)	103.9(16)	C(13)-C(13A)-C(14A)	33.6(5)
C(16)-C(13)-C(14)	135.4(14)	C(15A)-C(14)-C(14A)	139(2)
C(14A)-C(13)-C(14)	31.5(9)	C(15A)-C(14)-C(13)	105.5(13)

C(14A)-C(14)-C(13)	44.6(14)	C(13)#1-C(15)-C(14)	92.0(8)
C(15A)-C(14)-C(15)	18.0(11)	C(14)-C(15A)-C(15)	146(2)
C(14A)-C(14)-C(15)	156.9(17)	C(14)-C(15A)-C(14A)	20.9(11)
C(13)-C(14)-C(15)	118.6(8)	C(15)-C(15A)-C(14A)	166.6(16)
C(15A)-C(14)-C(16)	118.6(13)	C(14)-C(15A)-C(13)#1	135.3(15)
C(14A)-C(14)-C(16)	28.6(15)	C(15)-C(15A)-C(13)#1	68.8(12)
C(13)-C(14)-C(16)	16.0(6)	C(14A)-C(15A)-C(13)#1	120.2(10)
C(15)-C(14)-C(16)	133.4(8)	C(14)-C(15A)-C(13)	50.9(11)
C(14)-C(14A)-C(13)	104(2)	C(15)-C(15A)-C(13)	148.2(14)
C(14)-C(14A)-C(15A)	20.1(11)	C(14A)-C(15A)-C(13)	35.6(7)
C(13)-C(14A)-C(15A)	91.8(13)	C(13)#1-C(15A)-C(13)	85.4(7)
C(14)-C(14A)-C(16)	137(2)	C(14)-C(15A)-C(16)#1	153.9(15)
C(13)-C(14A)-C(16)	32.9(9)	C(15)-C(15A)-C(16)#1	44.1(11)
C(15A)-C(14A)-C(16)	123.2(14)	C(14A)-C(15A)-C(16)#1	144.1(10)
C(14)-C(14A)-C(13A)	153.8(19)	C(13)#1-C(15A)-C(16)#1	24.7(5)
C(13)-C(14A)-C(13A)	57.3(11)	C(13)-C(15A)-C(16)#1	108.5(8)
C(15A)-C(14A)-C(13A)	148.9(12)	C(13)-C(16)-C(13A)	133(2)
C(16)-C(14A)-C(13A)	28.0(7)	C(13)-C(16)-C(15)#1	75.0(14)
C(15A)-C(15)-C(16)#1	112.2(15)	C(13A)-C(16)-C(15)#1	139.1(18)
C(15A)-C(15)-C(13)#1	79.2(13)	C(13)-C(16)-C(14A)	43.2(10)
C(16)#1-C(15)-C(13)#1	33.1(6)	C(13A)-C(16)-C(14A)	101.8(16)
C(15A)-C(15)-C(14)	16.1(10)	C(15)#1-C(16)-C(14A)	115.8(15)
C(16)#1-C(15)-C(14)	124.3(11)	C(13)-C(16)-C(15A)#1	51.3(11)

C(13A)-C(16)-C(15A)#1	153.9(17)	C(13A)-C(16)-C(14)	113.1(14)
C(15)#1-C(16)-C(15A)#1	23.7(6)	C(15)#1-C(16)-C(14)	102.1(10)
C(14A)-C(16)-C(15A)#1	92.6(12)	C(14A)-C(16)-C(14)	14.6(7)
C(13)-C(16)-C(14)	28.7(10)	C(15A)#1-C(16)-C(14)	78.6(7)

Table A.53. Anisotropic displacement parameters ($\text{\AA}^2 \times 10^3$) for $\text{C}_{12}\text{H}_{36}\text{N}_4\text{Ge}_4\text{Si}_4$ (**14**).

Atom	U11	U22	U33	U23	U13	U12
Ge(1)	29(1)	35(1)	28(1)	-1(1)	12(1)	-1(1)
Ge(2)	28(1)	32(1)	29(1)	2(1)	6(1)	-4(1)
Ge(3)	27(1)	33(1)	31(1)	-5(1)	12(1)	-5(1)
Ge(4)	23(1)	40(1)	30(1)	0(1)	7(1)	-4(1)
Si(1)	22(1)	40(1)	35(1)	-3(1)	8(1)	-3(1)
Si(2)	38(1)	35(1)	41(1)	7(1)	17(1)	6(1)
Si(3)	32(1)	53(1)	33(1)	0(1)	16(1)	-9(1)
Si(4)	45(1)	35(1)	33(1)	-7(1)	5(1)	-8(1)
N(1)	26(2)	30(2)	31(2)	-4(1)	10(1)	-3(1)
N(2)	26(1)	32(2)	33(2)	-1(1)	12(1)	-1(1)
N(3)	26(2)	33(2)	32(2)	-2(1)	11(1)	-5(1)
N(4)	27(1)	33(2)	33(2)	-3(1)	8(1)	-5(1)
C(1)	37(2)	57(3)	72(3)	2(2)	21(2)	-14(2)
C(2)	41(2)	73(3)	67(3)	-19(3)	12(2)	14(2)
C(3)	40(2)	77(3)	41(2)	-1(2)	3(2)	-8(2)
C(4)	66(3)	53(3)	82(4)	22(3)	34(3)	-7(2)
C(5)	47(2)	52(3)	60(3)	-8(2)	18(2)	6(2)
C(6)	66(3)	75(3)	37(2)	16(2)	12(2)	25(2)
C(7)	54(3)	95(4)	32(2)	5(2)	13(2)	-12(2)
C(8)	49(2)	67(3)	60(3)	-10(2)	25(2)	-1(2)

C(9)	50(2)	60(3)	59(3)	13(2)	25(2)	-10(2)
C(10)	76(4)	57(3)	89(4)	-28(3)	28(3)	10(3)
C(11)	84(3)	64(3)	32(2)	-5(2)	2(2)	-18(3)
C(12)	64(3)	57(3)	56(3)	6(2)	1(2)	-27(2)

Table A.54. Hydrogen coordinates ($\times 10^4$) and isotropic displacement parameters ($\text{\AA}^2 \times 10^3$) for $\text{C}_{12}\text{H}_{36}\text{N}_4\text{Ge}_4\text{Si}_4$ (**14**).

Atom	x	y	z	U(eq)
H(1A)	3150	6654	3755	102(12)
H(1B)	3687	6546	4375	102(12)
H(1C)	3154	7048	4445	102(12)
H(2A)	3253	3268	4061	70(8)
H(2B)	3754	4044	4127	70(8)
H(2C)	3221	4115	3499	70(8)
H(3A)	3176	5378	5493	88(11)
H(3B)	3716	4846	5462	88(11)
H(3C)	3200	4096	5368	88(11)
H(4A)	2032	8386	3424	76(9)
H(4B)	1691	9039	2784	76(9)
H(4C)	2039	7997	2737	76(9)
H(5A)	431	7630	3175	75(9)
H(5B)	589	8779	2949	75(9)
H(5C)	924	8315	3652	75(9)
H(6A)	1113	6704	1796	114(13)
H(6B)	692	7675	1724	114(13)
H(6C)	568	6483	1931	114(13)
H(7A)	2003	4193	5793	71(9)
H(7B)	1615	4655	6145	71(9)
H(7C)	1931	5482	5846	71(9)

H(8A)	864	6634	4963	83(10)
H(8B)	550	5893	5309	83(10)
H(8C)	369	5895	4539	83(10)
H(9A)	468	3419	4469	71(9)
H(9B)	648	3289	5235	71(9)
H(9C)	1016	2799	4863	71(9)
H(10A)	2100	2400	2590	155(17)
H(10B)	1744	1313	2420	155(17)
H(10C)	2050	1651	3157	155(17)
H(11A)	556	3739	1873	106(12)
H(11B)	704	2652	1571	106(12)
H(11C)	1092	3693	1701	106(12)
H(12A)	1008	1509	3427	128(15)
H(12B)	627	1273	2698	128(15)
H(12C)	509	2295	3077	128(15)

Table A.55. Atomic Coordinates ($\times 10^4$) and Equivalent Isotropic Displacement Parameters ($\text{\AA}^2 \times 10^3$) for $\text{C}_{12}\text{H}_{36}\text{N}_4\text{Pb}_4\text{Si}_4$ (**15**).

Atom	x	y	z	U(eq)
Pb(1)	6905(1)	1604(1)	693(1)	22(1)
Pb(2)	6667	3333	1284(1)	21(1)
Si(1)	6667	3333	98(1)	29(1)
Si(2)	9972(2)	3757(3)	1092(1)	22(1)
N(1)	6667	3333	451(3)	20(2)
N(2)	8372(9)	3535(8)	970(1)	20(2)
C(1)	4880(13)	1903(14)	-42(2)	47(3)
C(2)	9657(13)	2116(12)	1286(3)	41(2)
C(3)	10784(11)	5289(11)	1347(2)	33(2)
C(4)	11249(11)	4115(12)	797(2)	40(2)

Table A.56. Interatomic Distances (Å) and Angles (°) for C₁₂H₃₆N₄Pb₄Si₄ (**15**).

Pb(1)-N(2)	2.298(7)	N(2)-Pb(1)-N(2)#1	81.4(4)
Pb(1)-N(2)#1	2.305(7)	N(2)-Pb(1)-N(1)	82.3(3)
Pb(1)-N(1)	2.312(6)	N(2)#1-Pb(1)-N(1)	82.1(3)
Pb(1)-Pb(1)#2	3.4621(6)	N(2)-Pb(1)-Pb(1)#2	41.31(17)
Pb(1)-Pb(1)#1	3.4621(6)	N(2)#1-Pb(1)-Pb(1)#2	84.2(2)
Pb(1)-Pb(2)	3.4693(7)	N(1)-Pb(1)-Pb(1)#2	41.52(17)
Pb(2)-N(2)#1	2.298(7)	N(2)-Pb(1)-Pb(1)#1	84.3(2)
Pb(2)-N(2)	2.298(7)	N(2)#1-Pb(1)-Pb(1)#1	41.16(18)
Pb(2)-N(2)#2	2.298(7)	N(1)-Pb(1)-Pb(1)#1	41.52(17)
Pb(2)-Pb(1)#1	3.4693(7)	Pb(1)#2-Pb(1)-Pb(1)#1	60.0
Pb(2)-Pb(1)#2	3.4693(7)	N(2)-Pb(1)-Pb(2)	40.98(19)
Si(1)-N(1)	1.693(13)	N(2)#1-Pb(1)-Pb(2)	41.01(19)
Si(1)-C(1)#2	1.883(12)	N(1)-Pb(1)-Pb(2)	85.0(3)
Si(1)-C(1)	1.883(12)	Pb(1)#2-Pb(1)-Pb(2)	60.069(7)
Si(1)-C(1)#1	1.883(12)	Pb(1)#1-Pb(1)-Pb(2)	60.069(7)
Si(2)-N(2)	1.716(9)	N(2)#1-Pb(2)-N(2)	81.6(3)
Si(2)-C(2)	1.869(10)	N(2)#1-Pb(2)-N(2)#2	81.6(3)
Si(2)-C(4)	1.872(10)	N(2)-Pb(2)-N(2)#2	81.6(3)
Si(2)-C(3)	1.877(10)	N(2)#1-Pb(2)-Pb(1)#1	41.00(19)
N(1)-Pb(1)#2	2.312(6)	N(2)-Pb(2)-Pb(1)#1	84.16(19)
N(1)-Pb(1)#1	2.312(6)	N(2)#2-Pb(2)-Pb(1)#1	41.17(18)
N(2)-Pb(1)#2	2.305(7)	N(2)#1-Pb(2)-Pb(1)	41.17(18)

N(2)-Pb(2)-Pb(1)	41.00(19)	C(2)-Si(2)-C(4)	109.7(5)
N(2)#2-Pb(2)-Pb(1)	84.16(19)	N(2)-Si(2)-C(3)	109.7(4)
Pb(1)#1-Pb(2)-Pb(1)	59.862(15)	C(2)-Si(2)-C(3)	106.8(5)
N(2)#1-Pb(2)-Pb(1)#2	84.16(19)	C(4)-Si(2)-C(3)	109.9(5)
N(2)-Pb(2)-Pb(1)#2	41.17(18)	Si(1)-N(1)-Pb(1)	120.2(3)
N(2)#2-Pb(2)-Pb(1)#2	41.00(19)	Si(1)-N(1)-Pb(1)#2	120.2(3)
Pb(1)#1-Pb(2)-Pb(1)#2	59.862(15)	Pb(1)-N(1)-Pb(1)#2	97.0(3)
Pb(1)-Pb(2)-Pb(1)#2	59.862(15)	Si(1)-N(1)-Pb(1)#1	120.2(3)
N(1)-Si(1)-C(1)#2	110.8(4)	Pb(1)-N(1)-Pb(1)#1	97.0(3)
N(1)-Si(1)-C(1)	110.8(4)	Pb(1)#2-N(1)-Pb(1)#1	97.0(3)
C(1)#2-Si(1)-C(1)	108.1(4)	Si(2)-N(2)-Pb(2)	119.1(3)
N(1)-Si(1)-C(1)#1	110.8(4)	Si(2)-N(2)-Pb(1)	120.6(4)
C(1)#2-Si(1)-C(1)#1	108.1(4)	Pb(2)-N(2)-Pb(1)	98.0(3)
C(1)-Si(1)-C(1)#1	108.1(4)	Si(2)-N(2)-Pb(1)#2	118.9(4)
N(2)-Si(2)-C(2)	110.0(4)	Pb(2)-N(2)-Pb(1)#2	97.8(3)
N(2)-Si(2)-C(4)	110.6(4)	Pb(1)-N(2)-Pb(1)#2	97.5(3)

Table A.57. Anisotropic displacement parameters ($\text{\AA}^2 \times 10^3$) for $\text{C}_{12}\text{H}_{36}\text{N}_4\text{Pb}_4\text{Si}_4$ (**15**).

Atom	U11	U22	U33	U23	U13	U12
Pb(1)	26(1)	22(1)	20(1)	-2(1)	0(1)	13(1)
Pb(2)	24(1)	24(1)	14(1)	0	0	12(1)
Si(1)	35(2)	35(2)	16(2)	0	0	17(1)
Si(2)	21(1)	28(1)	19(1)	0(1)	-2(1)	14(1)
N(1)	26(4)	26(4)	8(5)	0	0	13(2)
N(2)	25(4)	25(4)	13(4)	0(2)	2(2)	15(3)
C(1)	53(7)	62(8)	23(5)	-13(5)	-10(5)	27(6)
C(2)	47(6)	31(5)	52(7)	9(5)	0(5)	24(5)
C(3)	31(5)	32(5)	31(5)	-7(4)	-7(4)	13(4)
C(4)	31(5)	47(6)	35(6)	13(5)	14(4)	16(5)

Table A.58. Hydrogen coordinates ($\times 10^4$) and isotropic displacement parameters ($\text{\AA}^2 \times 10^3$) for $\text{C}_{12}\text{H}_{36}\text{N}_4\text{Pb}_4\text{Si}_4$ (**15**).

Atom	x	y	z	U(eq)
H(1A)	4653	998	35	50(20)
H(1B)	4929	1865	-240	50(20)
H(1C)	4157	2123	8	50(20)
H(2A)	8980	1918	1431	41(18)
H(2B)	10536	2273	1364	41(18)
H(2C)	9292	1322	1161	41(18)
H(3A)	10716	6076	1274	50(20)
H(3B)	11766	5575	1376	50(20)
H(3C)	10281	4991	1519	50(20)
H(4A)	11288	3269	757	260(100)
H(4B)	12180	4866	847	260(100)
H(4C)	10929	4391	636	260(100)

Table A.59. Atomic Coordinates ($\times 10^4$) and Equivalent Isotropic Displacement Parameters ($\text{\AA}^2 \times 10^3$) for $\text{C}_{12}\text{H}_{36}\text{N}_4\text{Sn}_4\text{Ge}_4$ (**16**).

Atom	x	y	z	U(eq)
Sn(1)	8611(1)	1497(1)	2195(1)	39(1)
Sn(2)	9964(1)	197(1)	1433(1)	39(1)
Ge(1)	10071(1)	2048(1)	4385(1)	41(1)
Ge(2)	7539(1)	-356(1)	1937(1)	44(1)
N(1)	8766(9)	289(6)	2216(8)	37(3)
N(2)	10042(10)	1431(6)	3425(8)	40(3)
C(1)	8632(15)	1842(13)	4688(12)	68(5)
C(2)	11395(13)	1758(10)	5371(10)	54(4)
C(3)	10242(17)	3073(9)	3973(13)	69(5)
C(4)	8227(19)	-1393(8)	2039(11)	66(6)
C(5)	6826(17)	-225(13)	2829(14)	80(6)
C(6)	6644(18)	-115(13)	747(15)	91(8)
O(1)	5226(9)	1520(6)	3453(8)	69(4)

Table A.60. Interatomic Distances (Å) and Angles (°) for C₁₂H₃₆N₄Sn₄Ge₄ (**16**).

Sn(1)-N(1)	2.169(11)	N(2)#1-Sn(2)-N(1)#1	81.6(4)
Sn(1)-N(2)#1	2.187(12)	N(2)-Ge(1)-C(2)	106.5(7)
Sn(1)-N(2)	2.201(12)	N(2)-Ge(1)-C(3)	105.4(7)
Sn(2)-N(1)	2.210(11)	C(2)-Ge(1)-C(3)	110.6(8)
Sn(2)-N(2)#1	2.219(11)	N(2)-Ge(1)-C(1)	106.2(7)
Sn(2)-N(1)#1	2.235(11)	C(2)-Ge(1)-C(1)	111.5(7)
Ge(1)-N(2)	1.855(12)	C(3)-Ge(1)-C(1)	115.8(8)
Ge(1)-C(2)	1.964(15)	N(1)-Ge(2)-C(5)	106.9(8)
Ge(1)-C(3)	1.977(17)	N(1)-Ge(2)-C(6)	106.8(8)
Ge(1)-C(1)	2.030(18)	C(5)-Ge(2)-C(6)	115.1(11)
Ge(2)-N(1)	1.865(12)	N(1)-Ge(2)-C(4)	104.3(7)
Ge(2)-C(5)	1.885(19)	C(5)-Ge(2)-C(4)	109.8(8)
Ge(2)-C(6)	1.91(2)	C(6)-Ge(2)-C(4)	113.1(9)
Ge(2)-C(4)	2.032(18)	Ge(2)-N(1)-Sn(1)	123.3(5)
N(1)-Sn(2)#1	2.235(11)	Ge(2)-N(1)-Sn(2)	118.2(6)
N(2)-Sn(1)#1	2.187(12)	Sn(1)-N(1)-Sn(2)	98.0(5)
N(2)-Sn(2)#1	2.219(11)	Ge(2)-N(1)-Sn(2)#1	118.5(6)
N(1)-Sn(1)-N(2)#1	82.8(4)	Sn(1)-N(1)-Sn(2)#1	97.1(4)
N(1)-Sn(1)-N(2)	83.5(4)	Sn(2)-N(1)-Sn(2)#1	96.3(4)
N(2)#1-Sn(1)-N(2)	81.5(5)	Ge(1)-N(2)-Sn(1)#1	119.8(5)
N(1)-Sn(2)-N(2)#1	81.2(4)	Ge(1)-N(2)-Sn(1)	119.2(6)
N(1)-Sn(2)-N(1)#1	83.0(4)	Sn(1)#1-N(2)-Sn(1)	98.2(5)

Ge(1)-N(2)-Sn(2)#1	120.7(6)
Sn(1)#1-N(2)-Sn(2)#1	97.2(5)
Sn(1)-N(2)-Sn(2)#1	96.6(4)

Table A.61. Anisotropic displacement parameters ($\text{\AA}^2 \times 10^3$) for $\text{C}_{12}\text{H}_{36}\text{N}_4\text{Sn}_4\text{Ge}_4$ (**16**).

Atom	U11	U22	U33	U23	U13	U12
Sn(1)	39(1)	33(1)	44(1)	2(1)	10(1)	3(1)
Sn(2)	44(1)	34(1)	38(1)	-2(1)	11(1)	-2(1)
Ge(1)	48(1)	34(1)	41(1)	-4(1)	12(1)	2(1)
Ge(2)	37(1)	35(1)	56(1)	2(1)	8(1)	-5(1)
N(1)	28(7)	40(7)	43(7)	-1(5)	11(5)	8(5)
N(2)	38(8)	29(6)	48(7)	-4(5)	7(6)	-9(5)
C(1)	46(11)	109(17)	53(11)	10(10)	20(9)	10(11)
C(2)	34(9)	73(12)	45(9)	2(8)	-4(7)	-6(8)
C(3)	91(15)	42(10)	74(13)	14(9)	23(11)	10(9)
C(4)	126(18)	31(8)	44(9)	-12(7)	30(10)	-45(10)
C(5)	62(14)	103(17)	83(15)	10(12)	36(12)	30(12)
C(6)	67(15)	94(17)	85(16)	26(13)	-19(12)	-16(12)
O(1)	35(6)	75(8)	97(9)	-86(7)	19(6)	-12(5)

Table A.62. Hydrogen coordinates ($\times 10^4$) and isotropic displacement parameters ($\text{\AA}^2 \times 10^3$) for $\text{C}_{12}\text{H}_{36}\text{N}_4\text{Sn}_4\text{Ge}_4$ (**16**).

Atom	x	y	z	U(eq)
H(1A)	8009	1912	4169	102
H(1B)	8577	2176	5146	102
H(1C)	8637	1342	4893	102
H(2A)	11301	1264	5558	81
H(2B)	11485	2092	5859	81
H(2C)	12041	1778	5172	81
H(3A)	10901	3100	3792	104
H(3B)	10299	3416	4449	104
H(3C)	9609	3196	3480	104
H(4A)	8999	-1352	2087	99
H(4B)	7855	-1676	1521	99
H(4C)	8147	-1635	2557	99
H(5A)	7372	-220	3403	119
H(5B)	6316	-624	2801	119
H(5C)	6430	236	2734	119
H(6A)	6179	301	764	137
H(6B)	6190	-532	491	137
H(6C)	7117	7	393	137

Table A.63. Atomic Coordinates ($\times 10^4$) and Equivalent Isotropic Displacement Parameters ($\text{\AA}^2 \times 10^3$) for $\text{C}_{12}\text{H}_{36}\text{N}_4\text{Sn}_8$ (**17**).

Atom	x	y	z	U(eq)
Sn(1)	998(1)	998(1)	998(1)	28(1)
Sn(2)	1903(1)	1903(1)	-1903(1)	32(1)
N(1)	887(3)	887(3)	-887(3)	29(1)
C(1)	3636(5)	1461(4)	-1461(4)	51(1)

Table A.64. Interatomic Distances (Å) and Angles (°) for C₁₂H₃₆N₄Sn₈ (**17**).

Sn(1)-N(1)#1	2.196(3)	Sn(1)#2-Sn(1)-Sn(1)#1	60.0
Sn(1)-N(1)#2	2.196(3)	N(1)#1-Sn(1)-Sn(1)#3	41.76(10)
Sn(1)-N(1)	2.196(3)	N(1)#2-Sn(1)-Sn(1)#3	41.76(10)
Sn(1)-Sn(1)#2	3.2757(9)	N(1)-Sn(1)-Sn(1)#3	85.27(15)
Sn(1)-Sn(1)#1	3.2757(9)	Sn(1)#2-Sn(1)-Sn(1)#3	60.0
Sn(1)-Sn(1)#3	3.2757(9)	Sn(1)#1-Sn(1)-Sn(1)#3	60.0
Sn(2)-N(1)	2.043(7)	N(1)-Sn(2)-C(1)#4	105.43(19)
Sn(2)-C(1)#4	2.139(5)	N(1)-Sn(2)-C(1)	105.43(19)
Sn(2)-C(1)	2.139(5)	C(1)#4-Sn(2)-C(1)	113.20(16)
Sn(2)-C(1)#5	2.139(5)	N(1)-Sn(2)-C(1)#5	105.43(19)
N(1)-Sn(1)#1	2.196(3)	C(1)#4-Sn(2)-C(1)#5	113.20(16)
N(1)-Sn(1)#2	2.196(3)	C(1)-Sn(2)-C(1)#5	113.20(16)
N(1)#1-Sn(1)-N(1)#2	83.1(2)	Sn(2)-N(1)-Sn(1)	120.54(15)
N(1)#1-Sn(1)-N(1)	83.1(2)	Sn(2)-N(1)-Sn(1)#1	120.54(15)
N(1)#2-Sn(1)-N(1)	83.1(2)	Sn(1)-N(1)-Sn(1)#1	96.5(2)
N(1)#1-Sn(1)-Sn(1)#2	85.27(15)	Sn(2)-N(1)-Sn(1)#2	120.54(15)
N(1)#2-Sn(1)-Sn(1)#2	41.76(10)	Sn(1)-N(1)-Sn(1)#2	96.5(2)
N(1)-Sn(1)-Sn(1)#2	41.76(10)	Sn(1)#1-N(1)-Sn(1)#2	96.5(2)
N(1)#1-Sn(1)-Sn(1)#1	41.76(10)		
N(1)#2-Sn(1)-Sn(1)#1	85.27(15)		
N(1)-Sn(1)-Sn(1)#1	41.76(10)		

Table A.65. Anisotropic displacement parameters ($\text{\AA}^2 \times 10^3$) for $\text{C}_{12}\text{H}_{36}\text{N}_4\text{Sn}_8$ (**17**).

Atom	U11	U22	U33	U23	U13	U12
Sn(1)	28(1)	28(1)	28(1)	-3(1)	-3(1)	-3(1)
Sn(2)	32(1)	32(1)	32(1)	5(1)	5(1)	-5(1)
N(1)	29(1)	29(1)	29(1)	1(1)	1(1)	-1(1)
C(1)	34(2)	59(2)	59(2)	6(3)	4(2)	-4(2)

Table A.66. Hydrogen coordinates ($\times 10^4$) and isotropic displacement parameters ($\text{\AA}^2 \times 10^3$) for $\text{C}_{12}\text{H}_{36}\text{N}_4\text{Sn}_8$ (**17**).

Atom	x	y	z	U(eq)
H(1A)	3677	1277	-656	42(16)
H(1B)	4134	2101	-1623	42(16)
H(1C)	3875	806	-1906	42(16)

Table A.67. Atomic Coordinates ($\times 10^4$) and Equivalent Isotropic Displacement Parameters ($\text{\AA}^2 \times 10^3$) for $\text{C}_{12}\text{H}_{36}\text{N}_4\text{Ge}_8$ (**18**).

Atom	x	y	z	U(eq)
Ge(1)	4070(1)	4070(1)	4070(1)	26(1)
Ge(2)	1796(1)	1796(1)	1796(1)	31(1)
N(1)	839(4)	839(4)	839(4)	27(2)
C(1)	3422(6)	1407(5)	1407(5)	49(2)

Table A.68 Interatomic Distances (Å) and Angles (°) for C₁₂H₃₆N₄Ge₈ (**18**).

Ge(1)-N(1)#1	2.002(4)	N(1)-Ge(2)-C(1)	106.6(2)
Ge(1)-N(1)#2	2.002(4)	N(1)-Ge(2)-C(1)#4	106.6(2)
Ge(1)-N(1)#3	2.002(4)	C(1)-Ge(2)-C(1)#4	112.2(2)
Ge(2)-N(1)	1.870(9)	N(1)-Ge(2)-C(1)#5	106.6(2)
Ge(2)-C(1)	1.937(7)	C(1)-Ge(2)-C(1)#5	112.2(2)
Ge(2)-C(1)#4	1.937(7)	C(1)#4-Ge(2)-C(1)#5	112.2(2)
Ge(2)-C(1)#5	1.937(7)	Ge(2)-N(1)-Ge(1)#6	121.1(2)
N(1)-Ge(1)#6	2.002(4)	Ge(2)-N(1)-Ge(1)#7	121.1(2)
N(1)-Ge(1)#7	2.002(4)	Ge(1)#6-N(1)-Ge(1)#7	95.7(3)
N(1)-Ge(1)#8	2.002(4)	Ge(2)-N(1)-Ge(1)#8	121.1(2)
N(1)#1-Ge(1)-N(1)#2	84.0(3)	Ge(1)#6-N(1)-Ge(1)#8	95.7(3)
N(1)#1-Ge(1)-N(1)#3	84.0(3)	Ge(1)#7-N(1)-Ge(1)#8	95.7(3)
N(1)#2-Ge(1)-N(1)#3	84.0(3)		

Table A.69. Anisotropic displacement parameters ($\text{\AA}^2 \times 10^3$) for $\text{C}_{12}\text{H}_{36}\text{N}_4\text{Ge}_8$ (**18**).

Atom	U11	U22	U33	U23	U13	U12
Ge(1)	26(1)	26(1)	26(1)	-2(1)	-2(1)	-2(1)
Ge(2)	31(1)	31(1)	31(1)	-5(1)	-5(1)	-5(1)
N(1)	27(2)	27(2)	27(2)	-1(2)	-1(2)	-1(2)
C(1)	29(4)	59(3)	59(3)	0(4)	-6(3)	-6(3)

Table A.70. Hydrogen coordinates ($\times 10^4$) and isotropic displacement parameters ($\text{\AA}^2 \times 10^3$) for $\text{C}_{12}\text{H}_{36}\text{N}_4\text{Ge}_8$ (**18**).

Atom	x	y	z	U(eq)
H(1A)	3524	571	1431	80(20)
H(1B)	3938	1769	1964	80(20)
H(1C)	3600	1689	634	80(20)

Table A.71. Atomic Coordinates ($\times 10^4$) and Equivalent Isotropic Displacement Parameters ($\text{\AA}^2 \times 10^3$) for $\text{C}_{12}\text{H}_{36}\text{N}_4\text{Pb}_4\text{Ge}_4$ (**19**).

Atom	x	y	z	U(eq)
Pb(1)	-673(1)	-673(1)	-10673(1)	36(1)
Pb(2)	-674(1)	-1823(1)	-5666(1)	34(1)
Ge(1)	-1163(2)	-1163(2)	-8838(2)	50(2)
Ge(2)	1179(2)	-1378(2)	-6189(2)	45(1)
N(1)	-585(9)	-585(9)	-9415(9)	48(9)
N(2)	552(8)	-1928(9)	-5581(8)	30(3)
C(1)	-1172(15)	-862(17)	-7802(16)	102(13)
C(2)	1730(60)	-2130(60)	-7140(60)	50(30)
C(2A)	1031(19)	-1683(19)	-7198(19)	64(9)
C(3)	2128(18)	-1867(19)	-6204(17)	63(10)
C(3A)	1780(90)	-2630(90)	-6520(90)	90(50)
C(4)	1230(30)	-360(30)	-5880(30)	48(12)
C(4A)	770(30)	-340(30)	-6190(20)	51(12)

Table A.72. Interatomic Distances (Å) and Angles (°) for C₁₂H₃₆N₄Pb₄Ge₄ (**19**).

Pb(1)-N(1)	2.303(14)	Ge(2)-C(2)	2.42(10)
Pb(1)-N(1)#1	2.303(14)	N(1)-Pb(1)#1	2.303(14)
Pb(1)-N(1)#2	2.303(14)	N(1)-Pb(1)#2	2.303(14)
Pb(1)-Pb(1)#1	3.467(2)	N(2)-Pb(2)#4	2.291(15)
Pb(1)-Pb(1)#2	3.467(2)	N(2)-Pb(2)#6	2.293(16)
Pb(1)-Pb(1)#3	3.467(2)	C(2)-C(3A)	1.46(16)
Pb(2)-N(2)	2.247(15)	C(2)-C(2A)	1.51(10)
Pb(2)-N(2)#4	2.291(15)	C(2)-C(3)	1.91(12)
Pb(2)-N(2)#5	2.293(16)	C(3)-C(3A)	1.64(16)
Pb(2)-C(3A)#5	2.73(15)	C(3A)-Pb(2)#6	2.73(15)
Pb(2)-Pb(2)#4	3.4525(15)	C(4)-C(4A)	1.03(6)
Pb(2)-Pb(2)#6	3.4718(13)	N(1)-Pb(1)-N(1)#1	81.8(9)
Pb(2)-Pb(2)#5	3.4718(13)	N(1)-Pb(1)-N(1)#2	81.8(9)
Ge(1)-N(1)	1.82(3)	N(1)#1-Pb(1)-N(1)#2	81.8(9)
Ge(1)-C(1)#7	1.96(3)	N(1)-Pb(1)-Pb(1)#1	41.2(4)
Ge(1)-C(1)#8	1.96(3)	N(1)#1-Pb(1)-Pb(1)#1	41.2(4)
Ge(1)-C(1)	1.96(3)	N(1)#2-Pb(1)-Pb(1)#1	84.4(6)
Ge(2)-N(2)	1.882(19)	N(1)-Pb(1)-Pb(1)#2	41.2(4)
Ge(2)-C(2A)	1.94(3)	N(1)#1-Pb(1)-Pb(1)#2	84.4(6)
Ge(2)-C(4)	1.95(5)	N(1)#2-Pb(1)-Pb(1)#2	41.2(4)
Ge(2)-C(3)	1.95(3)	Pb(1)#1-Pb(1)-Pb(1)#2	60.0
Ge(2)-C(4A)	2.04(5)	N(1)-Pb(1)-Pb(1)#3	84.4(6)

N(1)#1-Pb(1)-Pb(1)#3	41.2(4)	Pb(2)#4-Pb(2)-Pb(2)#5	60.184(12)
N(1)#2-Pb(1)-Pb(1)#3	41.2(4)	Pb(2)#6-Pb(2)-Pb(2)#5	59.63(2)
Pb(1)#1-Pb(1)-Pb(1)#3	60.0	N(1)-Ge(1)-C(1)#7	113.5(9)
Pb(1)#2-Pb(1)-Pb(1)#3	60.0	N(1)-Ge(1)-C(1)#8	113.5(9)
N(2)-Pb(2)-N(2)#4	80.1(7)	C(1)#7-Ge(1)-C(1)#8	105.2(10)
N(2)-Pb(2)-N(2)#5	80.5(7)	N(1)-Ge(1)-C(1)	113.5(9)
N(2)#4-Pb(2)-N(2)#5	79.6(7)	C(1)#7-Ge(1)-C(1)	105.2(10)
N(2)-Pb(2)-C(3A)#5	125(3)	C(1)#8-Ge(1)-C(1)	105.2(10)
N(2)#4-Pb(2)-C(3A)#5	140(3)	N(2)-Ge(2)-C(2A)	108.7(12)
N(2)#5-Pb(2)-C(3A)#5	75(3)	N(2)-Ge(2)-C(4)	111.6(16)
N(2)-Pb(2)-Pb(2)#4	40.9(4)	C(2A)-Ge(2)-C(4)	123.9(18)
N(2)#4-Pb(2)-Pb(2)#4	40.0(4)	N(2)-Ge(2)-C(3)	107.7(10)
N(2)#5-Pb(2)-Pb(2)#4	83.3(4)	C(2A)-Ge(2)-C(3)	88.7(13)
C(3A)#5-Pb(2)-Pb(2)#4	157(3)	C(4)-Ge(2)-C(3)	113.4(18)
N(2)-Pb(2)-Pb(2)#6	40.6(4)	N(2)-Ge(2)-C(4A)	106.0(14)
N(2)#4-Pb(2)-Pb(2)#6	82.9(5)	C(2A)-Ge(2)-C(4A)	102.3(15)
N(2)#5-Pb(2)-Pb(2)#6	40.7(4)	C(4)-Ge(2)-C(4A)	29.7(17)
C(3A)#5-Pb(2)-Pb(2)#6	98(3)	C(3)-Ge(2)-C(4A)	138.8(19)
Pb(2)#4-Pb(2)-Pb(2)#6	60.184(12)	N(2)-Ge(2)-C(2)	112(3)
N(2)-Pb(2)-Pb(2)#5	83.5(5)	C(2A)-Ge(2)-C(2)	39(3)
N(2)#4-Pb(2)-Pb(2)#5	40.8(4)	C(4)-Ge(2)-C(2)	137(3)
N(2)#5-Pb(2)-Pb(2)#5	39.6(4)	C(3)-Ge(2)-C(2)	50(3)
C(3A)#5-Pb(2)-Pb(2)#5	105(3)	C(4A)-Ge(2)-C(2)	132(3)

Ge(1)-N(1)-Pb(1)	119.6(6)	C(2A)-C(2)-Ge(2)	53(3)
Ge(1)-N(1)-Pb(1)#1	119.6(6)	C(3)-C(2)-Ge(2)	52(3)
Pb(1)-N(1)-Pb(1)#1	97.7(8)	C(2)-C(2A)-Ge(2)	88(5)
Ge(1)-N(1)-Pb(1)#2	119.6(6)	C(3A)-C(3)-C(2)	48(6)
Pb(1)-N(1)-Pb(1)#2	97.7(8)	C(3A)-C(3)-Ge(2)	93(6)
Pb(1)#1-N(1)-Pb(1)#2	97.7(8)	C(2)-C(3)-Ge(2)	78(3)
Ge(2)-N(2)-Pb(2)	121.2(7)	C(2)-C(3A)-C(3)	76(8)
Ge(2)-N(2)-Pb(2)#4	118.7(8)	C(2)-C(3A)-Pb(2)#6	128(10)
Pb(2)-N(2)-Pb(2)#4	99.1(6)	C(3)-C(3A)-Pb(2)#6	114(8)
Ge(2)-N(2)-Pb(2)#6	115.5(7)	C(4A)-C(4)-Ge(2)	80(5)
Pb(2)-N(2)-Pb(2)#6	99.8(7)	C(4)-C(4A)-Ge(2)	70(4)
Pb(2)#4-N(2)-Pb(2)#6	98.5(6)		
C(3A)-C(2)-C(2A)	117(10)		
C(3A)-C(2)-C(3)	56(8)		
C(2A)-C(2)-C(3)	105(6)		
C(3A)-C(2)-Ge(2)	80(8)		

Table A.73. Anisotropic displacement parameters ($\text{\AA}^2 \times 10^3$) for $\text{C}_{12}\text{H}_{36}\text{N}_4\text{Pb}_4\text{Ge}_4$ (**19**).

Atom	U11	U22	U33	U23	U13	U12
Pb(1)	36(1)	36(1)	36(1)	-4(1)	-4(1)	-4(1)
Pb(2)	35(1)	30(1)	36(1)	3(1)	-6(1)	3(1)
Ge(1)	50(2)	50(2)	50(2)	10(1)	10(1)	-10(1)
Ge(2)	45(1)	44(1)	45(2)	17(2)	6(1)	-12(1)
N(1)	48(9)	48(9)	48(9)	9(9)	9(9)	-9(9)
N(2)	29(8)	29(8)	32(9)	-6(7)	-11(7)	13(6)
C(1)	80(20)	140(30)	90(30)	60(20)	29(18)	0(20)

Table A.74. Hydrogen coordinates ($\times 10^4$) and isotropic displacement parameters ($\text{\AA}^2 \times 10^3$) for $\text{C}_{12}\text{H}_{36}\text{N}_4\text{Pb}_4\text{Ge}_4$ (**19**).

Atom	x	y	z	U(eq)
H(1A)	-1324	-1263	-7506	153
H(1B)	-1504	-465	-7740	153
H(1C)	-693	-712	-7661	153

Table A.75. Atomic Coordinates ($\times 10^4$) and Equivalent Isotropic Displacement Parameters ($\text{\AA}^2 \times 10^3$) for $\text{C}_{12}\text{H}_{28}\text{O}_8\text{Sn}_6$ (**21**).

Atom	x	y	z	U(eq)
Sn(1)	9299(1)	439(1)	3991(1)	34(1)
Sn(2)	9275(1)	2500	5694(1)	30(1)
Sn(3)	12070(1)	1435(1)	5139(1)	32(1)
Sn(4)	12103(1)	2500	3438(1)	31(1)
O(1)	8063(9)	2500	4572(6)	33(3)
O(2)	11549(11)	2500	6003(6)	33(3)
O(3)	11595(8)	1167(5)	3854(4)	32(2)
O(4)	10084(7)	1571(4)	5046(4)	23(2)
O(5)	12500(11)	2500	4576(5)	28(2)
O(6)	10093(10)	2500	3580(5)	25(2)
C(1)	6634(15)	2500	4589(10)	36(4)
C(2)	6160(20)	2500	3804(11)	55(6)
C(3)	6193(14)	1743(11)	4980(9)	58(4)
C(4)	11996(14)	2500	6753(10)	37(4)
C(5)	13500(20)	2500	6772(12)	83(9)
C(6)	11532(15)	1759(10)	7153(8)	57(4)
C(7)	12051(10)	447(8)	3484(7)	33(3)
C(8)	11628(17)	476(10)	2683(7)	59(4)
C(9)	13503(14)	437(10)	3534(9)	59(4)
C(10)	11519(18)	-289(9)	3852(8)	58(4)

Table A.76. Interatomic Distances (Å) and Angles (°) for C₁₂H₂₈O₈Sn₆ (**21**).

Sn(1)-O(4)	2.064(7)	O(6)-Sn(1)#1	2.065(5)
Sn(1)-O(6)	2.065(5)	C(1)-C(2)	1.48(3)
Sn(1)-O(1)	2.400(7)	C(1)-C(3)	1.501(18)
Sn(1)-O(3)	2.418(8)	C(1)-C(3)#1	1.501(18)
Sn(2)-O(4)	2.092(7)	C(4)-C(6)	1.493(18)
Sn(2)-O(4)#1	2.092(7)	C(4)-C(6)#1	1.493(18)
Sn(2)-O(1)	2.361(11)	C(4)-C(5)	1.55(2)
Sn(2)-O(2)	2.406(11)	C(7)-C(10)	1.484(18)
Sn(3)-O(4)	2.064(7)	C(7)-C(8)	1.498(18)
Sn(3)-O(5)	2.071(5)	C(7)-C(9)	1.498(18)
Sn(3)-O(3)	2.389(8)	O(4)-Sn(1)-O(6)	94.6(3)
Sn(3)-O(2)	2.399(8)	O(4)-Sn(1)-O(1)	74.6(3)
Sn(4)-O(5)	2.074(10)	O(6)-Sn(1)-O(1)	75.3(3)
Sn(4)-O(6)	2.085(10)	O(4)-Sn(1)-O(3)	74.3(3)
Sn(4)-O(3)	2.379(9)	O(6)-Sn(1)-O(3)	74.6(3)
Sn(4)-O(3)#1	2.379(9)	O(1)-Sn(1)-O(3)	134.2(3)
O(1)-C(1)	1.471(18)	O(4)-Sn(2)-O(4)#1	94.1(4)
O(1)-Sn(1)#1	2.400(7)	O(4)-Sn(2)-O(1)	75.0(3)
O(2)-C(4)	1.42(2)	O(4)#1-Sn(2)-O(1)	75.0(3)
O(2)-Sn(3)#1	2.399(8)	O(4)-Sn(2)-O(2)	74.9(3)
O(3)-C(7)	1.437(15)	O(4)#1-Sn(2)-O(2)	74.9(3)
O(5)-Sn(3)#1	2.071(5)	O(1)-Sn(2)-O(2)	135.2(4)

O(4)-Sn(3)-O(5)	94.6(4)	Sn(3)#1-O(2)-Sn(2)	94.0(3)
O(4)-Sn(3)-O(3)	74.9(3)	C(7)-O(3)-Sn(4)	123.1(6)
O(5)-Sn(3)-O(3)	74.6(3)	C(7)-O(3)-Sn(3)	121.9(7)
O(4)-Sn(3)-O(2)	75.6(3)	Sn(4)-O(3)-Sn(3)	94.8(3)
O(5)-Sn(3)-O(2)	75.0(3)	C(7)-O(3)-Sn(1)	121.3(6)
O(3)-Sn(3)-O(2)	135.1(3)	Sn(4)-O(3)-Sn(1)	94.3(3)
O(5)-Sn(4)-O(6)	94.4(4)	Sn(3)-O(3)-Sn(1)	94.0(3)
O(5)-Sn(4)-O(3)	74.7(2)	Sn(1)-O(4)-Sn(3)	116.7(3)
O(6)-Sn(4)-O(3)	75.1(2)	Sn(1)-O(4)-Sn(2)	115.3(3)
O(5)-Sn(4)-O(3)#1	74.7(2)	Sn(3)-O(4)-Sn(2)	115.4(3)
O(6)-Sn(4)-O(3)#1	75.1(2)	Sn(3)-O(5)-Sn(3)#1	115.9(5)
O(3)-Sn(4)-O(3)#1	135.0(4)	Sn(3)-O(5)-Sn(4)	115.7(3)
C(1)-O(1)-Sn(2)	120.8(10)	Sn(3)#1-O(5)-Sn(4)	115.7(3)
C(1)-O(1)-Sn(1)	122.6(5)	Sn(1)-O(6)-Sn(1)#1	115.7(5)
Sn(2)-O(1)-Sn(1)	95.0(3)	Sn(1)-O(6)-Sn(4)	115.9(3)
C(1)-O(1)-Sn(1)#1	122.6(5)	Sn(1)#1-O(6)-Sn(4)	115.9(3)
Sn(2)-O(1)-Sn(1)#1	95.0(3)	O(1)-C(1)-C(2)	107.9(14)
Sn(1)-O(1)-Sn(1)#1	93.5(4)	O(1)-C(1)-C(3)	108.2(10)
C(4)-O(2)-Sn(3)	122.4(5)	C(2)-C(1)-C(3)	110.0(10)
C(4)-O(2)-Sn(3)#1	122.4(5)	O(1)-C(1)-C(3)#1	108.2(10)
Sn(3)-O(2)-Sn(3)#1	94.1(4)	C(2)-C(1)-C(3)#1	110.0(10)
C(4)-O(2)-Sn(2)	122.2(9)	C(3)-C(1)-C(3)#1	112.5(18)
Sn(3)-O(2)-Sn(2)	94.0(3)	O(2)-C(4)-C(6)	110.4(10)

O(2)-C(4)-C(6)#1	110.4(9)	O(3)-C(7)-C(8)	108.6(10)
C(6)-C(4)-C(6)#1	109.8(16)	C(10)-C(7)-C(8)	110.0(13)
O(2)-C(4)-C(5)	110.1(14)	O(3)-C(7)-C(9)	108.0(10)
C(6)-C(4)-C(5)	108.0(10)	C(10)-C(7)-C(9)	109.4(13)
C(6)#1-C(4)-C(5)	108.0(10)	C(8)-C(7)-C(9)	110.3(12)
O(3)-C(7)-C(10)	110.5(10)		

Table A.77. Anisotropic displacement parameters ($\text{\AA}^2 \times 10^3$) for $\text{C}_{12}\text{H}_{28}\text{O}_8\text{Sn}_6$ (**21**).

Atom	U11	U22	U33	U23	U13	U12
Sn(1)	34(1)	40(1)	29(1)	-2(1)	-2(1)	-12(1)
Sn(2)	28(1)	36(1)	25(1)	0	8(1)	0
Sn(3)	26(1)	37(1)	33(1)	7(1)	2(1)	4(1)
Sn(4)	27(1)	40(1)	25(1)	0	5(1)	0
O(1)	18(5)	51(8)	29(6)	0	-2(4)	0
O(2)	31(6)	47(8)	22(6)	0	-7(5)	0
O(3)	36(4)	34(5)	26(4)	-6(3)	10(3)	-3(4)
O(4)	19(3)	23(4)	28(4)	-1(3)	2(3)	-2(3)
O(5)	41(6)	29(7)	14(5)	0	-1(5)	0
O(6)	23(5)	38(7)	15(5)	0	-3(4)	0
C(1)	17(7)	47(12)	44(10)	0	0(7)	0
C(2)	38(10)	81(17)	48(12)	0	-7(9)	0
C(3)	33(7)	69(12)	73(11)	15(9)	1(7)	-13(7)
C(4)	15(7)	53(13)	43(10)	0	-6(7)	0
C(5)	40(11)	180(30)	29(11)	0	-10(9)	0
C(6)	75(10)	66(11)	30(7)	6(7)	7(7)	22(9)
C(7)	20(5)	32(8)	48(7)	4(6)	10(5)	-2(5)
C(8)	100(13)	49(10)	26(7)	-12(6)	13(7)	15(9)
C(9)	54(9)	58(11)	65(10)	-24(8)	24(8)	-5(8)
C(10)	92(12)	29(9)	53(9)	1(6)	21(9)	-5(8)

Table A.78. Hydrogen coordinates ($\times 10^4$) and isotropic displacement parameters ($\text{\AA}^2 \times 10^3$) for $\text{C}_{12}\text{H}_{28}\text{O}_8\text{Sn}_6$ (**21**).

Atom	x	y	z	U(eq)
H(2A)	5243	2463	3800	80
H(2B)	6521	2049	3546	80
H(2C)	6425	2988	3565	80
H(3A)	6368	1286	4673	80(30)
H(3B)	5287	1775	5075	80(30)
H(3C)	6646	1688	5441	80(30)
H(5A)	13809	1964	6692	80
H(5B)	13789	2689	7245	80
H(5C)	13820	2846	6389	80
H(6A)	10610	1749	7153	34(19)
H(6B)	11840	1767	7654	34(19)
H(6C)	11853	1290	6906	34(19)
H(8A)	10707	495	2659	110(40)
H(8B)	11930	6	2430	110(40)
H(8C)	11978	946	2451	110(40)
H(9A)	13843	917	3316	60(30)
H(9B)	13830	-22	3273	60(30)
H(9C)	13758	408	4044	60(30)
H(10A)	11863	-332	4343	60(30)
H(10B)	11754	-755	3570	60(30)
H(10C)	10599	-250	3877	60(30)

Table A.79. Atomic Coordinates ($\times 10^4$) and Equivalent Isotropic Displacement Parameters ($\text{\AA}^2 \times 10^3$) for $\text{C}_{16}\text{H}_{36}\text{O}_8\text{Sn}_6$ (**22**).

Atom	x	y	z	U(eq)
Sn(1)	0	7500	125(1)	23(1)
Sn(2)	-1975(1)	6633(1)	-1259(1)	23(1)
O(1)	1776(3)	6842(3)	-382(2)	24(1)
O(2)	-479(2)	6254(2)	-655(1)	16(1)
C(1)	-2636(4)	8516(4)	132(2)	25(1)
C(2)	-3052(4)	7497(4)	589(3)	36(1)
C(3)	-3635(4)	9085(4)	-268(3)	39(1)

Table A.80. Interatomic Distances (Å) and Angles (°) for C₁₆H₃₆O₈Sn₆ (**22**).

Sn(1)-O(2)	2.091(3)	O(2)#2-Sn(2)-O(1)#1	74.84(10)
Sn(1)-O(2)#1	2.091(3)	O(2)-Sn(2)-O(1)#1	74.40(10)
Sn(1)-O(1)	2.379(3)	O(2)#2-Sn(2)-O(1)#2	75.11(10)
Sn(1)-O(1)#1	2.379(3)	O(2)-Sn(2)-O(1)#2	73.59(10)
Sn(2)-O(2)#2	2.067(3)	O(1)#1-Sn(2)-O(1)#2	133.41(13)
Sn(2)-O(2)	2.095(3)	C(1)#1-O(1)-Sn(1)	116.9(2)
Sn(2)-O(1)#1	2.383(3)	C(1)#1-O(1)-Sn(2)#1	125.4(3)
Sn(2)-O(1)#2	2.418(3)	Sn(1)-O(1)-Sn(2)#1	95.74(11)
O(1)-C(1)#1	1.423(5)	C(1)#1-O(1)-Sn(2)#3	122.5(2)
O(1)-Sn(2)#1	2.383(3)	Sn(1)-O(1)-Sn(2)#3	94.05(10)
O(1)-Sn(2)#3	2.418(3)	Sn(2)#1-O(1)-Sn(2)#3	94.97(10)
O(2)-Sn(2)#3	2.067(3)	Sn(2)#3-O(2)-Sn(1)	115.21(12)
C(1)-O(1)#1	1.423(5)	Sn(2)#3-O(2)-Sn(2)	116.51(12)
C(1)-C(3)	1.516(7)	Sn(1)-O(2)-Sn(2)	115.09(12)
C(1)-C(2)	1.520(6)	O(1)#1-C(1)-C(3)	110.8(4)
O(2)-Sn(1)-O(2)#1	95.57(14)	O(1)#1-C(1)-C(2)	110.3(4)
O(2)-Sn(1)-O(1)	75.57(10)	C(3)-C(1)-C(2)	110.7(4)
O(2)#1-Sn(1)-O(1)	74.57(10)		
O(2)-Sn(1)-O(1)#1	74.57(10)		
O(2)#1-Sn(1)-O(1)#1	75.57(10)		
O(1)-Sn(1)-O(1)#1	134.91(14)		
O(2)#2-Sn(2)-O(2)	94.85(14)		

Table A.81. Anisotropic displacement parameters ($\text{\AA}^2 \times 10^3$) for $\text{C}_{16}\text{H}_{36}\text{O}_8\text{Sn}_6$ (**22**).

Atom	U11	U22	U33	U23	U13	U12
Sn(1)	26(1)	22(1)	20(1)	0	0	-2(1)
Sn(2)	17(1)	22(1)	30(1)	3(1)	-1(1)	-3(1)
O(1)	20(2)	26(2)	26(2)	0(1)	-5(1)	3(1)
O(2)	14(1)	16(1)	18(1)	-1(1)	0(1)	-3(1)
C(1)	26(3)	23(2)	25(2)	-4(2)	5(2)	3(2)
C(2)	31(3)	36(3)	41(3)	6(2)	15(2)	2(2)
C(3)	38(3)	38(3)	40(3)	6(2)	13(2)	14(3)

Table A.82. Hydrogen coordinates ($\times 10^4$) and isotropic displacement parameters ($\text{\AA}^2 \times 10^3$) for $\text{C}_{16}\text{H}_{36}\text{O}_8\text{Sn}_6$ (**22**).

Atom	x	y	z	U(eq)
H(1)	-2303	9065	459	46(16)
H(2A)	-3360	6925	268	49(10)
H(2B)	-3632	7745	924	49(10)
H(2C)	-2424	7182	859	49(10)
H(3A)	-3360	9721	-548	45(9)
H(3B)	-4183	9348	86	45(9)
H(3C)	-3989	8544	-591	45(9)
